

# **Apelinergic system and its role in the development of resistance to antiangiogenic therapy in cancer treatment**

## **Dissertation**

Zur Erlangung der Würde des Doktors der Naturwissenschaften (Dr. rer. nat.)  
im Fachbereich Chemie, der Fakultät für Mathematik, Informatik und Naturwissenschaften  
der Universität Hamburg

vorgelegt von  
Zoran Knežević

Hamburg, 2020



The presented work was conducted from November 2016 until February 2020 externally in the Department of Oncology, Hematology and Bone Marrow Transplantation with the Section Pneumology (University Cancer Center Hamburg) at the University Medical Center Hamburg-Eppendorf under the supervision of Prof. Dr. Walter Fiedler. Prof. Dr. Elke Otjen co-supervised this work in the Department of Chemistry at the University of Hamburg.

November 2016 - February 2020  
Date of the disputation: 16.10.2020

*Evaluators*

Prof. Dr. Walter Fiedler  
Prof. Dr. Wolfgang Maison

*Examination committee*

Chair: Prof. Dr. Elke Oetjen  
Vice chair: Prof. Dr. Wolfgang Maison  
Member: PD Dr. Sabine Hoffmeister-Ullerich



*“Our virtues and our failings are inseparable, like force and matter.  
When they separate, man is no more.”*

Nikola Tesla



*Dedicated to my loved ones.*



*Посвећено мојим најмилијима.*





---

**Table of contents**

Table of contents .....	I
List of abbreviations.....	V
List of figures .....	VIII
List of tables.....	X
Summary .....	1
Zusammenfassung.....	3
1. INTRODUCTION.....	5
1.1 Physiological angiogenesis, molecular basis and mechanisms .....	5
1.1.1 Factors affecting angiogenesis .....	5
1.1.2 Mechanism of angiogenesis .....	7
1.2 Pathophysiological angiogenesis.....	9
1.2.1 Angiogenesis in solid tumors .....	9
1.2.2 Angiogenesis in acute myeloid leukemia.....	11
1.2.3 Contribution of the immune system to tumor angiogenesis.....	12
1.3 Metastatic odyssey.....	13
1.4 Angiogenesis inhibition.....	15
1.4.1 Therapeutic opportunities.....	15
1.4.2 Mechanisms of resistance to antiangiogenic therapy .....	18
1.5 Apelinergic system .....	20
1.6 Apelin receptor .....	22
1.6.1 Distribution and regulation of APJ expression.....	22
1.6.2 APJ signaling.....	23
1.7 Apelin .....	24
1.7.1 Distribution and regulation of Apelin expression .....	25
1.7.2 Analogs of Apelin .....	26
1.7.3 Antagonists of APJ.....	27
1.8 Pathophysiological role of the apelinergic system.....	28
1.8.1 Pathophysiological angiogenesis.....	28
1.8.2 Cancer.....	29
1.9 Thesis objectives .....	32
2. MATERIAL AND METHODS .....	33
2.1 Material.....	33
2.1.1 Laboratory equipment, kits and reagents .....	33

## TABLE OF CONTENTS

---

2.1.2	Apelin, Apelin analogs and APJ antagonists.....	42
2.1.3	Cells.....	43
2.1.4	Animals .....	44
2.1.5	Synthetic oligonucleotides .....	45
2.1.6	Plasmids and recombinant AAV vectors.....	46
2.1.7	Software, online tools, and databases.....	47
2.2	Methods .....	48
2.2.1	Cell culture .....	48
2.2.2	Monocyte to macrophage polarization .....	49
2.2.3	Functional assays.....	51
2.2.4	Gene and protein surface expression analyses .....	53
2.2.5	Protein quantification .....	54
2.2.6	General molecular biology methods.....	55
2.2.7	Cloning strategies .....	58
2.2.8	Virological methods .....	60
2.2.9	<i>In vivo</i> experiments .....	63
2.2.10	Immunohistochemistry .....	65
2.2.11	Statistics.....	65
3.	RESULTS.....	66
3.1	Apelin and APJ expression in immune and endothelial cells.....	66
3.1.1	Polarization to proangiogenic M <sub>2</sub> macrophage phenotype.....	66
3.1.2	APJ expression in M <sub>2</sub> macrophages .....	68
3.1.3	Regulation of apelinergic system in M <sub>2</sub> macrophages .....	68
3.1.4	APJ expression in PBMCs .....	71
3.1.5	Apelin and APJ expression in endothelial cells .....	72
3.1.6	Regulation of apelinergic expression in endothelial cells.....	73
3.2	Apelin and APJ expression in cancer .....	74
3.2.1	APJ expression in murine tumor tissue and tumor cell lines .....	74
3.2.2	APJ protein surface expression in human glioblastoma tissue.....	76
3.2.3	Apelin and APJ expression profile in human acute myeloid leukemia (AML) ....	77
3.2.4	Apelin concentration in plasma of ovarian carcinoma patients .....	78
3.2.5	Apelin and APJ expression in acute myeloid leukemia (AML) cell lines .....	79
3.2.6	Apelin and APJ expression in solid tumor cell lines.....	80
3.2.7	APJ expression regulation in tumor cell lines .....	82
3.3	Functional analyses .....	83

---

3.3.1	Proliferation of M <sub>2</sub> macrophages .....	84
3.3.2	Proliferation of wildtype AML cell lines .....	85
3.3.3	Proliferation of solid cancer cell lines .....	86
3.3.4	Proliferation of transduced AML cell lines .....	87
3.3.5	Clonogenicity of transduced AML cell lines .....	89
3.3.6	Role of the Apelin/APJ system in solid tumor cell migration.....	90
3.4	Apelinergic system's role in immunotherapy.....	91
3.4.1	Immunotherapy-dependent APJ regulation in AML cell lines .....	92
3.4.2	APJ-mediated cytotoxicity .....	93
3.5	Role of Apelin/APJ system <i>in vivo</i> .....	95
3.5.1	Subcutaneous tumor model .....	95
3.5.2	Efficiency of antiangiogenic therapy in subcutaneous model.....	97
3.5.3	Efficiency of antiangiogenic therapy in intravenous model.....	98
3.6	Targeting of the apelinergic system by AAV vectors .....	100
3.6.1	Specificity of AAVs to the lung endothelium .....	101
3.6.2	AAV-mediated targeting of apelinergic system in a lung metastasis model .....	103
4.	DISCUSSION .....	111
4.1	Apelinergic system in endothelial and proangiogenic immune cells .....	111
4.2	The function of the apelinergic system in macrophages .....	114
4.3	Direct link between apelinergic system and tumor .....	115
4.3.1	Tumor tissue .....	115
4.3.2	Tumor cell lines.....	117
4.4	Functional assays in tumor cell lines.....	119
4.4.1	Proliferation rates .....	119
4.4.2	Colony-forming properties of tumor cells.....	120
4.4.3	Migration properties of tumor cells.....	120
4.4.4	Effects of hypoxia on apelinergic expression in tumor cells.....	121
4.4.5	The role of apelinergic system in immunotherapy .....	121
4.5	Role of apelinergic system <i>in vivo</i> .....	122
4.5.1	Lung metastasis models.....	123
4.5.2	Effects of the genetic targeting of apelinergic system .....	124
5.	CONCLUSION .....	132
6.	REFERENCES .....	135
7.	Supplementary data .....	149
8.	Appendix .....	155

## TABLE OF CONTENTS

---

8.1 Hazard statements.....	155
8.2 Precautionary statements.....	155
8.3 Physical and health hazards pictograms.....	157
Acknowledgments.....	158
Eidesstattliche Versicherung / <i>Declaration on Oath</i> .....	163

---

**List of abbreviations**

7-AAD	7-Aminoactinomycin D
A. u.	Arbitrary units
AAV	Adeno-associated virus
ACE2	Angiotensin-converting enzyme 2
AGTRL1	Refer to APJ
AML	Acute Myeloid Leukemia
Ang II	Angiotensin II
Ang1	Angiopoietin 1
Apelin-OE	Apelin-overexpressing
APJ	Apelin receptor (protein/gene)
APJ-OE	APJ-overexpressing
APLN	Apelin (protein/gene)
APLNR	See APJ
AsNRs	Apelin-based synNotch receptors
AT <sub>1A</sub>	Angiotensin II receptor subtype 1A
BLI	Bioluminescence imaging
BMP	Bone morphogenetic proteins
cAMP	Cyclic adenosine monophosphate
CAR-T	Chimeric antigen receptor T cells
CD	Cluster of differentiation
CD11b	Cluster of differentiation molecule 11B: Integrin alpha M
CD163	Cluster of differentiation 163: Scavenger receptor cysteine-rich type 1 protein M130
CD206	Cluster of differentiation 206: The mannose receptor
CD3	Cluster of differentiation 3: T3 complex
CD31	Cluster of differentiation 31: Platelet endothelial cell adhesion molecule (PECAM-1)
CD80	Cluster of differentiation 80: T-Lymphocyte Activation Antigen
cDNA	Complementary DNA
CLL	Chronic lymphocytic leukemia
CMV	Cytomegalovirus
CNS	Central nervous system
CTC	Circulating tumor cells
ddH <sub>2</sub> O	Ultra-pure double-distilled water
DMEM	Dulbecco's Modified Eagle Medium
DNA	Deoxyribonucleic acid
<i>E. coli</i>	<i>Escherichia coli</i>
EC	Endothelial cell
EC <sub>50</sub>	Half maximal effective concentration
eGFP	Enhanced green fluorescent protein
ELISA	Enzyme-linked immunosorbent assay
FBS	Fetal bovine serum
FGF	Fibroblast Growth Factor
GAPDH	Glyceraldehyde-3-phosphate dehydrogenase

## LIST OF ABBREVIATIONS

---

gDNA	Genomic DNA
GOI	Gene of interest
gp	genomic particle(s)
GPCR	G-Protein coupled receptor
H&E	Hematoxylin and eosin
HIF-1 $\alpha$	Hypoxia-induced factor 1 $\alpha$
HUVEC	Human Umbilical Vein Endothelial Cells
IC <sub>50</sub>	Half maximal inhibitory concentration
IFN $\alpha$	Interferon-alpha
IFN $\gamma$	Interferon-gamma
IGF	Insulin-like growth factor
IHC	Immunohistochemistry
IMDM	Iscoe's Modified Dulbecco's Medium
ip	intraperitoneal
ITIM	Immunoreceptor tyrosine-based inhibition motif
iv	intravenous
IVC	Individually ventilated cages
IVI/EVI	<i>in vivo/ex vivo</i> imaging
KOR	$\kappa$ -opioid receptor
LUC	Firefly Luciferase gene
mAPJ	Murine APJ
MMPs	Matrix metalloproteinases
mRNA	Messenger ribonucleic acid
MVD	Microsvessel density
NF $\kappa$ B	Nuclear factor 'kappa-light-chain-enhancer' of activated B-cells
OD	Optical density
OE	Overexpressing
pAML	Primary Acute Myeloid Leukemia
PBMC	Peripheral Blood Mononuclear Cells
PBS	Phosphate Buffered Saline
PDGF	Platelet-Derived Growth Factor
PF4	Platelet factor IV
PFA	Paraformaldehyde
PIGF	Placental growth factor
RNA	Ribonucleic acid
RPMI	Roswell Park Memorial Institute Medium
sc	subcutaneous
SD	Standard deviation
SDF1	Stromal cell-derived factor 1
SN	Supernatant
Sp1	Specificity protein 1
Stat3	Signal transducer and activator of transcription 3
TAM	Tumor-associated Macrophages
TGF	Transforming Growth Factor
TIGIT	T-cell immunoreceptor with Ig and ITIM domains

TKI	Tyrosine Kinase Inhibitor
TNF $\alpha$	Tumor necrosis factor $\alpha$
TSP	Thrombospondins
UKE	University Medical Center Hamburg-Eppendorf
UV	Ultraviolet
VEGF	Vascular Endothelial Growth Factor
VEGFR2	Vascular Endothelial Growth Factor Receptor 2

Further standard abbreviations, especially for measurement units as well as common prefixes have been used without being listed in this table.

**List of figures**

Figure 1. Simplified mechanism of angiogenesis..... 7

Figure 2. Different mechanisms to form blood vessels ..... 9

Figure 3. Amino acid sequence of mature Apelin isoforms ..... 25

Figure 4. Representative flow cytometric analysis of isolated monocytes and M<sub>2</sub> macrophages ..... 66

Figure 5. Monocyte to M<sub>2</sub> macrophage polarization, morphology and marker surface expression. .... 67

Figure 6. Representative flow cytometric analysis of Apelin receptor expression profile..... 68

Figure 7. Flow cytometric analysis of APJ expression using Alexa Fluor 488-coupled APJ antibody .. 69

Figure 8. Apelinergic expression profile of M<sub>2</sub> macrophages under different conditions ..... 70

Figure 9. Effects of hypoxia on APLN/APJ gene expression in M<sub>2</sub> macrophages ..... 71

Figure 10. Flow cytometric analysis profile of freshly isolated PBMCs ..... 72

Figure 11. Analysis of APLN and APJ mRNA expression in human umbilical vein endothelial cells. 73

Figure 12. Regulation of apelinergic system in ECs upon antiangiogenic treatment..... 74

Figure 13. APJ gene expression in various murine tumors ..... 75

Figure 14. Apelinergic expression profile in murine solid tumor cell lines ..... 76

Figure 15. Flow cytometric analysis of human glioblastoma tissue..... 77

Figure 16. APJ surface expression on primary AML cells. .... 77

Figure 17. Apelinergic gene expression in cells from primary AML and M<sub>2</sub> macrophages ..... 78

Figure 18. Apelin plasma concentration in healthy donors and ovarian cancer patients ..... 79

Figure 19. Apelinergic expression profile in AML cell lines..... 80

Figure 20. Apelinergic expression profile in solid tumor cell lines ..... 81

Figure 21. APJ regulation in tumor cell lines upon stimulation with Apelin..... 82

Figure 22. Apelinergic gene expression profile under hypoxic conditions ..... 83

Figure 23. Proliferation properties of polarized M<sub>2</sub> macrophages upon APJ stimulation/inhibition .... 84

Figure 24. Effects of Apelin receptor stimulation and inhibition in AML cell lines..... 85

Figure 25. The proliferation rate of solid tumor cell lines upon stimulation and inhibition of APJ .... 86

Figure 26. Effect of APJ stimulation and inhibition in wildtype and APJ-expressing AML cell lines. 87

Figure 27. Effect of APJ stimulation and inhibition on proliferation in WT and APJ-OE AML cells . 88

Figure 28. Comparison of proliferation rates between wildtype and APJ-overexpressing cell lines .... 89

Figure 29. Colony formation assay for AML cell lines..... 89

Figure 30. Effect of apelinergic stimulation and inhibition on solid cancer cells migration abilities ... 91

Figure 31. Regulation of APJ expression after stimulation with IFN $\gamma$  ..... 92

Figure 32. Cytotoxic assays performed on AML cells as target cells ..... 94

Figure 33. Tumor aggressiveness in preliminary subcutaneous tumor model ..... 96

Figure 34. Qualitative analysis of murine lung metastases ..... 96

Figure 35. Effectiveness of antiangiogenic therapy on subcutaneous tumor growth ..... 98



---

Figure 36. Effect of DC101 on the lung metastatic burden.....	99
Figure 37. Quantification of metastatic burden in intravenous lung metastatic model.....	100
Figure 38. AAV pre-experimental setup.....	101
Figure 39. BLI of mice intravenously injected with AAVs expressing firefly luciferase.....	102
Figure 40. Experimental setup of the main AAV experiment.....	103
Figure 41. Effects of Apelin and F13A on the metastatic burden.....	104
Figure 42. eGFP expression analysis in murine lung tissue.....	105
Figure 43. Effect of Apelin and F13A on metastatic burden in the repeated main experiment.....	106
Figure 44. Analysis of the Apelin/F13A concentration in murine lung tissue.....	107
Figure 45. Representative IHC images of pulmonary metastatic tissue in Apelin-PBS and F13A-PBS mice subgroups.....	108
Figure 46. Immunohistochemical analysis of the murine lung tissue.....	109
Figure 47. Graphical representation of the results.....	131

**List of tables**

Table 1. Mediators involved in angiogenesis ..... 6

Table 2. Metastatic cascade..... 14

Table 3. Antiangiogenic therapeutical approaches..... 17

Table 4. The hallmarks of resistance to antiangiogenic therapy ..... 19

Table 5. Physiological significance of apelinergic system..... 21

Table 6. An overview of Apelin/APJ expression in cancer..... 30

Table 7. Laboratory equipment ..... 33

Table 8. Molecular biology kits and ready-to-use reagents..... 35

Table 9. Enzymes ..... 36

Table 10. Antibodies ..... 37

Table 11. Chemicals, reagents and cell culture supplements ..... 38

Table 12. Recipes for buffers and solutions ..... 41

Table 13. DNA-ladders ..... 41

Table 14. Apelin analogs..... 42

Table 15. Prokaryotic cells..... 43

Table 16. Eukaryotic cells ..... 43

Table 17. Synthetic oligonucleotides ..... 45

Table 18. Plasmids ..... 46

Table 19. Recombinant AAV vectors ..... 46

Table 20. Software, online tools and databases..... 47

Table 21. Plasmid composition for AAV production..... 60

Table 22. Plasmid composition for lentiviral production ..... 62

Table 23. Different cohorts in the main AAV experiment ..... 103

## Summary

It is well known that angiogenesis is one of the hallmarks of cancer. In last decades, much attention has been given to antiangiogenic therapy, especially to VEGF inhibition. Despite the initial period of enthusiasm, several studies showed that the effects of antiangiogenic therapy are usually only transient due to the interference of different resistance mechanisms. Apelin is a recently discovered peptide and, together with its cognate receptor APJ, is known to play a role in angiogenesis. Recent findings suggest that Apelin receptor (APJ) additionally has a role in cancer immunotherapy. This Ph.D. thesis aimed to investigate the effects of *in vitro* and *in vivo* targeting of Apelin/APJ system on tumor growth and development of resistance to antiangiogenic therapy, as well as their role in mediating tumor response to immunotherapy.

Protein surface and mRNA expression of Apelin and APJ had been broadly investigated in murine and human tumor tissue, immune and endothelial cells, as well as in various tumor-derived cell lines. The involvement of the apelinergic system in cancer pathophysiology was studied in *in vitro* and *in vivo* conditions. To investigate the effects of genetic targeting of apelinergic system on tumor cell homing and metastases, adeno-associated viral vectors (AAVs), that specifically target pulmonary endothelium and allow stable expression of the gene of interest, had been used.

The results of this study demonstrated that Apelin and APJ are highly expressed in isolated tumor tissue. In contrast, the majority of cell lines displayed only a low expression of Apelin/APJ. Accordingly, moderate effects of APJ stimulation and inhibition had been observed in *in vitro* functional assays, as well as in simulated conditions of immunotherapy, using cell lines. Differences between Apelin/APJ expression in tumors and tumor cell lines indicated that cells of the tumor microenvironment might have an influence on Apelin/APJ expression in tumor tissue *in vivo*. Furthermore, AAV-mediated genetic targeting of the apelinergic system in mouse lung metastasis model revealed that Apelin has a proangiogenic effect within tumor vasculature in terms of increased microvessel density, despite low Apelin concentration that was measured. Such effect was antagonized by the presence of F13A, an APJ antagonist. The lung metastasis model was not able to satisfy the expectations due to a low metastatic burden. No clear conclusions could be made on the effect of modulating apelinergic system on tumor cell engraftment.

## SUMMARY

---

Taken together, the results of this study have shown the potential of the apelinergic system to affect tumor vascularization, independent of antiangiogenic therapy. Experimental murine model with AAVs has the advantage of targeting the lung endothelium and therefore is relatively specific for lung metastases. Further studies should focus on optimizing the lung metastasis model, allowing better experimental reproducibility.

## Zusammenfassung

Die Angiogenese zählt zu den Markenzeichen von Krebserkrankungen und in den letzten Jahrzehnten wurde der antiangiogenen Therapie, insbesondere der VEGF-Hemmung, viel Aufmerksamkeit geschenkt. Trotz der anfänglichen Begeisterung zeigten mehrere Studien, dass die Auswirkungen der antiangiogenen Therapie aufgrund der Interferenz verschiedener Resistenzmechanismen meist nur vorübergehend sind. Apelin ist ein kürzlich entdecktes Peptid, das zusammen mit seinem zugehörigen Rezeptor APJ bei der Angiogenese beteiligt ist. Neuere Erkenntnisse deuten darauf hin, dass der Apelinrezeptor (APJ) zusätzlich eine Rolle bei der Immuntherapie von Tumorerkrankungen spielt. Ziel dieser Doktorarbeit war es, die Auswirkungen des gezielten Eingriffs in das Apelin/APJ-System *in vitro* und *in vivo* auf das Tumorstadium und die Entwicklung von Resistenzen gegen antiangiogene Therapien sowie ihre Rolle bei der Vermittlung der Tumorantwort auf eine Immuntherapie zu untersuchen.

Die Oberflächenprotein- sowie Genexpression von Apelin und APJ wurden in murinem und menschlichem Tumorgewebe, Primärzellen sowie in verschiedenen von Tumoren abgeleiteten Zelllinien umfassend untersucht. Die Beteiligung des apelinergen Systems an der Pathophysiologie von Krebserkrankungen wurde unter *in vitro*- und *in vivo*-Bedingungen untersucht. Um die Auswirkungen des genetischen Targetings des apelinergen Systems auf das Homing von Tumorzellen und die Entstehung von Metastasen zu untersuchen, wurden adeno-assoziierte virale Vektoren (AAVs) verwendet, die spezifisch auf das Lungenendothel abzielen und eine stabile Expression des Zielgens ermöglichen.

Die Ergebnisse dieser Studie haben gezeigt, dass Apelin und APJ in isoliertem Tumorgewebe eine hohe Expression aufweisen. In der Mehrzahl der Zelllinien hingegen wurde eine geringe Expression von Apelin/APJ gefunden. Dementsprechend wurden unter APJ-Stimulation und -Inhibition in funktionellen *in vitro* Tests sowie auch unter simulierten Bedingungen der Immuntherapie nur mäßige Effekte beobachtet. Unterschiede zwischen der Apelin/APJ-Expression in Tumorgewebe und Tumorzelllinien deuteten darauf hin, dass Zellen der Mikroumgebung des Tumors einen Einfluss auf die Apelin/APJ-Expression im Tumorgewebe *in vivo* haben könnten. Darüber hinaus zeigte das AAV-vermittelte genetische Targeting des apelinergen Systems im Lungenmetastasenmodell der Maus, dass Apelin trotz niedriger Apelin-Konzentration eine proangiogene Wirkung innerhalb des Tumorgefäßsystems in Form einer erhöhten Mikrogefäßdichte hat. Eine solche Wirkung wurde durch die Anwesenheit von F13A, einem APJ-Antagonisten, antagonisiert. Das Lungenmetastasenmodell konnte jedoch

## ZUSAMMENFASSUNG

---

die Erwartungen aufgrund einer geringen Metastasenlast nicht erfüllen. Es konnten keine eindeutigen Schlussfolgerungen zur Wirkung der Modulation des apelinergen Systems auf die Tumorzelltransplantation gezogen werden.

Insgesamt haben die Ergebnisse dieser Arbeit gezeigt, dass das apelinerge System das Potential hat, die Tumervaskularisierung unabhängig von einer antiangiogenen Therapie zu beeinflussen. Das experimentelle *in vivo* Modell mit AAVs hat den Vorteil, dass es auf das Lungenendothel abzielt und daher relativ spezifisch für Lungenmetastasen ist. Weitere Studien sollten sich auf die Optimierung des Lungenmetastasenmodells konzentrieren, um eine bessere experimentelle Reproduzierbarkeit zu ermöglichen.

## 1. INTRODUCTION

### 1.1 Physiological angiogenesis, molecular basis and mechanisms

To be able to survive and maintain themselves, cells need stable oxygen and nutrients supply. More complex organisms have blood vessels that nurture organs, fulfilling these tasks. In vertebrates, formation of blood vessels is accomplished by two complex physiological processes: vasculogenesis and angiogenesis.

#### 1.1.1 Factors affecting angiogenesis

While vasculogenesis represents *de novo* formation of blood vessels from endothelial cell progenitors, angiogenesis is primarily a process in which the new blood vessels arise from the pre-existing ones<sup>1-3</sup>. As a result of wide interactions between a variety of cells and molecules, this process starts early, during embryo development and continues in adulthood, occurring in several physiological processes, such as wound healing, organ development or regularly in the female genital system (ovulation)<sup>4</sup>. Angiogenesis can be positively and negatively regulated. Due to complex chemical signaling, blood vessels can be expanded, repaired or disrupted<sup>5</sup>. The balance between stimulating and inhibiting chemical signaling is critical for homeostasis. Some of the most important signaling molecules involved in angiogenesis are summarized in Table 1.

As a result of active angiogenesis, newly formed blood vessels contain two entities:

- Endothelial cells (ECs), the main building blocks of the endothelium, which are able to migrate and proliferate, allowing the formation of the structures called tubules<sup>6</sup>. Their function is not limited to providing a physical barrier to the surrounding environment, since ECs secrete a myriad of growth factors. This allows them to create a specific vascular niche in order to support the differentiation of progenitor cells<sup>7</sup>.
- Mural cells, such as pericytes and myofibroblasts, capable of lining up around and stabilizing the endothelium<sup>8</sup>. These cells communicate with endothelial cells via a panoply of different angiogenic molecules.

**Table 1. Mediators involved in angiogenesis**

<b>Mediator role</b>	<b>Member</b>	<b>Function</b>
Stimulatory	Vascular Endothelial Growth Factor (VEGF) Family (VEGF-A, VEGF-B, VEGF-C, VEGF-D, VEGF-E, and Placental Growth Factor (PlGF))	Group of essential cytokines that act as endothelium-specific mitogens, promoting differentiation of progenitor cells, proliferation, migration and vascular permeability <sup>9-11</sup> . VEGF-A is expressed in all developing organs, stimulating the survival and growth of the blood vessels in a paracrine fashion. Hypoxia is considered to be the main driving force for increased mRNA transcription of these factors <sup>10</sup> .
	Proteinase Families (Plasminogen activators, matrix metalloproteinases, heparanes, etc.)	Proteolytic degradation (allowing the migration of ECs), release of matrix-bound angiogenic activators, proteolytic activation of angiogenic chemokines <sup>12-14</sup> .
	Integrins (avb3, avb5)	Positive regulation of the angiogenic switch, migration, and invasion <sup>15</sup> .
	Members of the Notch signaling pathway	Role in the initiation of differentiation or preserving undifferentiated state of cells <sup>16</sup> .
	Angiopoietins	Vessel growth and stabilization <sup>17</sup> .
	VE-Cadherin	Interaction with VEGFR2 <sup>10</sup> .
	Ephrins	Attenuation of proliferative signaling <sup>18</sup> .
	Transforming Growth Factor (TGF) (Bone morphogenic protein (BMP), activins)	Concentration-dependent stimulation and inhibition of EC proliferation <sup>19</sup> .
	Platelet-Derived Growth Factor (PDGF-A to D)	Crucial role in stabilization of blood vessels through coverage with smooth muscle cells <sup>20</sup> .
	Fibroblast Growth Factor (FGF)	Crosstalk with VEGF family <sup>21</sup> .
	Chemokines	Recruitment of angiogenic leukocytes <sup>22</sup> .
	Coagulation factors (fibrin)	Triggering release of angiogenic factors <sup>20</sup> .
	Inhibitory	Platelet factor 4 (PF4), thrombospondins (TSP), angiostatin, type IV collagen



### 1.1.2 Mechanism of angiogenesis

Angiogenic activities in adults are not frequent since mature blood vessels are in the quiescent, an “off” state<sup>24</sup>. Angiogenesis gets triggered when the balance of proangiogenic and antiangiogenic molecules shifts toward the proangiogenic state<sup>25</sup>. Binding of angiogenic factors allows endothelial cells to proliferate and migrate toward the source of those factors, thus assembling into tubules that contain junctions specific for the endothelium (Figure 1).

First stage of angiogenesis starts with the formation of new vessel sprouts that contain leading cells, defined as “tip cells”. Tip cells do not proliferate in the presence of growth factors<sup>26</sup>. Their main function is to sense the surrounding environment by producing and extending their long, dynamic cytoplasmic projections, known as filopodia, which serve to direct the location of the future vascular bed. Filopodia of tip endothelial cells contain tyrosine kinase receptors, amongst all the Vascular Endothelial Growth Factor Receptor 2 (VEGFR-2). Certain authors claim that the selection of the tip cells is controlled by the Notch signaling pathway, because Notch family receptors and their ligands are influenced by the interaction of VEGF-A with endothelial cells<sup>27,28</sup>.

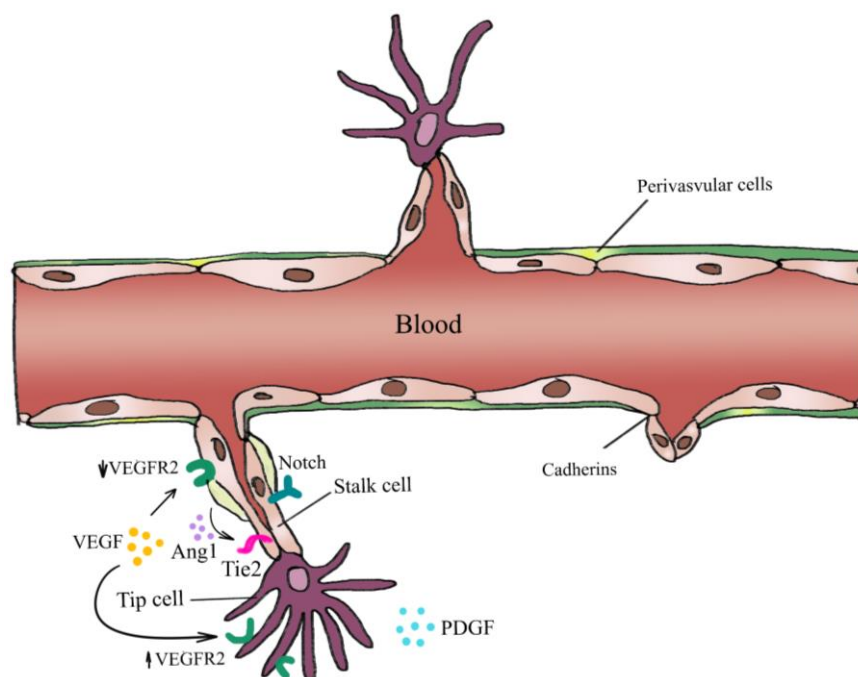


**Figure 1. Simplified mechanism of angiogenesis.** Tip cells are “exploring” the environment and directing the location of the future blood vessel. Stalk cells proliferate as a response to a variety of chemical signals. Mural cells are in close contact with the endothelial cells lining the capillaries, providing vascular stability.

## INTRODUCTION

---

The second stage is characterized by the proliferation of another subtype of endothelial cells, defined as “stalk cells”. Maintaining integrity of the forming sprout, stalk cells follow tip cells, produce fewer filopodia and respond directly to VEGF-A in terms of proliferation. Although tip and stalk cells differ in gene expression profile, many studies have still not been able to clearly define a specific marker for both endothelial cell subtypes<sup>29-31</sup>.

The third and final step in angiogenesis is vessel stabilization and it is orchestrated by interaction between endothelial and surrounding mural cells. Recruitment of mural cells is factor-dependent. Upon factor release from endothelial cells, mural cells tend to “sit” on top of the forming endothelium, thus allowing final enforcement of tight junctions to maintain the integrity and subsequent maturation of blood vessels<sup>32</sup>. Endothelial cells secrete platelet-derived growth factor, PDGF- $\beta$ , allowing mural cells to bond to the appropriate receptor on the membrane of pericytes, resulting in their proliferation and further recruitment. Similarly, pericytes express Angiopoietin-1 (Ang1), a factor that binds to the surface of endothelial cells via Tie2 receptor, fortifying the attachment of pericytes<sup>33</sup>. Such complexity of angiogenesis is a result of a team effort<sup>16,34,35</sup>.

According to several authors (studies and reviews), three ways to form blood vessels have been described so far (Figure 2)<sup>36-39</sup>:

1. Proliferation and migration into the extracellular matrix (sprouting angiogenesis), in which vascular endothelial cells divide as a response to proangiogenic factor stimulation (such as VEGF-A)<sup>40</sup>. Due to a cascade of stimulating signals, endothelial cells navigate toward the growth factor gradient and recruit pericytes to form the basement membrane. As the blood vessel continues to grow, smooth muscle cells are recruited to further stabilize the endothelium<sup>41,42</sup>.
2. Partitioning the vessel lumen by forming trans-capillary pillars (intussusceptive angiogenesis), which is, unlike sprouting angiogenesis, a much faster process, driven by mechanical stress or by a decrease of proangiogenic stimulation<sup>43,44</sup>.
3. Translocation of the blood vessels as a response to biomechanical forces (looping angiogenesis), where, due to the matrix contractility, blood vessels incorporate to form fully functional and perfused blood vessels<sup>38,45</sup>. In this process, contraction of the myofibroblasts allows successful incorporation of blood vessels. Finally, recruited blood vessels display all signs of maturity, compared to the existing ones<sup>38</sup>.

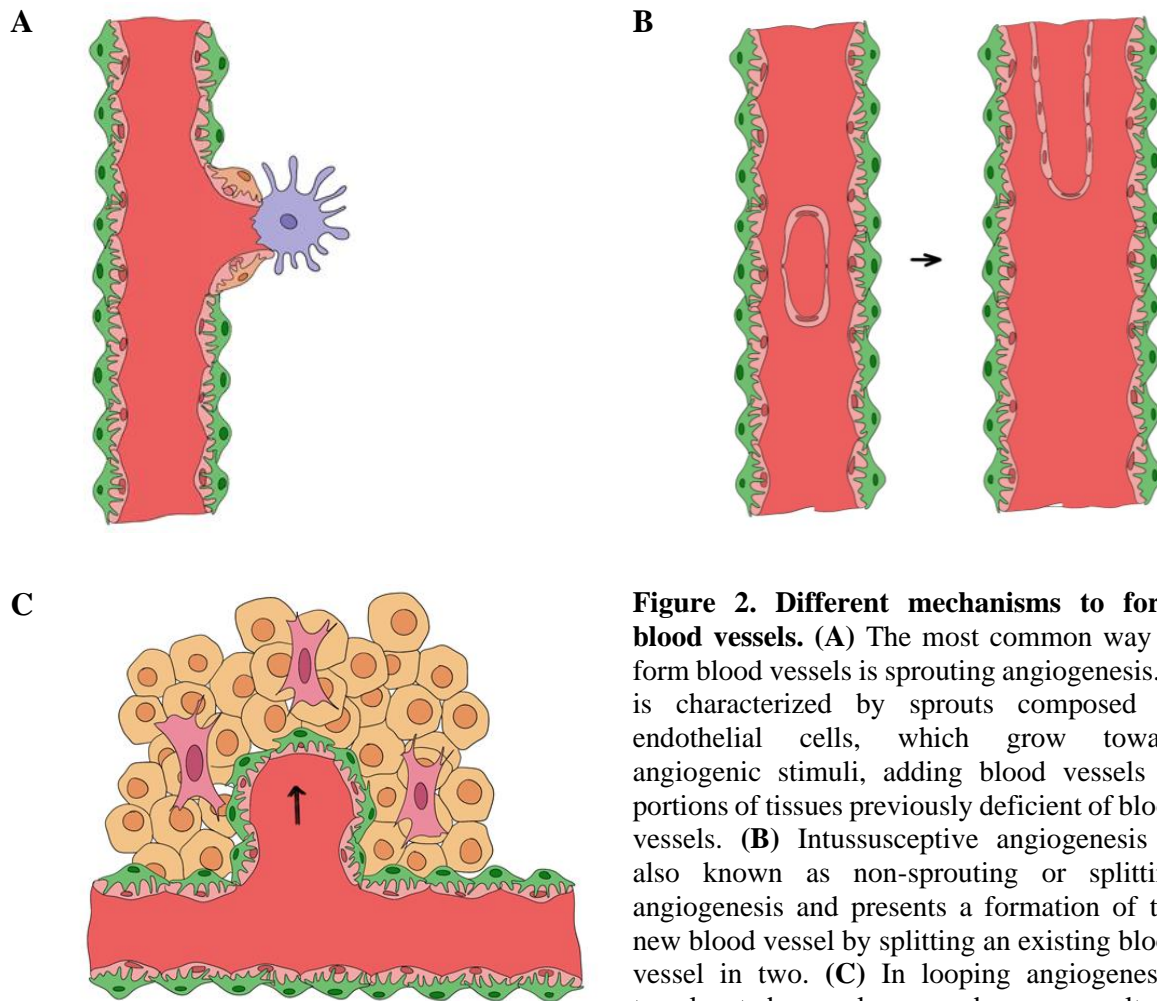


**Figure 2. Different mechanisms to form blood vessels.** (A) The most common way to form blood vessels is sprouting angiogenesis. It is characterized by sprouts composed of endothelial cells, which grow toward angiogenic stimuli, adding blood vessels to portions of tissues previously deficient of blood vessels. (B) Intussusceptive angiogenesis is also known as non-sprouting or splitting angiogenesis and presents a formation of the new blood vessel by splitting an existing blood vessel in two. (C) In looping angiogenesis, translocated vessels expand as a result of biomechanical forces.

## 1.2 Pathophysiological angiogenesis

### 1.2.1 Angiogenesis in solid tumors

During physiological embryogenesis and development, epithelial cells divide at a regular rate. In adulthood, these cells tend to multiply more scarcely. When a specific mutation occurs within these cells, they transform into tumor cells. As a result of their uncontrolled proliferation, tumors often extend to surface or protrude into lumen of the organ. These malignancies can be surgically removed if spotted on time. If not, the disturbed equilibrium between tumor cell proliferation and their apoptosis results in an increase in overall tumor size and mass.

## INTRODUCTION

---

In 1971, as a pioneer in the field of angiogenesis research, Dr. Folkman hypothesized that tumor growth is angiogenesis-dependent and that for every increase in tumor diameter, there must be a correspondent increase in tumor vascularization<sup>36</sup>. Therefore, angiogenesis is a crucial step in the progression of malignant tumors, allowing tumor growth and adaptation to hypoxic conditions<sup>46</sup>. Unlike healthy tissues, cancers always have angiogenesis switched on. As described by Weinberg and Hanahan, angiogenesis is one of the hallmarks of cancer, representing a pathophysiological process of creating new blood vessels from existing ones<sup>47</sup>. It has been extensively investigated in vascular tumors, since they are suitable for antiangiogenic treatment due to their extremely rich vascularization, compared to avascular tumors. Importantly, the process of tumor angiogenesis is regulated by proangiogenic and antiangiogenic factors produced from tumor cells as well as from surrounding cells of the tumor microenvironment<sup>48</sup>.

To be able to grow over a few millimeters in size as well as to function properly, fulfilling their own blood and oxygen supply, most tumors need to be well vascularized<sup>49</sup>. However, some of the inadequately oxygenated cancer cells tend to develop different ways to survive, shifting from highly aerobic to anaerobic metabolism<sup>50</sup>. In general, fast tumor growth often results in an oxygen delivery problem, subsequently driving the tumor cells to become hypoxic and to activate the hypoxia stress-response. Hypoxia triggers tumor neovascularization via plethora of different proangiogenic stimuli. Consequently, the existence of malformed permeable and leaky vessels, independent of normal blood vessels' hierarchy, leads to fluid buildup within the tumor microenvironment<sup>51</sup>.

Hypoxia is a key triggering power in tumor neovascularization, and it is carried out by the induction of hypoxia-induced factor 1 $\alpha$  (HIF-1 $\alpha$ )<sup>52</sup>. Under normal oxygen levels, hydroxylation of HIF-1 $\alpha$  is stimulating its own degradation, therefore keeping HIF-1 $\alpha$  levels low. This process is mediated by prolyl hydroxylases<sup>53</sup>. On the opposite, during hypoxia, HIF-1 $\alpha$  does not degrade, but instead accumulates within the cell and dimerizes with the constitutively expressed HIF-1 $\beta$ <sup>54</sup>. High expression of HIF complex further interacts with genes that encode for the VEGF family, FGF, IGF, integrins, MMPs, and proteins within the extracellular matrix<sup>55</sup>. Some of the other factors induced upon hypoxia include NF $\kappa$ B, JunB, Sp1, and Stat3<sup>56-59</sup>.

Several ways of tumor blood vessel formation have been described so far<sup>60</sup>. By mimicking chronic infection, tumors can recruit various tumor-stimulatory cells, utilizing them to release

proangiogenic factors<sup>61,62</sup>. Many tumor-associated cells can promote and maintain increased vascularization. Extensive research has been done on tumor-associated fibroblasts and macrophages. It has been proven that fibroblasts within the tumor can dramatically increase tumor angiogenesis and overall tumor growth<sup>63,64</sup>. Proven to secrete Stromal cell-derived factor-1 (SDF-1), these cells promote endothelial progenitor cell recruitment<sup>65</sup>. One of the persisting enigmas is population of tumor-associated macrophages, which are highly present in tumor tissue and whose complexity is being under investigation<sup>62</sup>. It is known that these cells specifically secrete matrix metalloproteinases that cleave VEGF from matrix sequestration, allowing it to act freely and to stimulate further vessel growth<sup>66</sup>.

During their development, tumor cells can hijack pre-existing blood vessels and transform them into tumor endothelium. Some of the solid tumor cells are very much alike endothelial cells, meaning that those tumors can use their own cells as building blocks in the newly formed endothelium<sup>67</sup>. Additionally, the majority of the endothelial progenitor cells are located in the bone marrow. Tumors can recruit those cells and stimulate their differentiation into functional endothelial cells<sup>68</sup>.

### 1.2.2 Angiogenesis in acute myeloid leukemia

Acute myeloid leukemia (AML) is a cancer of the hematopoietic system, which originates when mutation of the myeloid stem and progenitor cells within the bone marrow occurs. AML cells have a high tendency to proliferate and accumulate, leading to their domination in the hematopoietic bone marrow niche, therefore reducing the chance of patient survival<sup>69</sup>. Most AML studies are focused primarily on investigating the properties of leukemic cells. However, as reviewed by Behrmann *et al.*, the importance of the bone marrow microenvironment in pathophysiology has cast new light on the treatment of AML<sup>70</sup>.

Back in 1997, Fiedler *et al.* were first to find that AML cells have a role in exploiting angiogenic signaling in order to sustain their own survival and proliferation<sup>71</sup>. AML cells can originate from various progenitor cells. There are reports indicating that these cells have properties of leukemic hemangioblasts, meaning that they can proliferate into both malignant blasts and endothelial cells<sup>72,73</sup>.

Increased angiogenesis occurs in a high percentage of AML patients<sup>74</sup>. These patients have significantly increased microvessel density in the bone marrow, which is an important

component in providing oxygen and nutrients to the malignant cells and presents a negative prognostic factor<sup>74,75</sup>.

### 1.2.3 Contribution of the immune system to tumor angiogenesis

Due to the complexity of the immune system, its effect on angiogenesis cannot be simply controlled by one of the signaling pathways, but rather by controlling heterogeneous groups of signaling pathways. Myeloid cells, such as monocytes and macrophages, have an important role in angiogenic processes.

Precursors of these cells are located in the bone marrow. After their maturation, monocytes are distributed into the bloodstream and further migrate toward tissues, where they finally differentiate into resident tissue macrophages. Monocytes and macrophages have very distinct functions that highly depend on the environment where the cells are located<sup>76,77</sup>. Although a clear line between different phenotypes of macrophages cannot be drawn due to their complexity<sup>78</sup>, macrophages are often classified into two major groups:

- Proinflammatory macrophages (M<sub>1</sub>), a group of classically-activated macrophages, which have an important protective role and their presence in tumors often indicates a good prognosis<sup>79,80</sup>.
- Alternatively-activated macrophages (M<sub>2</sub>), which have an antiinflammatory and proangiogenic role in tumors. There are claims that antiinflammatory agents do not abrogate M<sub>1</sub> macrophage functions, but rather provide the alternative activation toward M<sub>2</sub> macrophages<sup>80,81</sup>.

In recent studies, there have been claims that macrophages, found in tumor periphery, modulate tumor growth as a response to the signaling from the tumor microenvironment. It was found that these macrophages display M<sub>2</sub> phenotype<sup>82</sup>. Tumors contain a large portion of M<sub>2</sub> macrophages, called tumor-associated macrophages (TAM). Their specific phenotype is being maintained by receiving signals from tumor cells<sup>83-85</sup>. Therefore, deciphering their definitive role and targeting TAMs can be of great significance in impairing tumor growth. In their review, Schmid and Varner discuss the most important roles of myeloid cells in tumor angiogenesis<sup>86</sup>.

Increase in TAM content within tumor tissue is claimed to be due to the recruitment of circulating monocytes by tumors, rather than from increase of tissue resident macrophages<sup>87</sup>. Strong evidence that TAMs regulate neovascularization exists, since TAM infiltration is known to correlate to microvascular density in several tumors types<sup>88-90</sup>. Additionally, certain authors indicate that TAM tumor infiltration might present a poor prognosis factor in some highly vascular cancers<sup>88,90</sup>. It has been proven that TAMs release various chemotactic factors, which can have a direct impact on tumor cells, affecting their migration, and therefore contributing to tumor invasion and metastasis<sup>91</sup>. Apart from monocytes and macrophages, other cells from myeloid lineage, such as MMP9- and VEGF-expressing myeloid cells, have the potential to promote tumor angiogenesis<sup>92</sup>.



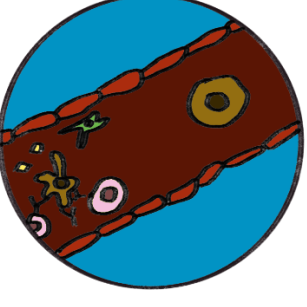
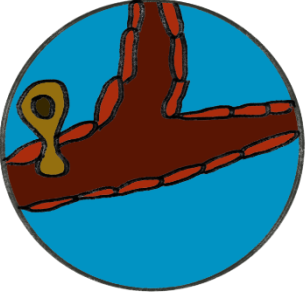

### 1.3 Metastatic odyssey

It is thought that, apart from brain, lung, liver and pancreas, primary cancers seldom cause death. The main reason for high cancer mortality is associated with a late step in tumor progression, termed metastasis<sup>93</sup>. By triggering metastasis, tumor cells transfer from place of origin to colonize distant parts of the body, such as lung, liver, brain and bone marrow. Fortunately, this is a highly inefficient process, because very few cells manage to survive throughout their journey<sup>94</sup>. Although the routes of metastasis can vary depending on cancer type, a cascade of sequential events is similar for most of the cancers (Table 2)<sup>95</sup>.

Immune-system-mediated angiogenesis has a high impact on metastasis. In their study, Ghouse *et al.* suggest that angiogenic switch in the mouse lungs prior to metastatic onset is influenced by myeloid cell lineage<sup>96</sup>. It has been proven that angiogenesis regulates premetastatic niche and that inhibiting this process might be beneficial to reduce or prevent metastasis. Those findings are also important for this Ph.D. thesis, since metastasis is investigated in conditions of stimulation and inhibition of angiogenesis.

Table 2. Metastatic cascade

---

	<p><b>1. Angiogenesis</b></p> <p>As a first step of metastasis, tumors develop a rich vascular network<sup>97</sup>. Newly formed vessels do not just nourish tumors, but also provide an efficient escape route. That way, tumor cells enter the circulation. Density of the vascular network within the tumor can be used as a prognostic marker for metastasis<sup>98</sup>.</p>
	<p><b>2. Intravasation</b></p> <p>Tumor cells usually have the strongest bonds with cells of their own kind. After epithelial to mesenchymal transition, they detach from the neighboring cells and migrate through the basement membrane of endothelium, entering the bloodstream<sup>99</sup>. Endothelia that are leakier can increase chances for the migration of tumor cells.</p>
	<p><b>3. Survival in circulation</b></p> <p>Being in circulation, tumor cells face unfavorable conditions. High number of cells die within a short time, destroyed mostly by the cells of the immune system (natural killer cells)<sup>100</sup>. Active immune surveillance is a vital protective mechanism against metastasis. Yet, some cells, such as platelets, play a role in protection of tumor cells<sup>101</sup>.</p>
	<p><b>4. Extravasation</b></p> <p>Tumor cells often find a way out of the vessels simply by migration through tight junctions between endothelial cells. Another possible mechanism includes diapedesis, a transcellular migration, which is typical for certain immune cells<sup>102</sup>.</p>
	<p><b>5. Secondary tumor formation</b></p> <p>After extravasation, the destiny of the tumor cell is not sealed – tumor cells can also get apoptotic or be eliminated by the immune cells. In some extreme cases, they remain dormant and further activate when the conditions become optimal<sup>103</sup>. Upon successful metastasis, tumors can migrate to secondary sites. This is considered as very poor prognostic factor for most of the patients with metastatic onset<sup>104</sup>.</p>

---



## 1.4 Angiogenesis inhibition

Cancer is as old as humankind and until this day, it remains to be a complex disease with no effective cure. For many years, clinicians have been using conventional chemotherapy as the only way to destroy rapidly dividing cancer cells. This approach, however, has limited efficacy due to the existence of the cancer hallmarks<sup>47</sup>. For example, during treatment, circulating tumor cells (CTCs) remain in lower division rates than “normal” tumor cells, and therefore do not respond to conventional therapy<sup>105</sup>. By existing in circulation, they tend to repopulate the tumor as soon as the treatment stops. Some types of tumors are intrinsically very aggressive and, therefore, resistant to conventional therapy<sup>106</sup>. Those tumors often migrate from the primary spot and populate distant parts of the body – they tend to metastasize.

Following past decades, a broad spectrum of targeted therapies has emerged, in which tumor cells are being harmed, keeping the normal cells intact. One of the indirect approaches includes antiangiogenic therapy. Tumor endothelium in aggressive types of cancer is presented by fast-growing vessels marked with unique structures<sup>107</sup>. Such blood vessel profile and its contribution to overall tumor growth highlight the antiangiogenic approach as a desirable adjunct to the existing cancer therapy or even suggests that treatment as a single therapeutic approach<sup>108-110</sup>.

### 1.4.1 Therapeutic opportunities

Folkman proposed the use of antiangiogenic agents for decreasing tumor blood vessels, and consequently, tumor shrinking<sup>36</sup>. Following that concept, it can be assumed that blocking tumor angiogenesis will lead to almost complete eradication of tumor blood vessels. Some of the promising approaches include prostate, colon, ovary, lung, breast cancers, as well as hepatocellular carcinoma<sup>111-116</sup>. However, until now, most of the therapeutic assessments have been a disappointment, demonstrating the failure of therapy<sup>117-119</sup>. Unfortunately, in most cases, blocking angiogenesis finally leads to even more aggressive growth of the tumor. Furthermore, due to tumor aggressiveness and the presence of leaky abnormal blood vessels, metastases often occur in patients treated with such therapy<sup>120</sup>. The complexity of compensatory proangiogenic pathways has been an insurmountable obstacle in cancer therapy by now.

It is known that all negative consequences occur since tumors simply become resistant to the therapy. Development of different signaling pathways to maintain oxygen and nutrients supply

leads to neoangiogenesis onset<sup>117,121</sup>. Deciphering the factors included in this process and improving the benefits of the therapy is one of the central starting points in fighting cancer. Therefore, identification and effective targeting of druggable pathways that are interconnected with pathophysiological angiogenesis are crucial.

Being a chaotic process characterized by leaky and partly formed, dilated vasculature, targeting angiogenesis can be accessed in two ways. The promising way to tackle cancer is by specifically destroying endothelial cells to prune blood vessels. On the other hand, normalization of the blood vessels could efficiently reduce metastatic potential, improve tumor vascularization, allowing efficient delivery of the chemotherapeutic drugs into the tumor<sup>122</sup>. That can be done by inhibiting the sprouting process and triggering the maturation by different mechanisms<sup>123</sup>. Some of the antiangiogenic therapeutic approaches are presented in Table 3.

The antiangiogenic approach is also effective in the treatment of hematologic malignancies, however, according to Dong *et al.*, it does not seem to be as effective as a single therapy<sup>124</sup>. Therefore, approaches that include a combination of existing cytotoxic chemotherapy with antiangiogenic drugs are being extensively investigated<sup>125</sup>.

**Table 3. Antiangiogenic therapeutical approaches**

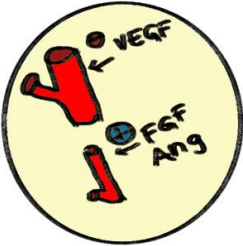
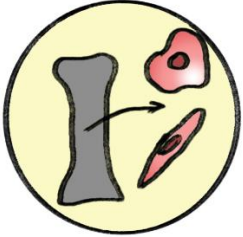
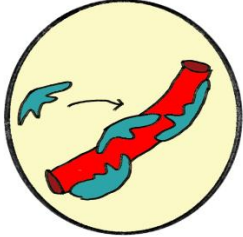
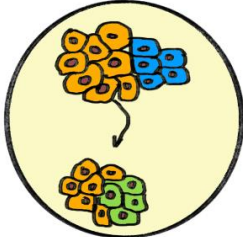
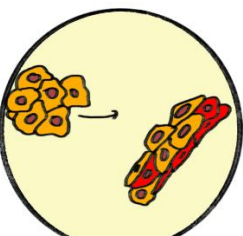
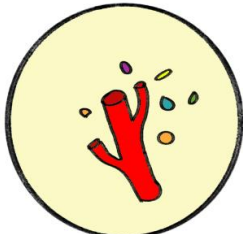
<b>Drug group</b>	<b>Examples</b>	<b>Mechanism of action</b>	<b>Approved for treatment</b>	<b>Notes</b>
Monoclonal antibodies directed against the VEGF Family	Bevacizumab, Ramucirumab	<ul style="list-style-type: none"> <li>• Bevacizumab contains human framework regions with antigen-binding regions of a humanized murine antibody that binds to VEGF</li> <li>• Ramucirumab binds to VEGF receptor 2 (VEGFR2) and prevents binding of its ligands</li> </ul>	<ul style="list-style-type: none"> <li>• Metastatic colon cancer<sup>126</sup></li> <li>• Metastatic breast cancer<sup>127</sup></li> <li>• Cell renal cell carcinoma in combination with interferon-<math>\alpha</math> (IFN<math>\alpha</math>)<sup>128</sup></li> <li>• Non-small cell lung carcinoma in combination with paclitaxel-carboplatin<sup>129</sup></li> </ul>	<ul style="list-style-type: none"> <li>• Bevacizumab was withdrawn for the treatment of metastatic breast cancer, as it failed to improve overall patient survival<sup>130</sup></li> <li>• Resistance to therapy develops rapidly, mainly driven by the activation of alternative proangiogenic signaling pathways<sup>131,132</sup></li> <li>• Phase III study for ramucirumab failed to hit its primary endpoint on progression-free survival among women with metastatic breast cancer<sup>133</sup></li> </ul>
Tyrosine kinase inhibitors (TKIs)	Sunitinib, Sorafenib	<ul style="list-style-type: none"> <li>• TKIs simultaneously target several proangiogenic signaling pathways<sup>134</sup></li> <li>• Binding to the ATP-binding pocket of the tyrosine kinase receptors<sup>134</sup></li> </ul>	<ul style="list-style-type: none"> <li>• Metastatic renal cell carcinoma patients<sup>135,136</sup></li> <li>• Metastatic neuroendocrine pancreatic cancer<sup>137</sup></li> <li>• Treatment of advanced hepatocellular carcinomas and metastatic renal cell carcinomas<sup>138</sup></li> </ul>	<ul style="list-style-type: none"> <li>• Relatively toxic, not to be used in a combination<sup>135,136</sup></li> </ul>

### 1.4.2 Mechanisms of resistance to antiangiogenic therapy

Back in 1971, Folkman emphasized that the mechanism, by which tumor affects neovascularization, needs to be well understood before any therapeutic option can be created<sup>36</sup>. It has been shown that, during antiangiogenic therapy, tumor blood perfusion is being reduced, and therefore tumors are unable to sustain a stable oxygen and nutrients supply<sup>48</sup>. That would logically lead to tumor hypoxia and weaken chemotherapy. However, as previously mentioned, recently published data suggest another antitumor concept of transient tumor vasculature normalization, allowing stable delivery of antitumor drugs<sup>139</sup>.

One way or another, antiangiogenic therapy results with increased progression-free survival. However, when the tumor enters hypoxia due to antiangiogenic therapy, the effects are usually only transient and no complete tumor regression is achieved since resistance to antiangiogenic therapy occurs. As a result, there is only a limited effect on overall survival. As reviewed by Bergers *et al.*, in some cancers, such as in hypovascularized pancreatic ductal adenocarcinoma, there is an immediate refractory to the treatment without even a transient benefit of the therapy<sup>131</sup>. Several mechanisms of resistance to antiangiogenic therapy have been described so far (Table 4)<sup>60,131</sup>.

**Table 4. The hallmarks of resistance to antiangiogenic therapy**

	<p><b>Activation of alternative proangiogenic signaling pathways</b></p> <p>Besides VEGF-A, certain cancers rely on additional factors that promote angiogenesis. Treatment of the mice with antibody targeting VEGFR2, led to overexpression of various proangiogenic factors, such as FGF1, FGF2, ephrins and angiopoietins. These factors induced neovascularization<sup>140</sup>. In humans, FGF2 expression increases in glioblastoma patients treated with VEGFR TKI<sup>141</sup>.</p>
	<p><b>Recruitment of bone marrow-derived cells</b></p> <p>Cells originated in bone marrow, such as monocytes, T-helper cells, granulocytes, and fibrocyte-like cells are able to mediate intrinsic resistance through the secretion of VEGF-A-independent proangiogenic factors, including FGF2 and Bv8<sup>132,142-144</sup>.</p>
	<p><b>Increased pericyte coverage and vessel maturation</b></p> <p>During pathophysiological angiogenesis, vessels are incompletely covered with pericytes. If the VEGF signaling pathway is blocked, tumor vessels tend to attract pericytes in order to achieve better coverage. These vessels are less sensitive to angiogenesis inhibitors<sup>145,146</sup>. One of the alternative ways to increase vessel pruning is targeting the pericytes<sup>145</sup>.</p>
	<p><b>Increased invasiveness</b></p> <p>Generated by antiangiogenic treatment, hypoxia and formation of nutrient-deprived environment will lead to increased tumor cell invasion through various mechanisms<sup>147</sup>. As an example, TKIs will reduce primary tumor growth, but accelerate the onset of multi-organ metastasis, affecting almost every step of the metastatic cascade<sup>148-150</sup>.</p>
	<p><b>Vascular mimicry and vessel co-option</b></p> <p>Tumor cells can grow along the existing vasculature and this process is often not sensitive to angiogenic inhibitors<sup>151</sup>. When endangered by hypoxia, tumor cells dedifferentiate and gain endothelial cell phenotype to form vascular-like structures<sup>152</sup>. This phenomenon has been described in various tumors<sup>153-155</sup>.</p>
	<p><b>Metabolic adaptation</b></p> <p>One of the newly described mechanisms. As a result of antiangiogenic treatment, induced hypoxia triggers HIF-1<math>\alpha</math> to affect metabolic reprogramming. Treatment with bevacizumab and TKIs can result in modulating glycolysis and metabolism of lipids in tumors<sup>156,157</sup>.</p>

### 1.5 Apelinergic system

Apelin and its cognate receptor, APJ (APLNR), are two major components of the apelinergic system and are co-expressed in a variety of peripheral tissues<sup>158,159</sup>. Their possible involvement in physiological and pathophysiological processes has intrigued scientists over the past three decades, leading to an increased number of articles published every year.

Apelinergic system was recently discovered: in 1993, a receptor for Apelin was found and five years later, its ligand, Apelin, was isolated from bovine stomach homogenates<sup>158,159</sup>. Results of several studies indicate that, during embryogenic development, APJ expression is predominantly restricted to endothelial and endothelial progenitor cells of blood vessels<sup>160-162</sup>. Additionally, there are reports that apelinergic system is highly expressed in endothelial cells of adult blood vessels<sup>163-165</sup>. Accordingly, the apelinergic system plays a regulatory role in various physiological functions, such as increasing heart contraction, vasodilation, modulation of glucose and insulin homeostasis, cardiovascular development. Some of those functions are summarized in Table 5.

On the other hand, Shin *et al.* describe a link between activation of the apelinergic system and several pathological conditions such as chronic heart failure, diabetes, obesity, cancer and other conditions<sup>166</sup>. Additionally, authors emphasize the potential of the apelinergic system for therapeutic targeting. In general, Apelin/APJ is a multifaceted system whose complexity arises from the presence of multiple ligand isoforms and a variety of intracellular signaling cascades that can be triggered.

**Table 5. Physiological significance of apelinergic system**

Physiological process	Role of apelinergic system
Processes related to cardiovascular system	<ul style="list-style-type: none"> <li>• Potent inotropic effect, increasing myocardial contraction and reducing the cardiac load<sup>167,168</sup></li> <li>• Cardioprotective effects, inhibiting apoptosis of glucose-deprived cultured cardiomyocytes<sup>169</sup></li> </ul>
Energy metabolism	<ul style="list-style-type: none"> <li>• Widely expressed in adipose tissue, role as adipokine<sup>170</sup>; high Apelin blood and plasma level correlate with obesity<sup>170,171</sup></li> <li>• Co-regulatory role with insulin in providing negative feedback for insulin production<sup>172</sup>; an increase in pancreatic islet cell mass<sup>173</sup></li> </ul>
Fluid homeostasis	<ul style="list-style-type: none"> <li>• Apelin opposes antidiuretic effect of vasopressin and decreases vasopressin expression<sup>174</sup>; another independent study shows conflicting data, suggesting the antidiuretic effect of Apelin<sup>175</sup></li> </ul>
Angiogenesis	<ul style="list-style-type: none"> <li>• Angiogenic factor, mitogen of endothelial cells<sup>176</sup></li> <li>• Essential for the normal development of frog heart and murine vasculature<sup>160,177</sup></li> <li>• Involvement in hypoxia-induced retinal angiogenesis<sup>178</sup></li> </ul>
Additional roles	<ul style="list-style-type: none"> <li>• Possible role in the regulation of hormone and gastric acid secretion in rats<sup>179-181</sup></li> <li>• Proposed involvement in the reduction of cytokine production in mouse spleen cells<sup>182,183</sup></li> <li>• APJ is a co-receptor of HIV entry into target cells, whereas Apelin blocks this process<sup>184,185</sup></li> <li>• Neuroprotective role in the hippocampal neurons<sup>186</sup></li> <li>• Increase in proliferation and survival in osteoblasts<sup>187,188</sup></li> </ul>

### 1.6 Apelin receptor

Apelin receptor, termed APJ (APLNR), belongs to the family of G protein-coupled receptors (GPCRs). G-protein-coupled receptors can be activated by a variety of different molecules, such as peptides, hormones or even ions. This receptor family is comprised of seven membrane-spanning domains and it is highly evolutionary conserved in the mammalian genome<sup>189</sup>. APJ shares this conventional GPCR structure, having N-terminal glycosylation, which is important for receptor expression and binding of ligands<sup>190</sup>. Structural studies have shown that both C- and N-terminals of APJ are required for internalization<sup>191,192</sup>.

APJ was first discovered as constitutively active orphan GPCR, until deorphanized, when its cognate ligand was extracted from the bovine stomach<sup>159</sup>. This receptor shares a very close structure to the angiotensin II (Ang II) receptor type AT<sub>1A</sub><sup>158</sup>. The human APJ gene is intronless and encodes for 377 amino acids, which constitute an intact receptor. Although it shares 31% sequence identity at the protein level with the angiotensin II receptor, it does not bind angiotensin II. Sequence homology between different mammalian Apelin receptors is high: humans and mice share 92% of their amino acid sequences. That homology goes even higher (96%) in the case of mouse and rat APJ<sup>193,194</sup>. On the other hand, in various species, such as rhesus macaque, cow or non-mammalian species (African clawed frog or zebrafish), that homology is lower than 50%<sup>195</sup>.

#### 1.6.1 Distribution and regulation of APJ expression

Until now, there is no complete data on the regulation of APJ gene expression. Studies in rats suggest that the promoter for APJ is regulated by Specificity protein 1 (Sp1), estrogen receptor, glucocorticoid receptor and others. Some authors consider Sp1 as a major regulator of APJ promoter activity<sup>196</sup>. APJ is susceptible to various single-nucleotide polymorphisms (SNPs), which can further result in higher susceptibility to brain infarction, heart failure, cardiomyopathy and hypertension<sup>197-199</sup>.

Many controversies arise when it comes to APJ expression regulation. O'Carroll *et al.* emphasize that APJ is most likely regulated in response to different stress factors<sup>200,201</sup>. Certain authors also claim that ligand of APJ, Apelin, is involved in APJ regulation within the gastrointestinal tract<sup>180</sup>. Since the apelinergic system is quite active in adipose tissue, some authors claim that insulin has a major role in the expression of APJ<sup>202</sup>.



APJ is broadly expressed in humans, rats, and mice<sup>203,204</sup>. In humans, the earliest known studies indicate that Apelin receptor (protein and mRNA) is widely distributed within certain central nervous system structures, such as the hippocampus, substantia nigra, medulla and spinal cord<sup>184,204,205</sup>. However, the functional role of APJ within these structures is still not fully known. Recent findings demonstrated APJ mRNA presence within bone marrow stromal cells<sup>206</sup>. Edinger *et al.* showed that APJ transcripts exist in spleen, intestine, colon and ovary<sup>184</sup>. That was confirmed by another study, reporting the strongest expression in the spleen<sup>204</sup>. Within these organ systems, APJ has a predominantly vascular location<sup>207</sup>. By immunohistochemical analysis, Kleinz *et al.* have discovered high expression of APJ in cardiac tissue, especially in cardiomyocytes, smooth muscle cells and endothelial cells<sup>208</sup>. Since it is expressed in endothelial cells, APJ can regulate the development of blood vessels synergistically with VEGF<sup>209</sup>.

Several studies have shown that mouse and rat APJ is significantly expressed throughout different brain regions, especially in the cerebellum, hypothalamus, hippocampus and olfactory bulb<sup>204,210,211</sup>. For both species, quantitative PCR revealed high levels of APJ in lung and heart tissue<sup>204,212</sup>. Pope *et al.* reported high levels of APJ binding sites in the anterior pituitary gland of the mouse<sup>203</sup>. However, conflicting findings of APJ mRNA expression in the rat pituitary gland have been described<sup>194,203,210</sup>. In their review, O'Carroll *et al.* describe APJ expression in more details<sup>201</sup>.

### 1.6.2 APJ signaling

In their review, Chapman *et al.* explain a portion of the many physiological effects that occur as a response to APJ activation and downstream signaling<sup>213</sup>. The canonical signaling pathway starts when APJ couples with G $\alpha$  subunit of G protein<sup>212,214</sup>. There are more G $\alpha$  subfamilies (G $\alpha$ i/o, G $\alpha$ q/11) APJ can couple with and binding to each of them is associated with a certain cellular effect<sup>167,215,216</sup>. It is known that the signaling mechanisms can vary from basic GPCR signaling to complex ones, which include heterodimerization with other GPCRs<sup>217</sup>. Several non-canonical pathways are still poorly understood and they might be involved in the phenomenon known as “biased agonism” or “functional selectivity”<sup>216</sup>. Chapman *et al.* describe that APJ signaling is heterologous, since the receptor shows affinity toward multiple G-proteins, therefore mediating different functional effects in different cell types<sup>213</sup>. The same authors claim that different isoforms of APJ ligands are able to exhibit qualitatively different physiological effect on cell, indicating potential ligand-specific variability in signaling.

Although it does not bind angiotensin II, it has been shown that APJ can dimerize with Ang II AT<sub>1A</sub> receptor and modify the affinity of angiotensin II for its receptor, thereby modulating angiotensin-converting enzyme 2 (ACE2) activity<sup>218-220</sup>. By dimerizing with other receptors, such as  $\kappa$ -opioid receptor (KOR) or neurotensin 1 receptor, apelinergic system can display synergistic effects<sup>217,221</sup>.

### 1.7 Apelin

APJ had been considered as an orphan receptor until the endogenous ligand of the apelinergic system was discovered back in 1998<sup>159</sup>. This ligand was later named Apelin – **APJ** endogenous binding **ligand**.

The gene which encodes for human Apelin (APLN) is found on chromosome Xq25–26.1 and has one intron within its open-reading frame<sup>201</sup>. Apelin genes for rat and mouse are located at chromosomal regions Xq35 and XA3.2, respectively. It is known that human Apelin cDNA encodes for 77-amino acid propeptide named preproapelin<sup>159</sup>. This molecule contains a hydrophobic-rich N-terminal region, which may have a role as a secretory signal sequence and in trafficking<sup>222</sup>. Apelin is highly conserved in vertebrates: humans and rat Apelin share 82% of sequence homology, with C-terminus having the highest level of conservation<sup>159,223</sup>. That terminus contains variable cleavage sites, suggesting the existence of different protein isoforms<sup>182</sup>.

Until now, the exact mechanism by which preproapelin is processed has not been fully understood and it has been thought to be affected by different cleavage sites in the C-terminus region<sup>224</sup>. Cleavage of preproapelin results mainly in proapelin formation, whose further cleavage requires the presence of several enzymes. Some known enzymes included in this process are angiotensin-converting enzyme 2 (ACE2) and pre-protein convertase subtilisin/kexin 3<sup>225-227</sup>. Certain authors emphasize the role of ACE2 in the regulation of Apelin peptide activity through additional cleavage<sup>228</sup>. There are several mature forms of Apelin, and their affinity to APJ depends on binding kinetics and receptor internalization<sup>229</sup>. For example, stimulation with mature form, Apelin-36, results in the receptor internalization and intracellular sequestration. On the other hand, Apelin-13 is able to cause internalization and recycling APJ back to the cell membrane<sup>229</sup>. The existence of different Apelin isoforms was predicted by structural analysis of the C-terminal end of preproapelin (Figure 3). That region of the molecule contains arginine and lysine residues and acts as a potential site for proteolytic cleavage<sup>230</sup>.

The potencies of different Apelin isoforms seem to correlate according to their size: APLN-13 > APLN-17 > APLN-36 > APLN-55<sup>231</sup>. In some cases, Apelin-13 cyclizes glutamine at its N-terminal to form pyroglutamated Apelin, [Pyr1]Apelin-13<sup>232</sup>. Certain studies indicate that [Pyr1]Apelin-13 is the most potent form of Apelin, however, other authors suggest equal potency between Apelin-13 and [Pyr1]Apelin-13<sup>233,234</sup>.

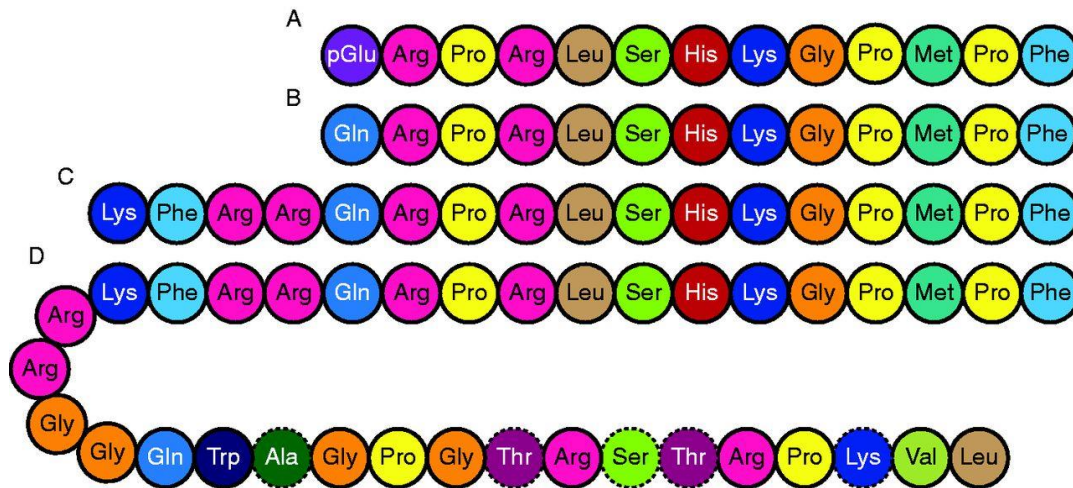


**Figure 3. Amino acid sequence of mature Apelin isoforms.** Amino acid sequences of (A) (Pyr1)Apelin-13, (B) Apelin-13, (C) Apelin-17 and (D) Apelin-36. Black circled residues are identical between human, bovine, rat and mouse. Adapted from O'Carroll *et al.*<sup>201</sup>

### 1.7.1 Distribution and regulation of Apelin expression

Similar to its putative receptor, regulation of Apelin gene expression is affected by different transcription factors. Activation of the transcription factors is mediated by several effectors. Hata *et al.* emphasize a possible role of Sp1 in the regulation of Apelin expression<sup>197</sup>. Furthermore, it has been reported that Apelin is secreted by adipocytes<sup>235</sup>. The secretion is influenced by tumor necrosis factor- $\alpha$  (TNF $\alpha$ ), a factor that induces Apelin gene expression in these cells<sup>235</sup>. Additionally, Jak/Stat pathway has been involved in the upregulation of murine Apelin<sup>236,237</sup>.

In humans, likewise its putative receptor, Apelin is widely distributed in central nervous system and peripheral tissues. The highest level of preproapelin transcripts can be found in the hippocampus and hypothalamus<sup>223</sup>. Certain authors observed strong Apelin mRNA expression in placenta, heart, lung and kidney<sup>204</sup>. Additionally, endothelial cells of large blood vessels, such as a of coronary artery, blood vessels of the kidney or endothelial cells of the atria and ventricles, have strong levels of Apelin expression<sup>238</sup>.

On the other hand, hypoxia seems to be the main inducer of Apelin expression<sup>160</sup>. Hypoxia responsive elements are present in the Apelin gene promoter and it has been shown that they influence regulation of the Apelin expression in cardiac myocytes<sup>239</sup>. Additionally, Apelin expression in adipocytes is regulated by the presence of HIF-1 $\alpha$ <sup>240</sup>.

### 1.7.2 Analogs of Apelin

#### *APELA*

Gene encoding a peptide that acts as an endogenous ligand for APJ was recently discovered<sup>241,242</sup>. This peptide has few names, some of which have humorous connotation: **Apelin Receptor Early Endogenous Ligand (Apela), Epiboly Late Because of Endoderm Late (Elabela) or simply Toddler<sup>241,243</sup>. Apela propeptide is not derived from preproapelin, but was rather predicted to consist of 54 amino acids, with mature peptide containing 32 amino acids<sup>244</sup>. It is interesting that the loss of this gene results in undeveloped heart in fish embryos, which is an effect similar to those of Apelin receptor gene loss<sup>244</sup>. Additionally, Yang *et al.* demonstrated the prevalent existence of Apela mRNA and peptide in adult human cardiovascular tissue, as well as in human blood vessels<sup>244</sup>. Although still not fully characterized, there has been some evidence that Apela plays an important role in a series of developmental signals<sup>241,243</sup>.**

#### *Salcut-NH<sub>2</sub>*

**Selective APL-36 Cutting and Amidation peptide (SCNH2) or Salcut-NH<sub>2</sub>, is a growth factor that is generated by the enzymatic processing of Apelin-36, and it presents the amide-derived form of Apelin-36<sup>245</sup>. This peptide was firstly discovered by Fang *et al.* and it is highly conserved in mammalian species<sup>245</sup>. Salcut-NH<sub>2</sub> stimulates growth of both blood and lymphatic vessels, mast cells and several anatomically different (by tumor origin) solid tumor cells at subnanomolar concentrations<sup>246</sup>. Interestingly, Fang *et al.* reported that Salcut-NH<sub>2</sub> is able to block Apelin-13-induced tube formation *in vitro*<sup>245</sup>. However, APJ antagonist did not inhibit Salcut-NH<sub>2</sub> effect, suggesting that Salcut-NH<sub>2</sub> activity is not dependent on the Apelin receptor. Same authors suggest that endogenous Salcut-NH<sub>2</sub> may play major roles in embryogenesis and carcinogenesis.**

### 1.7.3 Antagonists of APJ

#### *F13A*

F13A represents a peptide antagonist to APJ receptor and it is a result of the modification of pyroglutamated Apelin-13. This involves the replacement of the molecule's C-terminal phenylalanine residue (F in the single-letter amino acid code) with amino acid alanine (A in the single-letter amino acid code)<sup>201</sup>. F13A exhibits its effect by inhibiting forskolin-induced cAMP accumulation in rat APJ-overexpressing CHO cells<sup>210</sup>. Medhurst *et al.* reported lower potency of F13A on intracellular calcium mobilization and lower inhibition of cAMP accumulation, compared to [Pyr1]Apelin-13<sup>201</sup>. Additionally, it has been proven that F13A exhibits 2- to 14-fold lower receptor binding affinity for human APJ, expressed in different cell lines<sup>204</sup>. It is intriguing that in humans, binding of F13A to APJ results in calcium mobilization and internalization responses in rates similar to those of [Pyr1]Apelin-13<sup>230</sup>. This suggests a possible role of F13A as a competitive agonist of APJ. One of the goals of this Ph.D. thesis was to test the potential role of F13A as an Apelin antagonist.

#### *The M antagonists*

This is a group of non-peptide molecules that act as antagonists to APJ: ML221 and MM54.

In the last decade, Maloney *et al.* discovered and characterized ML221, the first small molecule antagonist of Apelin receptor with micromolar potency, from a high-throughput screening program<sup>247</sup>. This molecule exhibits a potent functional antagonism toward APJ in functional assays and it is proven that it binds to APJ 37 times more selectively than to APJ-closely related angiotensin II receptor<sup>247</sup>. Except for  $\kappa$ -opioid and benzodiazepinone receptors, ML221 did not show cross-reactivity to other G protein-coupled receptors<sup>247</sup>. However, its effectiveness is limited by its poor solubility in water and rapid metabolism.

MM54 is novel, even more potent antagonist to APJ. Macaluso *et al.* provided invaluable findings in the field of Apelin-related research, proving that MM54 has an antagonizing effect on inhibition of [Pyr1]Apelin-13 forskolin-induced cAMP accumulation in CHO-K1-APJ cells<sup>248</sup>. Following the MM54 discovery, the role of MM54 in cancer has been extensively investigated. It was reported to reduce tumor expansion, prolonging the survival time in a mouse xenograft model of glioblastoma<sup>249</sup>. MM54 was also a subject of *in vitro* studies in this Ph.D. project.

### *Protamine*

Recently, data from Le Gonidec *et al.* revealed a different pharmacological property of protamine – it acts as an antagonist to human APJ by displacing Apelin binding and abrogating G protein activation, as well as  $\beta$ -arrestin recruitment<sup>250</sup>. The same authors proved that the antagonistic activity of protamine could be reversed by heparin, which releases protamine that is bound to APJ<sup>250</sup>.

## **1.8 Pathophysiological role of the apelinergic system**

### 1.8.1 Pathophysiological angiogenesis

The apelinergic system is essential for physiological angiogenesis: during active angiogenesis, apelinergic signaling pathway cooperates with VEGF signaling, giving rise to new blood vessels<sup>251</sup>. On the other hand, recent findings have shed some light on the role of apelinergic system in pathophysiological angiogenesis. In their review, Wu *et al.* describe the enrollment Apelin/APJ in angiogenesis and myocardial infarction, ischemic stroke, retinal angiogenesis, obesity, as well as a role in tumor angiogenesis<sup>252</sup>. Additionally, Kasai *et al.* showed that the Apelin expression was significantly increased during hypoxia, with its overall expression being even higher than the one of VEGF<sup>178</sup>. Having discovered increased APJ expression within endothelial cells, the authors proved that the knockout of Apelin in mice lowered endothelial cell proliferation<sup>253</sup>. Therefore, HIF-1 $\alpha$  and the VEGF family can mediate angiogenesis together with the apelinergic system<sup>254</sup>.

Ishimaru *et al.* revealed that APJ antagonist, ML221, was able to suppress endothelial cell proliferation *in vitro*, however, the same antagonist showed no effect on the VEGF and VEGFR expression in the retina after its administration *in vivo*<sup>163</sup>. Interestingly, the same authors discovered that APJ was highly expressed in endothelial cells within abnormal vessels, unlike normal resting vessels, where its expression is low.

The specificity of apelinergic system to neoangiogenic processes has been presented most recently in the study of Wang *et al.*<sup>255</sup>. The authors designed and engineered cells with Apelin-based synNotch receptors (AsNRs), allowing them to interact exclusively with cells expressing APJ. APJ is claimed to have limited distribution in adulthood, being located mainly in endothelial cells during neovascularization. Since certain tumors require vascular support, it

has been shown that engineered cells successfully located endothelial cells within active endothelium of tumor.

In tumor angiogenesis, Apelin expression correlates with the increase of microvessel density and overall growth in tumors, such as in non-small cell lung cancer<sup>256</sup>. Additionally, an antagonist to APJ was able to inhibit the tumor growth indirectly, by decreasing blood vessel coverage in hepatocellular carcinoma<sup>257</sup>. Similar findings have been obtained in studies involving glioma models<sup>162</sup>. Mastrella *et al.* reported that in glioblastoma, Apelin expression decreases as a result of antiangiogenic therapy (anti-VEGF-A)<sup>258</sup>. Using an APJ antagonist (F13A), authors were able to reduce the angiogenesis and aggressiveness of glioblastoma. Pharmacological targeting of APJ demonstrated synergistic effect with existing antiangiogenic treatments in glioblastoma, eliminating the negative effects of resistance to antiangiogenic approach. That therapeutic strategy resulted in an overall improvement of antiangiogenic therapy. Contrary to some findings, certain authors demonstrated that knockout of Apelin stabilized vessel function, proving that the blockage of APJ is a key to reduce metastatic onset from the tumors that are resistant to receptor tyrosine kinase inhibitors<sup>150</sup>.

### 1.8.2 Cancer

During the past two decades, certain authors discussed that Apelin might have a role in tumor growth, migration of cancer cells, neoangiogenesis, as well as in induction of metastasis<sup>254</sup>. Indeed, several studies have proven the contribution of the Apelin/APJ system in the progression of cholangiocarcinoma, non-small cell lung cancer, gastrointestinal cancer, oral squamous cell carcinoma, glioblastoma, breast and ovarian cancer<sup>249,256,259-263</sup>.

The migration of tumor cells is a key factor for metastasis. Hashimoto *et al.* were the first to demonstrate the involvement of Apelin and APJ in cell migration, by stimulating APJ-overexpressing human embryonic kidney cells with Apelin<sup>264</sup>. Although there are still controversies about the mechanism that regulates cell migration, there are claims that Apelin elevates the migratory properties of different cancer cells, such as in certain human lung adenocarcinoma, gastric cancer, oral cell carcinoma as well as in ovarian cancer cells<sup>260,265-267</sup>. Furthermore, the expression profile of apelinergic system was investigated in certain cancer types: protein and gene expression analysis revealed differences in Apelin and APJ expression in comparison to healthy controls (Table 6).

**Table 6. An overview of Apelin/APJ expression in cancer.** Modified and adapted from Wysocka *et al.*<sup>254</sup>. ↑ Elevation; APLN (Apelin gene), APLNR (Apelin receptor gene), APJ (Apelin receptor protein).

Entity of disease	Patient/Tissue/Cell line, reference	mRNA	Protein	Synopsis
Brain	Glioblastoma <sup>162,249</sup>	APLN ↑	-	Involvement in the microvascular proliferation in glioblastoma.
Lung	Non-small lung cell carcinoma <sup>256</sup>	APLN ↑	-	Elevated microvessel density and poor overall survival.
	Lung adenocarcinoma <sup>268</sup>	-	APJ ↑	
Liver	Hepatocellular carcinoma <sup>257</sup>	APLN ↑	-	Promotion of arterial smooth muscle cell proliferation.
Multiple myeloma	Plasma <sup>269</sup>	-	Apelin ↑	Patients with advanced stage of disease had significantly poor prognosis when compared to healthy patients.
Cholangiocarcinoma	Tumor tissue <sup>259</sup>	APLN ↑	-	Autocrine/paracrine feedback regulates cholangiocarcinoma growth and angiogenesis.
		APLNR ↑	-	
	Cell lines <sup>259</sup>	-	Apelin ↑	
Gastrointestinal tract	Colorectal cancer patients <sup>270</sup>	APLN ↑	Apelin ↑	Patients with high tumor Apelin expression had a shorter overall survival period in comparison to those with low Apelin expression.
		APLNR ↑	APJ ↑	
	Gastric cancer <sup>271</sup>	-	APJ ↑	
Ovary	Ovarian cancer <sup>263</sup>	APLN ↑	-	Upon upregulation, Apelin induces ovarian cancer cell proliferation, acting as a mitogenic factor.
	Ovarian cancer cell lines <sup>267</sup>	APLNR ↑	-	
		-	Apelin ↑	
		APLNR ↑	APJ ↑	



Breast	Plasma of breast cancer patient <sup>272</sup>	-	Apelin ↑	Paracrine or autocrine mechanisms of apelin signaling. Significant cytoplasmic apelin immunoreactivity in mammary ductal and lobular epithelium in non-lactating state.
	Tissue of breast cancer patient <sup>262</sup>	-	Apelin ↑	
	Breast cancer cell line <sup>273</sup>	APLN ↑	-	
Kidney	Clear renal cell carcinoma <sup>274</sup>	APLNR ↑	APJ ↑	APLNR expression is an independent prognostic factor for survival.
	Cell lines <sup>274</sup>	APLNR ↑	APJ ↑	
Prostate	Prostate cancer <sup>275</sup>	APLN ↑	-	Apelin elevation is associated with tumorigenesis and aggressive progression of prostate cancer.
Blood	Chronic lymphocytic leukemia <sup>276</sup>	-	Elabela (Apela) ↑	ELA may contribute to the development of chronic lymphocytic leukemia.

### 1.9 Thesis objectives

The aim of this thesis was to examine the role of the apelinergic system in development of resistance against antiangiogenic therapeutics in cancer treatment. The main goal was investigation of the apelinergic system's role in solid tumor entities, as well as in acute myeloid leukemia, since angiogenic processes in the bone marrow are also involved in the pathophysiology of leukemias.

Primary objective was to study the effect of antiangiogenic treatment on tumor growth, metastasis onset and microvessel density in murine lung tumor tissue in conditions of overexpressed Apelin or APJ antagonist. Adeno-associated viral vectors (AAV) were therefore selected as tools that specifically target the lung endothelial cells and allow stable overexpression of gene of interest<sup>277</sup>. Since conventional antiangiogenic therapy generally does not lead to complete tumor regression, it is questioned whether the apelinergic system is a druggable target that can improve existing therapy.

Another goal was to examine potential role of Apelin/APJ system in paracrine interaction between proangiogenic immune cells, such as M<sub>2</sub> macrophages, and tumor endothelial cells. Also, this thesis was seeking to investigate direct effect of apelinergic system on tumor cells in *in vitro* conditions in terms of tumor cell proliferation and other functional properties.

In general, characterization of Apelin and APJ expression in tumor tissues, primary tissue-derived cells and immortalized tumor cell lines was envisaged as well.

## 2. MATERIAL AND METHODS

### 2.1 Material

#### 2.1.1 Laboratory equipment, kits and reagents

##### *Laboratory equipment*

Laboratory equipment used in this study is listed in Table 7.

**Table 7. Laboratory equipment**

<b>Equipment</b>	<b>Product name</b>	<b>Manufacturer/distributor</b>
Absorbance reader	Infinite® 200 PRO	Tecan (Männedorf, CH)
Agarose gel electrophoresis chamber	DNA Sub cell™	Bio-Rad (Hercules, CA, US)
Analytical scale	Pioneer™ PA213	Ohaus Corp. (Pine Brook, NJ, US)
Analytical scale	AT261 DeltaRange®	Mettler-Toledo GmbH (Greifensee, CH)
Benchtop Centrifuge I	Centrifuge 5424	Eppendorf (Hamburg, DE)
Biological safety cabinet	HeraSafe HS 9	Heraeus (Hanau, DE)
Biological safety cabinet	LaminAir HB 2448	Heraeus (Hanau, DE)
Benchtop Centrifuge II	Centrifuge 5804 R	Eppendorf (Hamburg, DE)
Benchtop Centrifuge IV	Centrifuge 5810 R	Eppendorf (Hamburg, DE)
Benchtop Centrifuge V	Labofuge 400 R	Heraeus (Hanau, DE)
Benchtop Microcentrifuge	myFuge™ Mini	Benchmark Scientific (Edison, US)
Benchtop mixer/shaker	Vortex Genie® 2	Thermo Fisher Scientific (Waltham, US)
Cell counter	Vi-Cell™ XR Cell Viability Analyzer	Beckman Coulter (Brea, US)
Chemiluminescence detection system	Fusion SL 3500 WL	Vilber Lourmat (Collégien, FR)
CO <sub>2</sub> -Incubator (cell culture)	Labotec Inkubator C200	Labotec (Göttingen, DE)
CO <sub>2</sub> -Incubator (cell culture, O <sub>2</sub> /CO <sub>2</sub> -adjustable)	Inkubator C16	Labotec (Göttingen, DE)
Documentation microscope (camera)	AxioCam MRc	Zeiss (Oberkochen, DE)
Electroporation system	Gene Pulser Xcell™ Microbial System	Biorad (Hercules, US)

## MATERIAL AND METHODS

Flow cytometer	FACS Calibur™	Becton Dickinson (Franklin Lakes, US)
Flow cytometer	FACS Canto™	Becton Dickinson (Franklin Lakes, US)
Freezing container	Mr. Frosty™	Nalgene, Thermo Scientific (Waltham, US)
Gel documentation system	Gene Genius Bio Imaging System	Syngene (Frederich, US)
Gel documentation system	EBOX VX2	Vilber Lourmat (Collégien, FR)
Heating block	Thermomixer Comfort	Eppendorf (Hamburg, DE)
<i>In vivo/ex vivo</i> imaging system	IVIS 200	Caliper Lifescience (Hopkinton, US)
Incubation shaker	Certomat® IS	B. Braun Biotech International (Melsungen, DE)
Incubator (Bacteria)	Heraeus® Kendro Typ B12	Heraeus (Hanau, DE)
Luminometer	Mithras LB 940	Berthold Technologies (Bad Wildbad, DE)
Magnetic stirrer	IKAMAG® RH	Janke & Kunkel, IKA (Staufen, DE)
Microbiological incubator	Kelvitron® t	Heraeus Instruments (Hanau, DE)
Microplate reader	Infinite® M200 Pro	Tecan Life Sciences (Männedorf, CH)
Microscope	Axiovert 25	Zeiss (Oberkochen, DE)
Microscopy system for migration assays	Incucyte™ microscopy system	Sartorius (Göttingen, DE)
Microtome	HM 355 S	Microm (Neuss, DE)
Migration assay 96-well plates	IncuCyte® ImageLock 96-well Plates	Sartorius (Göttingen, DE)
Neubauer counting chamber	Neubauer-Improved bright line	Paul Marienfeld GmbH & CO KG (Lauda-Königshofen, DE)
Nitrogen storage tank	CryoPlus™	Thermo Fisher Scientific (Waltham, US)
pH meter	pH 192, WTW	Xylem Analytics (Weilheim, DE)
Power supply	PowerPac™ Basic	Biorad (Hercules, US)
Power supply	PowerPac™ 300	Bio-Rad (Hercules, US)
Preparative ultracentrifuge	Optima™ LE-80K, Rotor: Type 70.1	Beckman Coulter (Brea, US)
Real-Time PCR cycler	LightCycler® 96	Roche (Basel, CH)
Roll shaker	Stuart® roller mixer SRT9D	Cole-Parmer (Staffordshire, UK)
Rotating Mixer	Test-tube-rotator 34528	Snijders (Tilburg, NL)
SDS-PAGE electrophoresis cell	XCell SureLock™ Electrophoresis Cell	Invitrogen, Thermo Fisher Scientific (Waltham, US)
Shaker	KM-2	Edmund Bühler GmbH (Bodelshausen, DE)

Shaker (bacteria)	Ceromat® IS	B. Braun Biotech International (Melsungen, DE)
Spectrophotometer	NanoDrop ND-1000	Thermo Fisher Scientific (Waltham, US)
Steam sterilizer	Varioklav®	HP Medizintechnik (Oberschleißheim, DE)
Tank Blotting chamber	Mini-PROTEAN® 3 Cell	Bio-Rad (Hercules, US)
Thermal gradient cycler	Mastercycler® gradient	Eppendorf (Hamburg, DE)
Thermo blocks	TB2/Thermoblock	Biometra (Göttingen, DE)
Thermocycler	T1 Thermocycler	Biometra (Göttingen, DE)
Tube topper/sealer	Quick-Seal Cordless Tube Topper	Beckman Coulter (Brea, CA, US)
UV-Vis Spectrophotometer	NanoDrop® Spectrophotometer ND-1000	PEQLAB (Erlangen, DE)
Vortexer	VF-2	Janke & Kunkel, IKA (Staufen, DE)
Water bath	GFL 1002	Gesellschaft für Labortechnik GmbH (Burgwedel, DE)
Water bath/circulator	Thermomix ME	B. Braun (Melsungen, DE)
Wound maker	IncuCyte® WoundMaker	Sartorius (Göttingen, DE)

### *Ready-to-use reagents and kits*

Ready-to-use reagents and kits used in this study are listed in Table 8.

**Table 8. Molecular biology kits and ready-to-use reagents**

<b>Kit or reagent</b>	<b>Manufacturer/distributor</b>	<b>Hazard and precautionary statements</b>	<b>GHS hazard</b>
DC Protein Assay Reagents Package	BioRad (Hercules, US)	-	-
DNA Gel Loading Dye (6X)	Thermo Fisher Scientific (Waltham, US)	-	-
DreamTaq™ Green PCR Master Mix	Thermo Fisher Scientific (Waltham, US)	-	-
Dual-Glo® Luciferase Assay System	Promega (Madison, US)	H: 225, 301, 311, 315, 318, 319, 331, 335, 370	GHS06, GHS07
ELISA Apelin-12 Extraction Free Kit (Spectrophotometry)	Phoenix Pharmaceuticals (Burlingame, US)	-	-
ELISA Apelin-12 Kit (Luminescence)	Phoenix Pharmaceuticals (Burlingame, US)	-	-
innuPREP RNA Mini Kit	Analytik Jena AG (Jena, DE)	H: 302, 312, 314, 332, 412	GHS05, GHS07

## MATERIAL AND METHODS

		P: 101, 102, 103, 260, 303+361+353, 305+351+338, 310, 405, 501	
Library Efficiency™ DH5α™ Competent Cells	Thermo Fisher Scientific (Waltham, US)	-	-
MycoAlert™ Mycoplasma Detection Kit	Lonza (Basel, CH)	H: 332, 373	GHS08
NucleoBond® Xtra Midi Plus	Macherey-Nagel (Düren, DE)	H: 226, 315, 319, 334 P: 210, 261sh, 304+340, 342+311	GHS03, GHS07
NucleoSpin® Gel and PCR Clean-up	Macherey-Nagel (Düren, DE)	H: 302, 412 P: 264W, 273, 301+312, 330	GHS07
NucleoSpin® Plasmid	Macherey-Nagel (Düren, DE)	H: 226, 302, 315, 319, 334, 336 P: 210, 260D, 261sh, 264W, 280sh, 301+312, 304+340, 330, 342+311	GHS02, GHS07
OptiPrep™ Density Gradient Medium (60% w/v iodixanol)	Axis-Shield (Dundee, UK)	-	-
Pan Monocyte Isolation Kit, human	Miltenyi Biotec GmbH (Bergisch Gladbach, DE)	-	-
Phusion High Fidelity Kit	Thermo Fisher Scientific (Waltham, US)	-	-
PrimeScript RT Master Mix	Takara Bio Inc. (Shiga, JP)	H302	-
TB Green Premix Ex Taq™ II (SYBR® Premix Ex Taq™ II)	Takara Bio Inc. (Shiga, JP)	-	GHS05
Cell Proliferation Reagent WST-1 (Tetrazolium salt)	Roche Diagnostics, (Mannheim, DE)	H: 315, 319, 335 P: 261, 305 + 351 + 338	GHS07

### Enzymes

Enzymes used in this study are listed in Table 9.

**Table 9. Enzymes**

Enzyme	Manufacturer/distributor
DNA Polymerase I, Klenow Fragment (5,000 U/ml)	New England Biolabs (Ipswich, US)
Fusion High Fidelity DNA Polymerase (2,000 U/ml)	Mobidiag (Espoo, FIN)

Proteinase K	Qiagen (Hilden, DE)
T4 DNA Ligase (400,000 U/ml)	Thermo Fisher Scientific (Waltham, US)
SacII (plus Buffer B)	Thermo Fisher Scientific (Waltham, US)
FastDigest StuI	Thermo Fisher Scientific (Waltham, US)
FastDigest BamHI	Thermo Fisher Scientific (Waltham, US)
FastDigest NotI	Thermo Fisher Scientific (Waltham, US)
FastDigest MscI	Thermo Fisher Scientific (Waltham, US)
FastDigest HindIII	Thermo Fisher Scientific (Waltham, US)
FastDigest EcorI	Thermo Fisher Scientific (Waltham, US)
FastDigest BsrGI	Thermo Fisher Scientific (Waltham, US)

### Antibodies

Antibodies used in this study are listed in Table 10.

**Table 10. Antibodies**

Denotation	Host	Clone	Isotype	Source
<b>Monoclonal</b>				
Alexa Fluor™ 488 anti-hAPJ (FAB8561G)	Mouse	#72133R	Alexa Fluor® 488 Mouse IgG1 $\kappa$ Isotype Control	R&D Systems (Minneapolis, US)
<i>APC anti-hAPJ (FAB856A) discontinued</i>	<i>Mouse</i>	<i>#72133</i>	<i>APC Mouse IgG3 Isotype Ctrl (FC)</i>	<i>R&amp;D Systems (Minneapolis, US)</i>
APC anti-hAPJ (FAB8561A)	Mouse	#72133R	APC Mouse IgG1, $\kappa$ Isotype Ctrl (FC)	R&D Systems (Minneapolis, US)
APC anti-hCD200R (329207)	Mouse	OX-104	APC Mouse IgG1, $\kappa$ Isotype Ctrl (FC)	Biologend (San Diego, US)
APC anti-hCD80 (305219)	Mouse	2D10	APC Mouse IgG1, $\kappa$ Isotype Ctrl (FC)	Biologend (San Diego, US)
FITC anti-hCD14 (325604)	Mouse	HCD14	FITC Mouse IgG1, $\kappa$ Isotype Ctrl (FC)	Biologend (San Diego, US)
FITC anti-hCD163 (333617)	Mouse	GHI/61	FITC Mouse IgG1, $\kappa$ Isotype Ctrl (FC)	Biologend (San Diego, US)
FITC anti-hCD206 (321103)	Mouse	15-2	FITC Mouse IgG1, $\kappa$ Isotype Ctrl (FC)	Biologend (San Diego, US)
PE anti-CD11b (301306)	Mouse	CRF44	PE Mouse IgG1, $\kappa$ Isotype Ctrl (FC)	Biologend (San Diego, US)
PE anti-Tie2 (FAB3131P)	Mouse	#83715	PE Mouse IgG1, $\kappa$ Isotype Ctrl (FC)	R&D Systems (Minneapolis, US)
<b>Polyclonal</b>				
Anti-APJ (1/100 - 1/1000 v/v)	Rabbit	-	IgG	Abcam (Cambridge, UK)

## MATERIAL AND METHODS

### *Chemicals and reagents*

Chemicals, reagents and cell culture supplements used in this study are presented in Table 11.

**Table 11. Chemicals, reagents and cell culture supplements**

<b>Substance/reagent</b>	<b>Producer</b>	<b>Hazard and precautionary statements</b>	<b>GHS hazard</b>
10 × Annexin V Binding Buffer	Becton Dickinson (Franklin Lakes, US)	-	
2-Propanol	Carl Roth GmbH, (Karlsruhe, DE)	H: 225, 319, 336 P: 210, 261, 305+351+338	GHS02, GHS07
AB-Serum	Bio-Rad (Hercules, US)	-	
Acrylamide 37%	Sigma-Aldrich (St. Louis, US)	H: 301, 312, 315, 317, 319, 332, 340, 350, 361f, 372 P: 201, 280, 301+310, 305+351+338, 308+313	GHS06, GHS08
Agarose	Lonza (Basel, CH)	- H: 317, 334	
Ampicillin	Sigma-Aldrich (Taufkirchen, DE)	P: 261, 272, 280, 285, 302+352, 304+341, 333+313, 342+311, 363	GHS08
Annexin V-APC	Biologend (San Diego, US)	-	-
Benzonase®	Sigma-Aldrich (Taufkirchen, DE)	-	-
BSA, Albumin Fraktion V	Carl Roth GmbH (Karlsruhe, DE)	-	-
Chloramphenicol	Sigma-Aldrich (St. Louis, US)	H351 P: 315, 319, 308 + 313 H: 302, 360, 373	GHS05, GHS08
Chloroquine	Sigma-Aldrich (St. Louis, US)	P: 201, 202, 260, 264, 280, 301+312, 308+313, 314, 330	GHS07, GHS08
DC101	Eli Lilly and Company (Indianapolis, US)	-	-
DEPC-Treated Water	Thermo Fisher Scientific (Waltham, US)	-	-
Dimethyl sulfoxide (DMSO)	Merck KGaA, (Darmstadt, DE)	H227 P: 210, 280	GHS07
EDTA	Sigma-Aldrich (St. Louis, US)	H: 332, 373 P314	GHS07
Endothelial Cell Growth Medium MV	Promocell GmbH (Heidelberg, DE)	-	-
Ethanol, absolute	Merck (Darmstadt, DE)	H: 225, 319, 335, 320, H315 + H320 P: 210, 240, 261 305+351+338, 403+233	GHS02, GHS07



		H: 317, 334	
Fast-Media® Amp Agar	InvivoGen (San Diego, US)	P: 261, 272, 280, 285, 302+352, 304+341, 333+313, 342+311, 363	GHS08
Fetal Bovine Serum (FBS)	Biochrom GmbH (Berlin, DE)	-	
Formafix 4 % buffered	Grimm med. Logistik GmbH (Torgelow, DE)	H: 302, 317, 341, 350 P: 261, 280, 302+352, 308+313	GHS07, GHS08
Gibco™ DPBS (1×), [-] CaCl <sub>2</sub> , [-] MgCl <sub>2</sub> , PBS	Thermo Fisher Scientific (Waltham, US)	-	-
Glycerol	Sigma-Aldrich (St. Louis, US)	-	-
GM-CSF (human, rekombinant)	PreproTech (Hamburg, DE)	-	-
Hexadimethrine bromide (Polybrene)	Sigma-Aldrich (St. Louis, US)	H302	GHS07
Interleukin 4 (IL-4)	PreproTech (Hamburg, DE)	-	
		H: 319, 335, 336	
Isoflurane, Forene®	Abbott GmbH & Co. KG, (Hannover, DE)	P: 264, 280, 235+2351+338, 337+313, 261, 271, 304+340, 312, 403+233, 405, 501 H: 302, 332	GHS07, GHS08
Ketanest® S (Ketamine) 25 mg/mL	Pfizer (New York City, US)	P: 261, 264, P301+312, P304+340, P330	-
Macrophage Colony Stimulating Factor, human, recombinant	PreproTech (Hamburg, DE)	-	-
		H: 255, 301, 311, 331, 370	
Methanol (MeOH)	Carl Roth GmbH + Co. KG, (Karlsruhe, DE)	P: 210, 233, 240, 241, 242, 243, 260, 264, 270, 271, 280, 301+310, 303+361+353, 308+311	GHS02, GHS06, GHS08
MethoCult™ H4230	STEMCELL Technologies (Vancouver, CA)	-	-
NaCl 0.9 %	B. Braun Biotech International (Melsungen, DE)	-	-
PBS-MK	Thermo Fisher Scientific (Waltham, US)	-	-
Penicillin-Streptomycin (10.000 U/10 mg/mL)	Sigma-Aldrich GmbH, (Steinheim, DE)	H: 315, 317, 320, 334, 335 360, 371 P: 302+352, 304+340, 201, 260, 333+313, 261	GHS07
Polyfect™ Transfection reagent	Qiagen (Hilden, DE)	-	-
Polysucrose 400 Trennmedium	BioClot GmbH (Aidenbach, DE)	-	-

## MATERIAL AND METHODS

Propidium iodide, 1 mg/mL solution	Thermo Fisher Scientific (Waltham, US)	-	-
Protease Inhibitor Cocktail tablets cOmplete™	Roche Diagnostics, (Mannheim, DE)	H: 302, 314 P: 260, 264, 270, 280, 301+312, 330, 501, 301+330+331, 303+361+353, 304+340+310, 305+351+338+310	GHS05
Proteinase K	Sigma-Aldrich GmbH, (Steinheim, DE)	H334 P: 261, 342+311	GHS07, GHS08
Puromycin dihydrochloride	Sigma-Aldrich (St. Louis, US)	H302	GHS07
RNAlater RNA Stabilization Reagent	Qiagen (Hilden, DE)	-	-
Rompun® (Xylazine) 2 % solution	Bayer AG (Leverkusen, DE)	H301 P: 264, 301+310, 330	GHS06
ROTI®GelStain	Carl Roth (Karlsruhe, DE)	-	-
SDS (Sodium dodecyl sulfate)	Sigma-Aldrich (St. Louis, US)	H: 228, 302, 311, 315, 319, 335 P: 210, 261, 280, 312, 305+351+338 H: 300, 400, 410	GHS02, GHS06
Sodium azide	Sigma-Aldrich (St. Louis, US)	P: 264, 270, 273, 301+310, 321, 330, 391, 405, 501	GHS06, GHS09
Sodium orthovanadate	Sigma-Aldrich GmbH, (Steinheim, DE)	H302 P301 + P312 + P330 H: 350, 351	GHS07
Trypan Blue solution, 0.4 % (w/v)	Sigma-Aldrich (St. Louis, US)	P: 201, 202, 280, 308+313, 233 H: 315, 319, 334, 335	GHS08
Trypsin	PAA Laboratories (Pasching, AT)	P: 261, 264, 271, 280, 285, 302+352, 304+340, 304+341, 305+351+338, 312, 321, 332+313, 337+313, 342+311	GHS07, GHS08
Turbofect™ Transfection reagent	Thermo Fisher Scientific (Waltham, US)	-	-

*Buffers and solutions*

The recipes for commonly used buffers and solutions are listed in Table 12.

**Table 12. Recipes for buffers and solutions**

<b>Description</b>	<b>Specification, note</b>
Erylysis buffer	155 mM NH <sub>4</sub> Cl, 10 mM KHCO <sub>3</sub> , 0.1 mM EDTA, <i>ad</i> 1 L, sterile filtered
FACS-buffer	10% AB-serum in PBS
Freezing solution	45% RPMI, 45% fetal bovine serum (FBS), 10% DMSO
2x HEPES-buffered saline transfection buffer (2x HBS)	pH 7.05-7.1
Ketanest®/Xylazin-narcotic	24 mL Ketanest®S (esketamine hydrochloride), 4 mL Xylazin (xylazine hydrochloride), 22 mL 0,9% NaCl
LB-Agar	40 g LB-Agar (Luria/Miller), <i>ad</i> 1 L ddH <sub>2</sub> O, sterilized by autoclaving
LB-Medium	25 g LB-Medium (Luria/Miller), <i>ad</i> 1 L ddH <sub>2</sub> O, sterilized by autoclaving
0.1 M Phosphate buffer	30 mL 0.1 M Na <sub>2</sub> HPO <sub>4</sub> , 10 mL 0.1 M NaH <sub>2</sub> PO <sub>4</sub>
10x Running buffer	29 g Tris base, 144 g Glycine, 10 g SDS, <i>ad</i> 1 L ddH <sub>2</sub> O
20% (w/v) Sodium dodecyl sulfate (SDS)	20.0 g SDS, <i>ad</i> 100 mL ddH <sub>2</sub> O
50x Tris-acetate- EDTA (TAE) buffer	40 mM Tris-HCl, 20 mM Sodium acetate, 1 mM EDTA, pH 8.2
10x Tris-buffered saline (TBS) buffer	24.2 g Tris base, 80.1 g NaCl, <i>ad</i> 1 L ddH <sub>2</sub> O, pH 7.6
1x TBS with Tween® 20 (TBS-T) buffer	100 mL 10x TBS, 1 mL Tween® 20, <i>ad</i> 1 L ddH <sub>2</sub> O
10x Transfer buffer	121.14 g Tris base, 144.89 g Glycine, <i>ad</i> 1 L ddH <sub>2</sub> O
0.5 M Tris-HCl, pH 6.8	15.0 g Tris base, <i>ad</i> 250 mL ddH <sub>2</sub> O; pH adjustment with 6M HCl to 6.8; storage at 4°C
1.5 M Tris-HCl, pH 8.8	90.8 g Tris base, <i>ad</i> 500 mL ddH <sub>2</sub> O; pH adjustment with 6M HCl to 8.8; storage at 4°C

*DNA ladders*

DNA-ladders used in this study are presented in Table 13.

**Table 13. DNA-ladders**

<b>Description</b>	<b>Catalog number</b>	<b>Manufacturer</b>
GeneRuler 1 kb Plus DNA Ladder, ready-to-use	SM1331	Thermo Fisher Scientific (Waltham, US)
GeneRuler 100 bp Plus DNA Ladder	SM0241	Thermo Fisher Scientific (Waltham, US)

## MATERIAL AND METHODS

---

### *Disposables*

Disposables were obtained from the following companies: Beckman Coulter, Biorad, Braun, Corning, Dako, Eppendorf, Greiner, Perkin Elmer, Pierce, Sarstedt, Whatman.

### 2.1.2 Apelin, Apelin analogs and APJ antagonists

#### *Apelin*

[Pyr1]Apelin-13 isoform was used for all functional studies. The peptide was purchased from Abcam (Cambridge, UK) and diluted in water to a stock concentration of 10 mM. This isoform has a binding affinity  $IC_{50}$  of  $5.7 \pm 0.3$  nM in the competitive binding assay and an  $EC_{50}$  of  $1.89 \pm 1$  nM in the forskolin-induced cAMP assay<sup>278</sup>.

#### *Apelin analogs*

Apelin analogs used during this study were a kind gift of Prof. Dr. Eric Marsault, Department of Pharmacology, Université de Sherbrooke. All substances were diluted in water to a stock concentration 1 mM. Substance names, including their sequence and molar mass presented in Table 14.

**Table 14. Apelin analogs**

Peptide	Sequence	Molar mass (g/mol)
AM01-182	Pyr-R-P-R-L-S-H-K-G-P-Nle-P-Tyr(OBn)	1621.9
AM01-190	Pyr-R-P-R-L-S-H-K-G-P-Nle-P-Bpa	1619.9
AM02-50	K-P-K-L-S-[AllylGly-K-G-P-AllylGly]-Tyr(OBn)	1273.5
KT01-3	Pyr-R-P-R-L-S-H-K-[AllylGly-P-M-P-AllylGly]	1477.7
KT01-11	Pyr-R-[AllylGly-R-L-S-AllylGly]-K-G-P-M-P-F	1447.7

#### *APJ antagonists*

Non-peptide APJ antagonist MM54 was purchased from Tocris Bioscience (Bristol, UK). MM54 was prepared in water at a stock concentration of 10 mM. According to the manufacturer, MM54 ( $K_i = 82$  nM;  $IC_{50} = 93$  nM) antagonizes the inhibitory effect of [Pyr1]-Apelin-13 on forskolin-induced cAMP accumulation in CHO-K1-APJ cells.

Peptide APJ antagonist F13A was purchased from Ontores Biotechnologies (Zhejiang, CN). F13A was prepared in water at a stock concentration of 20  $\mu\text{g}/\mu\text{L}$ .

## 2.1.3 Cells

*Prokaryotic cells (Escherichia coli)*

*E. coli* strains used for amplification of plasmid DNA are listed in Table 15.

**Table 15. Prokaryotic cells**

Denotation	Genotype
DH5 $\alpha$ <sup>TM</sup>	F- $\phi$ 80dlacZ $\Delta$ M15 ( <i>lacZYA-argF</i> ) U169 <i>deoR recA1 endA1 hsdR17</i> ( $\tau$ K-, mK+), <i>phoA supE44 <math>\lambda</math>- thi-1 gyrA69 relA1</i>
DH10BAC <sup>TM</sup>	F- <i>mcrA <math>\Delta</math>(mrr-hsdRMS-mcrBC) <math>\phi</math>80dlacZ<math>\Delta</math>M15 <math>\Delta</math>lacX74 <i>deoR recA1 endA1 araD139 (ara, leu)7697 galU galK <math>\lambda</math>- rpsL nupG bMON14272 pMON7124</i></i>

*Eukaryotic cells*

Immortalized cell lines used in this study are listed in Table 16.

**Table 16. Eukaryotic cells**

Denotation	Origin	Cultivation medium	ATCC/DSMZ number
<i>Suspension cell lines</i>			
HL-60	36-year-old Caucasian female with acute promyelocytic leukemia (1976)	RPMI + 10% FBS	ATCC® CRL-240
Kasumi 1	7-year-old Japanese male with AML (1989)	RPMI + 20% FBS	ATCC® CRL-2724
Molm13	20-year-old male with AML FAB M5a at relapse (1995)	RPMI + 10% FBS	ACC 554
MONO-MAC-1	64-year-old male with AML FAB M5 at relapse (1985)	RPMI + 10% FBS + 2 mM L-glutamine + 1x non-essential amino acids + 1 mM sodium pyruvate	ACC 525
MV4-11	10-year-old male with biphenotypic B-myelomonocytic leukemia (1987)	RPMI + 10% FBS	ATCC® CRL-9591
OCI-AML3	57-year-old male with AML FAB M4 (1987)	$\alpha$ -MEM + 20% FBS	ACC 582
OCI-AML5	77-year-old male with AML M4 in relapse (1990)	$\alpha$ -MEM + 20% FBS + 2.5 ng/mL GM-CSF	ACC 247
OCI-M1	62-year-old patient with AML M2 (1988)	RPMI + 10% FBS	ACC 529
TF-1	35-year-old Japanese male with severe pancytopenia (1987)	RPMI + 10% FBS + 2.5 ng/mL GM-CSF	ATCC® CRL-2003
THP-1	1-year-old male with AML at relapse (1978)	RPMI + 10% FBS	ACC 16

## MATERIAL AND METHODS

UKE-1	59-year-old female with secondary AML (1997)	IMDM + 10% FBS + 10% HS + 1 $\mu$ M Hydrocortison	-
<i>Adherent cell lines</i>			
A549	Initiated in 1972 through explant culture of lung carcinomatous tissue from a 58-year-old Caucasian male	DMEM + 10% FBS	ATCC® CCL-185™
HEK 293T	Adenovirus E1A/B and SV40 large T-antigen transformed human embryonic kidney cells	DMEM + 10% FBS	ATCC® CRL-1573™
HL-60	36-year-old Caucasian female with acute promyelocytic leukemia (1976)	RPMI + 10% FBS	ATCC® CRL-240
HT29	HT-29 line was isolated from a primary tumor of 44-year old Caucasian female	RPMI + 10% FBS	ATCC® HTB-38™
HUVEC	Human Umbilical Vein Endothelial Cells	EGM™-2 Endothelial Cell Growth Medium-2 BulletKit™ (10% FBS)	ATCC® CRL-1730™
LLC1	Isolated from mouse frozen lung tissue	DMEM + 10% FBS	ATCC® CRL-1642™
MC38	Derived from C57BL6 murine colon adenocarcinoma cells	DMEM + 10% FBS	-
MDA MB231	Mammary gland/breast; derived from metastatic site: pleural effusion	DMEM + 10% FBS	ATCC® CRM-HTB-26™
MDA MB468	Mammary gland/breast; derived from metastatic site: pleural effusion	DMEM + 10% FBS	ATCC® HTB-132™
MOLM13	20-year-old male with AML FAB M5a at relapse (1995)	RPMI + 10% FBS	ACC 554
OVCAR8	Established in 1982 by T.C. Hamilton <i>et al.</i> from the malignant ascites of a patient with progressive adenocarcinoma of the ovary <sup>279</sup>	RPMI + 20% FBS	ATCC® HTB-161™
U188	Glioblastoma of 50-year-old Caucasian male	DMEM + 10% FBS	ATCC® HTB-15™

### 2.1.4 Animals

All experiments involving animals were performed with female immunocompetent mouse strain CR57BL/6-5050 (*Mus musculus*), known as “Black Six”. The animals were purchased from the Janvier Lab (Le Genest-Saint-Isle, FR) or have been originated in the animal facility of the University Medical Center Hamburg-Eppendorf.

## 2.1.5 Synthetic oligonucleotides

All oligonucleotides used in this study were synthesized by Eurofins Genomics (Ebersberg, DE) and are listed in Table 17. Primers were diluted in ddH<sub>2</sub>O in accordance with the manufacturer's recommendation.

**Table 17. Synthetic oligonucleotides**

Denotation	Sequence 5' → 3'	GC%	No. Bases
<b>Primers used for cloning</b>			
Luc_fw(IRES)	ATACACCTGCAAAGGCGGCACAAC C	56	25
Luc_rev	GGCACCAGCAGCGCACTTTGAATC	58	24
hAPLN_pOTB7_fw	GTAAAACGACGGCCAGTAACTATA ACGG	46	28
NotI_hAPLN_pOTB7_rev	ATCAGCGGCCGCTCAGGAAACAGC TATGACCATGTGCC	58	38
LeGO_APJ_fw	AAAGAATTCAAGCTTGGATCCGAT ATCG	39	28
LeGO_APJ_rev	TTTAGGCCTTCTAGAGTATACTGGC GCG	50	28
<b>Sequencing primers</b>			
CMV teto2 -CMV_rev	GGGACTTTCCTACTTGGCA	19	53
Luc_rev	GGCACCAGCAGCGCACTTTGAATC	25	58
seqpLeGO-GOI(A)_fwI	CCGTACCACCACACTGGG	18	58
seqpLeGO-GOI(A)_fwII	AGGCCGGTGAGGCAGAAG	18	67
seqpLeGO-GOI(A)_fwIII	GGTCACCACCAGCACCAC	18	67
seqpLeGO-GOI(mAPJ)_fwI	TGTGGTGACTTTGCCACTGT	20	50
seqpLeGO-GOI(mAPJ)_fwII	CACCATCATGCTGACATGTTACT	23	43
seqpLeGO-GOI(mAPJ)_revI	GAGGTAGCTGCTGAGCTTGC	20	60
seqpLeGO-GOI(mAPJ)_revII	CTTCCGCAGGCCCTCAAT	18	61
seq_hAPLN-LeGOi-C2_rev1	AGATTCATGCTGCTCCTTGG	20	50
seq_hAPLN-LeGOi-C2_rev2	AAGGGAGTATTGGGAGGCAC	20	55
seq_hAPLN-LeGOi-C2_rev3	GGCATCAGGCTCTTGTCTTC	20	55
seq_hAPLN-LeGOi-C2_fw2	CCTAGCTTCCGTGAGGGG	18	67
seq_hAPLN-LeGOi-C2_fw1	AGCGTTTGCTCAGTTAAGGG	20	50
<b>Primers used for Real-time RT-qPCR</b>			
hAPLN 2002	GGAAGTGCAGCAGGAATAGC	55	20
hAPLN 2162	ACACACAAAGTTGGGCATCA	45	20
hAPJ 479	CTATGGGGCAGACAACCAGT	55	20
hAPJ 647	GATATCAGCTGAGCGCCTCT	55	20
hGAPDH for 822	GTCAGTGGTGGACCTGACCT	60	20
hGAPDH rev 1066	TGCTGTAGCCAAATTCGTTG	45	20
mGAPDH_fw_942	GGCATTGCTCTCAATGACAA	45	20
mGAPDH_rev_1178	GGCCCCTCTGTTATTATGG	55	20
mAPLNR_fw_712	GCCACAGCAGTCTTATGGGT	55	20
mAPLNR_rev_1035	GGTCACTACAAGCACCACGA	55	20
eGFP_fw_308	ACGACGGCAACTACAAGACC	55	20
eGFP_rev_415	TTGTACTCCAGCTTGTGCC	55	20
mgGAPDH_fw	GGGGCAGCTCTCAGGTTC	67	18
mgGAPDH_rev	GGAGATTGCTACGCCATAGG	55	20

## MATERIAL AND METHODS

### 2.1.6 Plasmids and recombinant AAV vectors

Plasmids used in this study are listed in Table 18.

**Table 18. Plasmids**

pXX2-187	AAV2 <i>rep/ AAV2 cap</i> R588ins, <i>Sfi</i> I sites, used for generation of single clone AAV2 R588 mutants	280
pXX6	Adenoviral helper plasmid containing E1A, E1B, E2A, E4-orf6, VA, used for production of rAAV vectors	281
pAAV-CMV-teto2-LUC	AAV expression cassette, containing the luciferase gene under control of the CMV promoter and the SV40 poly-A signal embedded between AAV2 ITRs	Jakob Körbelin
pEX-a128-Apelin13	Used to clone gene for mApelin; Selection antibiotic: ampicilin	Eurofins Genomics
pEX-a128-F13A	Used to clone gene for mApelin; Selection antibiotic: ampicilin	Eurofins Genomics
pMDLg/pRRE	LV packaging plasmid includes gag, coding for the virion main structural proteins; pol, responsible for the retrovirus-specific enzymes; and RRE, a binding site for the Rev protein which facilitates export of the RNA from the nucleus	Kristoffer Riecken
pRSV-Rev	Rev cDNA expressing plasmid in which the joined second and third exons of HIV-1 rev are under the transcriptional control of RSV U3 promote	Kristoffer Riecken
mAPJ VersaClone cDNA RDC0101	Shuttle vector, containing complete ORF for mAPJ, along with Kozak consensus sequence for optimal translation initiation. The gene insert is flanked with convenient multiple cloning sites	R&D Systems (Minneapolis, US)
hAPJ VersaClone cDNA RDC0100	Shuttle vector, containing complete ORF for hAPJ, along with Kozak consensus sequence for optimal translation initiation. The gene insert is flanked with convenient multiple cloning sites	R&D Systems (Minneapolis, US)
hAPLN in pOTB7	pOTB7 vector was constructed by Dr. Michael Brownstein, National Institute of Mental Health; plasmid is used to amplify hAPLN gene by PCR; Selection antibiotic: chloramphenicol	BioCat GmbH (Heidelberg, DE)
LeGO iG2 Puro <sup>+</sup>	Used to clone gene for hAPLNR; expresses eGFP as a reporter gene; Selection antibiotic: puromycin	Kristoffer Riecken
LeGO iC2 Puro <sup>+</sup>	Used to clone genes for hAPLNR, hAPLN; expresses mCherry as a reporter gene; Selection antibiotic: puromycin	Kristoffer Riecken

Recombinant AAV vectors used in this study are listed in Table 19.

**Table 19. Recombinant AAV vectors**

Denotation	Description
AAV-ESGHGYF-CMV-Apelin-IRES-Luc	AAV vector used for transduction of murine lung endothelium. Murine Apelin is cloned within the vector and Firefly luciferase gene serves as a reporter.
AAV-ESGHGYF-CMV-F13A-IRES-Luc	AAV vector used for transduction of murine lung endothelium. Murine Apelin receptor antagonist (F13A) is cloned within the vector and Firefly luciferase gene serves as a reporter.
AAV-ESGHGYF-CMV-Luc	Empty AAV vector, serves as a control. Firefly luciferase gene is integrated.



## 2.1.7 Software, online tools, and databases

Software, online tools, and databases used in this study are listed in Table 20.

**Table 20. Software, online tools and databases**

<b>Denotation</b>	<b>Source</b>	<b>Purpose</b>
Acrobat® Reader DC	Adobe® (San Jose, US)	Reading of PDF files
ApE 2.0 – A plasmid Editor (M. Wayne Davis)	<a href="http://biologylabs.utah.edu/29orgense/n/wayned/ape/">http://biologylabs.utah.edu/29orgense/n/wayned/ape/</a>	<i>In silico</i> DNA analyses
BLAST- Basic Local Alignment Search Tool	<a href="http://blast.ncbi.nlm.nih.gov/Blast.cgi">http://blast.ncbi.nlm.nih.gov/Blast.cgi</a>	Online alignment search for nucleic acid- or protein sequences
CellQuest Pro 5.2.1	BD Biosciences (New Jersey, US)	Flow cytometric analysis
Endnote X9®	ClarivateThomson Reuters/Adept Scientific (London, UK)	Literature management
Excel 365	Microsoft (Redmond, US)	Data editing
FACSDiva™	BD Biosciences (New Jersey, US)	Flow cytometric analysis
Fiji	<a href="http://fiji.sc/Fiji">http://fiji.sc/Fiji</a>	Analyses and graphic editing of fluorescence images
FlowJo	FlowJo LLC (Ashland, US)	Flow cytometric analysis
SnapGene	GSL Biotech LLC (San Diego, US)	Documentation of agarose gels
ImageJ	National Institute of Health (Bethesda, US)	Analyses and graphic editing of fluorescence images
Living Image®4.0	Caliper Lifescience (Waltham, US)	<i>In vivo</i> imaging
Magellan 2	Tecan (Männedorf, CH)	Measurement of absorbance
MikroWin 2000	Berthold Technologies (Oak Ridge, US)	Measurement of luminescence
Nanodrop 2000	Thermo Fisher Scientific (Waltham, US)	Measurement of nucleic acid concentration
Power Point 365	Microsoft (Redmond, US)	Graphic editing
Prism 7.0	GraphPad Software (San Diego, US)	Statistics and graphic editing of data
PubMed	<a href="http://www.ncbi.nlm.nih.gov/pubmed">http://www.ncbi.nlm.nih.gov/pubmed</a>	Online search for literature
Word 365	Microsoft (Redmond, US)	Text editing

### 2.2 Methods

#### 2.2.1 Cell culture

##### *General handling of the cells*

Cells in this study were regularly tested for mycoplasma contamination using the MycoAlert™ Mycoplasma Detection Kit, and only mycoplasma-free cells were used for experiments. Except for hypoxia experiments, cell cultures were incubated in a CO<sub>2</sub>-incubator at 37°C, 95% relative humidity and 5% CO<sub>2</sub>. Handling of all tissues and liquids were conducted under aseptic conditions in a sterile safety cabinet. Different cell lines were maintained under varying culture conditions. Refer to Table 16 for the corresponding cell culture medium.

Cryopreserved cells were quickly thawed by removing the vial from liquid nitrogen and placing the vial in a water bath at 37°C. Cells were then transferred to a 15 mL centrifuge tube with 10 mL of pre-warmed culture media and centrifuged once for 5 min at 300 x g (25°C). After discarding the DMSO-containing supernatant, cells were resuspended in pre-warmed fresh culture medium and transferred to a 25 cm<sup>2</sup> sterile culture flask for expansion, followed by a medium change on the next day.

For this study, both suspension and adherent cell lines were used. Suspension cell lines were cultivated in sterile polystyrene cell culture flasks (T25, T75). They were passaged three times a week, and the minimal and maximal cell densities, recommended by ATCC (American Type Culture Collection) and DSMZ (*Deutsche Sammlung von Mikroorganismen und Zellkulturen*), were maintained.

Depending on their confluence, adherent cells were kept in monolayers and passaged 2-3 times a week after reaching confluency of 80-90%. To detach the cells, medium was removed, and the cell layer was washed once with sterile PBS or 0.2% EDTA in PBS. For detachment, cells were incubated with 1x trypsin for 2-5 minutes at room temperature or in the incubator at 37°C. The reaction was stopped by adding culture medium (1:2 v/v) and the desired cell suspension volume was centrifuged for 5 minutes. The supernatant was removed, and the cells were resuspended in the appropriate medium and transferred back in a cell culture flask.

For long-term storage of eukaryotic cells, the cryopreservation method was used. After centrifugation, the cell pellet was resuspended in the 1.6 mL of cryopreservation medium

(containing 10% DMSO to prevent the crystal formation within cell suspension), distributed to cryopreservation tubes, which were slowly frozen in a cooling rate of 1°C/hr down to -80°C. This was achieved using a cryopreservation chamber filled with isopropanol, known as Mr. Frosty™. After 24 hr, frozen cells were transferred to liquid nitrogen for long-term storage.

### *Cell counting*

Cell concentration and cell viability of a cell suspension were determined using trypan blue exclusion method. For that purpose, a manual or automated hemocytometer was used. To count the cells manually, the cell suspension was mixed with trypan blue solution (1:1 v/v) and added to a Neubauer chamber. Trypan blue is a substance that can only penetrate through non-intact cell membranes, therefore, it can be used to distinguish between dead and live cells. Viable (unstained) and non-viable (stained) cells of four large squares (1 mm<sup>3</sup>, each containing 16 small squares) were counted using the 10x objective of the microscope and the concentration of cells in the initial cell suspension was calculated using the following formula:

$$\text{Viable cells / mL} = \text{counted viable cells} * 2 \text{ (dilution factor)} * 10^4$$

The viability of the cell solution was calculated by using the following formula:

$$\text{Viability [\%]} = \text{viable cells} / (\text{viable} + \text{dead cells}) * 100$$

The automated hemocytometer Vi-Cell™ XR uses the same method to determine the viable cell number and viability of a cell solution.

### 2.2.2 Monocyte to macrophage polarization

#### *Isolation of PBMCs*

Peripheral blood mononuclear cells were isolated from healthy donors from the fraction of the blood sample, which is rich in the white blood cells and platelets (Buffy Coat), by polysucrose density gradient centrifugation.

Peripheral blood was diluted with PBS in ratio 1:1 (v/v). The sample was slowly and carefully layered on top of polysucrose solution and centrifuged for 30 minutes at 400 x g, at room temperature with the brake function switched off, which resulted in the formation of three layers. Separated according to their density, the PBMC could be found in the intermediate layer between the polysucrose medium and residual blood plasma. To ensure complete lysis of the

## MATERIAL AND METHODS

---

erythrocytes, isolated PBMCs were treated with 3-5 mL of erylisis (erythrocyte lysis) buffer for 5 minutes followed by a washing step in PBS.

### *Monocyte isolation*

To obtain the M<sub>2</sub>-macrophage phenotype, PBMCs from healthy donors were used to isolate and further stimulate the polarization of monocytes. Human monocytes were isolated from PBMCs by Monocyte Isolation Kit using negative selection settings, as described by the manufacturer.

### *Polarization to macrophages*

Polarized macrophages were obtained by two different methods.

In the first method (direct), uncommitted, M<sub>0</sub> macrophages were obtained by culturing freshly isolated monocytes for 6 days in RPMI 1640, supplemented with 10% FBS and 50 ng/ml Macrophage Colony Stimulating Factor (M-CSF) in 6-well plates at a density of  $2 \times 10^6/2$  mL/well. Polarization to M<sub>1</sub> and M<sub>2</sub> phenotype was obtained by removing the existing culture medium and culturing cells for additional 24 hr in RPMI 1640 supplemented with 10% FBS, 100 ng/ml LPS and 20 ng/ml IFN $\gamma$  (for M<sub>1</sub> polarization) or 20 ng/ml interleukin 4 (IL-4) (for M<sub>2</sub> polarization).

In the second method (indirect), PBMCs were seeded in a 6-well cell culture plate at a density of  $5 \times 10^6/5$  mL/well in RPMI 1640, supplemented with 10% FBS and 1 ng/mL M-CSF. After two days, the medium has been changed daily. On the sixth day, IL-4 was added at a concentration of 20 ng/mL to induce 24 hr polarization toward M<sub>2</sub> macrophages. Twenty four hours after the last change, the medium was changed again. In addition, half of the cells were stimulated with [Pyr1]Apelin-13 at a concentration of 10-50 pmol/L for 6 hr. The remaining cells served as negative control and were mixed with standard medium, supplemented with 10% FBS, M-CSF and IL-4. No M<sub>1</sub> macrophages were polarized indirectly. The cells were then either analyzed at the transcriptional level or the expression of different surface proteins was investigated by flow cytometry.

### 2.2.3 Functional assays

#### *Proliferation assays (cell count analysis)*

Effects of Apelin and MM54 on the proliferation rate of control and APJ-overexpressing AML cell lines was evaluated by the count of viable cells after stimulation/inhibition. For APJ-overexpressing cells, the assay was performed in the presence of selection antibiotic (puromycin, 2  $\mu\text{g/mL}$ ). Transgenic cell lines were tested for APJ expression by flow cytometry and RT-qPCR prior to the experiments (refer to supplementary material). Cells were seeded in triplicates in a 24-well plate at cell concentration of  $0.3 \times 10^6$  cells/mL. After three to four days of incubation, the cell number was determined with the trypan blue exclusion on Vi-Cell™ XR. Initial cell concentration was confirmed by double count at the Vi-Cell™ XR after seeding the cells and it was included in the analysis of the results.

#### *WST-1 assay*

According to the manufacturer, this test is based on the reduction of a tetrazolium salt, which can be used to quantify the cell proliferation or cell viability<sup>282</sup>. The salt is broken down to formazan by the mitochondrial dehydrogenase succinate-tetrazolium reductase, which is present in metabolically active cells. Therefore, WST-1 assay can be used to measure the overall metabolic activity inside a cell. The rate of WST-1 cleavage by mitochondrial dehydrogenases correlates with the number of viable cells in the culture.

To conduct this assay, solid tumor cell lines were used. Cells were seeded in an optimized seeding density of 10 000 cells/100  $\mu\text{L}$ /well and stimulated with Apelin and MM54 at different concentrations, following the incubation period for 24-48 hr. Upon incubation, WST-1 was added to each well and absorbance measured against a background control using a microplate reader at 440 nm at different time points. Second reading at 630 nm was recorded and subtracted from the 440 nm reading to control for artifacts. The effect of the substance on proliferation was quantified by measuring the absorbance of treated cells and comparing this to vehicle control cells, following the normalization of the proliferation rate.

#### *Colony formation assays*

The effects of stimulation and inhibition of APJ on the cell colony-forming abilities were examined on wildtype and APJ-overexpressing AML cell lines. As a semi-solid cell suspension medium, MethoCult™ H4230 was thoroughly mixed with basal IMDM medium with no

## MATERIAL AND METHODS

---

addition of growth factors since AML cell lines normally do not require these factors for colony formation. Cells were seeded in triplicates at a density of 250 cells/mL. Carefully avoiding the formation of air bubbles, 1.1 mL of cell suspension was plated onto 3.5 cm-Petri dishes. Cells were incubated for seven days at 37°C, 21% O<sub>2</sub>, 5% CO<sub>2</sub>, and 95% relative humidity. The colony count was assessed by manual counting under an inverted microscope. For transgenic cell lines, the assay was performed in the presence of the appropriate selection antibiotic (puromycin, 2 µg/mL). Cells used in the assays were verified for the presence transgenes by flow cytometry and RT-qPCR, as well as by microscopic observation of eGFP positivity.

### *Migration assay*

Automated cell migration assay was performed in collaboration with the research group of Prof. Dr. Manfred Jücker (with the kind help of Dr. Daniel Smit), using Incucyte™ microscopy system. Cells were grown to 90 - 95% confluency in a 96-well plate specialized for migration assays. Prior to stimulation with Apelin and MM54, a scratch was made in every well using IncuCyte® WoundMaker. After placement of the wound, cell media and floating cells were removed and the wells were washed once with basal medium. After washing step, cell medium was replaced with fresh one and supplemented with [Pyr1]-Apelin-13 or MM54. Water was used as solvent control. Having a built-in camera, the device was able to record cell migration status every 1 hr. The score of migrated cells was obtained by scanning the surface of the gap between cell fractions.

### *Hypoxia assay*

For performing experiments under hypoxic conditions, solid tumor cell lines were cultured in the hypoxia incubator at 37°C in the atmosphere containing 1% O<sub>2</sub> and 5% CO<sub>2</sub>. Prior to hypoxia experiments, cells were seeded in 6-well plates and were kept under normoxic conditions until reaching 80% confluency. After transferring to the hypoxia incubator, cells were kept for 2, 4, 8 and 24 hours. Cells were then detached from the surface using a cell scraper and stored in RNAlater until RNA extraction. Extracted RNA was reverse transcribed to cDNA and the samples were further subjected to RT-qPCR.

### *IFN $\gamma$ stimulation experiments*

To examine the effect of IFN $\gamma$  on Apelin receptor expression, AML cell lines, as well as on solid cell lines, were seeded in triplicates in defined optimal density in 12-well plates. Upon seeding, when the solid cells became adherent, interferon-gamma (IFN $\gamma$ ) was added to each

triplicate in three different concentrations. After 72 hours, solid tumor cells were trypsinized according to the general protocol and, together with AML cell lines, were washed once with PBS. Cells were further stained with the antibody against APJ and surface expression of APJ was measured by flow cytometry. Additionally, cells were stained for live/dead population with Annexin V, according to the manufacturer's recommendation. As a control for live/dead cell population, 50% of control, viable cells, were exposed to fatal 70°C for 10 minutes, and after cooling they were mixed with live, untreated cells, following the live/dead staining. This ensured that the control contains both live and dead groups in order to confirm the efficient binding of Annexin V.

#### *Killing assay - cytotoxic assay*

Killing assays were performed by incubating AML cell lines as target cells with peripheral blood mononuclear cells (PBMCs) as effector cells. Cells expressing enhanced green fluorescent protein (eGFP) were used as vector control. AML control (eGFP) and APJ-overexpressing cells were co-cultured with PBMCs of healthy donors in a ratio 1:5 and incubated with 0.1 ng/mL CD33-CD3 BiTE (bi-specific T-cell engager) antibody construct, as well as with 10 µg/mL of a T-cell immunoreceptor with Ig and ITIM domains (TIGIT) antibody or the corresponding isotype controls. After 24 hr of incubation, flow cytometric analysis was performed using 7-AAD as a marker for eGFP<sup>+</sup> dead cells.

#### 2.2.4 Gene and protein expression analyses

##### *Flow cytometric analyses*

Flow cytometry is a technique that enables the characterization of single cells within a cell suspension based on their size and granularity as well as fluorescent labeling. Fluorophore-conjugated antibodies are used to label cell surface as well as intracellular proteins, to determine their expression. Moreover, fluorescent protein expression, such as expression of eGFP or members of mFruits family (mCherry), can be detected by flow cytometry. Hydrodynamic focusing allows the cells to enter the laser beam one by one. The laser beam is scattered when it strikes the cell and the light scattering is detected as forward scatter (FSC) and side scatter (SSC). Fluorophores or expressed fluorescent proteins are excited by the laser and their emitted light can be detected.

## MATERIAL AND METHODS

---

For the purpose of this study, flow cytometric analyses were performed on either FACS Calibur with the software CellQuest Pro or FACS Canto with the software FACS Diva. Java-based FlowJo software was additionally used to analyze the raw data. Cell sorting was performed on a FACS Aria IIIu at the FACS Core Facility (UKE). Antibodies used for fluorescent labeling of the cells are shown in Table 10.

### *Stainings for flow cytometric analysis*

Typical staining conditions included cell washing with PBS, followed by resuspension of cells in 100  $\mu$ L FACS buffer (10% AB v/v serum). Cells were stained with the appropriate amount of antibody (according to the manufacturer's recommendation) and incubated at 4°C in dark for up to 30 minutes. Cells were then washed with PBS and resuspended in 300-400  $\mu$ L PBS, depending on a cell number. Depending on the research application/question, cells were additionally stained for live/dead populations using FITC-coupled Annexin V, according to the manufacturer's recommendation. Isotype and live/dead control were included for certain experiments.

### *Gene expression analysis*

Gene expression analysis was performed by real-time reverse transcription quantitative polymerase chain reaction (RT-qPCR). Refer to General molecular biology methods (2.2.6).

## 2.2.5 Protein quantification

### *Total protein quantification in animal tissues*

This protocol was adapted from Andersen *et al.*<sup>283</sup>. After isolation, lung tissues were kept at -80°C following homogenization in lysis buffer, RIPA (approximately 5 ml/g of tissue), supplemented with protease inhibitor cocktail for mammalian cell and tissue extracts (cOmplete™ Protease Inhibitor Cocktail tablets, stock solution 50x) and sodium orthovanadate (1 mM). Samples were kept on ice for 30 minutes and were vortexed every 10 minutes. Upon incubation, samples were centrifuged at 7000 xg at 4°C for 10 min. Supernatants were collected and protein levels in animal tissues were determined using Bio-Rad DC Protein Assay, which is a modified version of Bradford's assay<sup>284</sup>.



*Apelin quantification from plasma samples and tumor tissues*

To quantify the level of Apelin (F13A) in human plasma and mouse lung tissue, two different ELISA kits were used, depending on a sample. Human plasma samples were diluted 1:1 v/v and further processed using spectrophotometric Apelin-12 Extraction-Free EIA Kit (spectrophotometric), following the manufacturer's instructions. Supernatant from homogenized lung tissue was diluted 1:75 v/v and all samples were quantified using chemiluminescent Apelin-12 EIA Kit (chemiluminescent), following the manufacturer's instructions. All samples were analyzed in duplicates and detection of Apelin was confirmed with a positive control (diluted standard Apelin peptide was provided in the kit).

*Western blot\**

To perform Western blot analysis for the presence of Apelin receptor, SDS-PAGE was carried out to separate denatured proteins by size. The proteins were prepared for electrophoresis by cell lysis using RIPA Buffer and mixing whole cell lysate containing 20 µg protein with Lane Marker Reducing Sample Buffer (5X) to a final concentration of 1x in a total volume of 20 µL. The samples were denatured for 5 minutes at 95°C prior loading to the SDS-gel. All further steps (protein transfer, blocking with 5% BSA, incubation with antibody) were performed according to the antibody manufacturer's recommendation.

## 2.2.6 General molecular biology methods

*Sample preparation, RNA extraction*

Maximum number of  $5 \times 10^6$  cells were washed once with PBS and either used immediately for the extraction or stored in RNAlater stabilization solution at -80°C. To isolate RNA, cells in RNAlater were thawed and centrifuged at 20 000 xg for 10 minutes at room temperature. Up to 20 mg of tissue per sample was homogenized in PBS and RNA isolation was performed. The innuPREP RNA Mini Kit 2.0 was used according to the manufacturer's instructions for total RNA extraction.

The total RNA concentration was determined photometrically with the NanoDrop™ by measuring the absorbance at 260 nm and samples were stored at -80°C. RNA purity was

---

\* Due to high unspecific binding of the primary anti-APJ antibody in all processed samples, analysis of Western blot data are not presented. Therefore, the method is only briefly described in this section.

## MATERIAL AND METHODS

---

assessed by examining the absorbance ratios (A260/A280 and A260/A230 ratio). According to the manufacturer, ratios of 2.0 indicated pure RNA. All materials and reagents that have been used were RNase-free.

### *cDNA synthesis*

Synthesis of complementary DNA (cDNA) was performed by transcribing 1 µg of isolated RNA with the commercial Kit PrimeScript™ RT Master Mix, according to the manufacturer's instructions. The transcribed cDNA was diluted 1:5 v/v with DEPC-treated water and stored at -20°C or used directly for RT-qPCR.

### *Primer design and reconstitution*

The majority of PCR primers for this study were designed manually using Primer3Plus software<sup>285</sup>. When possible, intron-spanning primers and intron-exon boundary primers were used for RT-qPCR. All primers were synthesized by Eurofins Genomics and were reconstituted in RNase-free water to a final concentration of 100 µM. Primer efficiencies were validated by MTA Gabi Vohwinkel.

### *Real-time reverse transcription quantitative polymerase chain reaction (RT-qPCR)*

The gene expression analysis was performed by Real-time reverse transcription quantitative polymerase chain reaction (RT-qPCR). The principle of RT-qPCR is based on the intercalation of a fluorescent dye SYBR Green in the double-stranded PCR products and continuous measuring of the fluorescence intensity. Hence, the fluorescence intensity is proportional to the amount of PCR product.

The Kit TB Green Premix Ex Taq™ II and the plate-based Real-time quantitative PCR system LightCycler® 96 were used for all RT-qPCR analyses according to the manufacturer's instructions. Samples, standards, and controls were measured in triplicates. The general reaction condition used for RT-qPCR is shown in Supplemental data.

For quantification of the gene expression, Pfaffl<sup>286</sup>,  $\Delta\text{Ct}$  ( $2^{-\Delta\text{Ct}}$ ) or  $\Delta\Delta\text{Ct}$  ( $\Delta\text{Ct}$  with normalization to control sample) method was used. Results were normalized to the expression of the housekeeping gene GAPDH (glyceraldehyde 3-phosphate dehydrogenase). Using the Pfaffl method, the efficiency of each primer was taken into account.

### *Clean-up of the PCR product*

Purification of PCR product was achieved using the kit NucleoSpin® Gel and PCR Clean-up in accordance with the manufacturer's instructions. Purified DNA was eluted with DEPC-treated water and the concentration and sample quality was determined photometrically with the NanoDrop™.

### *Digestion*

Depending on their final concentration, purified PCR product and vector were each digested with 1 µL of the Fast Digest restriction enzymes in a total volume of up to 30 µL for a maximum of 1 hr at 37°C. Digestion longer than 1 hr was avoided due to the STAR activity of Fast digestion enzymes.

### *Ligation*

For successful ligation of the purified insert into the linearized vector, T4 DNA Ligase was used. Ligation was performed in 1:1 – 1:7 molar ratio (vector:insert) with up to 100 ng of vector-DNA. The ligation mix was incubated for 15 minutes at 16°C, followed by 4°C overnight and completed on the next day for 10 minutes at 22°C. Depending on the need, the reaction was stopped at 65°C for 10 minutes.

### *Sequencing*

The sequencing of all cloned plasmids, including hAPJ-LeGO iG2/Puro<sup>+</sup>, hAPJ-LeGO iC2/Puro<sup>+</sup>, hAPLN-LeGO iC2/Puro<sup>+</sup>, mAPJ-LeGO iC2/Puro<sup>+</sup>, mApelin-AAV-Luc, mF13A-AAV-Luc was performed by the company Eurofins Genomics GmbH (Ebersberg, DE), according to the company's instructions.

### *Transformation of Escherichia coli*

Competent *Escherichia coli* (*E. coli*) bacteria (Library Efficiency™ DH5α™ Competent Cells, competent DH10B) were used to replicate foreign plasmid DNA. To transform bacteria, heat shock and electroporation methods were carried out. Electroporation was performed with the kind help of Prof. Dr. Jakob Körbelin, using the device and the recommended settings of Dr. Körbelin's research group (AG Trepel). Heat shock was adapted from a nonprofit plasmid repository, Addgene<sup>287</sup>. The transformation-mix was plated on LB agar plates containing the

## MATERIAL AND METHODS

---

appropriate selection antibiotic (100 µg/mL ampicillin, 25 µg/mL chloramphenicol). The plates were incubated overnight at 37°C.

### *Qualitative colony-PCR*

To check for the presence of a specific gene region in bacterial clones, qualitative PCR was used. To accomplish this, a single colony from the LB agar plate was picked and transferred to 20 µL sterile water. In parallel, 10 µL of the suspension was used to inoculate 5 mL LB medium containing ampicillin (100 µg/mL) or chloramphenicol (25 µg/mL). The remaining suspension was used as a DNA template for the qualitative PCR, using the DreamTaq™ Green PCR Master Mix according to the manufacturer's instructions. For a general program used for colony-PCR, see supplemental data.

### *Extraction of plasmid DNA from E. coli*

For optimal bacterial replication of transformed bacteria, LB-medium containing the appropriate antibiotic (100 µg/mL ampicillin, 25 µg/mL chloramphenicol) was inoculated with the desired clone. Clones were taken from an LB agar plate (when confirmed by qualitative PCR) or from a glycerol stock and incubated overnight at 37°C (or 30°C in case of pAAV plasmid) and 180 rpm in a bacterial shaker. Plasmid extraction was performed by using the NucleoSpin® plasmid kit or the NuclioBond® Xtra Midi Plus kit, according to the manufacturer's instructions. The DNA concentration was determined photometrically with the NanoDrop™.

### *Agarose gel electrophoresis*

Agarose gel electrophoresis was performed to determine the DNA product size. Gels containing 1% agarose (with the addition of ROTI®GelStain nucleic acid stain) were run at 100 V in 1x TAE buffer for 30 - 60 min, dependent on the length of gel and size of the product. All gels were run with DNA ladders of different sizes. UV-light was used to visualize the DNA bands.

### 2.2.7 Cloning strategies

The vectors containing the gene of interest (GOI) were created using restriction cloning. Methods used for cloning are described in more detail in the following sections. All kits, enzymes and buffers were used as recommended by the manufacturer. Upon cloning, the ligation product was further transformed into competent *E. coli* cells and positive clones

(confirmed by colony-PCR) were selected for plasmid isolation. Verification of successful cloning was performed by Sanger sequencing of the recombinant plasmid, using sequencing primers specific for the region of interest. To produce multiple copies of plasmid, DNA was extracted from inoculated bacteria using a commercially available kit. For PCR conditions used for cloning, refer to supplemental data.

#### *Cloning Apelin and F13A in AAV vectors*

Adeno-associated viral vectors (AAV, in particular pAAV-CMV-Luc was used for cloning), which specifically target mouse lung endothelial cells, were designed and kindly provided by Prof. Dr. Jakob Körbelin<sup>277</sup>. In this technically complex process, genes for murine Apelin and F13A were cloned together with firefly luciferase (LUC) inside AAV. The completed plasmid was comprised of Apelin/F13A and firefly luciferase gene, separated by the Internal ribosome entry site (IRES) sequence. These elements are cis-acting RNA regions that promote internal initiation of protein synthesis using cap-independent mechanisms<sup>288</sup>. IRES sequence was cloned from LeGO plasmid, generously provided by PD Dr. Kristoffer Riecken.

Part of LUC gene (part\_LUC) was amplified from pAAV-CMV-Luc with overhanging BsrGI and MscI restriction sites. After digestion with the aforementioned enzymes, part\_Luc was cloned into LeGO-iG2 vector. LeGO-iG2 vector (with part\_Luc) and pAAV-CMV-Luc were then digested with EcoRI and HindIII, following blunting with the Klenow fragment. To get the new plasmid (pAAV-CMV-IRES-Luc), sequences were digested both with BsrGI, and IRES-part\_LUC sequence from digested LeGO vector was ligated to the larger part of digested pAAV-CMV-Luc sequence. After amplification, pAAV-CMV-IRES-Luc and pAX28 plasmid (containing Apelin or F13A gene) were digested with StuI and SacII, and Apelin/F13A sequence was ligated to pAAV-CMV-IRES-Luc, forming pAAV-CMV-(Apelin/F13A)-IRES-Luc plasmid.

#### *Luminescence assay and confirmation of successful cloning*

To test for the presence and functionality of a reporter gene within AAV plasmid, luminescence assay was performed using Dual-Glo® Luciferase Assay System, which enables fast and simple quantitation of a stable luminescent signal from firefly luciferase reporter gene (LUC) in a sample. HEK293 cell were seeded in an optimal density of 10 000 cells/200 µL/well in 96-well plate. Upon their attachment to the surface, 0.2 µg of DNA was mixed with TurboFect™ Transfection reagent and used to transiently transfect the cells with AAV plasmid containing

## MATERIAL AND METHODS

---

the gene of interest. Following the incubation period of 24-48 hours, luminescence was measured.

### *Cloning APJ and APLN in lentiviral vectors*

To use the lentiviral vector system for transduction of solid tumor and leukemic cell lines, LeGO plasmids (including helper plasmids) were kindly provided by PD Dr. Kristoffer Riecken. Vector maps and sequence data for the mentioned vectors are available at his webpage<sup>289</sup>. The cloning was performed by PCR amplification of the gene of interest to create overhangs with specific restriction sites.

Human APLN gene was amplified from hAPLN\_pOTB7 plasmid using previously designed primers (for sequences, see Table 17). Due to lack of restriction sites in pOTB7 plasmid, reverse primer contained NotI overhang sequence. Amplicon and LeGO iC2 plasmid were digested with EcoRI and NotI and digested amplicon was ligated to the larger sequence of digested LeGO plasmid.

Human APJ gene was amplified from Versa Clone APJ plasmid. Due to the lack of restriction sites in the aforementioned plasmid, primers were manually designed to contain EcoRI and StuI restriction sites (see Table 17). Amplicon and LeGO iG2 plasmid were digested with EcoRI and StuI and digested amplicon was ligated to the larger sequence of digested LeGO plasmid.

### 2.2.8 Virological methods

#### *AAV production in HEK 293T cells*

This protocol was part of the doctoral thesis of Prof. Dr. Jakob Körbelin<sup>290</sup> and it was adapted from Xiao *et al.*<sup>281</sup>. Embryonal kidney cells (HEK 293T) were kept in Petri dishes until 70% confluency. For each cell dish following composition was prepared and thoroughly mixed (Table 21).

**Table 21. Plasmid composition for AAV production**

12.00 µg	DNA total:
3 µg	ITR-containing plasmid e.g. reporter plasmids
3 µg	AAV <i>rep/cap</i> plasmid without ITRs
6.00 µg	Ad-pXX6 (containing E1A, E1B, E2A, E4-orf6, VA)
ad 450.00 µl	serum-free DMEM (Gibco)
120.00 µl	Polyfect transfection reagent (Qiagen)

After incubating to allow complex formation, the mixture was filled up with complete DMEM medium. The complete mixture was evenly distributed dropwise on the cells and mixed by gentle swirling. One day after transfection, the medium was exchanged by fresh supplemented DMEM medium and cells were incubated for another 2-3 days.

Transfected cells were carefully washed with PBS and detached from the surface of the cell dishes with a cell scraper. The cells were rinsed with PBS and transferred to tubes. Cell suspension was centrifuged, supernatant was discarded, and the cell pellet was resuspended with PBS-MK (phosphate-buffered saline, 1 mM MgCl<sub>2</sub>, 2.5 mM KCl). The viral particles were released from the cells by three repeated freeze/thaw cycles. Cellular nucleic acids were digested with nuclease (Benzonase) and the lysate was clarified by centrifugation. Supernatants containing the viral particles were stored at -80 °C until further purification by iodixanol density gradient centrifugation. The whole procedure was supervised by Prof. Dr. Jakob Körbelin.

#### *Iodixanol density gradient centrifugation*

This protocol is fully described in the doctoral thesis of Prof. Dr. Jakob Körbelin<sup>290</sup> and it was adapted from Hermens *et al.*<sup>291</sup>. The iodixanol gradient in this protocol is composed of steps intended to separate contaminants from an impure AAV preparation and it was performed in order to enrich AAV fraction. The whole process was supervised and assisted by Prof. Dr. Jakob Körbelin. After purification and enrichment, AAV particles were stored at -80 °C until titration and further use.

#### *Production of lentiviral particles*

This method was adapted from Weber (Riecken) *et al.*<sup>292</sup>. Lentiviral particles were used in order to transduce cell lines. To achieve the safety requirements during this study, third generation lentiviral system was used. Co-precipitation with calcium phosphate was used to transfect the target cells, human embryonal kidney cells (HEK 293T), with plasmids of the lentiviral system (Table 22). For safety reasons, all the work was carried out under the conditions of biological safety level S2.

**Table 22. Plasmid composition for lentiviral production**

Plasmid	Quantity
LeGO	10 µg
pMDLg/pRRE	10 µg
pRSV-Rev	5 µg
phCMV-VSV-G	2 µg

Calcium chloride ( $\text{CaCl}_2$ ) was added to the plasmid mixture to a final concentration 0.25 M. DNA- $\text{CaCl}_2$  mix was added dropwise under air bubbles to 100 µL 2x HEPES-buffered saline buffer (HBS). To produce lentiviral particles for overexpression of gene of interest (GOI), HEK 293T cells were seeded for each construct in a 10 cm cell culture dish at a density of  $5 \times 10^6$  cells/dish. Following the cell incubation, medium was replaced with 10 mL fresh DMEM + 10% FBS, supplemented with 25 µM chloroquine. Chloroquine inhibits the lysosomal degradation of the DNA which is taken up by the cells, therefore improving transfection efficiency<sup>293,294</sup>. Prepared calcium-phosphate-DNA co-precipitate was added dropwise in a final volume of 1 mL. After 24 hr of incubation, the supernatant was replaced with 8 mL fresh DMEM + 10% FBS. Virus-containing supernatant was harvested after 24 hours and stored at  $-80^\circ\text{C}$ .

#### *Transduction with lentiviral vector system*

To establish an effective and stable transgene integration into the genome of host cells, transduction was performed using lentiviral vector system. The likelihood of the multiple insertions, which may present the risk for mutations, was minimized by not exceeding the maximum transduction efficiency of 50%. All work was carried out under the conditions of biological safety level S2. Transduced cells were handled under the conditions of biological safety level S2 until one week after transduction (at least three splitting or medium changes) and later on under conditions of biological safety level S1.

Virus supernatants were used directly to transduce cells. For AML cell lines, 100 000 cells in 1 mL cell medium supplemented with 10 µg/mL polybrene were seeded in a 24 well-plate and treated with 1 - 150 µL virus supernatant in duplicates, depending on the cell line. Solid tumor cell lines were seeded in 24-well plates and kept in culture until reaching optimal confluence for transduction (80%). Following the centrifugation for 1 hr at 2000 rpm and the cells were



incubated overnight. After the medium replacement, the cells were further incubated up to four days, depending on the cell line. Adherent cells were detached and transduction efficiency was determined by flow cytometry, based on the percentage of eGFP<sup>+</sup> or mCherry<sup>+</sup> cells. The selection of transgenic cells was started by supplementing the medium with 2 µg/mL puromycin.

#### *Evaluation of the transduction efficiency*

The flow cytometric analysis of the transduced cells was assessed by following the general laboratory protocol of our research group (AG Akute Leukämien). Following the cell transduction, evaluation of the transduction efficiency was performed. The percentage of eGFP<sup>+</sup> or mCherry<sup>+</sup> cells was determined four days after transduction. To avoid the potential viral infection risk, freshly transduced cells were handled under biological safety level S2 conditions following the fixation with formaldehyde solution (Formafix 4%). Cells were then centrifuged in a capped FACS-tubes (round bottom) and resuspended in Formafix 4%. After 30-minute incubation at room temperature, the cells were washed once with PBS, resuspended in 300-400 µL PBS and analyzed at a flow cytometer. As a control, wildtype cell sample was included in the experiment. For general flow cytometric method, refer to section Gene and protein expression analyses (2.2.4).

#### *Cell sorting of transduced cells*

To exclude the wildtype cells and to further purify transduced cell population, after every transduction, a fluorescence-activated cell sorting (FACS) was performed. For the purpose of all *in vivo* experiments as well as for the functional assays, transduced cells were sorted at a FACS Aria IIIu (at UKE FACS Core Facility) based on eGFP or mCherry positivity. All transduced cells are shown in the supplemental data. For general flow cytometric method, refer to section Gene and protein expression analyses (2.2.4).

#### *2.2.9 In vivo experiments*

All experiments at the University Medical Center Hamburg-Eppendorf (UKE) involving animals were conducted in accordance with the German animal protection code (*Tierschutzgesetz*). The local authority and the ethics review board (*Behörde für Soziales, Familie, Gesundheit und Verbraucherschutz – Lebensmittelsicherheit und Veterinärwesen, Hamburg, DE*) granted Approval (in German, „*Die Bedeutung des Rezeptor-Liganden-Systems*

## MATERIAL AND METHODS

---

*APJ/Apelin in der Pathophysiologie von Krebserkrankungen*“, 18/63). Animals were housed in individually ventilated cages (IVCs) with a 12 hr light cycle at the UKE animal facility. Female C57BL/6 mice were kept under pathogen-free conditions and handled in accordance with the European Community recommendations for experimentation. All *in vivo* experiments were carried out with the generous help of Dr. Stefan Horn.

### *Subcutaneous mouse model*

In order to assess spontaneous lung metastasis formation and to find the optimum cell number for induction of metastasis, cell titration experiments were performed. Three C57BL/6 mice per group were subcutaneously injected with  $1 \times 10^5$ ,  $3 \times 10^5$ ,  $1 \times 10^6$ ,  $3 \times 10^6$  and  $1 \times 10^7$  cells of three murine cell lines, Lewis lung carcinoma (LLC1), colon adenocarcinoma (MC38) and melanoma cell line (B16). Mice were sacrificed after reaching critical tumor size, following the lung extraction. Prior to further analysis, lungs were fixed in formaldehyde, embedded in paraffin and slices were made at the Anatomy Department (UKE). Subcutaneous tumors were used as a control for immunohistochemical analysis.

### *Intravenous model of tumor metastasis*

The formation of metastasis was initiated by injecting tumor cells directly via the tail vein of the mice. Experiment was started by intravenously injecting  $2 \times 10^6$  LLC1 or MC38 cells into the mouse tail vein. Prior to injection, tumor cells were stably transduced using a lentiviral vector system to express an enhanced green fluorescent protein (eGFP). To quantify tumor metastatic burden, flow cytometry was performed, based on the eGFP positivity of tumor cells.

### *Anti-angiogenic and AAV treatment*

For treatment, DC101, an anti-angiogenic monoclonal antibody targeting the receptor for Vascular Endothelial Growth Factor (VEGFR-2), was used. For all models, treatment was initiated four days after transplantation and the mice were injected intraperitoneally two times per week with 40  $\mu\text{g/g}$  DC101 until sacrificing. AAV vectors were intravenously injected two days after tumor cell injection ( $1.5 \times 10^{11}$  viral particles per mouse).

### *Bioluminescence imaging (BLI)*

For analyses of luciferase transgene expression, BLI was performed prior to sacrificing the mice using Xenogen IVIS 200 imaging system in *In vivo* optical imaging core facility (UKE). After

intraperitoneally injecting 100  $\mu$ l/mouse firefly D-luciferin potassium salt (30 mg/ml in PBS) under gas anesthesia (2% (v/v) isoflurane, 98% (v/v) oxygen), representative images were taken when luminescence (photons/sec/cm<sup>2</sup>) reached the highest intensity (around 15 min after administration of D-luciferin). Luminescence was measured over a period of 5-10 min/measurement, with a binning of 1. Data were analyzed with the software Living Image. After sacrificing, *ex vivo* imaging was carried out on extracted lungs.

#### 2.2.10 Immunohistochemistry

With kind help of Dr. Stefan Horn, lung tissues were extracted from C57BL/6 mice injected with tumor cells. The lungs were split in two parts. Larger (right) lung parts were fixed in 4% paraformaldehyde (PFA) for up to 24 hr, washed, transferred to PBS and stored at 4 °C. Further processing of the lung tissue, including slicing, immunohistochemical staining and slide scanning, was carried out by Mouse Pathology Facility of UKE. Lung tissue slides were stained with CD31, CD3, eGFP and CD11b antibodies (provided by Facility).

Microvessel density was assessed by adaptation of the previously described protocol<sup>295</sup>. Angiogenic hotspots were detected with kind help and assistance of a pathologist, Dr. Daniela Bajdevska. Tumor tissue was identified by eGFP positivity. Scaling and division of whole slide images was done using the pathology slide viewing software, Aperio ImageScope (Leica Biosystems), which is well suited to handle extremely large images > 500 MB. Color deconvolution, thresholding and subsequent quantification was performed by the creation of a macro for Fiji/ImageJ version 1.52p with Java version 1.8.0\_172 (refer to supplemental data).

#### 2.2.11 Statistics

All the statistical work was carried out with the program Graph Pad Prism. Values are shown as mean  $\pm$  standard deviation (SD). For most of the analyses, statistics were performed as unpaired and paired t-test (two-tailed) and repeated-measures one-way ANOVA followed by Tukey's or Dunnett's multiple comparison test. The following levels of significance were defined: ns = non-significant;  $p < 0.05 = *$ ;  $p < 0.01 = **$ ;  $p < 0.001 = ***$ .

### 3. RESULTS

#### 3.1 Apelin and APJ expression in immune and endothelial cells

As a continuation of preliminary findings from our research group<sup>296</sup>, Apelin/APJ gene and protein surface expression were examined in primary cells, tumor tissue and tumor cell lines. Since proangiogenic macrophages are often found in tumors, it was hypothesized that their communication with the endothelial cells is carried out via apelinergic signaling.

##### 3.1.1 Polarization to proangiogenic M<sub>2</sub> macrophage phenotype

Several methods of *in vitro* macrophage polarization have been tested. To confirm successful macrophage polarization, flow cytometric analysis of the specific pattern of marker expression was performed before and one week after the stimulation of monocytes. Expression of seven markers for monocytes and polarized M<sub>2</sub> macrophages was compared. The following markers are surface receptors (CD14, CD11b, Tie2, APJ, CD200R), including M<sub>2</sub>-phenotype-specific costimulatory receptors, such as CD163 (hemoglobin scavenger receptor) and CD206 (mannose receptor). Example of comparison for markers CD14, CD163 and CD206 is shown on Figure 4.

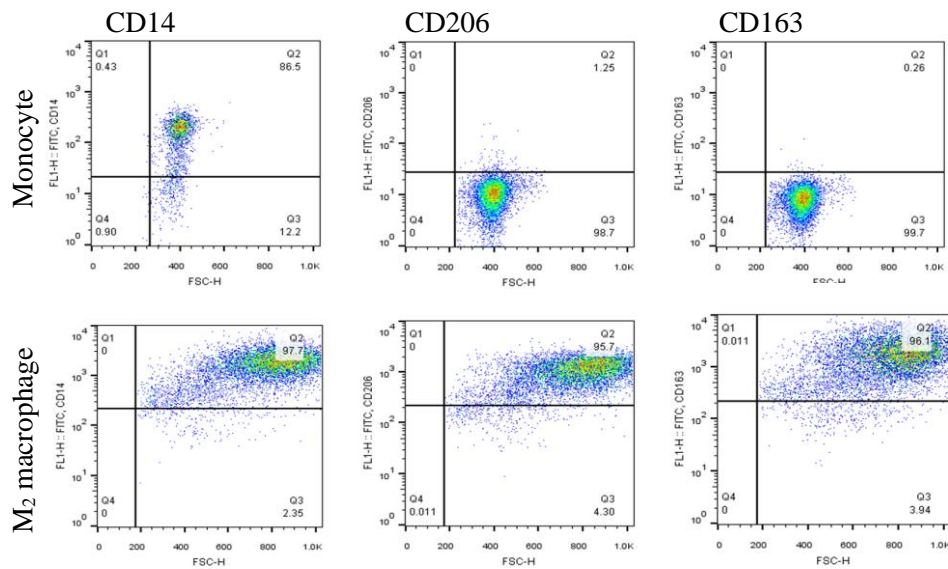


**Figure 4. Representative flow cytometric analysis of freshly isolated monocytes and M<sub>2</sub> macrophages.** Cell debris, as well as dead cells, were excluded during every analysis and surface expression of the specific markers is presented for both monocytes and M<sub>2</sub> macrophages (CD14, CD206, and CD163). In comparison to monocytes, high expression of CD163 and CD206 was seen on M<sub>2</sub> macrophages.

Monocyte-derived macrophages showed higher CD206 expression in comparison to freshly isolated monocytes, indicating that IL-4/M-CSF phase-polarization was sufficient to induce M<sub>2</sub> macrophage phenotype. High surface expression of CD14 was constantly present in both monocytes and polarized macrophages. Cumulative expression profiles of freshly isolated monocytes and polarized macrophages are shown in Figure 5. Further examination into different M<sub>2</sub> macrophage subtypes was not assessed in this study.

To support previous findings, polarization was confirmed by comparing morphological features between monocytes and macrophages. Unlike monocytes, which remained in suspension, M<sub>2</sub> macrophages remained completely adherent. In comparison to uncommitted M<sub>0</sub> phenotype with classical fried egg large, round, and flattened morphology, M<sub>2</sub> cells kept more spread morphology, appearing as adherent and stretched, “spindle-like” cells<sup>297-299</sup> (Figure 5).

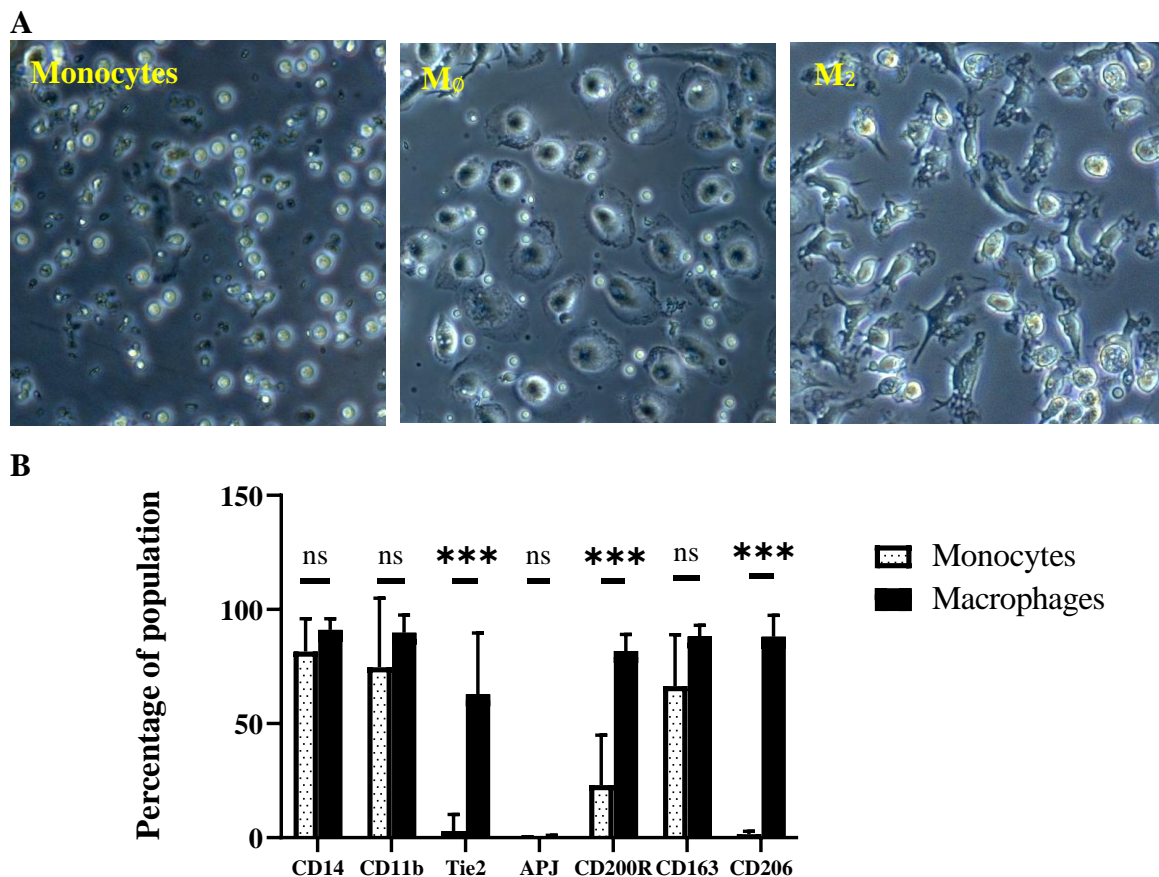


**Figure 5. Monocyte to M<sub>2</sub> macrophage polarization, their morphology and marker surface expression.** (A) Monocytes, uncommitted M<sub>0</sub> and M<sub>2</sub> macrophages, plated on 6-well plate. M<sub>0</sub> show different (fried egg) morphology in comparison to polarized M<sub>2</sub> macrophages (spindle formed); (B) Comparison of marker surface expression profiles of freshly isolated monocytes and polarized M<sub>2</sub> macrophages (n=9). Results are presented as mean + SD. Levels of significance: ns (non-significant), for  $p \geq 0.05$ ; \*  $p < 0.05$ ; \*\*\*  $p < 0.01$ . Paired two-tailed t-test.

## RESULTS

Relatively high expression of Tie2, cell-surface receptor for angiopoietin, was observed on M<sub>2</sub> macrophages, suggesting a possible monocyte polarization toward tumor-associated macrophages (TAM) or Tie2-expressing macrophages (TEM)<sup>300</sup>. Additionally, the expression level of CD200R was found to be significantly increased in M<sub>2</sub> macrophages, compared to monocytes.

### 3.1.2 APJ expression in M<sub>2</sub> macrophages

Contrary to the previous findings of our research group<sup>296</sup>, using APC-labeled antibody directed against Apelin receptor (APJ), minor or no differences between APJ protein surface expression on both monocytes and M<sub>2</sub> macrophages were found (Figure 6). It is worth noticing that the antibody used in this Ph.D. project was not the same as the one used in earlier experiments (see discussion section). Using the new APC-labeled antibody (different antibody clone), it was not possible to detect APJ epitopes neither on polarized M<sub>2</sub> macrophages nor on any cell line claimed to have a stable endogenous expression of APJ (as it will also be addressed in further sections).

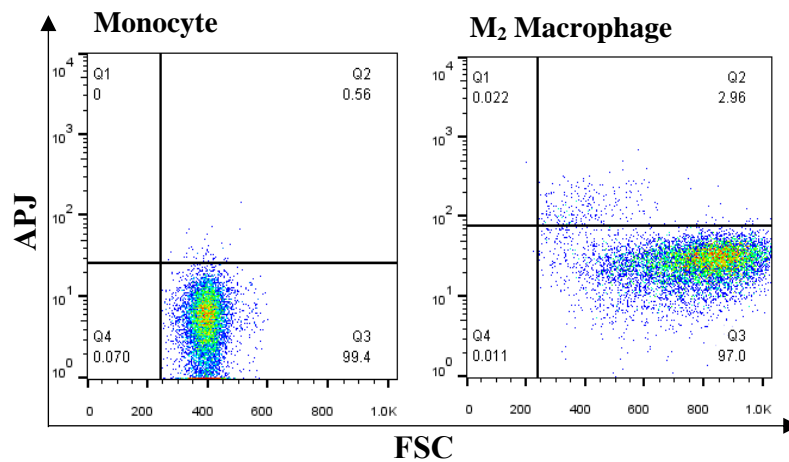


**Figure 6. Representative flow cytometric analysis of Apelin receptor expression profile.** Low protein surface expression of APJ was observed on both monocytes and polarized M<sub>2</sub> macrophages.

### 3.1.3 Regulation of apelinergic system in M<sub>2</sub> macrophages

In order to exclude biases that may have arisen from a non-functional antibody, Alexa Fluor 488-coupled anti-APJ antibody was used to examine the APJ surface expression on M<sub>2</sub>

macrophages\*. Prior to the flow cytometric analysis, monocytes were phase-polarized to M<sub>2</sub> macrophages either directly (after monocyte isolation) or indirectly (stimulation of monocytes within PBMCs as an indirect co-culture system). Contrary to previous results, obtained with APC-coupled antibody, Alexa Fluor 488-coupled antibody was able to detect the higher expression of APJ on M<sub>2</sub> macrophages polarized both directly and indirectly (Figure 7).

To investigate the role of Apelin in APJ regulation, M<sub>2</sub> macrophages were stimulated 24 hr with [Pyr1]Apelin-13 (in further text Apelin). Flow cytometric analysis of indirectly polarized macrophages revealed moderately higher APJ expression, compared to control (Figure 7).

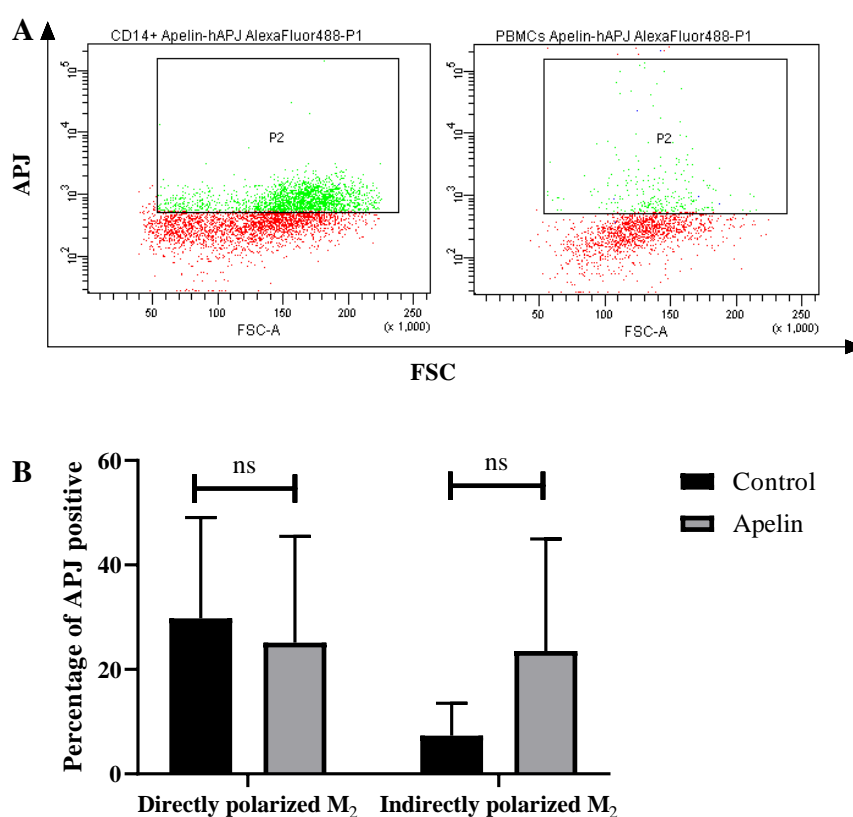


**Figure 7. Flow cytometric analysis of APJ expression using Alexa Fluor 488-coupled anti-APJ antibody.** (A) Surface expression of APJ was analyzed on M<sub>2</sub> macrophages polarized directly, upon monocyte isolation (left plot) or by selective polarization of monocytes co-cultured with the rest of PBMCs (right plot). Directly and indirectly polarized macrophages were further stimulated with pyroglutamated Apelin-13. (B) Unlike directly polarized macrophages, moderately increased APJ protein surface expression was observed in indirectly polarized macrophages upon Apelin stimulation (10 pM), compared to unstimulated (control) macrophages. Results are presented as mean + SD and

\* The aforementioned antibody was obtained at the end of this Ph.D. project and could not be used for repetition of previously performed experiments. Antibody manufacturer claims that Alexa Fluor 488-coupled anti-APJ antibody represents the same clone as APC-coupled antibody used in this study. For antibody catalog number, refer to the Material section.

## RESULTS

were obtained from three independent experiments. Paired t-test. Levels of significance: ns (non-significant).

To extend the insight into endogenous APJ expression in another macrophage phenotype, freshly isolated monocytes were polarized to the M<sub>1</sub> macrophage phenotype in parallel with M<sub>2</sub> polarization, by previously established protocol<sup>301</sup>. APJ expression levels were quantified by RT-qPCR and flow cytometry (with APC-labeled antibody). Interestingly, in both groups of macrophages, gene and surface expression of APJ was found low (data not shown).

Furthermore, the effects of APJ agonist and antagonist, as well as the effects of supernatants from tumor and endothelial cells on apelinergic expression profile in M<sub>2</sub> macrophages, had been investigated (Figure 8). No significant changes in APJ mRNA levels were observed between treated groups, since APJ level remained low. On the other hand, addition of supernatant from endothelial cells significantly increased Apelin gene expression, compared to the control group.

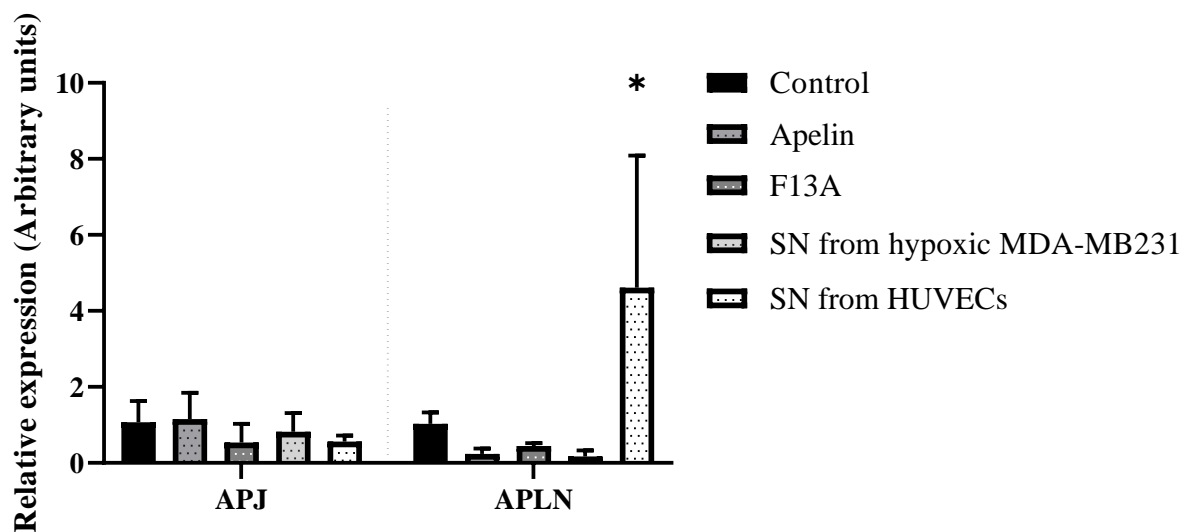


**Figure 8. Apelinergic expression profile of M<sub>2</sub> macrophages under different conditions.** Phase-polarized macrophages were treated with pyroglutamated Apelin-13 (20 nM), APJ receptor antagonist F13A (20 nM), supernatant from triple-negative breast carcinoma cell line (MDA MB231) cultured under hypoxic conditions (1% O<sub>2</sub>) and normoxic supernatant from human umbilical vein endothelial cells (HUVEC). Water was used as a vehicle control. Relative expression was determined using the  $\Delta\Delta C_t$  method and normalized to the expression of the glyceraldehyde-3-phosphate dehydrogenase (GAPDH). Results are presented as mean + SD and were obtained from four independent experiments. Levels of significance: \*  $p < 0.05$ . Ordinary one-way ANOVA followed by Tukey's multiple comparisons test.

Since the majority of tumor-associated macrophages (TAM) are found within tumor tissue, it is known that, due to antiangiogenic therapy, both TAMs and tumor cells enter into hypoxia. To examine the effect of hypoxic conditions on apelinergic expression profile of M<sub>2</sub>



macrophages, cells were kept under hypoxic conditions for 24 hr (1% O<sub>2</sub>). While APLN gene expression was found to be 5-fold higher, only moderate increase in APJ mRNA expression was found, when compared to the control cells (Figure 9).

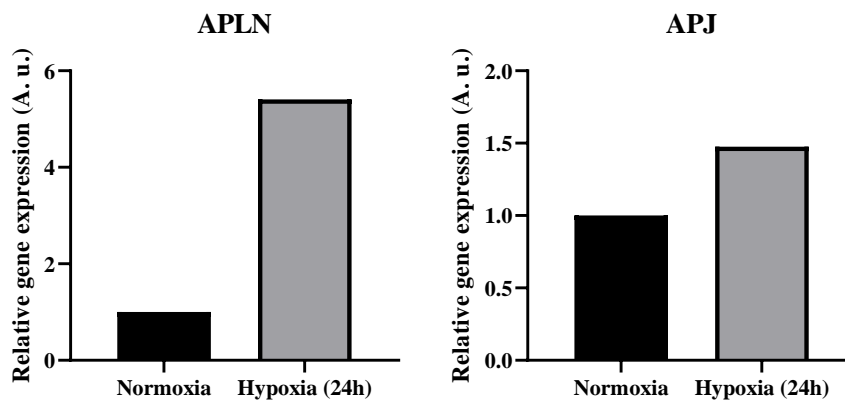


**Figure 9. Effects of hypoxia on APLN/APJ gene expression in M<sub>2</sub> macrophages.** M<sub>2</sub> macrophages have been kept under hypoxic conditions 24 hr. Macrophages from the same donor were subjected to normoxic conditions and served as a control. Expressions were normalized to the expression of glyceraldehyde-3-phosphate dehydrogenase (GAPDH). Results were analyzed in triplicates and evaluated using Pfaffl method.

#### 3.1.4 APJ expression in PBMCs

Since the surface expression on M<sub>2</sub> macrophages was found to be low, APJ surface expression was additionally examined within peripheral blood mononuclear cells (PBMCs). Therefore, freshly isolated PBMCs were analyzed by flow cytometry for three different cell surface markers per sample. Every marker combination represented specific fraction of PBMCs. The results presented in Figure 10 show significantly higher percentage of triple-positive CD11b/CD14/APJ and CD14/Tie2/APJ cell fractions in comparison to most of the analyzed cell groups. This implies that the major percentage of APJ-positive cell population is likely to be found in the monocytic lineage within PBMCs.

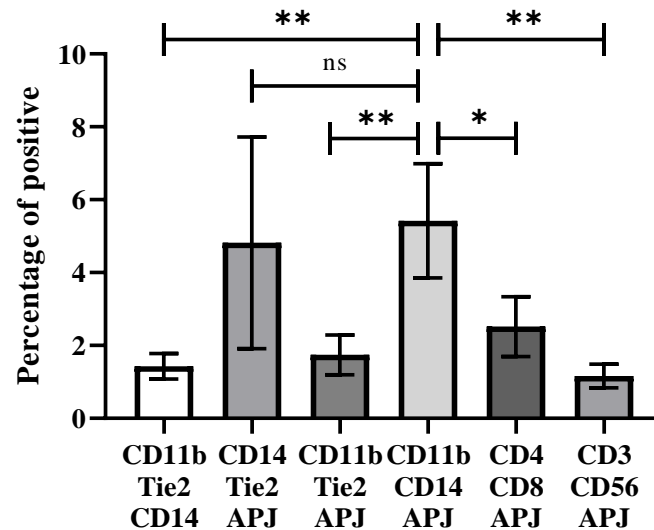


**Figure 10. Flow cytometric analysis profile of freshly isolated PBMCs.** Higher surface expression of APJ was observed within CD14<sup>+</sup>/Tie2<sup>+</sup> and CD11b<sup>+</sup>/CD14<sup>+</sup> cell populations. Results were obtained from five healthy donors and are presented as mean ± SD. n=5; Levels of significance: ns (non-significant), \* p < 0.05; \*\* p < 0.01. Unpaired t-test.

### 3.1.5 Apelin and APJ expression in endothelial cells

Previous findings from our research team revealed high expression of Apelin mRNA in several types of endothelial cells, suggesting the existence of apelinergic signaling in an autocrine or paracrine manner. To further verify these findings, mRNA levels of APLN and APJ were analyzed by RT-qPCR in human umbilical endothelial vein cells (HUVECs) at different cell passages.

Results of the gene expression analysis revealed that APLN mRNA level was significantly higher than the one of APJ (Figure 11). Furthermore, APLN gene expression was shown not to change in the higher passages of endothelial cells, which indicates that these cells have a high endogenous APLN gene expression. On the other hand, APJ mRNA constantly remained at a low level, despite the cell passage.

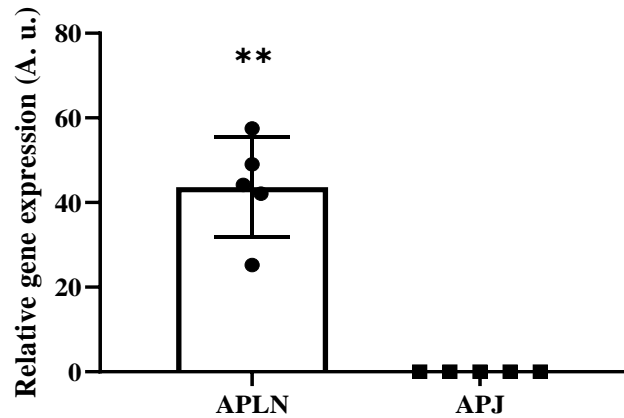


**Figure 11. Analysis of APLN and APJ mRNA expression in human umbilical vein endothelial cells.** The analysis was performed by means of RT-qPCR and results were normalized to the expression of the glyceraldehyde-3-phosphate dehydrogenase (GAPDH). For evaluation, the  $\Delta C_t$  method was used. Results from the graphical representation are presented as mean  $\pm$  SD and were obtained from five independent experiments (n=5). Levels of significance: \*\*\*p = 0.0012; Paired two-tailed t-test.

### 3.1.6 Regulation of apelinergic expression in endothelial cells

It is known that the antiangiogenic approach targets endothelial cells of active endothelium, mostly by inhibition of the VEGF-signaling pathway. However, little is known on how inhibition of VEGF-signaling affects apelinergic expression profile in those cells. To examine if VEGF-signaling inhibition alters apelinergic system expression, endothelial cells were treated with anti-VEGF antibody (bevacizumab) and tyrosine kinase inhibitor (sunitinib) during five cell passages. After every cell passage, APLN and APJ gene expression were analyzed (Figure 12).

It was shown that APLN gene expression remained mostly unaffected by the presence of bevacizumab, whereas sunitinib decreased that expression. On the other hand, both concentrations of bevacizumab were able to upregulate APJ expression until the end time point. Similar effect on ECs was displayed only by a lower concentration of sunitinib. Moreover, except for lower bevacizumab concentration, it could be seen that both antiangiogenic agents initially tend to downregulate APJ expression until higher cell passages, when upregulation occurs.

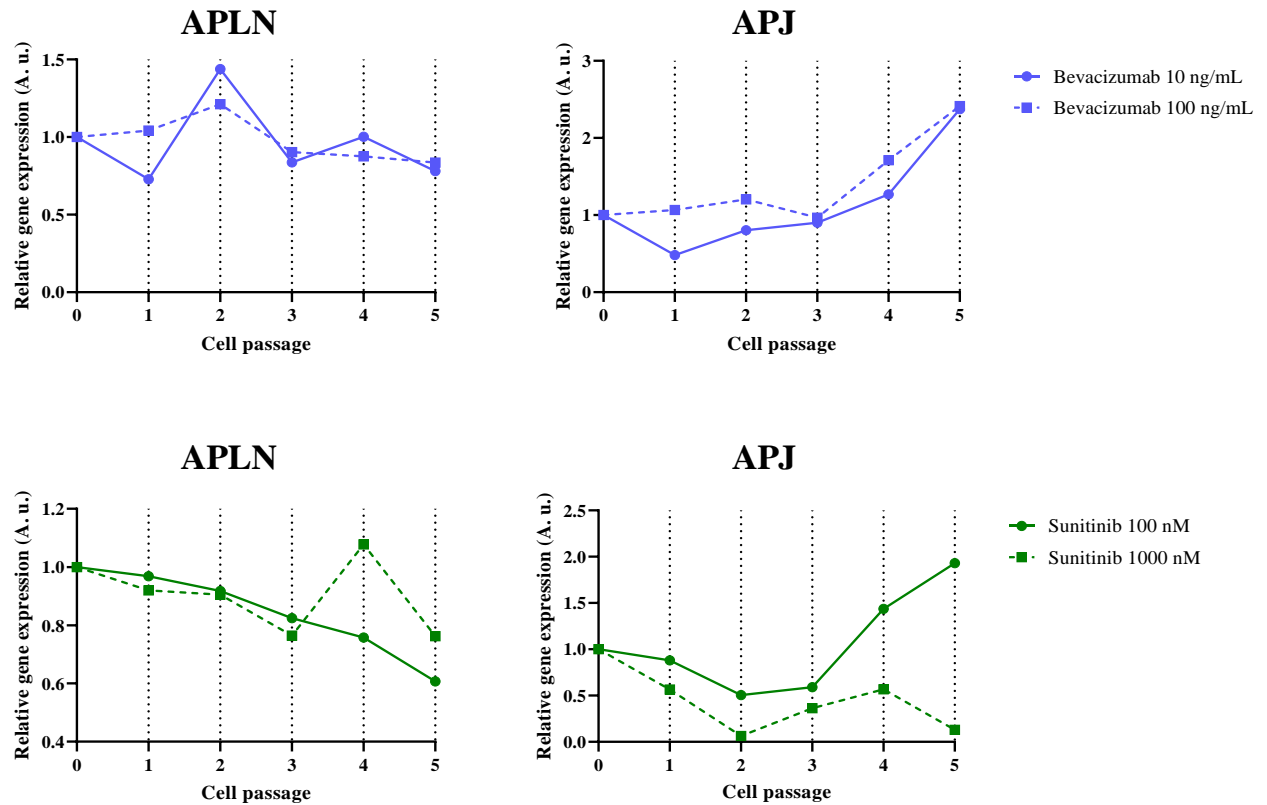


**Figure 12. Regulation of apelinergic system in ECs upon antiangiogenic treatment.** HUVECs were grown in the presence of antiangiogenic agents (bevacizumab or sunitinib) in two different concentrations. Untreated cells were used as a control. mRNA was extracted after every cell passage and expressions were normalized to the expression of glyceraldehyde-3-phosphate dehydrogenase (GAPDH). Results were analyzed in triplicates and evaluated using Pfaffl method.

### 3.2 Apelin and APJ expression in cancer

During this Ph.D. study, Apelin and APJ upregulation was reported in several cancer types<sup>267,270,274</sup>. In order to examine potential direct contribution of Apelin/APJ system to cancer, profound screening of apelinergic expression profile was carried out. Apelin/APJ expression, including mRNA and protein surface expression levels were analyzed in primary material (tumor tissue, bone marrow and periferal blood samples from patients), acute myeloid leukemia (AML) cell lines, as well as in solid cancer cell lines that were available in the laboratory of our research group.

#### 3.2.1 APJ expression in murine tumor tissue and tumor cell lines

Gene expression of APJ in murine tumors was quantified by RT-qPCR. Due to lack of our own murine tumor material, tissue samples from several murine tumors were kindly provided by the

neighboring research group, led by Prof. Dr. Dr. Sonja Loges. Since murine tumor tissues were kept intact at  $-80^{\circ}\text{C}$  and then thawed, flow cytometric analysis of the provided samples, therefore, could have not been performed due to the very low viability of tumor cells.

Interestingly, APJ mRNA expression was found to be extremely high in most of the analyzed material, and it was characterized by low Ct values. Since such Ct values can sometimes indicate genomic DNA (gDNA) contamination of the sample, murine tumor tissues were tested by RT-qPCR using primers that specifically bind to sequences of the genomic DNA (gene encoding for gGAPDH), to exclude possible contamination. Results of the analysis confirmed that the majority of tumor samples were gDNA-free and high APJ mRNA level was confirmed in analyzed samples (Figure 13). Although some of the analyzed tumors were treated with antiangiogenic therapy, no differences in APJ expression between untreated and treated tumors were found. Accordingly, very high APLN mRNA expression was detected in all samples (data not shown).

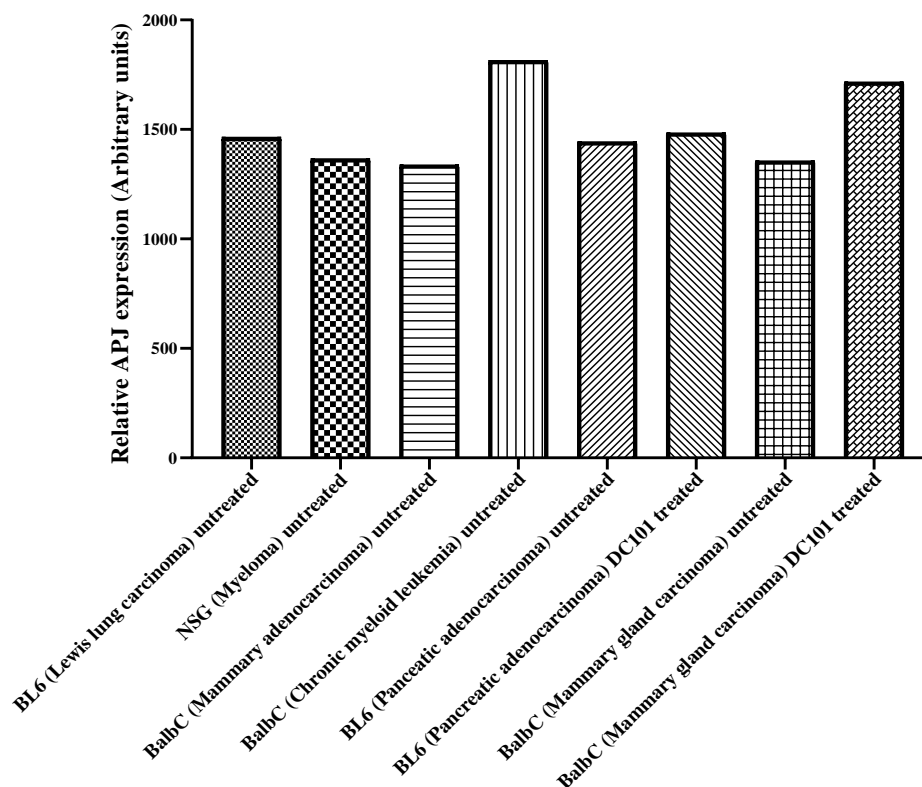


**Figure 13. APJ gene expression in various murine tumors.** APJ mRNA expression in murine tumor tissue was determined by RT-qPCR, and normalized to the expression of glyceraldehyde-3-phosphate dehydrogenase (GAPDH). The data presented were analyzed in triplicates and evaluated by  $\Delta\text{Ct}$  method.

## RESULTS

Additionally, APLN/APJ gene expression was investigated in three murine tumor cell lines, which were used in *in vivo* experiments (as will be addressed in further sections). Despite extremely high expression that was observed in tumor tissue, all three cell lines displayed low APJ mRNA levels (Figure 14). On the other hand, APLN gene expression levels in colon adenocarcinoma (MC38) and Lewis lung carcinoma (LLC1) cell lines were remarkably high. It is important to notice that APJ expression in primary Lewis lung carcinoma was almost  $10^5$ -fold higher than in cell line derived from the same tumor type.

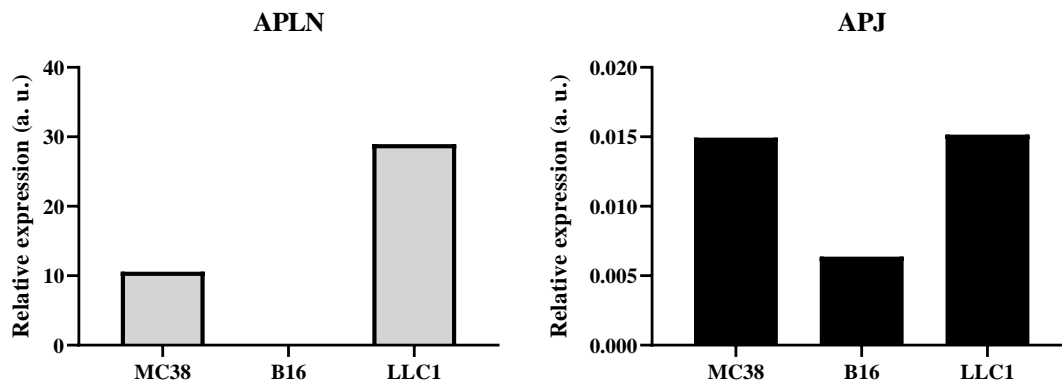


**Figure 14. Apelinergic expression profile in murine solid tumor cell lines.** APLN/APJ gene expression was analyzed in mouse colon adenocarcinoma (MC38), melanoma (B16) and Lewis lung carcinoma cell lines. Expressions were normalized to the expression of glyceraldehyde-3-phosphate dehydrogenase (GAPDH). Results were analyzed in triplicates and evaluated by  $\Delta$ Ct method. APLN expression in B16 cell line was characterized by very high Ct values.

### 3.2.2 APJ protein surface expression in human glioblastoma tissue

Surface expression of APJ was measured in glioblastoma samples from four patients. Tumor samples were generously provided by Dr. Cécile Maire. APJ surface expression was found to be moderate in all human glioblastoma samples (Figure 15). However, the number of biological replicates was a limiting factor and, due to the lack of normal brain tissue, no statistical analysis could have been performed. Low surface expression was later confirmed by RT-qPCR (data not shown).

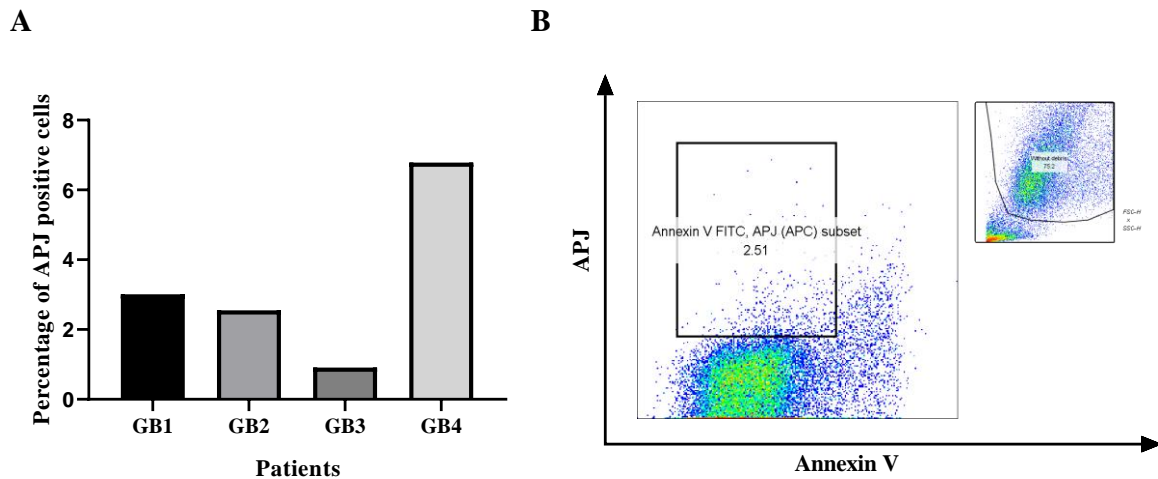


**Figure 15. Flow cytometric analysis of human glioblastoma tissue.** (A) Analysis of four tumor samples isolated from patients suffering from glioblastoma. No statistical analysis was performed due to a lack of healthy brain tissue serving as a control. (B) Representative flow cytometric analysis of a glioblastoma sample. GB (glioblastoma) abbreviations were assigned randomly to the samples.

### 3.2.3 Apelin and APJ expression profile in human acute myeloid leukemia (AML)

To investigate APJ surface expression in primary patient material, flow cytometric analysis was performed on cells that were isolated from bone marrow (leukemic blasts - pAML cells) and peripheral blood of patients suffering from AML. For all material, written informed consent was obtained from each patient. Results of the flow cytometric analysis revealed low to moderate APJ surface expression in the bone marrow and cells from peripheral blood. Additionally, no differences between APJ surface expression in both examined compartments were found (Figure 16).

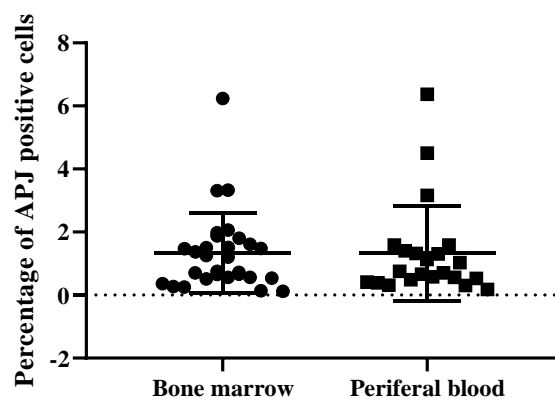


**Figure 16. APJ surface expression on primary AML cells.** Surface expression analysis was performed on cells from AML patients isolated from two body compartments: bone marrow and peripheral blood. Results indicate low APJ expression on the majority of samples, and no difference in

## RESULTS

surface expression was observed between two analyzed compartments. The analysis was performed on a total number of 29 patients (n=29).

Apelin and APJ gene expression in leukemic blasts was analyzed and compared to the gene expression in M<sub>2</sub> macrophages serving as a control (Figure 17). Accordingly, results of RT-qPCR analysis revealed generally low mRNA expression levels of APLN and APJ, characterized by mostly high Ct values for gene of interest (GOI) (above 30). While APLN expression in pAML samples was shown to be lower, somewhat higher APJ expression could be observed, compared to M<sub>2</sub> macrophages. Moreover, in pAML samples, APJ seemed to have had moderately higher expression than APLN (Figure 17, B).

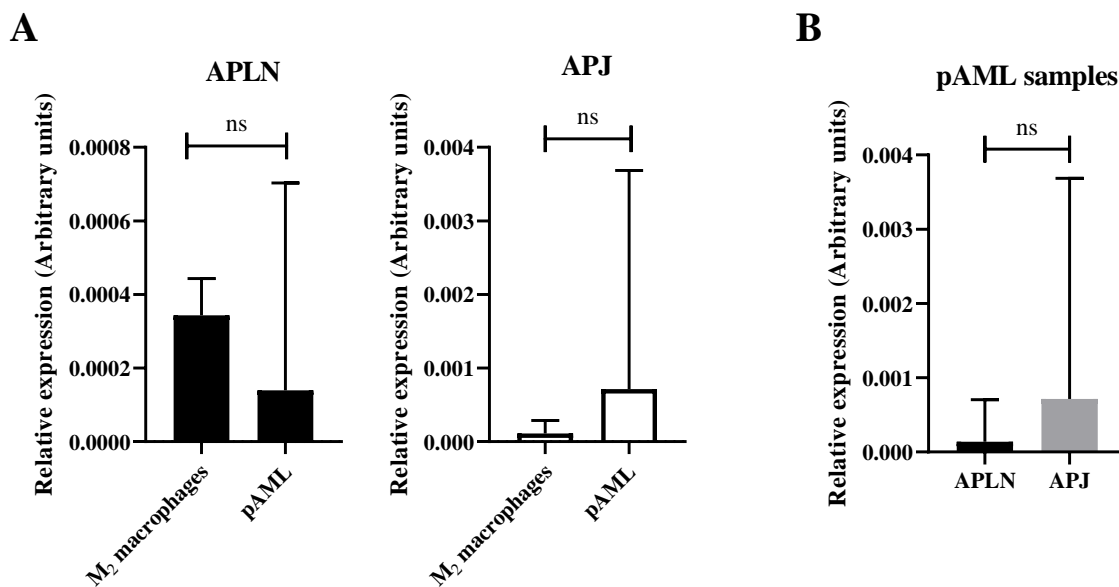


**Figure 17. Apelinergic gene expression in cells from primary AML and M<sub>2</sub> macrophages.** (A) Differences in APLN and APJ gene expression profile were observed between pAML (n=24) and M<sub>2</sub> macrophages (n=3). (B) Comparison between APLN and APJ gene expression in pAML samples. The graphical representation is based on mean + SD and all samples were analyzed in triplicates using  $\Delta$ Ct method. Expressions were normalized to the expression of glyceraldehyde-3-phosphate dehydrogenase (GAPDH). Levels of statistical significance: ns (non-significant); Unpaired t-test.

### 3.2.4 Apelin concentration in plasma of ovarian carcinoma patients

In order to examine the differences in plasma Apelin protein levels between healthy donors and those of ovarian carcinoma patients, samples were quantitatively analyzed using a commercially available ELISA Kit. Plasma samples from ovarian cancer patients were kindly provided by PD Dr. Leticia Oliveira-Ferrer and Prof. Dr. Heidi Schwarzenbach.



Interestingly, it was shown that the protein level of Apelin was significantly decreased in the plasma of ovarian cancer patients in comparison to the plasma of healthy donors (Figure 18).

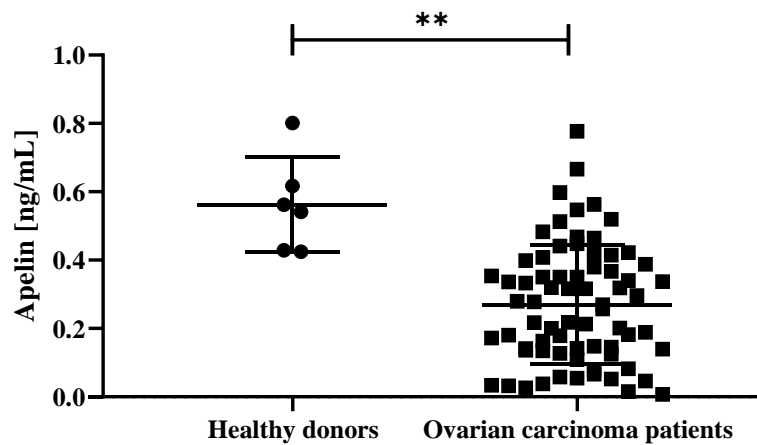


**Figure 18. Apelin plasma concentration in healthy donors and ovarian cancer patients.** Quantitative analysis of Apelin plasma concentration was performed in healthy donors (n=6) and ovarian cancer patients (n=71). The analyses were done using commercially available ELISA Kit that detects all active Apelin forms. The graphical representation is based on mean  $\pm$  SD and all samples were analyzed in duplicates. Levels of statistical significance: \*\* p = 0.0025; Unpaired t-test followed by Welch's correction.

### 3.2.5 Apelin and APJ expression in acute myeloid leukemia (AML) cell lines

In a recently published study, it was proven that, in comparison with healthy donors, serum levels of Apela (Elabela, Toddler), APJ receptor ligand, was increased in patients with chronic lymphocytic leukemia (CLL)<sup>276</sup>. Knowing that Apela was increased in CLL, it was hypothesized that the similar scenario might occur in acute myeloid leukemia.

In order to test the possible involvement of apelinergic system in AML, surface and gene expression analyses were performed in several AML cell lines (Figure 19). Consistent with the previous findings, the APJ expression on protein and gene level was found to be low in the majority of tested cell lines.

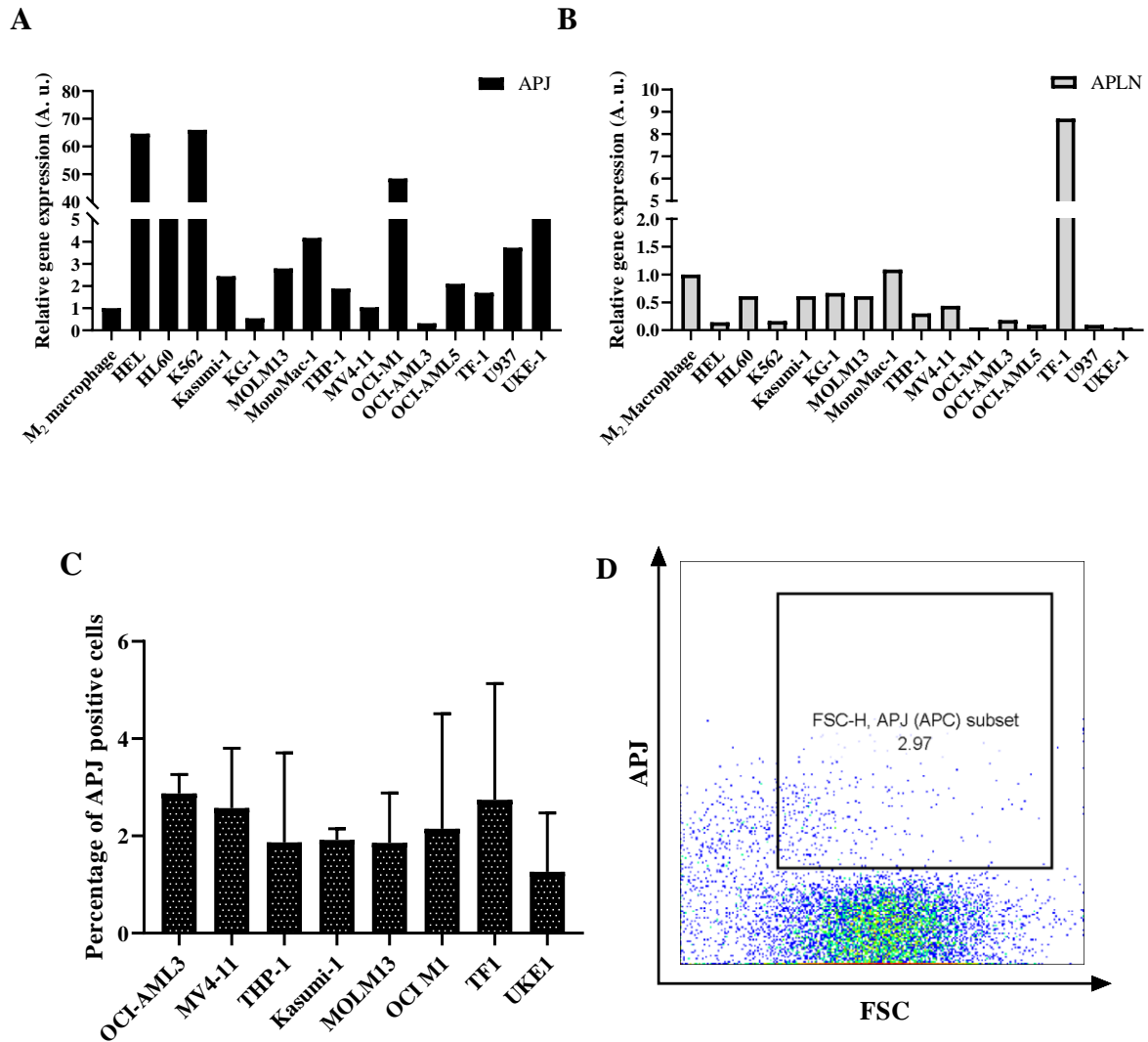


**Figure 19. Apelinergic expression profile in AML cell lines.** (A and B) APLN and APJ mRNA levels were quantified in AML cell lines by RT-qPCR and gene expression was compared to the M<sub>2</sub> macrophage as a control. Results were evaluated using Pfaffl method. All samples were analyzed in triplicates and the results were normalized to the expression of glyceraldehyde-3-phosphate dehydrogenase (GAPDH). (C) Flow cytometric analysis of eight AML cell lines. Results are presented as mean + SD and were obtained from five independent flow cytometric measurements (n=5). (D) Representative flow cytometry plot of MOLM13 cell line after gating for APJ-positive cells.

### 3.2.6 Apelin and APJ expression in solid tumor cell lines

Similar to the previous approach, RT-qPCR and flow cytometry were used to analyze endogenous APLN and APJ expression in solid tumor cell lines. APJ mRNA level was found to be low in most of the solid tumor cell lines, followed by high Ct values (Figure 20). Interestingly, U118 and HT29 are, respectively, human glioblastoma and colon adenocarcinoma cell lines, claimed to have a high endogenous expression of Apelin receptor. Accordingly, the usage of those cell lines as APJ positive control has been suggested by the

antibody manufacturer (for reference on antibody, see Material section). Surprisingly, flow cytometric analysis showed very low APJ expression in those cell lines (for detailed flow cytometric analysis of U118 cell line, see Supplementary data).

On the other hand, APJ surface expression was significantly increased in human breast cancer cell line, SKBR-3 (Figure 20). Interestingly, this expression was found to be even higher than expression in assumed APJ-positive cell line control (U118).

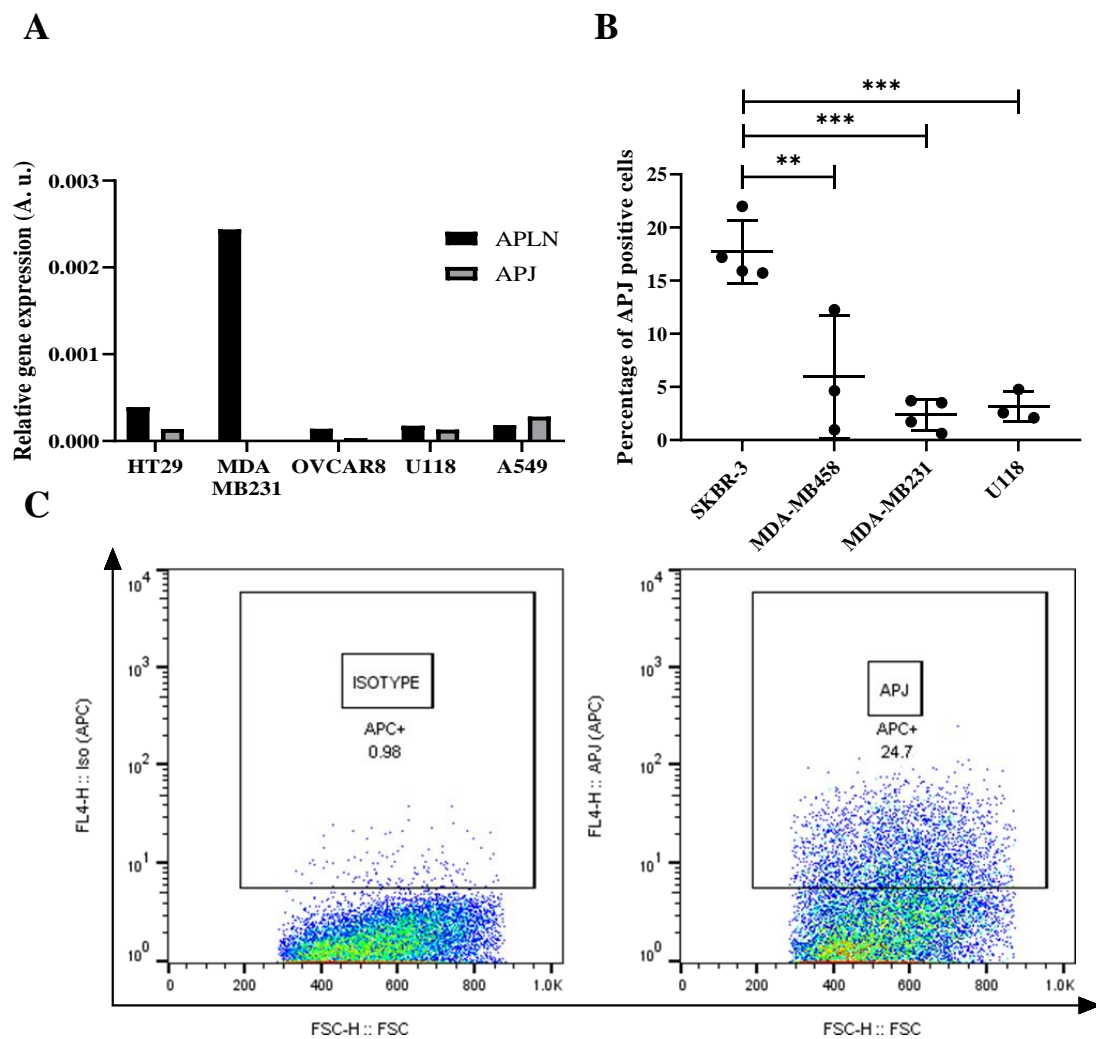


**Figure 20. Apelinergic expression profile in solid tumor cell lines.** (A) APLN/APJ gene expression analysis in five solid tumor cell lines revealed low mRNA levels. (B) Breast carcinoma cell lines were analyzed by flow cytometry; HER2-overexpressing breast cancer cell line (SKBR) displayed higher APJ expression in comparison to triple-negative breast cancer cell lines. Results from (B) are presented as mean  $\pm$  SD and were obtained from a minimum of three independent flow cytometric measurements (n=3). (C) Representative flow cytometry plot of SKBR3 cell line after gating for APJ-positive cells.

## RESULTS

Levels of significance: ns non-significant; \*\*p < 0.01 \*\*\*p < 0.001; One-way ANOVA followed by Tukey's multiple comparisons test.

### 3.2.7 APJ expression regulation in tumor cell lines

Gene expression has been additionally investigated in both AML and solid cell lines upon Apelin stimulation (Figure 21). Stimulation with Apelin for 24 hr resulted in APJ mRNA decrease in HepG2 cell line, whereas APJ gene expression was increased in A549 cell line. No similar effects in AML cell lines were observed. After 48 hr, an increase in APJ mRNA expression could be observed in both solid tumor cell lines.

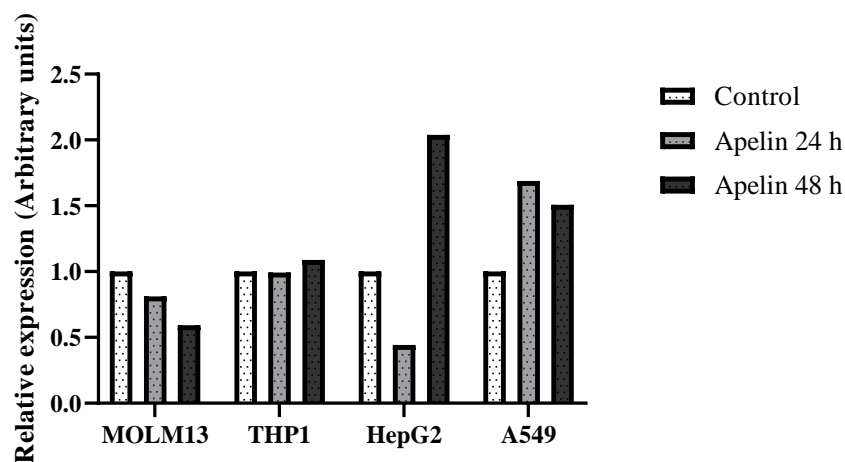


**Figure 21. APJ regulation in tumor cell lines upon stimulation with Apelin.** AML and solid tumor cell lines were incubated for 24 hr and 48 hr with 100 nM [Pyr1]Apelin-13. Gene expression was analyzed by the Pfaffl method. All samples were analyzed in triplicates and the results were normalized to the expression of glyceraldehyde-3-phosphate dehydrogenase (GAPDH).

APLN/APJ expression profile has been additionally analyzed in solid tumor cells that were exposed to hypoxic conditions (Figure 22).

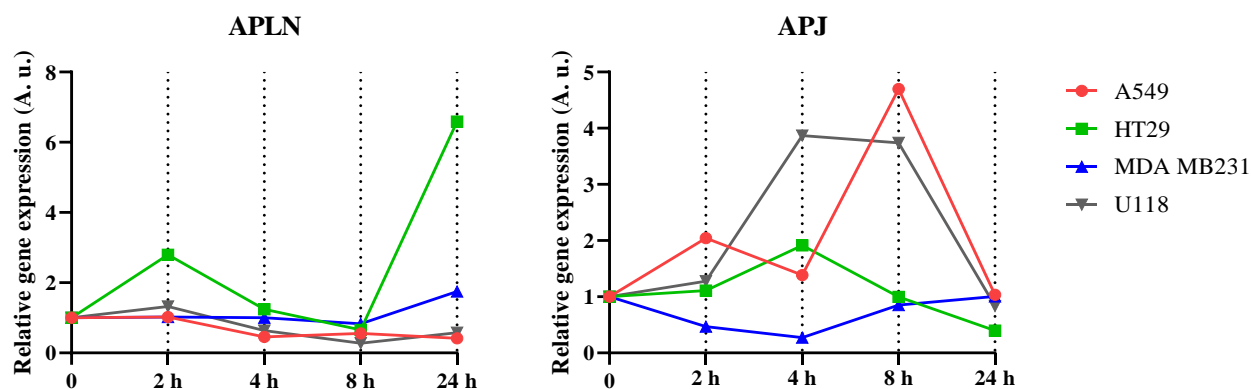


**Figure 22. Apelinergic gene expression profile under hypoxic conditions.** Solid tumor cells were kept under hypoxia for 24 hr. RNA was isolated after 2 hr, 4 hr, 8 hr and 24 hr. Cells kept under normoxic conditions served as a control. Gene expression was compared to the relevant cell line controls and data were analyzed using Pfaffl method. All samples were analyzed in triplicates and results were normalized to the expression of glyceraldehyde-3-phosphate dehydrogenase (GAPDH).

APLN mRNA level remained mostly unchanged, except for HT29 cell line at the end time point, where a 6-fold increase in gene expression was observed. On the other hand, change in APJ expression was likely to be more influenced by hypoxic conditions. Unlike MDA MB231 cell line, where APJ expression even decreased, other cell lines displayed a peak in APJ expression between 4 hr and 8 hr after initiation of hypoxia. However, this effect seemed to have been only transitory, since APJ expression returned back to the control level after 24 hr.

### 3.3 Functional analyses

Results of the expression analysis in M<sub>2</sub> macrophages, endothelial cells and majority of tumor cell lines revealed relatively low endogenous APJ expression. The primary objective of functional assays was to investigate if proangiogenic M<sub>2</sub> macrophages, as well as tumor cell lines, react to the presence of APJ agonists/antagonists, despite low APJ expression that was found. Assays, including cellular proliferation and clonogenicity, cell viability, cytotoxicity and migration have been carried out to monitor the functional properties of cells in culture after treatment with various stimulatory/inhibitory molecules. It was assumed that apelinergic expression profile could be altered in certain conditions, and therefore, changes in expression profile, as a result of stimulation or inhibition, might lead to the different physiological responses upon APJ stimulation or inhibition.

## RESULTS

### 3.3.1 Proliferation of M<sub>2</sub> macrophages

Cell proliferation in terms of viability was examined using WST-1 proliferation assay. Macrophages were stimulated with Apelin and its analogs upon polarization to M<sub>2</sub> phenotype. Additionally, to evaluate the effect of Apelin/APJ targeting on their proliferation, macrophages were treated with MM54, a small molecule inhibitor that acts as a competitive APJ antagonist. Unstimulated macrophages were used as a control.

Compared to unstimulated control, Apelin and peptide analogs of Apelin were able to show moderate, though not a significant increase in proliferation rate of M<sub>2</sub> macrophages (Figure 23). On the other hand, MM54 in higher concentration was able to decrease proliferation rate (in terms of viability), compared to Apelin-13 and AM01-182-treated macrophages. No similar effects could be observed either with lower concentrations of MM54, or with the rest of Apelin analogs.

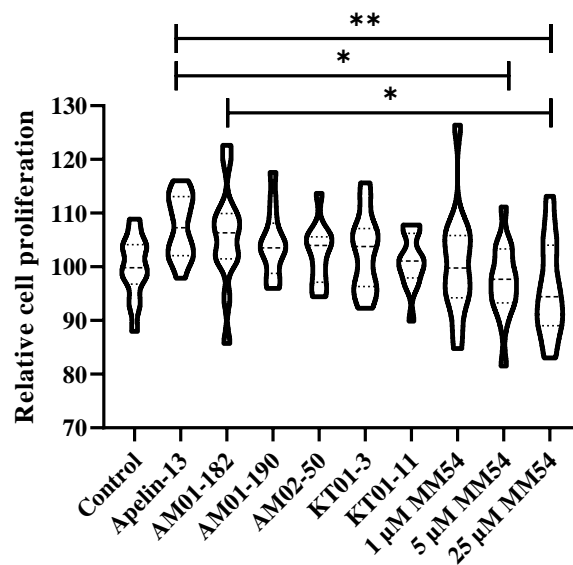


**Figure 23. Proliferation properties of polarized M<sub>2</sub> macrophages upon APJ stimulation/inhibition.** Proliferation rate was evaluated using WST-1 proliferation assay. Cell proliferation was analyzed after treatment with [Pyr1]Apelin-13, AM01-182, AM01-190, AM02-50, KT01-3, KT01-11 (20 nM) and MM54 (1, 5 and 25 μM) for 48 h and normalized to vehicle control. The graphical representation is based on mean ± SD. Data represent the results of three independent experiments, each with 3-5 replicates per group. \* p < 0.05; \*\* p < 0.01 One-way ANOVA followed by Tukey's multiple comparisons test.

### 3.3.2 Proliferation of wildtype AML cell lines

To examine their proliferation rates in terms of cell count, several AML cell lines were treated with pyroglutamated Apelin-13 and a peptide antagonist to Apelin receptor (F13A) in three different concentrations. After 72 hours of incubation, the cell number was evaluated by automatic cell counting. During this experiment, some cells in culture became adherent and due to this behavior, they were excluded from further analysis.

Incubation of selected AML cell lines with Apelin peptide (0.1 - 10  $\mu\text{M}$ ) did not result in a statistically significant elevation of cell proliferation in any cell line analyzed (Figure 24). Additionally, Apelin antagonist was found to have no effect on cell proliferation.

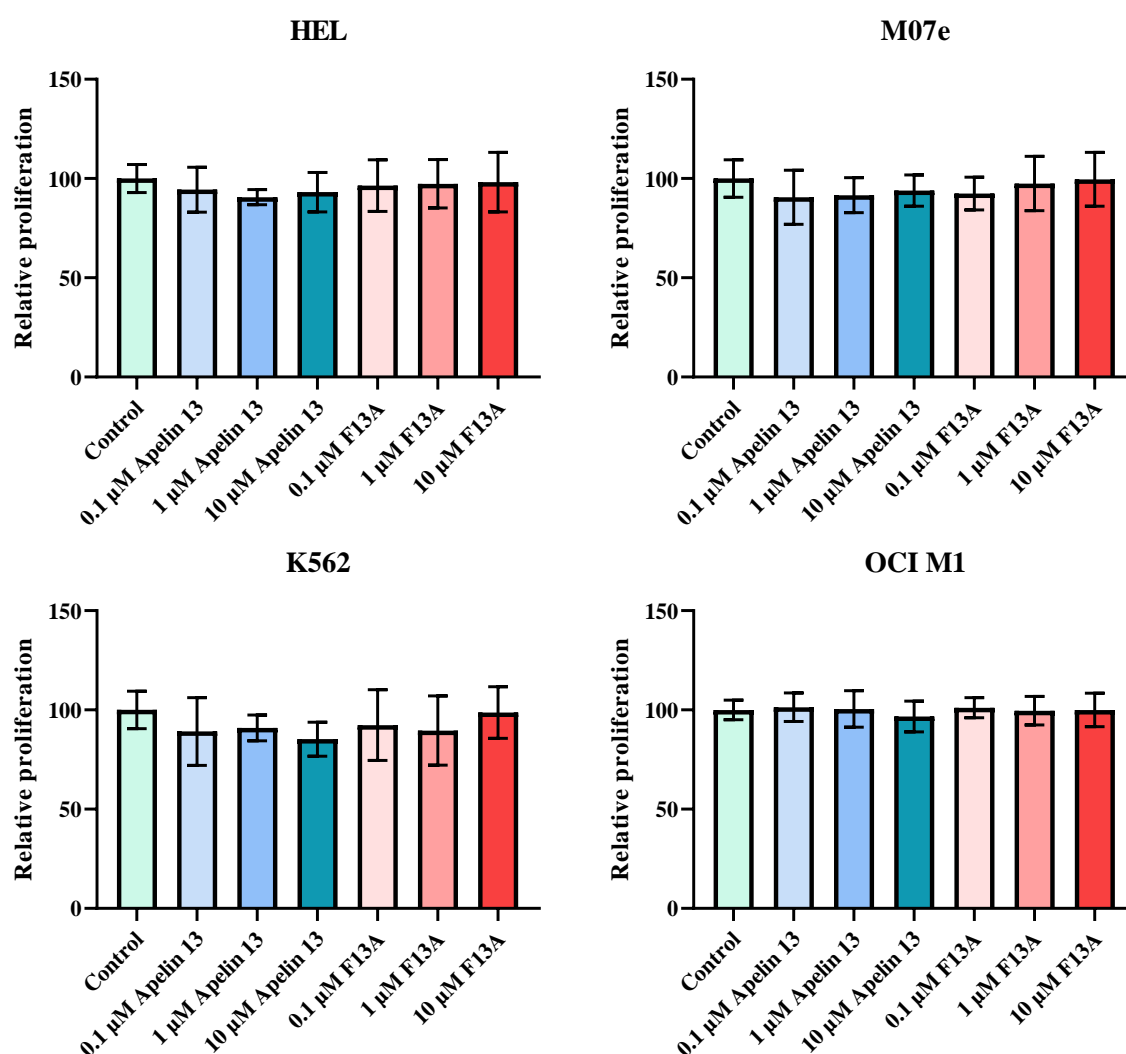


**Figure 24. Effects of Apelin receptor stimulation and inhibition in AML cell lines.** Cells were seeded at a defined density and treated with the [Pyr1]Apelin-13 and F13A. Stimulation was performed with single substances and water as solvent control. After three days of incubation, the cell number was

## RESULTS

determined using automatic counting device. The results are normalized to the respective control and presented as mean value  $\pm$  standard deviation of the relative proliferation from two independent experiments in triplicates. Statistical analysis of the differences between the control and the single treatments was performed using one-way ANOVA followed by Tukey's multiple comparisons test.

### 3.3.3 Proliferation of solid cancer cell lines

Proliferation potential and viability of four solid cancer cell lines in similar conditions had been investigated using WST-1 assay. Cells were incubated with different concentrations of pyroglutamated Apelin-13 and MM54 at nanomolar levels. Following the incubation time of 48 hours, proliferation rates were evaluated. It could be seen that cell lines HT29, MDA MB231, A549 and OVCAR8 did not respond to either stimulation or inhibition of APJ since no differences in cell proliferation were observed (Figure 25).

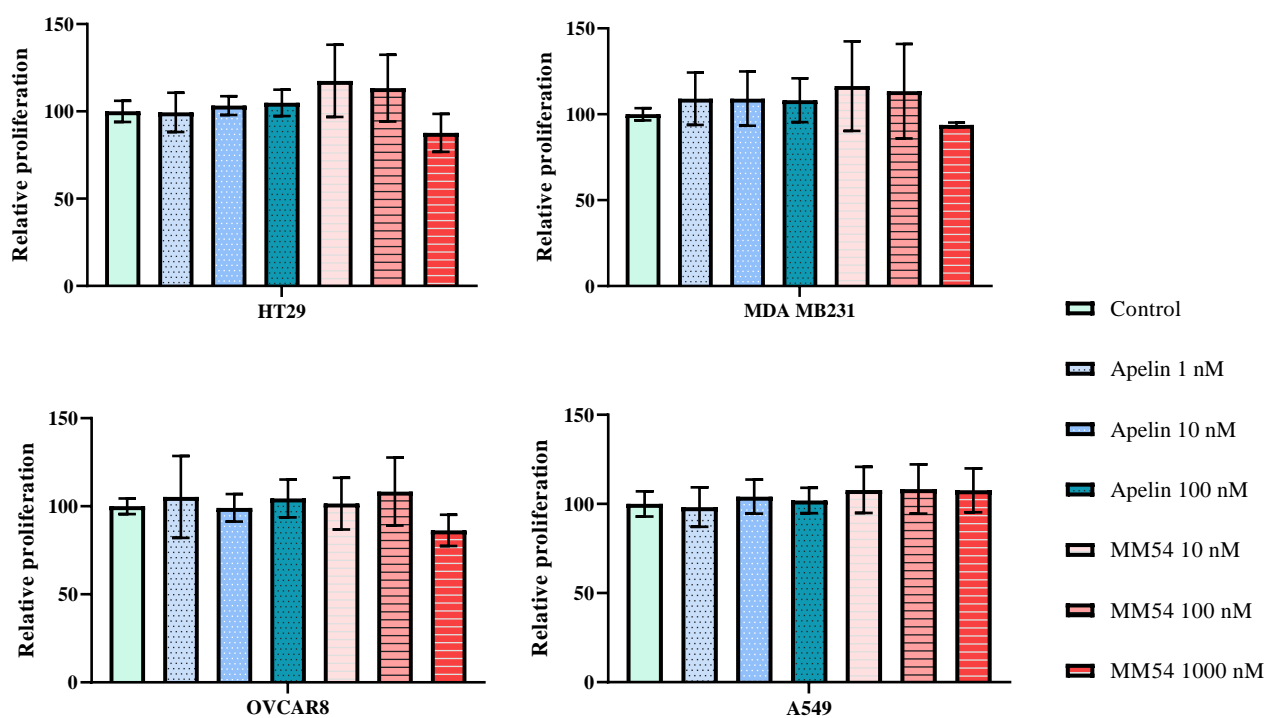


**Figure 25. The proliferation rate of solid tumor cell lines upon stimulation and inhibition of APJ.** The proliferation was assessed using WST-1 proliferation assay. Cell viability was evaluated after treatment with [Pyr1]Apelin-13 (1, 10 and 100 nM) and MM54 (10, 100 and 1000 nM) for 48 h. In total, two independent experiments were performed with 3 replicates per each group (n=2). The graphical representation is based on mean  $\pm$  SD. No statistically significant differences were found in either cell line. One-way ANOVA followed by Tukey's multiple comparisons test.



### 3.3.4 Proliferation of transduced AML cell lines

Since APJ endogenous expression in the majority of tumor cell lines was found to be very low, insufficient gene expression had been overcome by cell transduction with APJ-overexpressing lentiviral vector system. In order to investigate whether transgenic cell lines respond to the presence of exogenous Apelin, proliferation assays were carried out using APJ-overexpressing THP1 and MOLM13 cell lines. Wildtype THP1 and MOLM13 were also included in these assays, to serve as a control. All cells were treated with three different concentrations of pyroglutamated Apelin-13 (Figure 26).

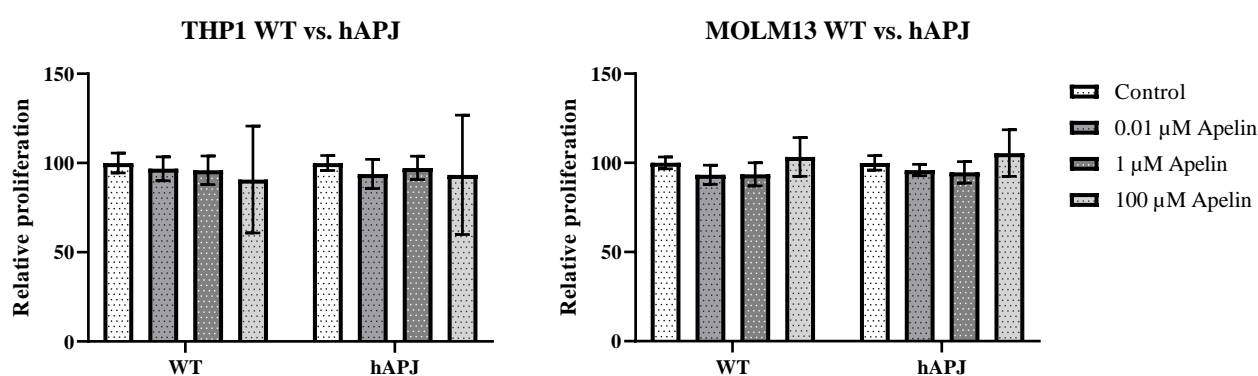


**Figure 26. Effect of APJ stimulation and inhibition in wildtype and APJ-expressing AML cell lines.** Cells were seeded at a defined density and treated with [Pyr1]Apelin-13 in three different concentrations. After three days of incubation, cell numbers were determined by automatic counting device. The results are presented as mean value  $\pm$  SD from minimum of three independent experiments, performed in triplicates. Proliferation rate is normalized to the respective vehicle control. Statistical analysis of the differences between the control and the single treatments was performed using one-way ANOVA followed by Tukey's multiple comparisons test.

The presence of the Apelin receptor in transgenic cell lines seemed not to have had any effect on AML cells proliferation, since no significant differences between control and treated samples in both wildtype and APJ-overexpressing cells could be observed.

According to the manufacturer, [Pyr1]Apelin-13 and APJ antagonist, MM54, have effective concentration ( $EC_{50}$ ) and half maximal inhibitory concentration ( $IC_{50}$ ) at nanomolar levels (see Material section). Therefore, it was assumed that the change in cell proliferation might be manifested in the presence of Apelin and MM54 in lower concentrations. In order to investigate if the lower concentration gradient affects cell proliferation, proliferation assays were repeated with different experimental setup. Concentrations of Apelin and MM54 were within declared  $EC_{50}$  and  $IC_{50}$  range and both substances were used at five different nanomolar concentrations,

## RESULTS

which varied from 0.01 nM - 100 nM for Apelin, while the concentration of M54 was in range from 0.1 nM - 1000 nM.

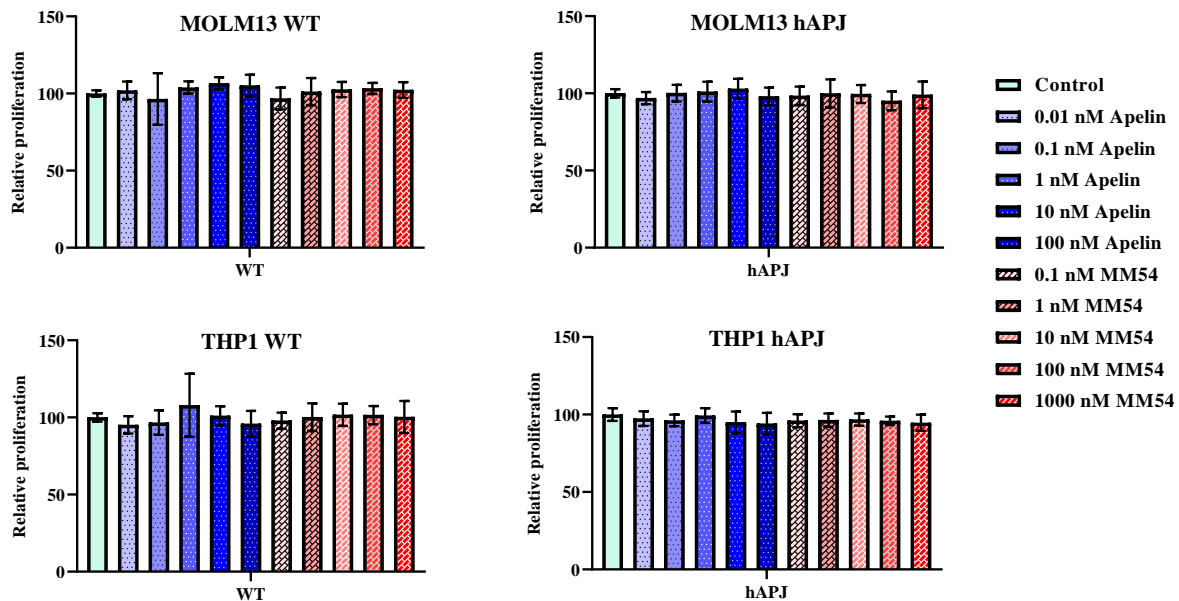


**Figure 27. Effect of APJ stimulation and inhibition on proliferation in wildtype and APJ-overexpressing AML cells.** Cells were seeded at a defined density and treated with the [Pyr1]Apelin-13 and MM54 in five different concentrations. After three days of incubation, the cell numbers were assessed by automatic cell counting. The results represent the mean value  $\pm$  SD of the proliferation, normalized to the solvent control. Results were obtained from a minimum of three independent experiments, performed in triplicates. Statistical analysis of the differences between the control and the single treatments was performed using one-way ANOVA followed by Tukey's multiple comparisons test.

Despite experiment repetition, lower concentration gradients of Apelin and MM54 did not affect wildtype cell proliferation (Figure 27). Surprisingly, similar scenario could also be seen in transgenic cell lines. Despite stable APJ expression in the cells, Apelin did not increase cell proliferation. Accordingly, MM54 showed no effect in any concentration present.

In addition, proliferation rates of APJ-overexpressing cells have been compared to those of wildtype cells (without stimulation). APJ-overexpressing cells in both cell lines displayed moderately higher proliferation rates, however, no statistically significant difference could be seen. Overall, proliferation in transgenic cells was not affected by the presence of APJ.

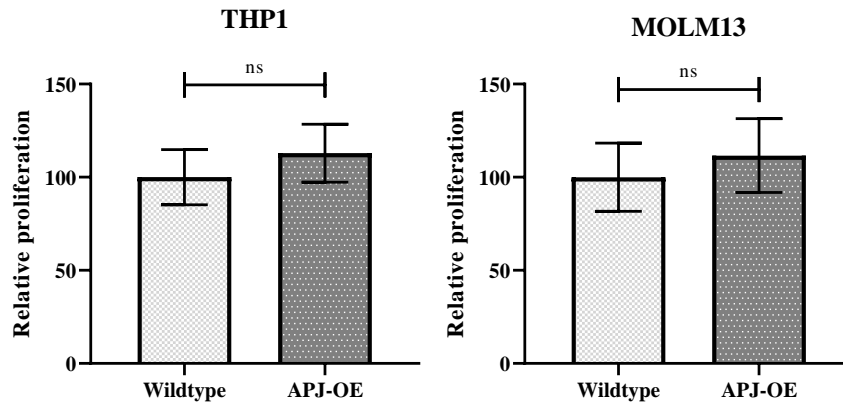


**Figure 28. Comparison of proliferation rates between wildtype and APJ-overexpressing cell lines.** Cell number was determined after three days of incubation using an automatic count device. Results were normalized to the respective wildtype control. Levels of significance: ns (non-significant). Unpaired t-test.

### 3.3.5 Clonogenicity of transduced AML cell lines

To obtain further insight into the Apelin/APJ system's role in self-renewal properties of acute myeloid leukemia cells, colony-forming assays were performed using wildtype and APJ-overexpressing AML cell lines. In accordance with the experimental setup from the proliferation assays, cells were treated with Apelin and MM54. Colony counting was assessed seven days after cell incubation (Figure 29).

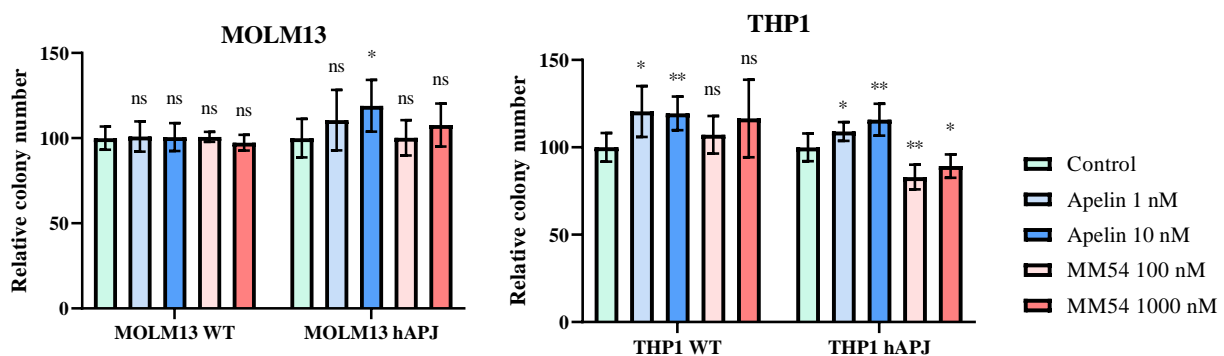


**Figure 29. Colony formation assay for AML cell lines.** Wildtype and APJ-overexpressing MOLM13 and THP1 cells were cultured on semisolid medium in the presence of [Pyr1]Apelin-13 and MM54. After seven days, colony number was retrieved by manual counting and normalized to the vehicle control. Results are presented as mean  $\pm$  SD of three independent experiments. Levels of significance: ns (non-significant); \*  $p < 0.05$ , \*\* $p < 0.01$ . Unpaired t-test.

## RESULTS

---

Apart from moderate effect of Apelin in APJ-overexpressing cells, no significant increase or decrease in colony number upon stimulation could be seen on either wildtype or transgenic MOLM13 cell line.

On the other hand, significant changes in clonogenicity have been observed in THP1 cell line, especially in APJ-overexpressing cells, compared to their respective controls. Stimulation with Apelin resulted in an increase of colony number, both in wildtype and APJ-overexpressing THP1 cells. Additionally, MM54-mediated APJ antagonism in transgenic cells resulted in decreased number of colonies compared to untreated control.

### 3.3.6 Role of the Apelin/APJ system in solid tumor cell migration

The effect of stimulation and inhibition of APJ on cell migration was examined in solid tumor cell lines by performing the automated IncuCyte® migration assays. Solid tumor cell lines with three different phenotypes had been used in experiment: wildtype (WT), APJ-overexpressing (APJ-OE), and Apelin-overexpressing (Apelin-OE) cell lines.

While migratory properties of WT MDA-MB231 cells remained unaffected, stimulation with Apelin significantly increased the speed of wound closure in APJ-overexpressing cell line (Figure 30). These migratory changes were specific to APJ presence where, compared to the control (untreated) APJ-OE cells, Apelin significantly increased migration. It was expected that MM54 would have the opposite effect on the migration rate of the cells, resulting in decreased cell migration. Contrary to expectations, APJ inhibitor showed stimulatory effect on cell migration, similar to that of Apelin. However, similar scenario could not be seen in A549 cell line due to unstable APJ expression in OE cells (for gene expression, see Supplementary data). Except for MM54-treated WT A549 cell line, no significant changes in cell migration were observed in wildtype cells, regardless of APJ stimulation/inhibition.

In Apelin-OE cell lines, APJ antagonism did not cause any change in the migration rates. Further gene expression analysis, however, revealed that APJ was expressed at a very low level in both MDA-MB231 and A549 cell lines.

In general, wound closure took more time to occur in control MDA MB231 (50 hr until wound closure) in comparison to A549 cell line (20 hr until wound closure), suggesting the differences in migratory properties between cell lines.

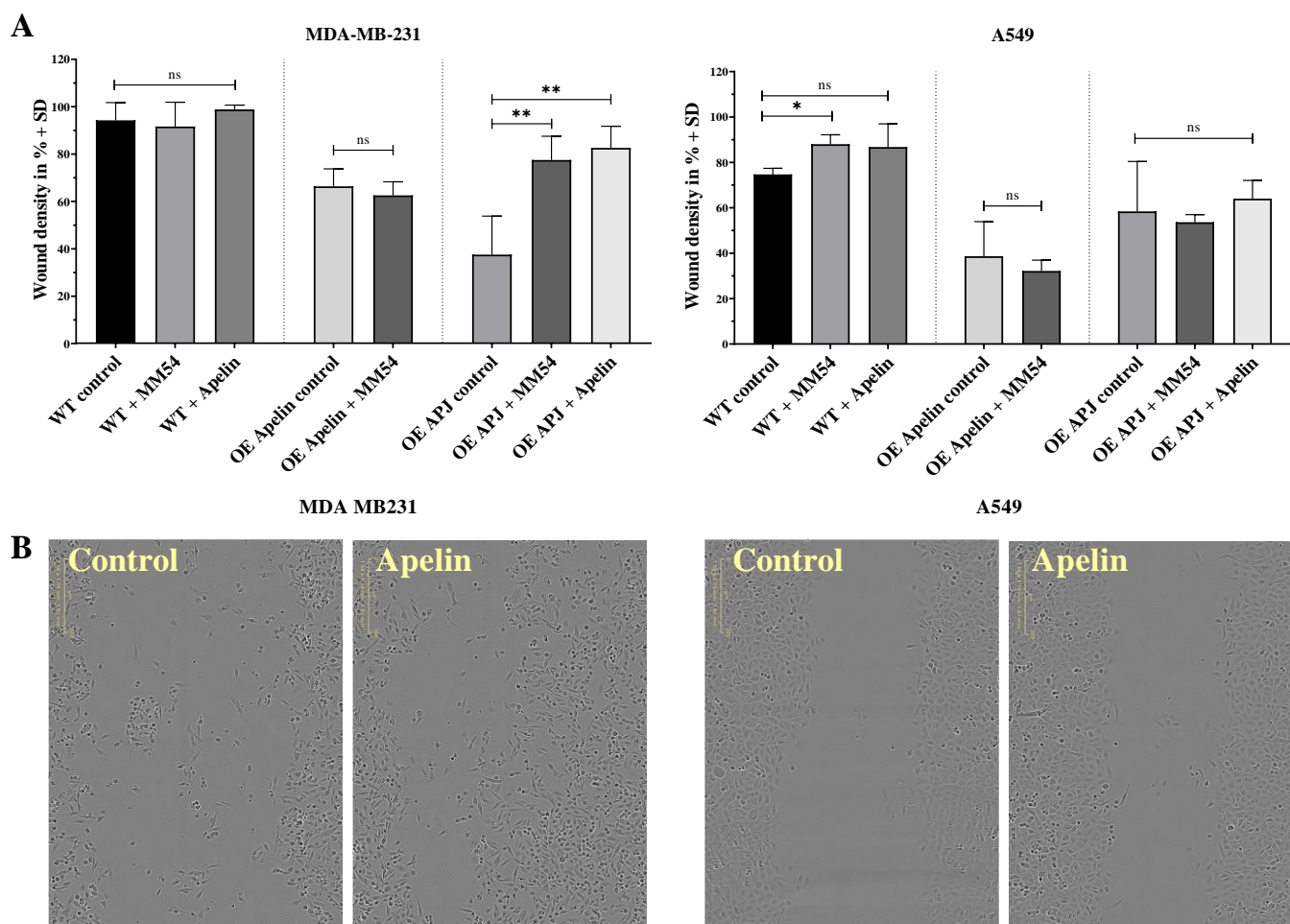


**Figure 30. Effect of apelinergic stimulation and inhibition on solid cancer cells migration abilities.** (A) Migration rates of MDA MB231 and A549 cancer cells were continuously measured and analyzed upon incubation with Apelin (10 nM) and MM54 (1000 nM). WT and APJ-OE cells were treated with Apelin or MM54, while Apelin-OE cells were treated only with MM54. Water-treated samples served as a vehicle control. (B) Representative images of APJ-OE cell lines at time point 12 h (MDA MB231, left) and 10 h (A549, right). Results are expressed as mean (wound closure) + SD of one experiment with 4 replicates per each group. Levels of significance: \*  $p < 0.05$ , \*\*  $p < 0.01$ ; One-way ANOVA and unpaired followed by Dunnett's multiple comparison test.

### 3.4 Apelinergic system's role in immunotherapy

In recently published studies, certain authors identified APJ as one of the key factors that influence immunotherapy mediated killing<sup>302</sup>. Using chimeric antigen receptor T cells (CAR-T) as effector cells and melanoma as target cells, it was managed to prove that loss of APJ results in more than 50% resistance to CAR-T cell-mediated lysis. These findings served as a conceptual basis for further experimental approach.

## RESULTS

### 3.4.1 Immunotherapy-dependent APJ regulation in AML cell lines

As a part of gene expression analyses, it was investigated whether AML and solid tumor cell lines are able to upregulate APJ expression in conditions that simulate immunotherapy. AMLs and tumor solid cell lines were treated with supernatant from cytokine-induced killer cells (CIK) from three different donors, as well as with interferon-gamma ( $\text{IFN}\gamma$ ) in three different concentrations.

While supernatant from CIK had a moderate effect on its expression, it could be seen that some AML cell lines, stimulated with  $\text{IFN}\gamma$ , showed concentration-dependent increase of APJ expression. Despite the apoptotic effect of  $\text{IFN}\gamma$ , the highest upregulation could be seen in MOLM13 cell line (Figure 31). On the other hand, these results were only partially confirmed by gene expression analysis since high variability in APJ expression was observed.

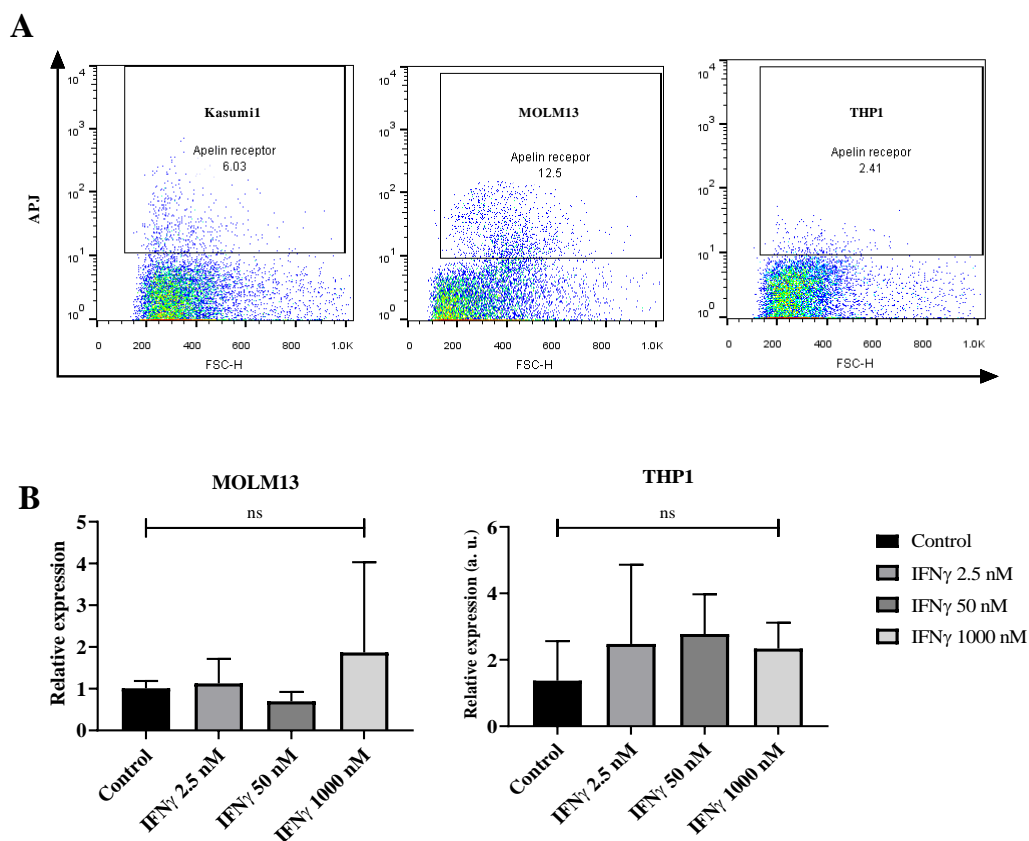


**Figure 31. Regulation of APJ expression after stimulation with  $\text{IFN}\gamma$ .** Three AML cell lines were incubated with 2.5, 50 and 1000 nM of  $\text{IFN}\gamma$ . (A) Representative flow cytometry plots of Kasumi1, MOLM13, and THP1 cell lines, stimulated with 50 nM  $\text{IFN}\gamma$ . (B) Comparison between APJ surface expression profile after treatment with  $\text{IFN}\gamma$ . Gene expression was compared to the relevant cell line controls and data were analyzed using  $\Delta\Delta\text{Ct}$  method. All samples were analyzed in triplicates and results were normalized to the expression of glyceraldehyde-3-phosphate dehydrogenase (GAPDH). Results

are presented as on the mean + SD of three independent experiments. Levels of significance: ns non-significant. Paired two-tailed t-test.

### 3.4.2 APJ-mediated cytotoxicity

To reproduce already documented cytotoxicity assays in our laboratory conditions<sup>303,304</sup>, AML cells as target cells had been incubated with PBMCs as effector cells. Immunotherapy was simulated *in vitro* by the addition of bi-specific T-cell engager (BiTE) and T-cell immunoreceptor with Ig and ITIM domains (TIGIT) antibody to cell suspension.

As a vector control for cytotoxicity assays, eGFP overexpressing cells with endogenous APJ expression were used. Dead cell exclusion dye, 7-Aminoactinomycin D (7-AAD), was used to differentiate apoptotic and healthy cells, based on cell membrane integrity. After incubation with BiTE and TIGIT antibody or their respective controls, the amount of apoptotic cells was measured by flow cytometry, based on eGFP positivity. The analysis of the cytotoxicity assay results is presented in Figure 32.

Visible effects of BiTE and TIGIT antibody on cell apoptosis have been observed in both APJ-overexpressing and control cells when compared to their respective controls (control BiTE and IgG2a). In general, addition of BiTE seemed to have had higher contribution to immune-mediated cytotoxicity. Preliminary experiments showed that the immune-mediated cytotoxic effects were substantially higher in THP1 APJ-overexpressing cells in comparison to the control cells (data not shown), indicating that APJ presence potentiates the effect of immunotherapeutics. However, repeated experiments in all three AML cell lines showed no differences in immune-mediated cytotoxicity between two phenotype groups (Figure 32).

Since transgenic cells were verified for APJ expression, it could be observed that, according to the flow cytometric analysis, some of the cells downregulated APJ expression over time, which could have been a possible reason for a decrease in cytotoxic effects (data not shown).

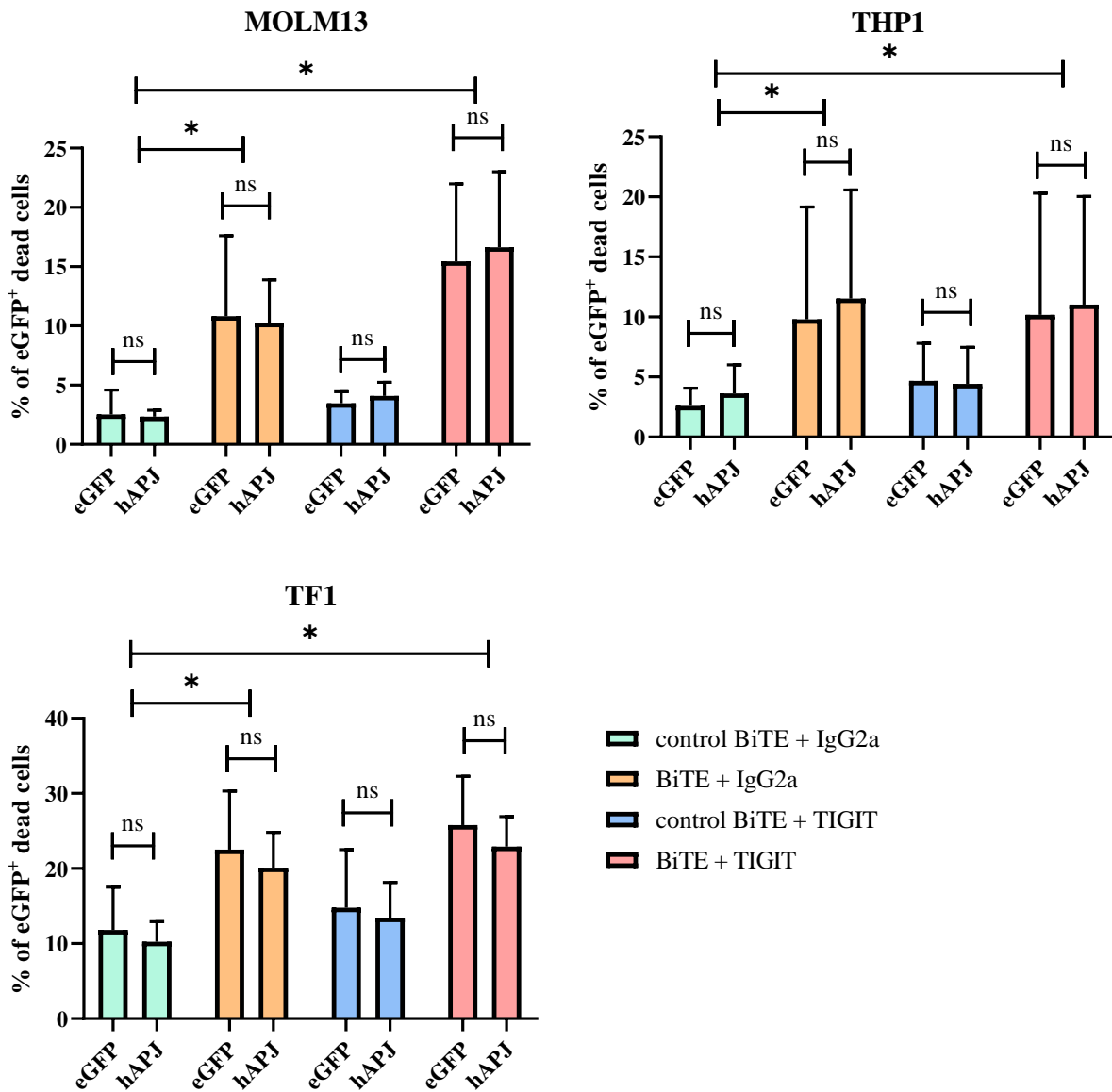


**Figure 32. Cytotoxic assays performed on AML cells as target cells.** AML control (eGFP) and APJ-eGFP overexpressing cells were co-cultured with peripheral mononuclear cells of healthy donors in a 1:5 ratio and incubated with a CD33-CD3 BiTE (bi-specific T-cell engager) antibody construct, as well as with immune checkpoint inhibitor antibody (TIGIT). Control BiTE and IgG2a treated cells served as treatment control. After 24 hr of incubation, flow cytometric analysis was performed using 7-AAD as a marker for GFP<sup>+</sup> dead cells. Results are presented as mean + SD of three independent experiments. Levels of significance: ns non-significant; \* p < 0.05. Two-tailed t-test.



### 3.5 Role of Apelin/APJ system *in vivo*

Conducted *in vivo* experiments aimed to investigate the effects of genetic targeting of Apelin/APJ system on metastatic burden, angiogenesis in tumors, and to study its role in development of resistance to antiangiogenic therapy. To test the existing hypotheses, murine lung tissue was chosen as a model of metastasis, since it is prone to be one of the primary metastatic targets<sup>305</sup>.

#### 3.5.1 Subcutaneous tumor model

As a first step toward establishing an appropriate lung metastasis model, the experiment was initiated by subcutaneously injecting three murine tumor cell lines, Lewis lung carcinoma (LLC1), colon adenocarcinoma (MC38) and melanoma (B16) into female C57BL/6J mice. Mice were sacrificed after reaching critical tumor size, following the lung extraction. Subcutaneous tumors and lung tissues were sliced and stained with hematoxylin and eosin (H&E).

Interestingly, subcutaneous tumors of all three cell lines that were injected, behaved very aggressively, which finally had fatal consequences to the mice in relatively short period (Figure 33). The tumor size increased nearly exponentially from day 7-10, when the majority of the subcutaneous tumors were considered as engrafted. Despite the differences between the number of injected tumor cells, survival rates did not significantly differ and high tumor aggressiveness remained the same. In case of murine melanoma cell line, it was noticed that there was a tendency of metastatic colonization of other organs besides lung tissue, such as liver and gastrointestinal system, making the cell line even more aggressive.

## RESULTS

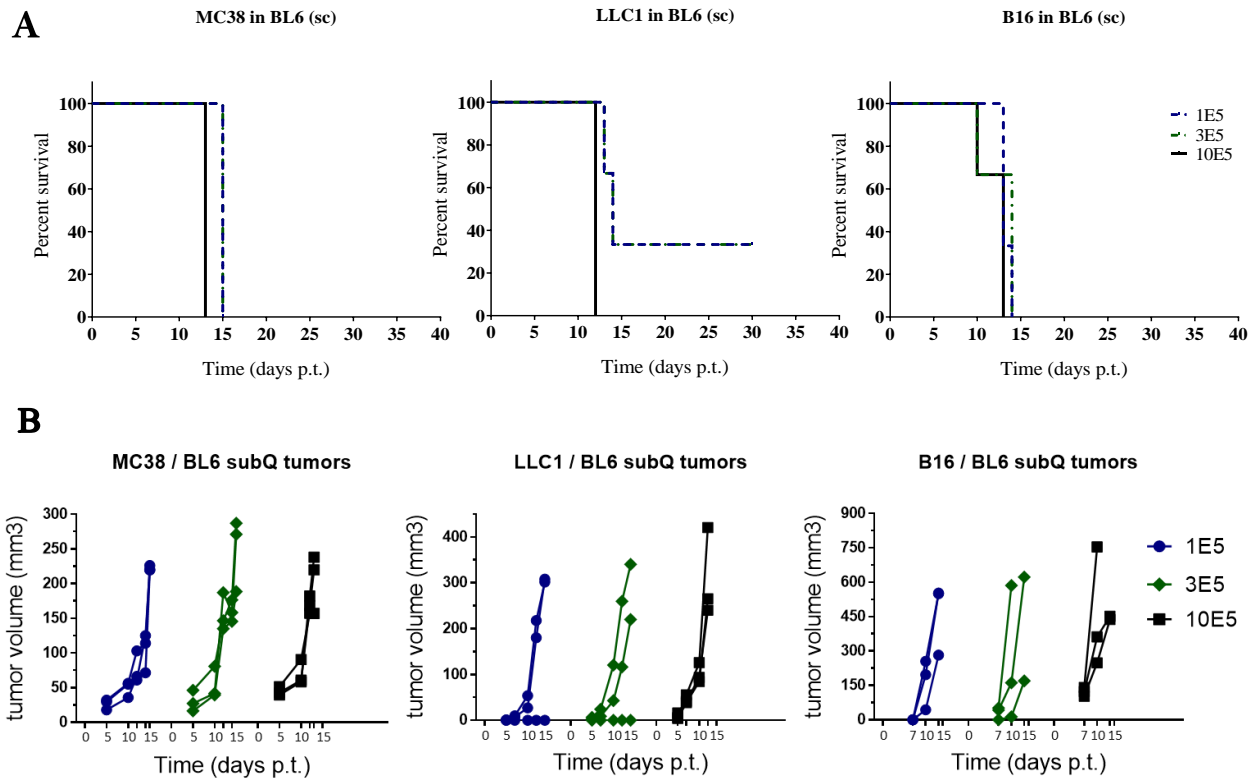


**Figure 33. Tumor aggressiveness in preliminary subcutaneous tumor model.** (A) Three cell lines, injected subcutaneously into C57BL/6J mice revealed high aggressiveness, resulting in low survival rate. Injection of lower number of LLC1 cells did not result in metastatic engraftment. (B) Critical tumor volume within all groups was reached in maximum of 15 days after the initiation of experiment.

On the other hand, within three tumor mouse groups, except for few samples, macroscopically visible metastatic regions on the surface of the lungs could not be seen. However, after microscopic evaluation of the H&E stained samples, it was possible to observe and distinguish micrometastases within the lung tissue (Figure 34).

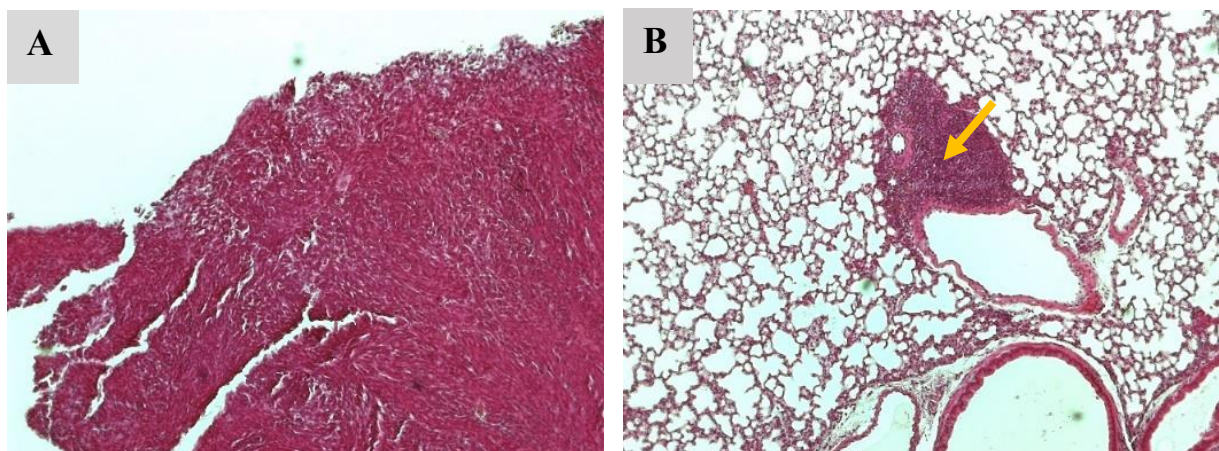


**Figure 34. Qualitative analysis of murine lung metastases.** Prior to analysis, lungs were fixed in formaldehyde, embedded in paraffin and 4  $\mu$ m thick slices were made. (A and B) Hematoxylin and

Eosin-stained sections of murine tissue. **(A)** H&E stained subcutaneous tumors were used as a positive control to identify the tumor tissue. **(B)** Lung metastasis was confirmed in comparison with the control tumor (yellow arrow).

Despite the fact that it was possible to detect the micrometastases, their overall number was very low and, therefore, could not satisfy the model requirements. Additionally, semiquantitative analysis revealed that more than half of all isolated lungs did not even contain metastases. Surprisingly low lung tumor engraftment was due to high subcutaneous tumor aggressiveness, since the mice had to be sacrificed after reaching critical tumor volume. Insight into literature suggested that higher lung metastatic burden could have been achieved in case of continuous removal of subcutaneous tumors, which would have significantly prolonged the duration of the experiment<sup>305</sup>. This was, however, from the time point of view, not in accordance with the model expectations.

The preliminary subcutaneous model did not satisfy the requirement of obtaining the significant number of lung macrometastasis, which was considered as essential for the next set of experiments. Moreover, due to the fact that biased micrometastatic quantification could have led to imprecise results, it was decided to proceed further with a different lung metastasis model by intravenous injection of tumor cells. Due to its extremely high aggressiveness, murine melanoma model cell line (B16) was not used for further mouse experiments.

### 3.5.2 Efficiency of antiangiogenic therapy in subcutaneous model

In order to start the main mouse experiments (including genetic targeting of the apelinergic system), it was important to test the effectiveness of antiangiogenic therapy on tumor growth. Similar to the previous experiment, LLC1 tumor cells were subcutaneously injected into female C57BL/6J mice. For treatment, DC101, an antiangiogenic monoclonal antibody targeting the receptor for Vascular Endothelial Growth Factor (VEGFR-2) was used, which is a mouse analog for human ramucirumab. Treatment was initiated four days after transplantation and mice were treated two times per week. The results of the experiment confirmed the positive effect of antiangiogenic treatment in terms of reducing tumor growth (Figure 35).

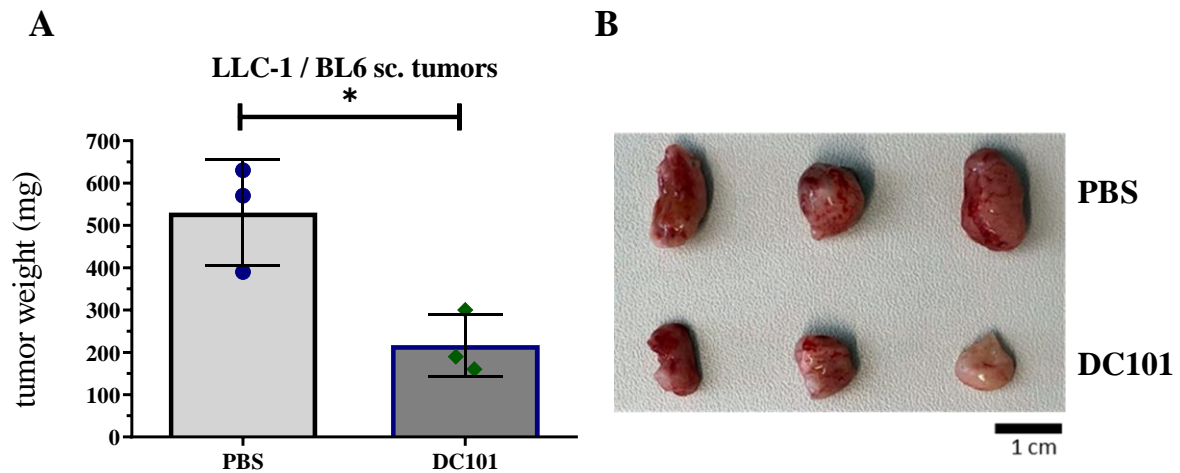


**Figure 35. Effectiveness of antiangiogenic therapy on subcutaneous tumor growth.** (A) Subcutaneous tumor weight of DC101-treated mice was compared to untreated control (PBS). (B) Antiangiogenic treatment resulted in observably low tumor diameter. Results are presented as mean  $\pm$  SD. Levels of significance: \*  $p < 0.05$ ; Unpaired t-test.

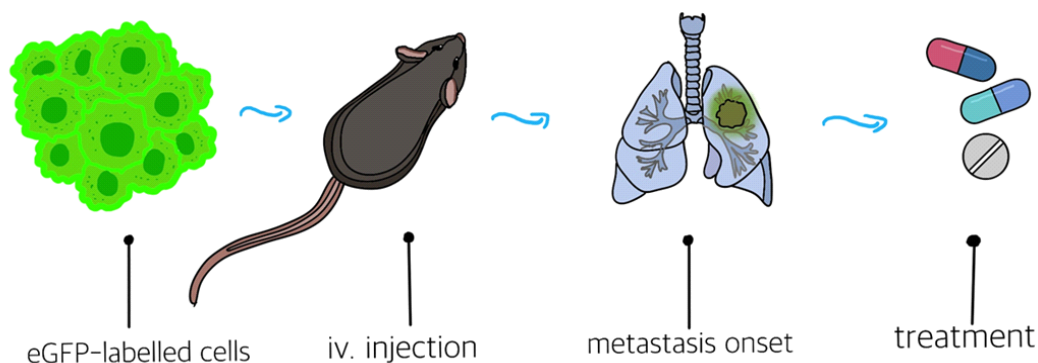
Suppression of subcutaneous tumor growth in DC101 treated mice could be observed after a relatively short exposure to the drug (up to two weeks) and it was considered as a sign of therapy effectiveness in this model.

### 3.5.3 Efficiency of antiangiogenic therapy in intravenous model

After analyzing the efficiency of the antiangiogenic therapy in subcutaneous model, next set of experiments was carried out by intravenously injecting MC38 and LLC1 cells into female C57BL/6J mice. Tumor cells were transduced using a lentiviral vector system to allow the stable expression of an enhanced green fluorescent protein (eGFP). The idea behind this was to estimate lung metastatic burden more precisely through the number of engrafted eGFP positive tumor cells. eGFP-labeled cells are easily detected and hence their presence can be quantified by flow cytometry.

In accordance with previously conducted subcutaneous experiments, treatment with DC101 was able to lower the lung metastatic burden, resulting in decreased number of lung macrometastasis, compared to the untreated group (PBS) (Figure 36). However, the reduced metastatic burden was not statistically significant. Therefore, in comparison to its efficiency in subcutaneous tumor model, antiangiogenic therapy displayed moderate effects on inhibiting lung metastases formation and onset.

A



B

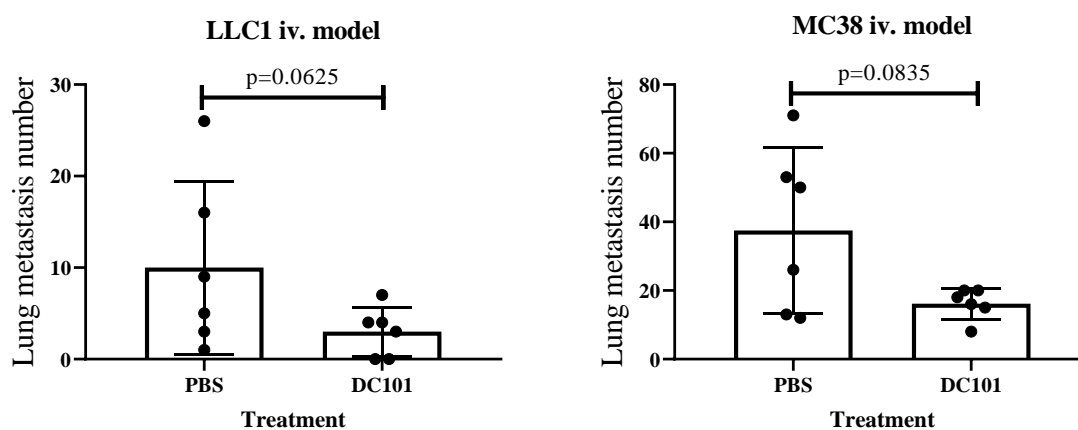


**Figure 36. Effect of DC101 on the lung metastatic burden.** (A) Schematic representation of the experimental setup: LLC1 and MC38 cells were transduced with the LeGO-iG2 vector system to stably overexpress eGFP. After the metastatic engraftment, the antiangiogenic treatment was initiated. (B) Treatment with DC101 resulted in a moderate reduction in number of observable lung macrometastases for both LLC1 and MC38 intravenous models. Results are presented as mean  $\pm$  SD and levels of significance are presented above bars. Paired two-tailed t-test.

Whereas the existence of metastasis was undoubtedly confirmed by macroscopic observation, contrary to the expectations, lung metastatic burden in either model could not be quantified by flow cytometry. Constantly low overall eGFP expression was present in isolated lung tissue, as it is shown in Figure 37. Nevertheless, the evidence of moderate effectiveness of antiangiogenic therapy was considered as enough in order to conduct the main experiments.

## RESULTS

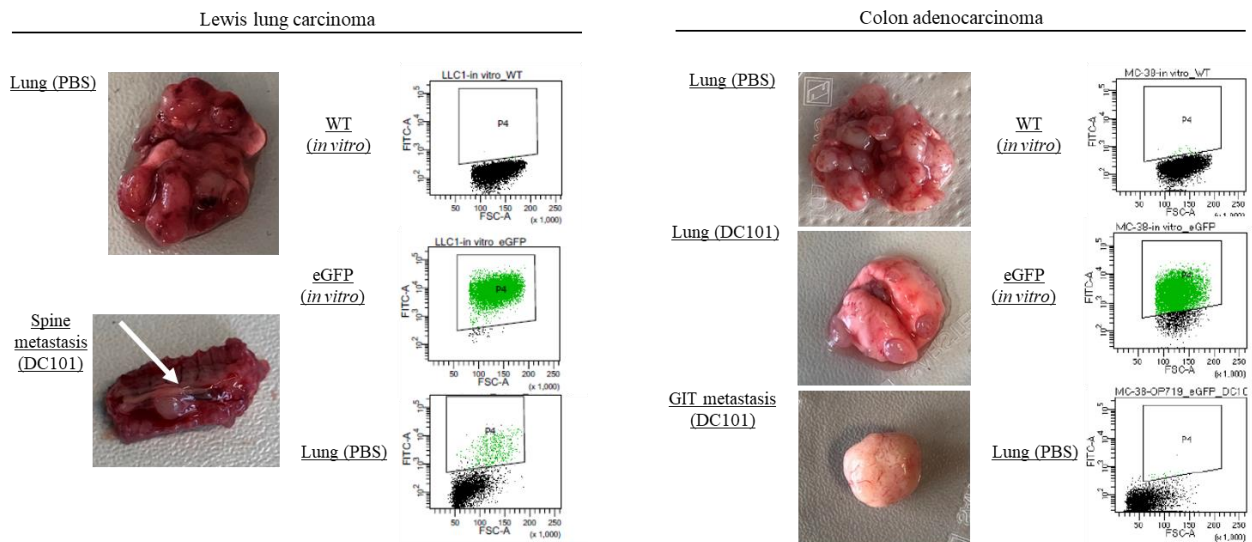


**Figure 37. Quantification of metastatic burden in intravenous lung metastatic model.** Although macroscopically visible, it was not possible to detect and quantify lung metastatic burden based on eGFP positivity of tumor cells within the lung tissue. On the contrary, in *in vitro* conditions, it was possible to clearly distinguish the presence of eGFP signal in cultured eGFP<sup>+</sup> LLC1 and MC38 cells, compared to wildtype cells. Other metastases (spine, gastrointestinal tract, left and right, respectively) were not assessed.

### 3.6 Targeting of the apelinergic system by AAV vectors

To examine the effects of vector-mediated inhibition/stimulation of the apelinergic system on tumor vascularity and overall growth, as well as on lung metastasis, adeno-associated viral (AAV) vectors were used. Effective targeting of lung endothelial cells by AAVs in therapeutically highly relevant pulmonary vasculature as target tissue has been described by Körbelin *et al.*<sup>277</sup>. Therefore, genes for mouse Apelin and APJ antagonist, F13A, were cloned into AAVs. Choosing this strategy, based on organ-specific vector homing to the endothelium after intravenous administration, was considered as applicable for *in vivo* gene delivery in the experimental conditions.

#### *Luciferase – a reporter gene for Apelin/F13A expression*

Gene encoding for firefly luciferase was cloned into AAV vector system to serve as a reporter, ensuring that specific targeting of lung endothelial cells has been achieved. Upon successful homing of the viral particles, *in vivo/ex vivo* imaging (IVI/EVI) can be used to detect the location of the reporter signal. To confirm the presence of the GOI within AAV, the vector was sequenced two times and it was used to transfect HEK293 cells transiently. Luminescence was measured 24 hours after cell transfection (Figure 38).

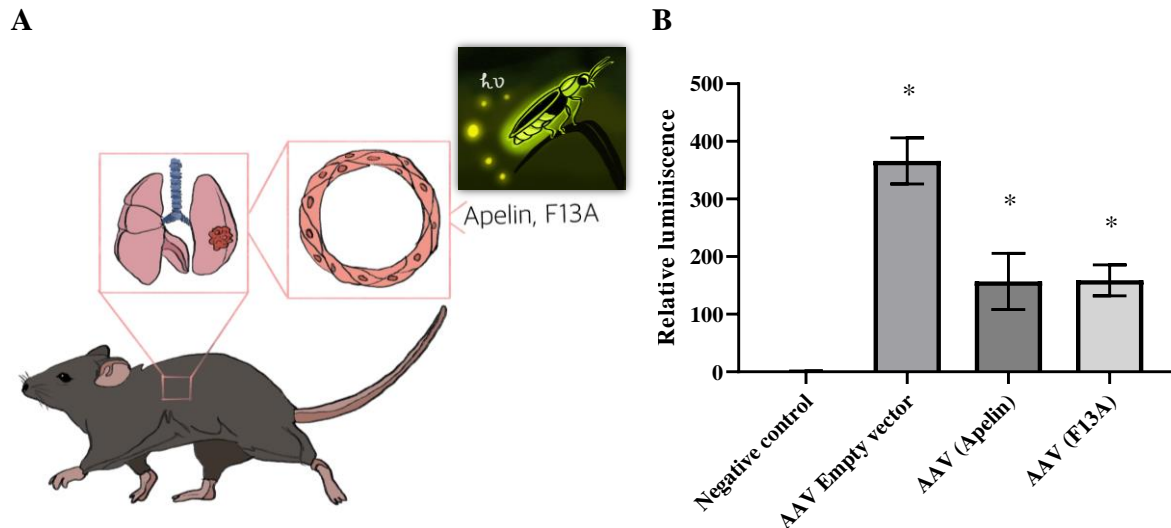


**Figure 38. AAV pre-experimental setup.** (A) Schematic illustration of murine lung endothelium, which expresses Apelin or F13A and firefly luciferase upon AAV transduction. After injection, luciferin undergoes a reaction of oxidative decarboxylation in the presence of ATP, oxygen, and a firefly luciferase and consequent luminescence occurs. (B) *In vitro* luminescence assay was carried out to confirm the presence of the reporter gene in transfected cells: HEK293 cells that are successfully transfected with plasmid containing Apelin (F13A)-Luc sequence express both Apelin (F13A) and firefly luciferase genes. Results are presented as mean  $\pm$  SD. Levels of significance: \*  $p < 0.05$ . Unpaired t-test.

### 3.6.1 Specificity of AAVs to the lung endothelium

To confirm the claimed specificity of the AAV vectors toward endothelial cells of the murine pulmonary tissue, AAVs were intravenously injected into female mice, assembling the experimental setup into four groups:

- No-AAV control (PBS)
- AAV-Luciferase (empty vector)
- AAV-Apelin-Luciferase
- AAV-F13A-Luciferase

After injection, mice have been kept healthy under normal conditions in an animal facility over a five-week period. Prior to sacrifice, mice have been injected with luciferin and tissue targeting of the AAV vectors was visualized by imaging the CMV-driven luciferase expression. Although the number of replicates per group was low, imaging of the mouse organs revealed that the long-lasting presence of the luciferase signal was restricted to the lungs.

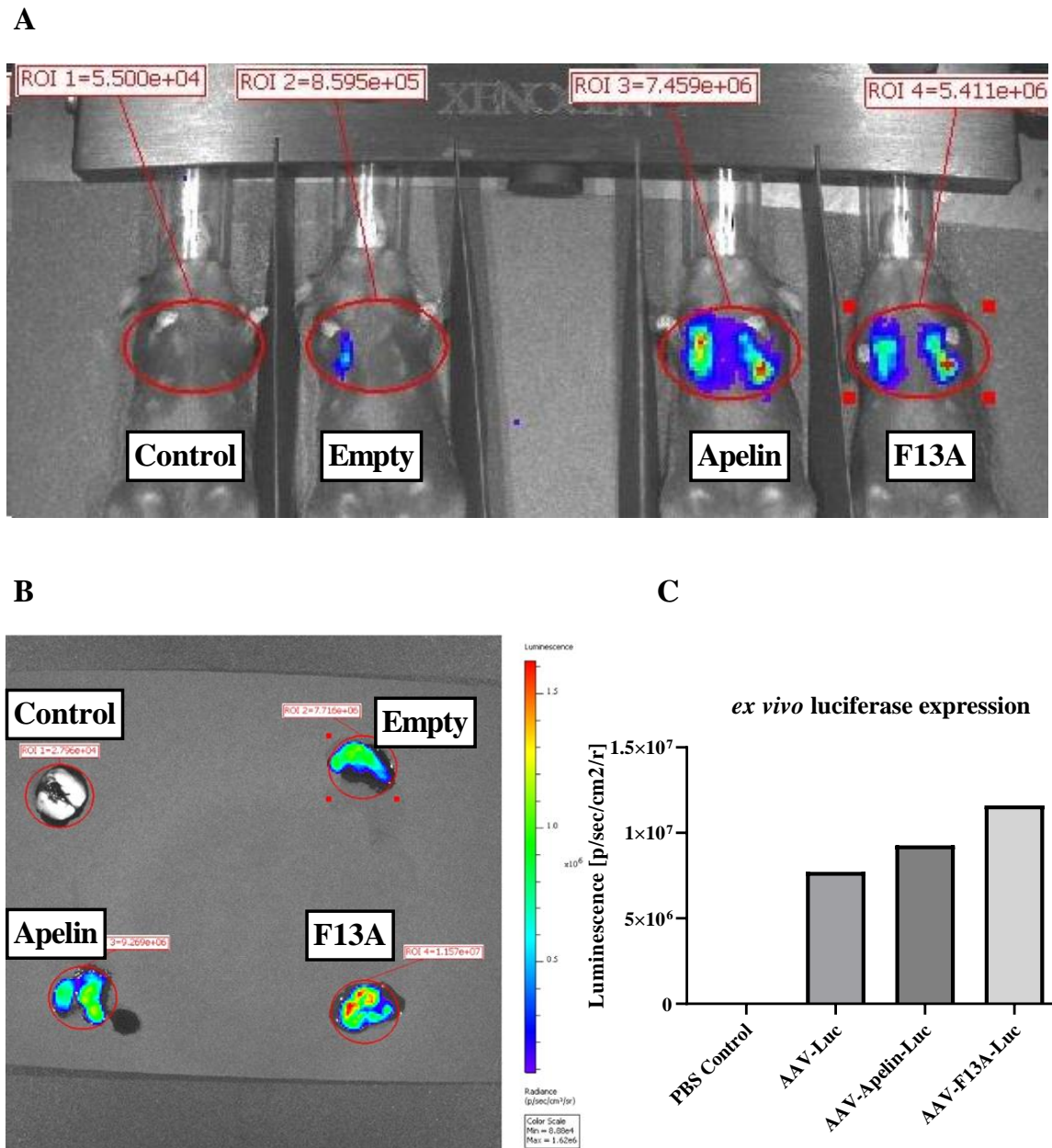


**Figure 39. Bioluminescence imaging (BLI) of mice intravenously injected with AAVs expressing firefly luciferase.** Recombinant AAV vectors carrying the luciferase gene under control of the CMV promoter were administered into the tail vein of mice at a dose of  $1.5 \times 10^{11}$  gp/mouse. (A) Mice were imaged when luminescence reached peak values after ip administration of luciferin potassium salt. (B) *Ex vivo* bioluminescent imaging revealed that AAV specifically targets pulmonary endothelium. (C) High luciferase expression was detected in the lung tissue in all AAVs groups.

Additionally, these findings had been validated *ex vivo*, measuring bioluminescence of the extracted lungs. While bioluminescent signal was not found present in the control group, high signal intensity was observed in all Luc-expressing groups. The results of preliminary AAV experiments indicated successful targeting of the endothelial cells located within murine lungs (Figure 39).



### 3.6.2 AAV-mediated targeting of apelinergic system in a lung metastasis model

#### Main experiment

After evaluation of specificity toward pulmonary endothelium, as well as the efficiency of antiangiogenic therapy, Apelin/F13A-expressing AAV vectors were used in combination with antiangiogenic treatment to examine their effects on the metastatic burden. The schematic representation of the experimental design is shown in Figure 40.

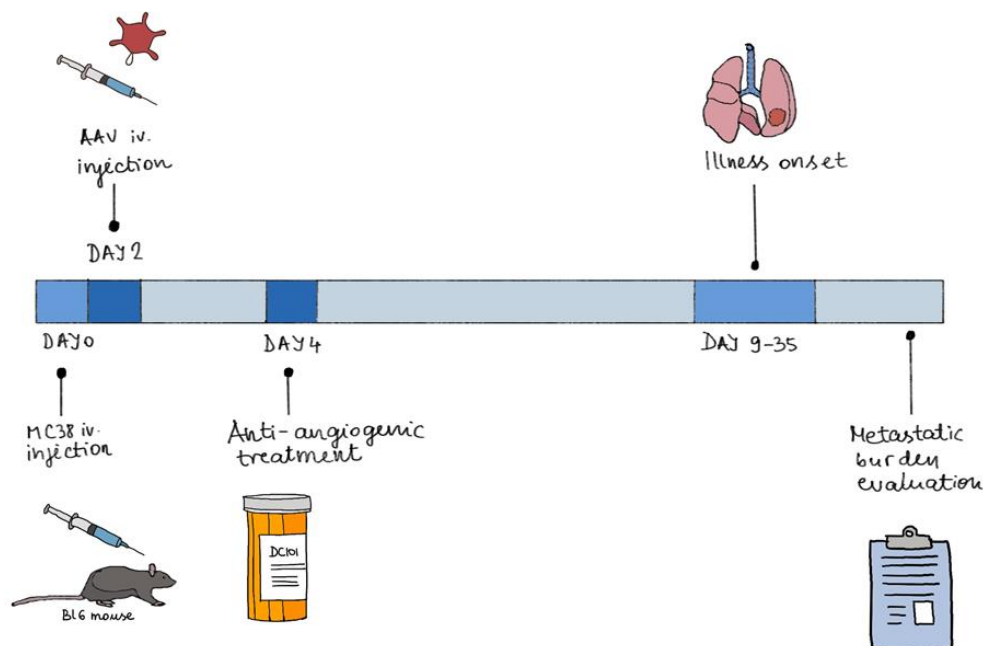


**Figure 40. Experimental setup of the main AAV experiment.** MC38 cells were intravenously injected into mice, to induce lung metastasis, followed by AAV injection on the second day. Four days after the tumor cell injection, antiangiogenic treatment with mouse anti-VEGFR-2 antibody, DC101, was started.

Depending on the treatment and the administration of AAV vectors containing the specific gene of interest, mice were divided into six cohorts (Table 23). All mice were sacrificed at the same time point ( $n=36$ ), however, during the early experimental phase, four mice died of unknown causes.

**Table 23. Different cohorts in the main AAV experiment.**

Cohort number	Gene of interest in AAV	Antiangiogenic treatment (DC101)
1	Empty	No
2	Empty	Yes
3	Apelin	No
4	Apelin	Yes
5	F13A	No
6	F13A	Yes

## RESULTS

Surprisingly, analysis of the results showed that previously highly metastatic MC38 cell line caused a generally low metastatic burden within all observed groups (Figure 41). Unexpectedly low tumor cell engraftment could also be seen in the control group. On the other hand, the highest metastatic number (15-30) has been observed in just two mice from F13A (treated and untreated) group. This was, however, significantly lower in comparison with the preliminary intravenous lung metastasis model, where metastasis burden reached two-fold higher number.

Dark red spots in the lungs, indicating internal bleeding, could be seen in all cohorts. The presence of internal bleeding within the pulmonary tissue, as well as low metastatic burden, suggested another role of AAV vectors in metastasis onset, irrelevant to the Apelin/APJ system's activation/inhibition. Moreover, these findings indicated the potential immunostimulatory effect of AAVs on lung tissue and the possibility of triggering immune cell infiltration, which further could have prevented the metastatic onset.

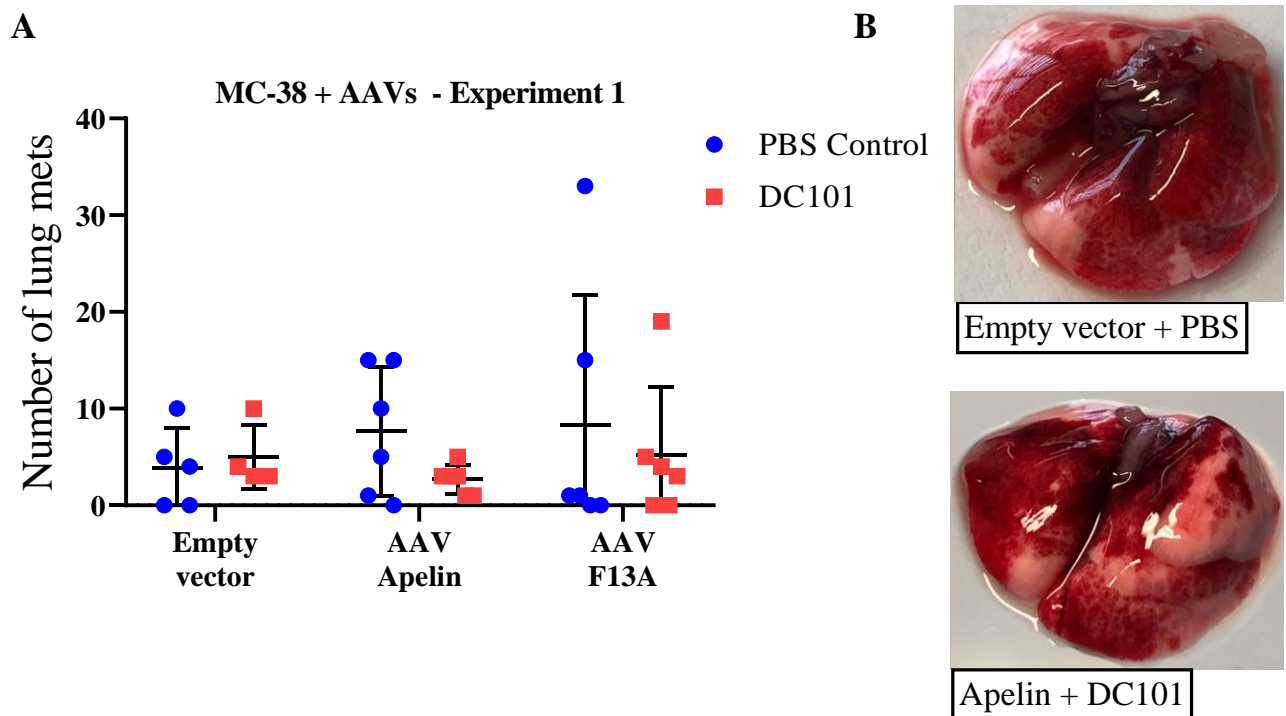


**Figure 41. Effects of Apelin and F13A on the metastatic burden.** (A) Unexpectedly, macroscopic analysis revealed low lung metastatic burden that was present in all six mouse cohorts and no differences between groups could be observed. (B) Internal bleeding was present in all AAV cohorts. Results are presented as mean  $\pm$  SD. Levels of significance: ns (non-significant); One-way ANOVA followed by Tukey's multiple comparisons test.

Following macroscopic analysis, RT-qPCR was performed to further quantify metastatic colonization of the left lung half on behalf of eGFP gene expression (Figure 42). The results of gene expression analysis were similar to those from the macroscopic analysis. Except for one

sample, eGFP could be detected in all analyzed groups. However, high variability was observed and no significant difference could be seen between groups.

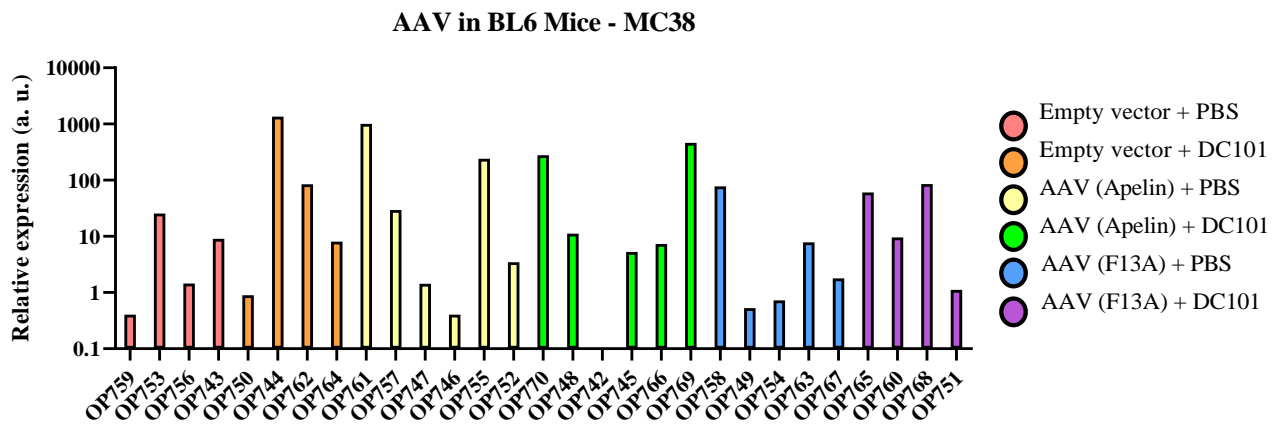


**Figure 42. eGFP expression analysis in murine lung tissue.** To provide further details on the metastatic burden within tested groups, expression analysis of the gene encoding for enhanced green fluorescent protein (eGFP) was performed. The expression of eGFP directly correlates with the amount of tumor cells present in the lung compartment. OP is a name assigned to the group member to randomize the analysis. No differences in eGFP expression between the groups were observed.

#### *Repeated main experiment*

Due to unexpected and contradictory results in the AAV C57BL/6J lung metastasis model, the previous experiment was repeated. Hence, to avoid possible biases that might have arisen from the earlier experiment, additional control group (non-AAV treated mice) was included in the experimental setup.

Macroscopic analysis from repeated experiment indicated that the high variability remained the same as the previous experiment showed (Figure 43). Hence, the lung metastatic burden of control groups was again not as high as expected, since the highest number of metastasis was 10, in comparison to 71, what has been seen in the preliminary intravenous model. On the other hand, the analysis revealed better engraftment in other groups when compared to the preceding experiment. Still, no significant differences in number of lung metastases have been observed between the different mouse cohorts: neither within different AAV vector cohorts, nor in groups with or without antiangiogenic treatment. Interestingly, non-AAV (no-vector) cohort seemed to have had the similar metastatic burden as other AAV groups (both Apelin and F13A), independent of DC101 treatment. Therefore, the application of the AAV vector in general, was unlikely to have had an impact on lung metastasis onset in this experimental model.

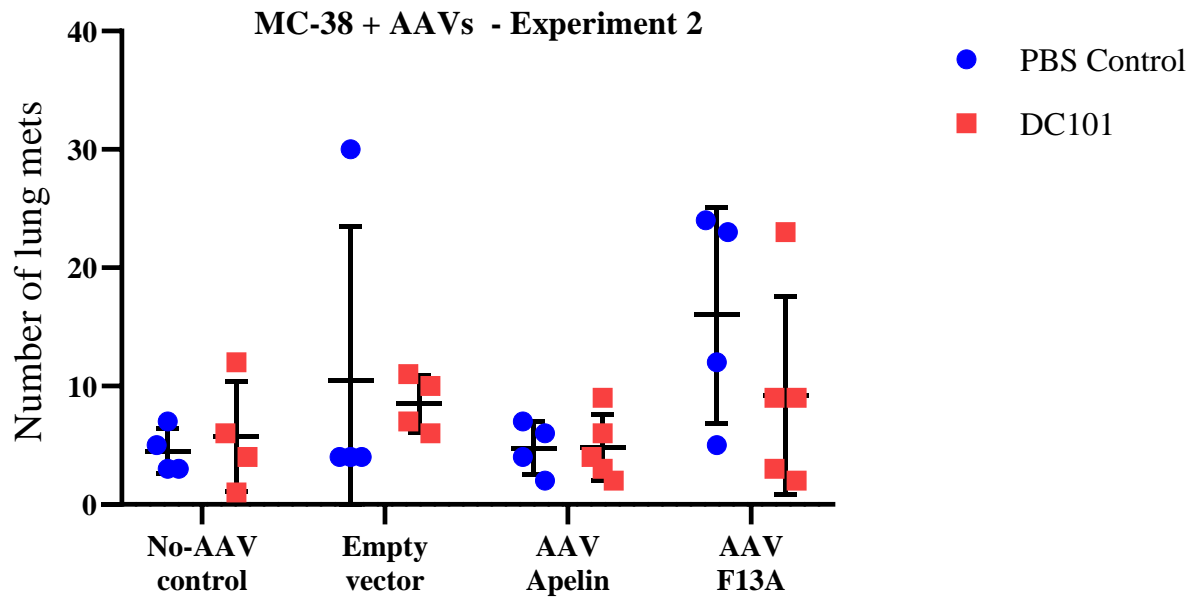


**Figure 43. Effect of Apelin and F13A on metastatic burden in the repeated main experiment.** Results of the macroscopic analysis revealed that a low lung metastatic burden remained low in all groups without significant observable differences between the groups. Results are presented as mean  $\pm$  SD. Levels of significance: ns non-significant; One-way ANOVA followed by Tukey's multiple comparisons test.

#### *Presence of Apelin and F13A in AAV-treated pulmonary tissue*

To elaborate on the effect of Apelin and F13A level on the metastatic burden, murine left lung lobe was used for the protein extraction and subsequent quantification of Apelin. Due to its structural similarity with Apelin, F13A level in pulmonary tissue was also quantified using the same ELISA Kit.

The results showed that Apelin concentration remained mostly at the endogenous level, since no differences in Apelin concentrations between the groups could be observed (Figure 44). In comparison to AAV-untreated control, as well as to empty-vector control, AAV-Apelin group showed no increase in Apelin concentration. Therefore, Apelin level remained constantly low, regardless of the AAV vector used for Apelin overexpression within lung endothelium.

On the other hand, moderate, but significant increase in F13A concentration was observed in AAV-F13A group. Compared to Apelin level in non-AAV group, total F13A concentration in pulmonary homogenates was found almost two times higher (Figure 44, A). However, this difference could not be observed when the raw data were relativized to the total concentration of all extracted proteins (Figure 44, B).

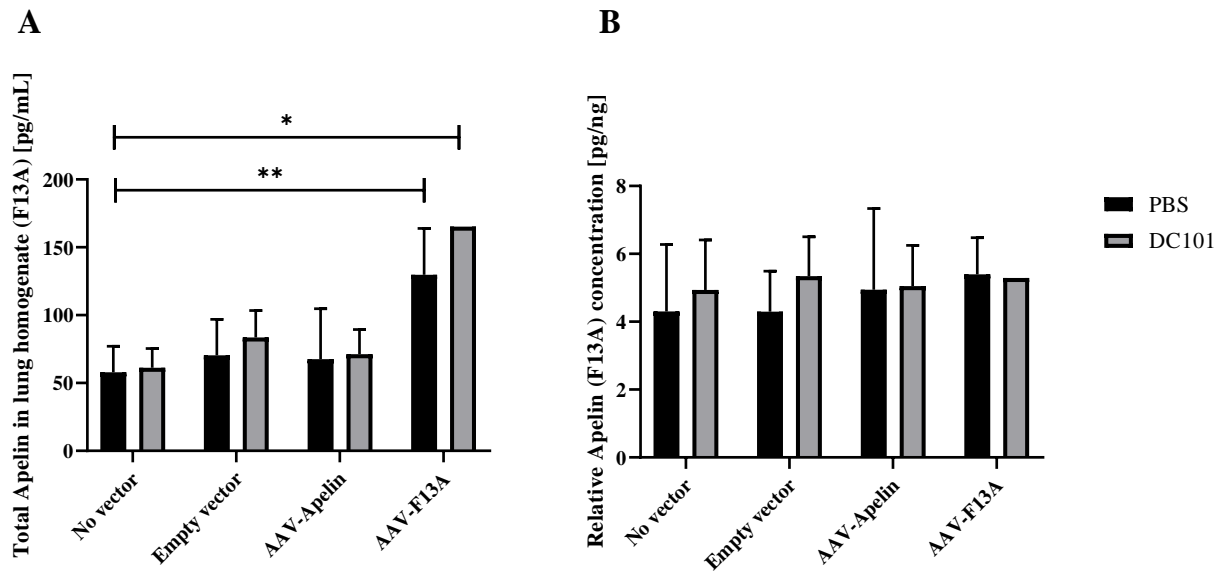


**Figure 44. Analysis of the Apelin/F13A concentration in murine lung tissue.** Enzyme-linked immunosorbent assay (ELISA) kit was used to detect and quantify Apelin (F13A) levels in the left lobe of murine lungs. Results are presented as total Apelin per lung half (A) or concentration of Apelin was normalized to the measured total protein level (B). In the AAV-F13A group, the concentration in four samples could not be measured due to very low concentration (below measurable level declared by the manufacturer). Each measurement was performed in duplicates. Results are presented as mean + SD. Levels of significance: \*  $p < 0.05$ ; \*\*  $p < 0.01$ ; ns non-significant. One-way ANOVA, followed by Dunnett's multiple comparisons test.

#### *Immune cell infiltration and microvessel density in metastases*

To evaluate microvessel density (MVD) and the infiltration of the immune cells in the tumor tissue, murine right pulmonary lobe was used for immunohistochemical staining. Samples were stained with antibodies directed against CD31 to investigate vascularity of the metastatic tissue, while CD3 and CD11b served to evaluate immune cell infiltration (Figure 45). Additionally, to identify tumor tissue, samples were stained with eGFP antibody, since MC38 cells had stable eGFP expression. Prior to the MVD quantification, tumor areas with angiogenic hotspots were manually selected by the pathologist.

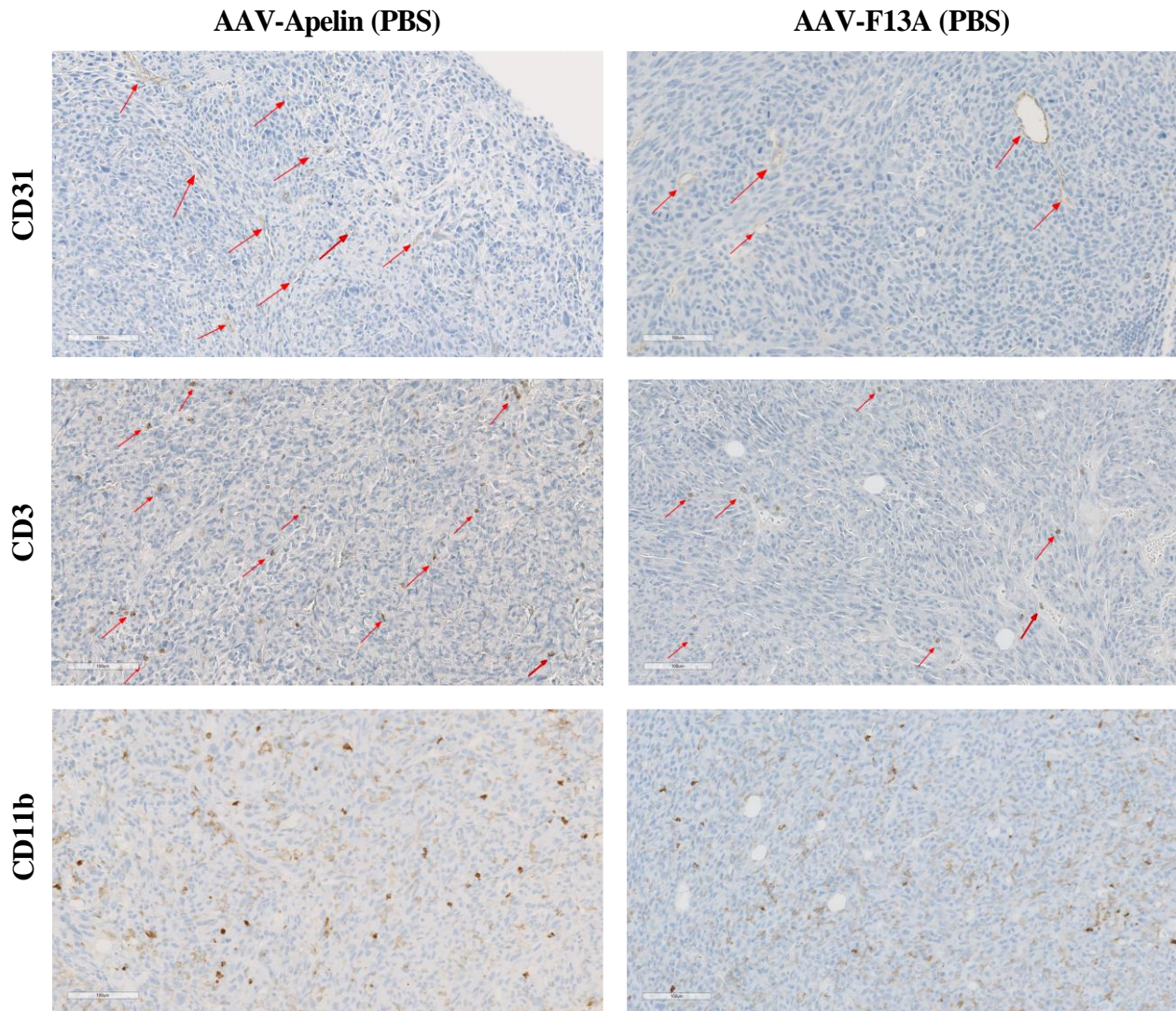


**Figure 45. Representative IHC images of pulmonary metastatic tissue in Apelin-PBS and F13A-PBS mice subgroups.** Histological staining was performed to determine changes in vascular density (CD31) and immune cell infiltration (CD3 and CD11b). Red arrows indicate blood vessels (CD31) and individual cells (CD3). Scale bars = 100  $\mu$ m.

Interesting results have been obtained after analyzing intratumoral microvessel density (Figure 46). In comparison to no-vector control, Apelin group (PBS and DC101 treated) displayed a significant increase in CD31 coverage. Furthermore, the vascularity in DC101-treated empty-vector group seemed to have been reduced when compared to untreated empty vector group. This decrease in MVD, however, was not statistically significant, due to high variability in CD31 positive area within both groups.

The most significant differences in MVD were observed when comparing Apelin and F13A groups (treated and untreated). While antiangiogenic treatment within Apelin and F13A subgroups had no effect on CD31 coverage, significant differences were noted between MVD

of untreated Apelin and untreated F13A groups. It could be observed that both treated and untreated F13A groups displayed a reduced CD31-positive area.

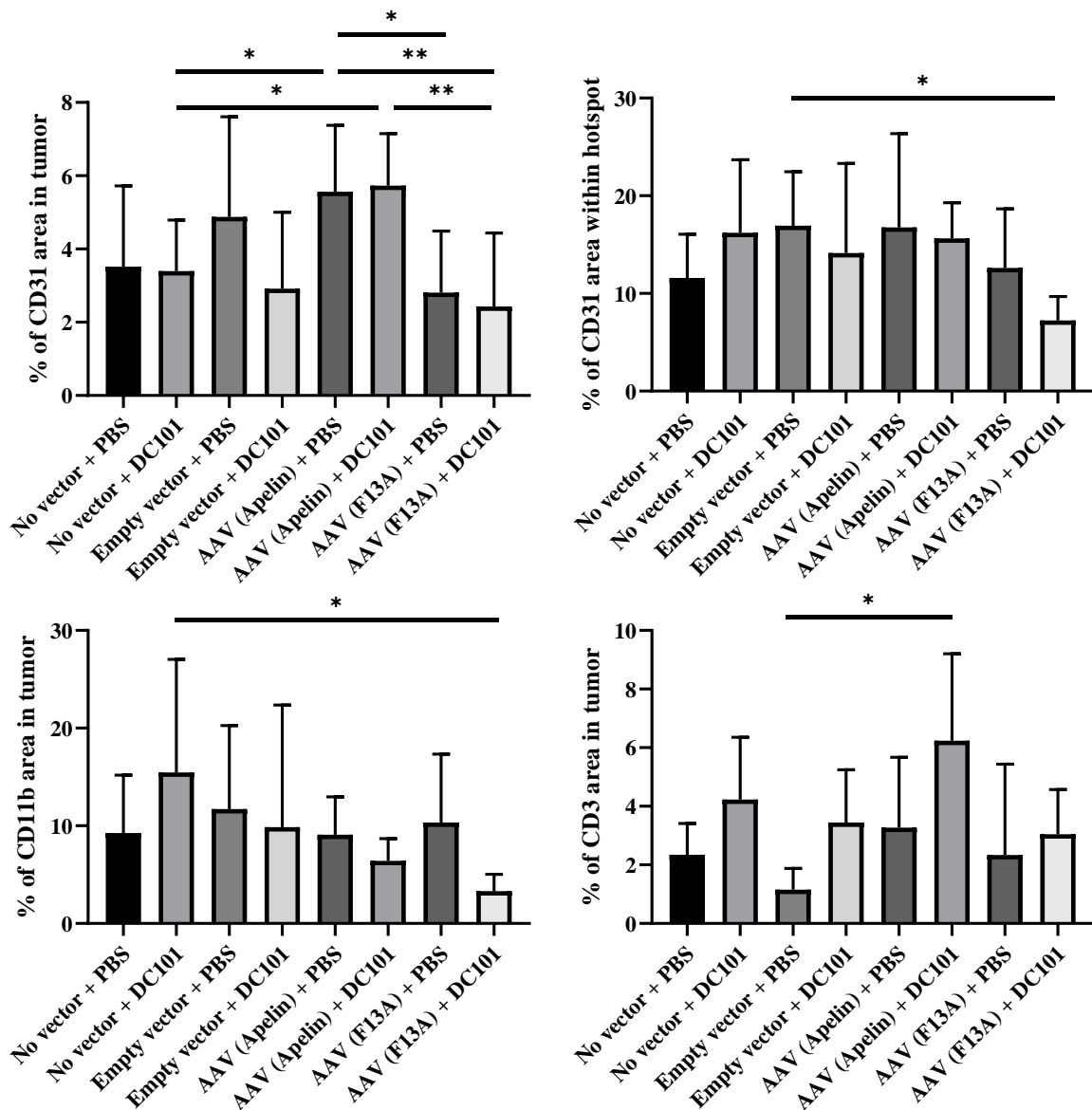


**Figure 46. Immunohistochemical analysis of the murine lung tissue.** Right lung lobes were fixed in formalin and embedded in paraffin, prior to IHC staining. MVD was assessed by analyzing the percentage of CD31 positive area within the tumor and by measuring the total C31 positive area within the angiogenic hotspots. Infiltration of the immune cells was assessed by staining against CD11b and CD3 areas. Unspecific stainings were excluded from data analysis. Results are expressed as mean percentage of positive area + SD. Levels of significance: \*  $p < 0.05$ ; \*\*  $p < 0.01$ . One-way ANOVA followed by Tukey's multiple comparisons test.

On the other hand, MVD was not affected by antiangiogenic treatment in case of no-vector cohort, since no differences between PBS and DC101-treated group was found.

## RESULTS

---

In general, the infiltration of immune cells seemed not to have been affected by the presence of Apelin/F13A or antiangiogenic treatment. It is worth noticing that groups with basal Apelin expression (no-vector and empty-vector) had to a certain extent higher infiltration of myeloid, CD11b-positive cells, compared to DC101-treated F13A group. In the case of CD3 cells infiltration, significantly increased coverage was present in the DC101-treated Apelin group. However, due to a high variability detected in other analyzed groups, no additional statistically significant differences in immune cell infiltration were found.



## 4. DISCUSSION

### 4.1 Apelinergic system in endothelial and proangiogenic immune cells

Prior to the beginning of this project, our working group showed that M<sub>2</sub>-like macrophages, found in patients suffering from pulmonary hypertension, have a higher expression level of Apelin receptor, APJ<sup>296</sup>. In accordance with these preliminary findings, primary hypothesis was that the APJ existence may present a part of the mechanism by which tumor-associated macrophages (TAM) communicate with the cells of active endothelium. This assumption was supported by previously published studies, which proved that during active angiogenesis, the effect of APJ ligand, Apelin, is expressed synergistically with VEGF signalization<sup>209</sup>.

Since higher APJ surface expression in macrophages was previously found in our research group, it was hypothesized that Apelin, secreted from tumor endothelial cells, actively mediates communication with macrophages, polarized by the influence of the tumor microenvironment. Results from this Ph.D. project demonstrate that Apelin is secreted from endothelial cells, regardless of the cell passage, meaning that there is a high probability that the same scenario happens *in vivo*. However, despite the findings of high endogenous Apelin expression, the presence of the putative receptor, APJ, could not be confirmed in endothelial cells. On the other hand, when endothelial cells were exposed to VEGF-A blockage (bevacizumab) and tyrosine kinase inhibition (sunitinib), APJ upregulation could be seen. Therefore, we can assume that the impairment of VEGF signaling pathway may alternatively trigger apelinergic signaling. Since del Toro *et al.* claim that APJ expression is restricted to stalk endothelial cells<sup>306</sup>, it should be taken into account that APJ upregulation may indicate activation of this cell phenotype. However, in order to get more clear insights, it is important to analyze more than one endothelial cell line. Hence, endothelial cells, isolated directly from tumors, would be a sample of choice for further investigation.

Isolation of viable macrophages from tumor tissue (TAMs) is known to be a tedious task, as the cells tend to become apoptotic and low cell number is a limiting factor in the analysis. Moreover, it is still not possible to genetically label this cell population due to a lack of specific TAM-associated markers<sup>307</sup>. Therefore, monocytes were artificially polarized toward macrophages with M<sub>2</sub> phenotype, assuring that the similar condition for the purpose of this analysis is established, since M<sub>2</sub> macrophages are closely related to TAMs<sup>308,309</sup>. Different methods of monocyte polarization were tested in order to acquire M<sub>2</sub> macrophages. After the

## DISCUSSION

---

optimization, it was found that the most efficient method was the phase polarization, in which the macrophages were treated first with M-CSF, following the stimulation with IL-4. To confirm M<sub>2</sub> phenotype, cells were tested for the presence of already known specific markers CD163 and CD206<sup>310</sup>. Finally, these markers were found present in polarized macrophages, which confirmed that they displayed proangiogenic M<sub>2</sub> phenotype.

Although with the optimized polarization strategy it was possible to confirm the proangiogenic macrophage phenotype, it was not likely to detect high presence of APJ on macrophages. Moreover, the results of flow cytometric analysis occasionally showed even lower expression of APJ in comparison to the isotype control for the antibody. This obstacle could have been surpassed neither with the antibody titration, nor by lowering the concentration of isotype control, which finally raised doubt about antibody functionality. It is worth noticing the differences between the APC-labeled antibody used in the previous work of our research group and the one used in this study. Unlike the APC-labeled antibody used in this study, the “older” antibody, raised from different clone, was fully functional and observable differences in APJ expression in comparison to control could be seen. Unfortunately, the antibody used in previous studies was discontinued, and next choice was using the most similar one (produced by the same manufacturer). Furthermore, as it will be discussed in the following sections, the “new” APC-labeled antibody displayed low binding capacity when used on various primary cells and cell lines. Finally, the low functionality of this antibody was shown in a separate experiment (see Supplementary data).

Contradictory to the results obtained from APC-coupled antibody, generally higher APJ surface expression was found using another antibody labeled with a different fluorophore (Alexa Fluor 488). These data were yet in accordance with the findings from another research group from our clinic<sup>311</sup>. However, main reasons for finding higher expression of APJ in M<sub>2</sub> macrophages were not clear, since Alexa Fluor 488-coupled antibody was raised from the same clone as APC-coupled antibody used in this study.

To get more insight into the APJ presence, a series of quantitative analyses of APJ mRNA expression in polarized macrophages were conducted. Once again, the results indicated a low APJ expression in M<sub>2</sub> macrophages. In general, constantly high Ct values and no positive control for APJ mRNA level were the limiting factors in gene expression analysis and no clear conclusion could be drawn regarding the APJ expression in macrophages. Until now, there has been no report on the mRNA expression level of APJ in alternatively polarized macrophages.

The conflicting results of flow cytometric analysis and RT-qPCR imply the need for a reliable control for the experimental setup. The relatively low abundance of Apelin receptor may even be considered as “normal”, in case that low quantities of the ligand can trigger apelinergic system’s signaling pathway. On the other hand, gene expression analysis has shown moderate, but visible upregulation of apelinergic system under hypoxia. Since tumors tend to exploit the immune system, especially in hypoxic conditions, we can speculate that apelinergic system becomes “a bigger player” and “line of communication” in such events. Again, the most valuable information is likely to be seen after gene expression analysis of TAMs.

Based on defined panel for flow cytometric analysis of M<sub>2</sub> macrophages, surface expression of Tie2 receptor, one of the crucial factors in the angiogenic process, has been analyzed. Although low APJ expression was reported and therefore did not confirm the primary hypothesis, interestingly, it was discovered that polarized M<sub>2</sub> macrophages have substantially higher expression of Tie2 receptor, compared to monocytes and M<sub>1</sub> macrophages. Prior studies proved that Tie2-expressing macrophages foster tumor angiogenesis and additional studies confirmed that these cells could only be found in the cancerous tissues<sup>312,313</sup>. In accordance with these claims, Atanasov *et al.* confirmed that the presence of M<sub>2</sub> polarized macrophages expressing Tie2 receptor is associated with decreased overall survival in patients with cancer<sup>314,315</sup>. Therefore, it was confirmed that M<sub>2</sub> macrophages from this experimental system were indeed proangiogenic.

According to flow cytometric analysis using APC-labeled antibody, APJ level remained very low in myeloid cells (monocytes, M<sub>1</sub> and M<sub>2</sub> macrophages). Therefore, the investigation was broadened on peripheral blood mononuclear cells (PBMC). PBMC pool was divided into several cell lineage groups, based on a specific pattern of marker surface expression. The idea behind this was to prove the existence of the cell fraction, which exclusively expresses APJ. It was found that monocytic, CD14/CD11b cell fraction, together with CD14/Tie2 cell population, have the highest proportion of APJ positive cells. Although it was possible to isolate the cell fraction with possible proangiogenic potential, the overall APJ expression within that fraction was less than expected. In order to obtain more precise results and to avoid biases, the quantification method for APJ has to be further optimized.

### 4.2 The function of the apelinergic system in macrophages

As already mentioned, previous findings did not confirm APJ expression at the expected level. Nevertheless, it was sought to examine the possibility to induce APJ upregulation in M<sub>2</sub> macrophages and for that purpose, cells were stimulated with several agents. Some of them were likely to display agonistic effect (AM01-182, AM01-190, AM02-50, Apelin), while from other molecules (KT01-3, KT01-11, MM54, F13A) antagonism toward APJ was expected. Additionally, to mimic the *in vivo* conditions, in which M<sub>2</sub> macrophages communicate with endothelial and tumor cells, stimulation with supernatant from endothelial cells and tumor cells under hypoxia was performed. Yet, no significant changes in APJ expression were observed. Quantification of APLN mRNA level additionally showed that M<sub>2</sub> macrophages are likely to secrete Apelin in higher amounts when stimulated with supernatant from endothelial cells, which indicated the potential communication between proangiogenic macrophages and endothelial cells. However, it was not possible to clearly prove that the connection between alternatively polarized macrophages and endothelial cells is directly achieved via the apelinergic system.

Regardless of the apelinergic system's presence, viability of M<sub>2</sub> macrophages as a response to stimulation and inhibition of the receptor was examined. It was found that APJ inhibition with MM54 moderately lowered cell viability/proliferation, compared to Apelin-treated macrophages. However, neither Apelin nor any other Apelin analog significantly affected cell viability/proliferation, compared to the control group. Low expression of both APLN and APJ may indicate the insufficiency of the experimental system to simulate *in vivo* conditions in this case. Tumor microenvironment, which is essential to understand the function of immune cells, could not have been fully reproduced in the applied experimental setup. From *in vitro* experiments, no strong evidence on Apelin/APJ contribution to macrophage viability was provided.

On the other hand, the conflicting conclusion in the literature on this topic reveals a substantial gap in understanding the role of apelinergic system in macrophages. One may assume that the applied experimental setup did not accomplish the sufficient level of macrophage polarization and therefore it was not possible to observe an effect of activation or inhibition of the apelinergic system. Latroche *et al.* showed that Apelin is a central molecule that participates in the myogenesis and angiogenesis by modulation of macrophage functions, indicating the presence and function of the receptor<sup>316</sup>. These findings again may lead to the conclusion that

presence of the apelinergic system indeed depends on the state of polarized macrophages influenced by specific conditions. Such conditions, however, could not be simulated *in vitro*.

It is also worth to mention that certain studies reported that APLN/APJ pathway may not affect macrophage functions. For example, Hara *et al.* showed that activated macrophages have a similar profile of proinflammatory cytokines and migration properties, regardless of the Apelin presence<sup>317</sup>. Generally, results presented in this thesis suggest that macrophage functions might be even more complex. The alterations of the Apelin effects on macrophages should be considered in parallel with important proinflammatory molecules, such as cytokines. From that point of view, macrophages isolated directly from tumors would be a better option to examine the significance of the apelinergic system.

### **4.3 Direct link between apelinergic system and tumor**

Over the past decade, it was noted that the Apelin/APJ system plays an important role in tumor biology<sup>257,266,268,318,319</sup>. Before the beginning of this thesis, limited information was achieved in deciphering the exact mechanism of that role. In this study, the interest in the role of apelinergic system in cancer was extended by performing a wide search for the Apelin/APJ presence in tumor cell lines, as well as in tumor tissue. With that in regard, different aspects of investigation were assessed:

- Gene expression in tumor tissue and cell lines,
- Functional properties of the tumor cells as a response to stimulation/inhibition of the apelinergic system,
- Generation of an appropriate model to study effect of the apelinergic system in the tumor environment.

#### **4.3.1 Tumor tissue**

The search for the specific gene, whose expression is altered in cancer tissue, has been a key step in understanding tumor pathogenesis and patient prognosis for decades<sup>320</sup>. As mentioned in the introduction section, it is known that in the past few years, the expression of the apelinergic system has been documented in several cancer types. However, limiting and contradictory information about the apelinergic system's exact location has not yet been fully clarified. It is still not entirely known whether the apelinergic system can be found only within

## DISCUSSION

---

the extensive tumor vasculature or its location is also in tumor cells. This again creates confusion, since certain tumors are highly vasculogenic<sup>321</sup>: cells of such tumors exhibit vascular mimicry and are able to even differentiate into endothelial cells.

Apelinergic expression was examined in human and murine tumor tissue. During this project, a group of authors came out with data in which was claimed that APJ is highly upregulated in glioblastoma and that targeting of the apelinergic system impairs the growth of the tumor<sup>249</sup>. For the purpose of APJ expression screening, glioblastoma samples from patients that were treated in the clinic were analyzed. However, the results were not in agreement with the published study, since APJ expression was found to be very low. It is worth noticing that the samples were analyzed using flow cytometry with the antibody of questionable functionality and our considerations need to relate to the limitation of the number of biological replicates.

On the other hand, analysis of the murine tumor tissue revealed very high levels of mRNA for both APLN and APJ genes. Findings of increased apelinergic system's expression was thought to have been influenced by the possible contamination of samples with genomic DNA. However, after designing primers that specifically bind gDNA, results of gene expression analysis excluded suspected contamination, since the majority of samples were gDNA-free. This may indicate again that the tumor microenvironment specifically upregulates the expression of both APLN and APJ, which is hardly possible to reproduce in *in vitro* conditions. In these experimental conditions, it was unlikely to show in which tumor compartment Apelin/APJ has the highest expression, since murine tumor tissue was frozen and no isolation of viable cells was possible. However, based on findings that have been published in the course of this study<sup>322</sup>, one can speculate that the tumor endothelium is primary location of APJ.

The expression levels of APLN and APJ mRNA have also been investigated on cells isolated from the bone marrow of patients suffering from acute myeloid leukemia (AML). APJ mRNA expression was found to be moderately expressed, yet not as low as it was observed in M2 macrophages. Surprisingly, APLN was found on a very low level. This once again raised the question about the role of tumor microenvironment in the regulation of the apelinergic system. Since pathophysiology of AML is highly influenced by the extensive vascular network within the bone marrow niche<sup>70</sup>, it can be assumed that Apelin, secreted by endothelial cells, is a signaling molecule that interacts with AML cells.

To further corroborate these findings with present hypotheses, Apelin plasma levels of patients suffering from ovarian tumors were analyzed. Surprisingly, analysis of the results showed low

levels of Apelin in plasma of most ovarian cancer patients, compared to the healthy ones. This implies that serum/plasma Apelin may not serve as a good prognostic marker for cancer patients. Also, these findings seem to be in agreement with those published by Feng *et al.*, where correlation between the serum Apelin and prognostic markers could not be made. Moreover, these authors have proven that Apelin isolated from tumors, and not from serum, is associated with the worsened overall prognosis<sup>260</sup>. Therefore, the presence of physiological Apelin should not be confused with the overall outcome in cancer patients and should be taken with care. The limitation of this study was the unlikelihood to get insight into Apelin levels within ovarian cancers. This once again leads to the conclusion that the function of the apelinergic system in cancer is limited to the tumor compartment. From one point of view, this can be considered as useful, since it makes the apelinergic system more “targetable”, in case that apelinergic system is exclusively upregulated in tumor tissue. This assumption, however, must be further investigated.

One can also assume that the upregulation of APLN and APJ genes can easily be assigned to the tumor endothelial cells which make microvascular proliferation found in many solid tumors, as well as in leukemia. That way, tumor ECs potentially contribute to the higher expression that has been seen in some tumor samples. If we assume that the changes in mRNA expression are a result of an increased number of endothelial cells present in tumor tissue in general, rather than changes of expression in tumor cells alone, then the expression of the whole apelinergic system is less likely to contribute to the pathogenesis directly, but has a hardly known role in tumor blood vessel formation. These assumptions are, however, closely related to the findings of Kidoya *et al.*<sup>319</sup>.

#### 4.3.2 Tumor cell lines

In a recently published study, it was proven that, in comparison with healthy volunteers, serum levels of Apela, a ligand for APJ receptor, was increased in patients with chronic lymphocytic leukemia (CLL). In the same study, it was concluded that Apela is worth of research in targeted cancer treatment<sup>276</sup>. Knowing that this molecule was increased in CLL, it was hypothesized that the similar scenario may occur in acute myeloid leukemia. As a consequence of high Apela expression, the possibility of the upregulation of the putative receptor was assumed. Following analysis of the results obtained from primary tumor material, a profound screening of tumor-derived cell lines from solid tumors and AML was carried out.

## DISCUSSION

---

It was confirmed by both flow cytometric analysis and RT-qPCR that the majority of analyzed tumor cell lines have moderate to low APJ surface and gene expression. As mentioned in the results section, it was sought to reveal a stable expression, especially in case of glioblastoma (U118) and colon adenocarcinoma (HT29) cell lines, since the antibody manufacturer was constantly claiming to have been used these cell lines as a standard. Contrary to these claims, significant differences in expression were not observed. Additionally, similar results from the expression analysis of the majority of AML cell lines were obtained, revealing a variable, but overall low to moderate expression of both APLN and APJ.

It is plausible that the tested cell lines merely have low expression of APJ and APLN. This occurrence has already been seen, as Sorli *et al.* reported that APJ mRNA was not detectable in the well-established TS/A breast cancer cell line and that APLN mRNA was only detectable at a high cycle threshold (Ct of 34)<sup>323</sup>. Similar observations with glioblastoma cell lines were described in the Ph.D. thesis of Venkatesh<sup>324</sup>.

On the other hand, the study from Wang *et al.* has shown higher levels of APLN and APJ mRNA in another breast cancer cell line (Hs 578T), as well as in breast cancer tissue<sup>262</sup>. It is worth noticing that substantially higher APJ surface expression was found in the SKBR-3 breast carcinoma cell line. This may suggest that although primary tumor cells (not to be confused with tumor-derived cell lines) and tumor tissue may express high levels of Apelin and APJ, tumor cell lines may lose expression over time. Finally, the low expression of both Apelin and APJ in cell lines may be assigned to the likelihood that tumor cell lines simply do not express abundant amounts of these molecules. As previously mentioned, the other cell types that make up the tumor mass, such as vascular cells, could also express high levels of APLN and APJ. Another study has reported mRNA expression of APLN and APJ at more detectable levels in colorectal cancer cell lines<sup>318</sup>, which was in conflict with results obtained from this study. The gradual loss of apelinergic expression in cell culture is a critical limiting factor in representing *in vivo* conditions. Comparison of the Apelin and APJ levels, measured at both protein and gene levels, using the pre-established “standard” cell line would confirm this claim.



#### 4.4 Functional assays in tumor cell lines

##### 4.4.1 Proliferation rates

Regardless of the apelinergic system's absence in tumor cells, it was sought to test whether functional changes in cells upon APJ stimulation or inhibition can occur. For that reason, several functional *in vitro* assays were conducted. The majority of the cell lines that have already been screened for the presence of Apelin and APJ were used. Proliferation rates and viability status of the cells that have previously been treated with agonists and antagonists to APJ were assessed. The first set of assays were conducted using wildtype AML cell lines. However, it was not possible to observe any effect of either inhibition or stimulation of APJ, regardless of the concentration of substances used in functional assays. Until now, no similar data on AML cell lines have been published.

The obtained results led to an assumption that, in order to be able to observe any effect, APJ receptor should be artificially expressed in examined cells. Finally, to mitigate the absence of APJ mRNA expression in the majority of cell lines, as well as the lack of response to exogenous Apelin or APJ antagonist, a lentiviral vector system that allows stable Apelin and APJ overexpression on different cell lines was consequently used. Generating the overexpressing cell lines to model the apelinergic system was challenging to test in this system, since there was no valid method to confirm the stable expression, besides RT-qPCR. In general, one of the reasons for the biased quantification of protein surface expression is likely to be due to complex nature of G protein-coupled receptors<sup>325-327</sup>, such as APJ.

After the repetition of proliferation assays, using APJ overexpressing AML cell lines, it was not possible to observe any significant effect of APJ modulation. Similar results were found in solid tumor cell lines, with the exception of the moderate effect of MM54 on wildtype HT29, MDA MB231 and OVCAR8 cell lines. It was observed that the antagonism of APJ led to moderate, however, statistically non-significant effect in these cell lines in lowering their viability. These results were partially in accordance with the results obtained from previous studies, where it was proven that antagonizing APJ leads to lower proliferation rates of the tumor cells<sup>267,328</sup>. These findings, however, showed that apelinergic system may not be an essential factor of tumor cell survival, but rather, it can be speculated about the role of this system as an aiding factor.

### 4.4.2 Colony-forming properties of tumor cells

In additional functional assays, such as in colony formation assays, *in vitro* investigation of the clonal proliferation and differentiation potential of leukemic cells was carried out. It was sought to examine whether Apelin and APJ antagonist MM54 affect self-renewal properties of the tumor cells (both wildtype and APJ-overexpressing cells). Clonogenicity assays were performed on two AML cell lines, such as MOLM13 and THP1 (certain cell lines were excluded from the analysis due to their adherent behavior). Results from these functional assays showed that both, Apelin and MM54, display an effect on clonogenicity of the THP1 cell line. While Apelin was able to increase the number of colonies, MM54 decreased colony formation, indicating an antileukemic behavior of APJ antagonism. This effect was, however, partially shown in case of MOLM13 cell line, where only higher concentration of Apelin increased the number of colonies. It is worth noticing that the overall effect of stimulation and inhibition of APJ was more visible in APJ-overexpressing cell lines, demonstrating the requirement of APJ presence in the cells in order to affect functional properties. To conclude on the role of apelinergic system in cell self-renewal, these results should, however, be further confirmed in other cell lines.

### 4.4.3 Migration properties of tumor cells

Results of the migration assays showed partial dependence of cell migration on the presence and activation of the apelinergic system. It was previously mentioned that the absence of APJ and APLN had been overcome by successful transduction using overexpression vectors. In accordance with that, it was possible to observe different response of breast cancer cells in terms of their migration after stimulation and inhibition of APJ. Interestingly, cells reacted to both Apelin and MM54 yet in a similar way, enhancing the migration rate, and it was manageable to prove that the differences between the migration rates exist between wildtype and overexpressing cells. Moreover, it was possible to clarify why there was no difference in another observed cell line, HT29. Results of the RT-qPCR analysis indicated that transgenic HT29 cells lost expression of apelin receptor, as the APJ expression profile was the same as that in wildtype cells. This is, however, not a unique case, since loss of gene of interest expression in overexpressing cells may happen due to the silencing of the promoter. Furthermore, in APLN-overexpressing cell lines, it was intended to antagonize the effect of secreted Apelin by treating the cells with MM54. It was expected that Apelin inhibition would result in a different migration rate. However, no effect could be observed, since no APJ

expression had existed in the first place. Therefore, further experimental setup should surpass the absence of both Apelin and APJ. It is worth to notice that during the course of this thesis, results of a similar study have partially confirmed the changes in cell migration properties that occur as a response to modulated apelinergic signaling<sup>328</sup>.

#### 4.4.4 Effects of hypoxia on apelinergic expression in tumor cells

It is known that, as a result of antiangiogenic treatment, well-vascularized tumors often enter into hypoxia<sup>148,329</sup>. As mentioned in the introduction section, hypoxia is one of the triggering forces in the formation of new blood vessels and it is also the indirect cause of metastasis initiation. With that in mind, it was sought to examine how the malignant as well as normal cells react to hypoxic conditions *in vitro* in terms of apelinergic system expression. It was hypothesized that, upon upregulation, tumor cells can utilize the apelinergic system as a way of communication with tumor microenvironment, which could result in recruitment of “helper” cells, assuming that apelinergic signaling exists within tumor microenvironment. Surprisingly, exposing the cancer cells to 1% of oxygen at different time periods did not reveal significant APLN and APJ upregulation in tumor cell lines. This was not in accordance with the findings of Heo *et al.*, since they showed that Apelin upregulation is affected by hypoxia in oral cancer cell lines<sup>266</sup>. On the other hand, the expression of APLN increased with time in case of endothelial cells (EC), indicating that this pathway seems to be physiologically present in ECs, which was in accordance with the study published by Eyries *et al.*<sup>330</sup>.

#### 4.4.5 The role of apelinergic system in immunotherapy

The immune system has surveillance and modulating roles in various cancers. Therefore, enhancing the surveillance and subsequent cancer cell recognition presents a rational strategy in fighting cancer. In their study, Obara *et al.* hypothesized the association between the apelinergic system and the immune system, highlighting their role in modulating immune cell functions<sup>331</sup>. Recent reports showed that APJ interacts with the transcription factor Janus kinase-1 (JAK1) to modulate interferon gamma (IFN $\gamma$ ) response, as well as that APJ abrogation reduces the efficacy of immune therapy<sup>302</sup>. The mentioned findings support the present hypothesis that moderate to low APJ expression found in tumor cells, may present a limiting factor for the immune system in recognition of these cells.

By mimicking immune system response, it was sought to investigate whether the treatment with IFN $\gamma$  will have an effect on APJ expression. While supernatant from cytokine-induced killer cells displayed moderate effects, it was found that AML and some solid tumor cells, treated with IFN $\gamma$ , responded in terms of a concentration-dependent APJ upregulation. On the other hand, it should be noted that IFN $\gamma$  exhibited an observable apoptotic effect on most of the cells that have been analyzed. These findings might imply that, although APJ expression remained constantly low, even small changes in its expression are likely to cause an effect.

In this study, the role of APJ in cancer immunotherapy has been tested *in vitro* by performing cytotoxicity assays. The idea behind this was to compare the cytotoxic effect of effector cells (PBMCs) on target cells (vector-control and APJ-overexpressing cells). Effects of bi-specific T-cell enhancer (BiTE) and T-cell immunoreceptor with Ig and ITIM domains (TIGIT) antibody on PBMC-mediated AML cell apoptosis have already been described in our and other research groups<sup>303,304,332</sup>. In this experimental setup, it was intended to compare the effectiveness of documented immunotherapy between control and APJ-overexpressing groups. The data were contradictory: although the results of the preliminary experiment showed a significant difference between the two treated groups, repeated experiments did not confirm that, since there was no increase in number of apoptotic APJ-overexpressing cells. It can be assumed that, since allogeneic settings have been used, the experimental setup does not mirror the situation in the patient, which might explain different results in the assays. These findings can lead to the conclusion that the *in vitro* conditions are simply a restricting factor that only can be bridged by performing *in vivo* experiments, as the immune system's complexity is not limited to PBMCs only being effector cells. Future experiments should concentrate on comparing the effects of immunotherapy between the wildtype and transgenic APJ mice.

### **4.5 Role of apelinergic system *in vivo***

Experiments *in vivo* were designed with the purpose of overcoming the obstacles that have been faced in conducted *in vitro* experiments. The research goal was to investigate the effect of genetic targeting of APJ on metastases onset in conditions of diminished VEGF-signaling. Before the beginning of this thesis, no such data on the effect of apelinergic signaling have been published.

#### 4.5.1 Lung metastasis models

##### *Preliminary subcutaneous model*

The purpose of preliminary experiments was finding an optimal model of lung metastasis, which, from the theoretical point of view, seemed like a simple task to perform. The idea behind this approach was to induce the spontaneous formation of metastases as a result of subcutaneous tumor presence. The likelihood to represent the entire metastatic cascade was assumed as the possible advantage of this model.

Despite the expectation that the metastasis onset will take place in a short time period, no more than one macroscopically visible metastasis per lung could be detected. These findings were also supported by microscopic analysis, since no expected metastatic burden was achieved. Moreover, cell lines used in this system exhibited extreme aggressiveness, resulting in short time fatality to the mouse subjects. Taken together, this experimental limitation, caused by low metastatic burden, could have been overcome by performing constant excision of subcutaneous tumors, and expecting for the metastasis to occur. This approach has already been described by several authors in cancers like mammary tumors and melanoma, where resection of the primary tumor was needed to allow the onset of metastasis<sup>333,334</sup>. However, despite the possible advantage of that system in terms of allowing certain therapies and conditions to be tested, due to the time limitation of this study, it was not possible to operate in that way.

##### *Intravenous lung metastasis model and efficiency of antiangiogenic therapy*

Taking into account the limitations observed in the subcutaneous model, it was decided to establish the lung metastasis model by intravenous injection of tumor cells, understanding that the lungs are one of the primary organs prone to metastasis formation<sup>305</sup>. However, the limitation of this model is that direct intravenous application of cancer cells circumvents the early steps of the metastatic pathway<sup>335</sup>, especially the invasion of cancer cells into the surrounding tissue and subsequent intravasation. This experimental system has reproduced the homing of tumor cells applied directly into the bloodstream to secondary organs, such as lungs. Therefore, for the purpose of investigating early steps of the metastatic cascade, establishing spontaneous metastasis would have been a more appropriate approach.

Prior to the main experiment of this project, the research goal was to confirm the effect of antiangiogenic therapy. Ramucirumab, a direct VEGFR2 antagonist that binds with high affinity to the extracellular domain of VEGFR2, has recently been approved for the treatment

## DISCUSSION

---

of metastatic non-small-cell lung carcinoma (NSCLC), based on the REVEL trial<sup>336</sup>. Murine analog of ramucirumab, DC101, has been used in this study to test its efficiency in both subcutaneous and intravenous models. It was possible to prove that DC101 has a therapeutic effect on tumor growth in the subcutaneous model. On the other hand, a more moderate effect was observed in intravenous model, especially in LLC1 cohort. Obtained findings were in accordance with previously published studies<sup>337</sup>. Yet, it remained unclear why only moderate effect on lung metastasis onset in the intravenous model was observed. One of the explanations for this phenomenon may be the existence of tumors that develop a resistance to antiangiogenic therapy in random order. Similar situation has been described in the study of Jaiprasart *et al.*<sup>338</sup>. Using the inhibitors of the VEGF pathway, authors have been able to follow-up the tumor growth in mice: tumors that were able to regrow after initial shrinking were defined as treatment-resistant. Similar situation may have happened in this study.

Although the intravenous model satisfied the expectations in terms of macroscopically observable high lung metastatic colonization, the experimental system faced issues in lung metastases quantification method. It has previously been mentioned that the cells used for the intravenous metastasis model had been transduced in order to stably express enhanced green fluorescent protein (eGFP). Therefore, it was expected to precisely quantify the metastatic burden simply by flow cytometric analysis of eGFP positive cells in murine lung tissue. Surprisingly, it was unlikely to quantify eGFP positive cells even though lungs were visibly composed of more than 80% of tumor tissue. The explanation for this technical issue could be the spontaneous loss of eGFP expression within the tumor or cell damage during sample processing, which was more unlikely to have happened.

### 4.5.2 Effects of the genetic targeting of apelinergic system

In the study published a few months before the ending of this thesis, Jaiprasart *et al.* have been able to follow the growth of antiangiogenic-resistant tumors<sup>338</sup>. In their study, authors have successfully identified the group of mice bearing tumors that have gained adaptive resistance to antiangiogenic drugs, such as bevacizumab and sorafenib. Resistant tumors (RT) resumed angiogenesis and cell proliferation despite the continuation of applied treatment. Finally, they found that, amongst other genes, APJ and APLN were among the top enriched genes within the stroma of resistant tumors and demonstrated that regulation of these genes has a strong connection to resistance to antiangiogenic therapy.

Before the beginning of this project, a research group from our department has already published the study on successful targeting of pulmonary endothelial cells by using adeno-associated viral vectors (AAV)<sup>277</sup>. The authors showed that a selected capsid variant allows AAV entry exclusively into the endothelium of the pulmonary vasculature after intravenous injection and therefore assures efficient delivery of the gene of interest to the selected entity. This finding was alluring for the purpose of further investigation in this study, since AAV vectors could be utilized in order to genetically “impose” the stable expression of Apelin to the murine lung endothelium. Overexpressing Apelin was expected to give valuable information on its effect on tumor cell homing and, finally, insights into metastatic onset. Having tested the intravenous lung metastasis model, technically complex cloning of Apelin inside AAV was performed. Furthermore, to include the effect coming from the inhibition of apelinergic signaling into the experimental setup, the gene encoding for F13A was cloned into AAV vector. AAV vectors additionally contained a gene encoding for firefly luciferase, which could be easily used as a reporter of a stable AAV integration. Results from *in vitro* experiments and sequencing have confirmed successful cloning. Additionally, the goal was to confirm the specificity of AAV in used experimental conditions. Based on the results from bioluminescent imaging and already published findings, successful and specific targeting of lungs was achieved.

Contrary to all expectations, the main *in vivo* experiment showed entirely different results. Substantially decreased tumor cell engraftment revealed a low metastatic burden that was present within all study groups. Due to these findings, no antiangiogenic effect could be detected in comparison to any vehicle control group (PBS subgroups). Accordingly, no clear conclusion on apelinergic system’s influence on metastasis onset could be made, since some of the observed lung samples were even metastasis-free. These unusual findings were further confirmed by analyzing the gene expression of eGFP, expecting it to correlate with the number of tumor cells present in the lungs. It is worth noticing that the infiltration and engraftment of tumor cells were not as optimal as it was observed in the preliminary intravenous lung metastasis model.

Yet, the reason for low metastatic colonization was not clear, because the same cells and the matched mouse subjects (in regard to sex and age) were used in both experiments. Although their substrains were equal (6J) and therefore could not be considered as different, C57BL mice from the first and last two intravenous experiments were obtained from two sources (inbred and from commercial supplier Janvier, respectively). Therefore, one can speculate that the animal

## DISCUSSION

---

immune system or microbiome might have been changed and consequently had an impact on cell engraftment after tumor cell injection. Although differences in the genetics were likely to exist, this scenario was excluded, since all inbred lines are regularly re-constituted in the facility and at Janvier to minimize the possibility of genetic drift.

The limiting factor of the first conducted AAV experiment was the deficiency of a control group with no AAV treatment, since in this experimental setup, all groups were treated with AAV vectors (including AAV empty vector group). As a possible explanation for the unusual results, it was hypothesized that the applied vectors might somehow manifest an immune-mediated effect on tumor cell engraftment. Therefore, it was thought that the immune system, triggered by the presence of AAV vectors in lung endothelium, simply eliminates the tumor cells and that these events occur randomly, as shown by the variations of the lung metastatic burden between different groups. Ambiguous results from the previous experiments led to the assumption that the immune system, activated by presence of AAV vectors might influence the cell engraftment. From personal communication with Prof. Dr. Jakob Körbelin, who designed the lung-EC-specific vector, it was known that no observable influence on tumor colonization due to AAV injection was previously noted. However, these claims must be taken with caution, since different mouse models have been tested and therefore, an influence of the immune system in this experimental system cannot be excluded.

Since the first conducted experiment was lacking the no-AAV control group, the main mouse experiment was repeated by including an additional control group (no-AAV, vector-free mice). However, even with the improved experimental setup, results similar to the ones from the first experiment were obtained. On the other hand, it is worth noticing that the engraftment was moderately higher in comparison with the first experiment, but the high variability between all groups remained the same. No clear conclusion on the effect of any group parameter (agonistic or antagonistic effect of Apelin/F13A or antiangiogenic therapy) on metastatic burden could have been made after macroscopic observation.

One may, however, question the choice of mouse strain. The potential lung metastasis model in immunodeficient NSG mice would be more appropriate, since it is expected that mice without immune system would be more likely to have had higher metastatic colonization in comparison to those with a fully functional immune system. Indeed, several metastatic models have already been described<sup>339,340</sup>. However, it must be pointed out that the main research goal of this study was to investigate the role of immune system and apelinergic signaling on tumor



cell homing and metastatic onset, as well as on antiangiogenic treatment. For that reason, C57BL6 mice, with an intact immune system, were chosen as a model. Poor engraftment that was shown in both experiments was the limiting factor of this study. Although tumor engraftment is highly dependent on the mouse strain, this part of the experimental setup remained unchanged. Certain tumors, such as prostate carcinoma, do not engraft well in some mouse strains, and therefore high engraftment rate is unlikely to be achieved<sup>341</sup>. In this study, the engraftment abilities of MC38 cell line that has been used in main experiment, can also be speculated. On the one hand, metastatic potential of MC38 cells in intravenous models has already been evaluated by Kryczek *et al.*<sup>342</sup>. Additionally, in preliminary intravenous lung metastasis model, MC38 cells displayed the highest capacity to generate metastasis. However, that capacity was not retained using passaged cells for the main experiments. We could also assume that the viability of applied tumor cells could have been the reason for low metastatic burden, since the effective implementation of this model requires a higher degree of technical precision. On the other hand, in some cases, certain subpopulations of the cancer cells have been shown to be more efficient at generating tumors in mice compared to other cell subpopulations<sup>343</sup>. Therefore, it might have happened that during the passaging, cells have lost their engraftment potential. Taken together, the likelihood that MC38 cells suffered a phenotypic change cannot be excluded. Most of the limitations of this model could have been overcome by other approaches, such as activating the oncogenes like c-Neu oncogene, driven by a mouse mammary tumor virus promoter<sup>344</sup>, which has been proven to be of use in the study of Uribealgo *et al.*<sup>150</sup>. That way, more reproducible results could have been obtained.

Immunohistochemical (IHC) analysis of the lung tissues revealed to some extent a similar infiltration rate of the immune cells in all observed groups. In the majority of analyzed groups, high variability in CD3, as well as in CD11b area, was observed. In case of myeloid cell lineage (CD11b) it could be seen that their infiltration was lower in F13A-DC101 group, compared to all other groups. Yet, statistically significant difference was observed only when compared to DC101-treated no-vector group. Interestingly, the myeloid cell infiltration was shown to be decreased in apelin-KO mouse model heart tissue in study of Tatin *et al.*<sup>345</sup>. In the experimental settings used in this project, it can be assumed that presence of F13A was the reason for a decreased percentage of CD11b positive area. However, these findings need to be confirmed in a separate experimental setup.

On the other hand, T-cell marker (CD3) positive area was shown to be the highest in DC101-treated Apelin group. The increase in CD3 coverage was contrary to the results of

## DISCUSSION

---

Yamazaki *et al.*, who showed that infiltration of T cells is significantly inhibited by Apelin secretion in another pathological condition<sup>346</sup>. Since mice from analyzed Apelin group in this experimental system were treated with antiangiogenic therapy, results may indicate that DC101 abrogated the effect of Apelin, and that this could have been sufficient to induce infiltration of CD3 cells. On the other hand, these findings were partially in agreement with the research of Tatin *et al.* The authors have analyzed distribution of immune cell populations in the heart of apelin-KO mice compared with control mice and did not observe any changes in the ratio of CD3-positive T lymphocytes<sup>345</sup>.

In terms of microvessel density, moderate differences in CD31 tumor coverage between different groups could be observed. As previously mentioned, it was speculated that the apelinergic system has a central role in tumor endothelium. Compared to DC101-treated no-vector control, both Apelin groups displayed significantly higher CD31 tumor coverage. This may indicate that Apelin, secreted from pulmonary endothelial cells, additionally increased tumor microvessel density. However, if we compare two Apelin subgroups (control and DC101-treated), no changes in MVD could be observed, suggesting the possibility that DC101 effect could have been inhibited by the presence of Apelin. Similar situation could be seen in F13A group, since there was no difference between control and treated subgroup. On the other hand, differences in terms of MVD become more evident if we compare Apelin and F13A groups. Significantly decreased MVD in F13A group can be explained by antagonism of APJ by F13A. These findings were in accordance with the recently published study<sup>150</sup>. Still, it is of high importance to confirm these findings by additional experimental setup, since high variability in analysis of MVD can present a potential bias. Therefore, these results should be taken with caution.

Despite the proven specificity of the AAV vectors toward mouse lung endothelium, one can speculate that Apelin or F13A level might not have been secreted by pulmonary endothelial cells in sufficient quantity to influence tumor metastasis onset. Therefore, Apelin protein level in all murine lungs was quantified. Accordingly, the analysis revealed low Apelin protein level in all processed lung tissues and no differences between control and AAV-Apelin groups could have been observed. However, concentration of F13A was higher compared to all other groups. One can imply that the low Apelin protein level might have been the reason for variations of metastatic burden, but still affected MVD. Yet, antiangiogenic treatment did not have an expected effect in treated groups, probably due to a random effect in cell engraftment that has been present. It can be concluded that these experimental conditions were not optimal for the

complexity of the desired model, indicating that the next model will require substantial reassessment in terms of higher controllability and reproducibility.

In the beginning of this project, studies with similar hypotheses were conducted from separate working groups. In the experimental system using oncogene-driven spontaneously induced mammary cancer, Uribealgo *et al.* have proven that loss of Apelin reduced tumor angiogenesis and impaired tumor growth<sup>150</sup>. As an advantage, the authors used a previously established model of Apelin-KO mice, which was a more controllable system in comparison to the one used in this thesis. Their system allowed an insight into the effect of Apelin produced from the tumor cells and tumor-microenvironment-derived Apelin. Finally, authors managed to prove that the depletion of Apelin from any of the mentioned compartments is sufficient to reduce tumor growth. Apelin depletion was also proven to be the key factor for tumor microenvironment remodeling, resulting in improved vessel leakiness and a decrease in the infiltration of immune-suppressive subset of neutrophil lineage<sup>150</sup>.

Likewise, Mastrella *et al.* investigated the contribution of tumor cell-derived Apelin on tumor angiogenesis and discovered that the apelinergic system has a dichotomous role in angiogenesis and invasion in glioblastoma tumor models<sup>258</sup>. The mentioned study also emphasized the importance of F13A molecule, questioning its proposed antagonistic effect to APJ. Similar to therapeutic setup in this project, the authors proved that co-administration of DC101 and F13A was able to synergistically blunt both vascularization and invasive properties of the tumor. However, complete diminishing of Apelin by terms of knocking down tumor-derived (tumor cell APLN-KD) and knocking out host-derived APLN (APLN-KO mice), tumor invasiveness increased. It was hypothesized that Apelin and F13A produced similar effect on APJ in terms of receptor-binding, however, downstream pathways might have been different depending on a ligand. Possible explanation that authors provide for this phenomenon is that F13A may not be able to sufficiently activate APJ in endothelium, but has a sufficient effect on tumor cells to stop the invasion and increase the overall survival<sup>258</sup>.

During this study, it became clear that this system requires optimization due to constant and random changes in metastatic burden, regardless of the experimental system's invariability. Addressing this issue presents a challenge and this model evidently requires a reporter that proves efficient cell engraftment. Moreover, re-evaluation of AAV vector's functionality is necessary to ensure sufficient protein quantities in the targeted tissue. Finally, this experimental system needs to consider the usage of transgenic mice in terms of Apelin or even APJ depletion

## DISCUSSION

---

(KO mice). It is worth noticing that usage of APJ-KO mice would disclose a valuable information on *in vivo* role of APJ in immunotherapy. On the other hand, it would be valuable to reveal the difference between the effects of cell- and host-derived APLN/APJ on metastasis formation in antiangiogenic conditions. However, in addition to the advantages from usage of Apelin-KO mice, it is worth to mention that such mice are completely Apelin-deficient which might result in undesired phenotype as physiological Apelin lacks in all tissues. The model used in this study still has a great potential and advantage only to target the lung ECs and should, therefore, be relatively specific for lung metastases – given that it would have worked and Apelin would have been overexpressed or antagonized sufficiently (F13A). Therefore, the improvement of this model would be of great interest for future work.

Few days before the conclusion of this thesis, the importance of the apelinergic system in contribution to tumor angiogenesis has been recognized in the study of Wang *et al.*<sup>255</sup>. Authors have successfully engineered Apelin-based synthetic Notch receptors (AsNRs) that can specifically interact with APJ and further stimulate synNotch pathways. That way, immune cells, engineered to express such receptor, were able to specifically target active tumor endothelium. The authors once more confirmed that apelinergic system is one of the key factors and a druggable target in inhibiting tumor angiogenesis. The potential of this system emerges slowly and may shed some necessary light in the area of such complexity as tumor angiogenesis.

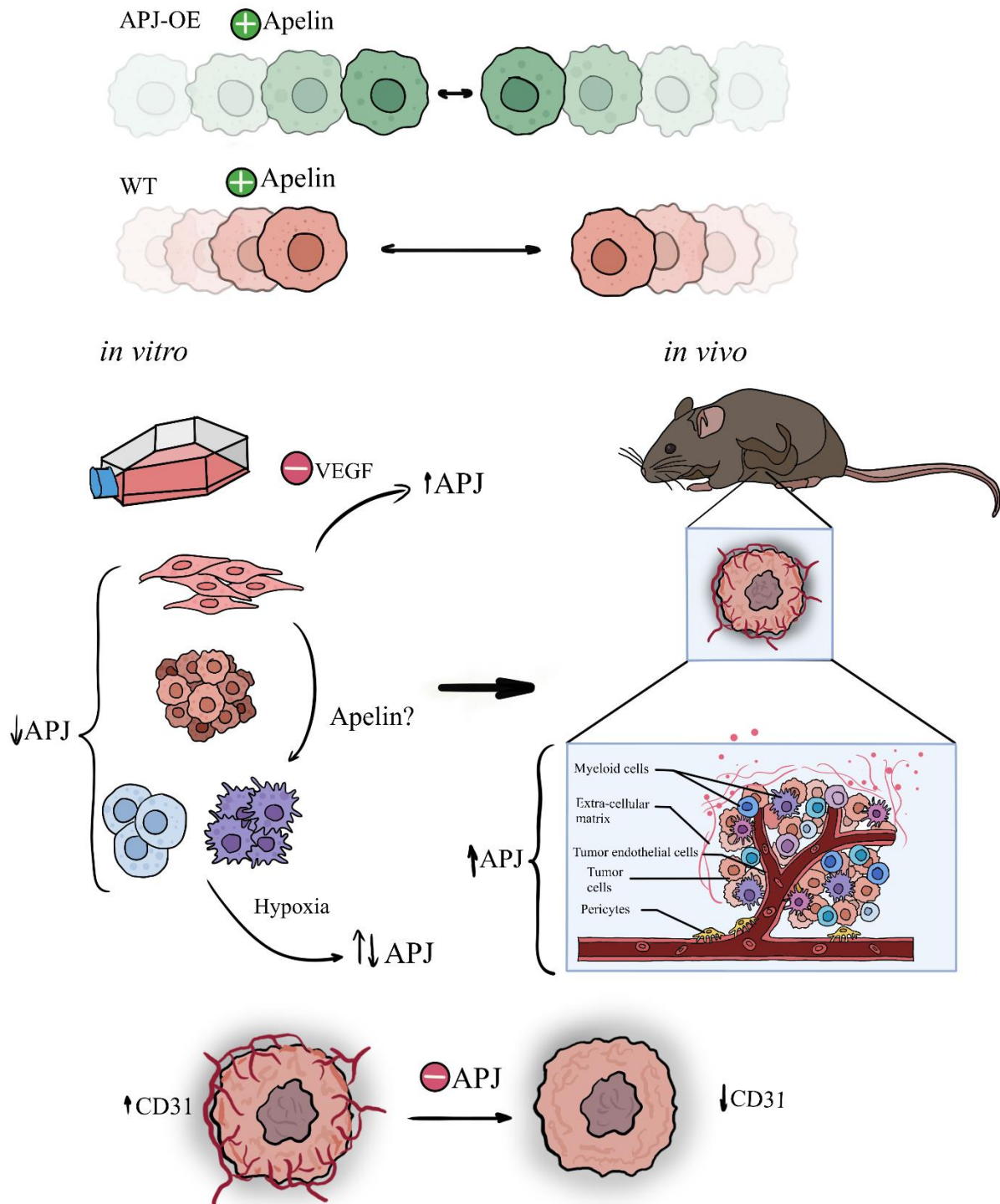


Figure 47. Graphical representation of the results

### 5. CONCLUSION

The presented thesis investigated the direct and indirect role of the apelinergic system in cancer development. This project was highly focused on its role in the onset of metastasis in the conditions of genetic targeting of the apelinergic system.

The *in vitro* experimental system did not reveal a significant role of Apelin and its putative receptor APJ in functional properties of either primary cells, such as alternatively polarized M<sub>2</sub> macrophages, or tumor cells, due to their unusually low expression levels. Numerous tumor-derived cell lines had been experimentally assessed to evaluate the Apelin/APJ expression. It was concluded that the investigated cell lines do not simulate the conditions of high APJ expression, which was reported in cancer tissue. The results from this study indicate the insufficiency of the *in vitro* experimental system to represent the potential interaction of the tumor cells with a multicellular tumor niche.

APJ deficiency has been partially overcome by experimental induction of apelinergic system in the examined tumor cell lines. In *in vitro* conditions, the presence of APJ-overexpressed cells demonstrated that effective apelinergic signaling can partially influence functional properties, such as cell migration and self-renewal properties, but had no effect on proliferation of the examined cells. Therefore, Apelin/APJ signaling in tumor-derived cell lines is not likely to play a direct and unique role in cancer survival *in vitro*, but rather possess an indirect role such as in cell migration properties. Since the highest expression of apelinergic system was found to be in tumor tissue, such properties should be re-envisaged in *in vivo* conditions.

Finally, it has been envisioned to target apelinergic system *in vivo* by lung endothelial cell-specific modification of Apelin expression in murine lung metastasis model. The primary endpoint of this model, number of lung metastases, did not fulfill the expectation due to a lack of sufficient tumor cell engraftment. The experimental system was not able to reproduce the previously established model of lung metastasis, although the same conditions have been applied. It is speculated that this is due to the random effect in cell engraftment of MC38 cell line. Therefore, a profound reassessment in terms of lung metastasis induction is required.

The effect of genetic targeting of apelinergic system was found to be promising, since antagonism of APJ resulted in decreased microvessel density in tumors and the opposite effect was demonstrated in case of Apelin overexpression. It can be concluded that Apelin/APJ system would be a promising therapeutic target for angiogenesis-related diseases, especially in cancer.

For future research on apelinergic system's contribution to cancer, finding of optimal models and improving quantification techniques is of critical importance. One of the promising ways to optimize the lung metastasis model would be employing genetically engineered mouse models, which would provide better reproducibility in events such as tumor progression and angiogenesis. Therefore, inevitable biases that arise from intravenously injecting tumor cells could be easily circumvented. AAVs are emerging as a revolutionary tool to target not only normal, but also tumor endothelium. Due to its specificity, such approach would be of great significance in investigation of Apelin-mediated events in tumor vasculature.

Moreover, further research should be more focused on detailed investigation of downstream signaling pathways in tumor endothelium upon antiangiogenic therapy. RNA-sequencing of isolated tumor endothelium is likely to provide the necessary information on changes in gene expression profile that may change as a result of the antiangiogenic approach.

Taken together, the work presented in this thesis may be of significance in narrowing the directions in future research of apelinergic system in malignant diseases.





## 6. REFERENCES

1. Carmeliet, P., *et al.* Abnormal blood vessel development and lethality in embryos lacking a single VEGF allele. *Nature* **380**, 435-439 (1996).
2. Risau, W., *et al.* Vasculogenesis and angiogenesis in embryonic-stem-cell-derived embryoid bodies. *Development* **102**, 471-478 (1988).
3. Risau, W. & Flamme, I. Vasculogenesis. *Annu Rev Cell Dev Biol* **11**, 73-91 (1995).
4. Carmeliet, P., De Smet, F., Loges, S. & Mazzone, M. Branching morphogenesis and antiangiogenesis candidates: tip cells lead the way. *Nat Rev Clin Oncol* **6**, 315-326 (2009).
5. Carmeliet, P. Angiogenesis in life, disease and medicine. *Nature* **438**, 932-936 (2005).
6. De Smet, F., Segura, I., De Bock, K., Hohensinner, P.J. & Carmeliet, P. Mechanisms of vessel branching: filopodia on endothelial tip cells lead the way. *Arterioscler Thromb Vasc Biol* **29**, 639-649 (2009).
7. Borovski, T., De Sousa, E.M.F., Vermeulen, L. & Medema, J.P. Cancer stem cell niche: the place to be. *Cancer Res* **71**, 634-639 (2011).
8. Burri, P.H., Hlushchuk, R. & Djonov, V. Intussusceptive angiogenesis: its emergence, its characteristics, and its significance. *Dev Dyn* **231**, 474-488 (2004).
9. Ferrara, N. Role of vascular endothelial growth factor in the regulation of angiogenesis. *Kidney Int* **56**, 794-814 (1999).
10. Breier, G. Angiogenesis in embryonic development--a review. *Placenta* **21 Suppl A**, S11-15 (2000).
11. Gluzman-Poltorak, Z., Cohen, T., Shibuya, M. & Neufeld, G. Vascular endothelial growth factor receptor-1 and neuropilin-2 form complexes. *J Biol Chem* **276**, 18688-18694 (2001).
12. Pepper, M.S. Extracellular proteolysis and angiogenesis. *Thromb Haemost* **86**, 346-355 (2001).
13. Jackson, C. Matrix metalloproteinases and angiogenesis. *Curr Opin Nephrol Hypertens* **11**, 295-299 (2002).
14. Bergers, G., *et al.* Matrix metalloproteinase-9 triggers the angiogenic switch during carcinogenesis. *Nat Cell Biol* **2**, 737-744 (2000).
15. Hynes, R.O. A reevaluation of integrins as regulators of angiogenesis. *Nat Med* **8**, 918-921 (2002).
16. Phng, L.K. & Gerhardt, H. Angiogenesis: a team effort coordinated by notch. *Dev Cell* **16**, 196-208 (2009).
17. Xu, Y. & Yu, Q. Angiopoietin-1, unlike angiopoietin-2, is incorporated into the extracellular matrix via its linker peptide region. *J Biol Chem* **276**, 34990-34998 (2001).
18. Iruela-Arispe, L. Angiogenesis: novel and basic science insights and human therapy - keystone symposium. *IDrugs* **7**, 111-113 (2004).
19. Goumans, M.J., *et al.* Balancing the activation state of the endothelium via two distinct TGF-beta type I receptors. *EMBO J* **21**, 1743-1753 (2002).
20. Carmeliet, P. Manipulating angiogenesis in medicine. *J Intern Med* **255**, 538-561 (2004).
21. Liekens, S., De Clercq, E. & Neyts, J. Angiogenesis: regulators and clinical applications. *Biochem Pharmacol* **61**, 253-270 (2001).
22. Bernardini, G., *et al.* Analysis of the role of chemokines in angiogenesis. *J Immunol Methods* **273**, 83-101 (2003).
23. Ferrara, N. VEGF and the quest for tumour angiogenesis factors. *Nat Rev Cancer* **2**, 795-803 (2002).
24. Ehling, M., Adams, S., Benedito, R. & Adams, R.H. Notch controls retinal blood vessel maturation and quiescence. *Development* **140**, 3051-3061 (2013).
25. Helfrich, I. & Schadendorf, D. Blood vessel maturation, vascular phenotype and angiogenic potential in malignant melanoma: one step forward for overcoming anti-angiogenic drug resistance? *Mol Oncol* **5**, 137-149 (2011).
26. Gerhardt, H., *et al.* VEGF guides angiogenic sprouting utilizing endothelial tip cell filopodia. *J Cell Biol* **161**, 1163-1177 (2003).
27. Sainson, R.C., *et al.* Cell-autonomous notch signaling regulates endothelial cell branching and proliferation during vascular tubulogenesis. *FASEB J* **19**, 1027-1029 (2005).

## REFERENCES

---

28. Liu, Z.J., *et al.* Regulation of Notch1 and Dll4 by vascular endothelial growth factor in arterial endothelial cells: implications for modulating arteriogenesis and angiogenesis. *Mol Cell Biol* **23**, 14-25 (2003).
29. Motherwell, J.M., Anderson, C.R. & Murfee, W.L. Endothelial Cell Phenotypes are Maintained During Angiogenesis in Cultured Microvascular Networks. *Sci Rep* **8**, 5887 (2018).
30. Chen, W., *et al.* The endothelial tip-stalk cell selection and shuffling during angiogenesis. *J Cell Commun Signal* **13**, 291-301 (2019).
31. Blanco, R. & Gerhardt, H. VEGF and Notch in tip and stalk cell selection. *Cold Spring Harb Perspect Med* **3**, a006569 (2013).
32. Stratman, A.N., *et al.* Interactions between mural cells and endothelial cells stabilize the developing zebrafish dorsal aorta. *Development* **144**, 115-127 (2017).
33. Armulik, A., Abramsson, A. & Betsholtz, C. Endothelial/pericyte interactions. *Circ Res* **97**, 512-523 (2005).
34. Ribatti, D. The Discovery of Tumor Angiogenesis Factors: A Historical Overview. *Methods Mol Biol* **1464**, 1-12 (2016).
35. Ribatti, D., Vacca, A., Nico, B., Presta, M. & Roncali, L. Angiogenesis: basic and clinical aspects. *Ital J Anat Embryol* **108**, 1-24 (2003).
36. Folkman, J. Tumor angiogenesis: therapeutic implications. *N Engl J Med* **285**, 1182-1186 (1971).
37. Caduff, J.H., Fischer, L.C. & Burri, P.H. Scanning electron microscope study of the developing microvasculature in the postnatal rat lung. *Anat Rec* **216**, 154-164 (1986).
38. Kilarski, W.W., Samolov, B., Petersson, L., Kvanta, A. & Gerwins, P. Biomechanical regulation of blood vessel growth during tissue vascularization. *Nat Med* **15**, 657-664 (2009).
39. Carmeliet, P. Mechanisms of angiogenesis and arteriogenesis. *Nat Med* **6**, 389-395 (2000).
40. Ribatti, D. & Crivellato, E. "Sprouting angiogenesis", a reappraisal. *Dev Biol* **372**, 157-165 (2012).
41. Tomanek, R.J. & Schatteman, G.C. Angiogenesis: new insights and therapeutic potential. *Anat Rec* **261**, 126-135 (2000).
42. Pauty, J., *et al.* A Vascular Endothelial Growth Factor-Dependent Sprouting Angiogenesis Assay Based on an In Vitro Human Blood Vessel Model for the Study of Anti-Angiogenic Drugs. *EBioMedicine* **27**, 225-236 (2018).
43. Styp-Rekowska, B., Hlushchuk, R., Pries, A.R. & Djonov, V. Intussusceptive angiogenesis: pillars against the blood flow. *Acta Physiol (Oxf)* **202**, 213-223 (2011).
44. Hlushchuk, R., *et al.* Tumor recovery by angiogenic switch from sprouting to intussusceptive angiogenesis after treatment with PTK787/ZK222584 or ionizing radiation. *Am J Pathol* **173**, 1173-1185 (2008).
45. Benest, A.V. & Augustin, H.G. Tension in the vasculature. *Nat Med* **15**, 608-610 (2009).
46. Lin, E.Y. & Pollard, J.W. Tumor-Associated Macrophages Press the Angiogenic Switch in Breast Cancer. *Cancer Research* **67**, 5064-5066 (2007).
47. Hanahan, D. & Weinberg, R.A. Hallmarks of cancer: the next generation. *Cell* **144**, 646-674 (2011).
48. De Palma, M., Biziato, D. & Petrova, T.V. Microenvironmental regulation of tumour angiogenesis. *Nat Rev Cancer* **17**, 457-474 (2017).
49. Bergers, G. & Benjamin, L.E. Tumorigenesis and the angiogenic switch. *Nat Rev Cancer* **3**, 401-410 (2003).
50. Venning, F.A., Wullkopf, L. & Erler, J.T. Targeting ECM Disrupts Cancer Progression. *Front Oncol* **5**, 224 (2015).
51. Nagy, J.A. & Dvorak, H.F. Heterogeneity of the tumor vasculature: the need for new tumor blood vessel type-specific targets. *Clin Exp Metastasis* **29**, 657-662 (2012).
52. Lee, J.W., Ko, J., Ju, C. & Eltzschig, H.K. Hypoxia signaling in human diseases and therapeutic targets. *Exp Mol Med* **51**, 1-13 (2019).
53. Fan, L., Li, J., Yu, Z., Dang, X. & Wang, K. The hypoxia-inducible factor pathway, prolyl hydroxylase domain protein inhibitors, and their roles in bone repair and regeneration. *Biomed Res Int* **2014**, 239356 (2014).
54. Krock, B.L., Skuli, N. & Simon, M.C. Hypoxia-induced angiogenesis: good and evil. *Genes Cancer* **2**, 1117-1133 (2011).

55. Harris, A.L. Hypoxia--a key regulatory factor in tumour growth. *Nat Rev Cancer* **2**, 38-47 (2002).
56. Schmidt, D., *et al.* Critical role for NF-kappaB-induced JunB in VEGF regulation and tumor angiogenesis. *EMBO J* **26**, 710-719 (2007).
57. Schorpp-Kistner, M., Wang, Z.Q., Angel, P. & Wagner, E.F. JunB is essential for mammalian placentation. *EMBO J* **18**, 934-948 (1999).
58. Arcondeguy, T., Lacazette, E., Millevoi, S., Prats, H. & Touriol, C. VEGF-A mRNA processing, stability and translation: a paradigm for intricate regulation of gene expression at the post-transcriptional level. *Nucleic Acids Res* **41**, 7997-8010 (2013).
59. Niu, G., *et al.* Constitutive Stat3 activity up-regulates VEGF expression and tumor angiogenesis. *Oncogene* **21**, 2000-2008 (2002).
60. van Beijnum, J.R., Nowak-Sliwinska, P., Huijbers, E.J., Thijssen, V.L. & Griffioen, A.W. The great escape; the hallmarks of resistance to antiangiogenic therapy. *Pharmacol Rev* **67**, 441-461 (2015).
61. Zijlstra, A., *et al.* Proangiogenic role of neutrophil-like inflammatory heterophils during neovascularization induced by growth factors and human tumor cells. *Blood* **107**, 317-327 (2006).
62. Squadrito, M.L. & De Palma, M. Macrophage regulation of tumor angiogenesis: implications for cancer therapy. *Mol Aspects Med* **32**, 123-145 (2011).
63. Orimo, A. & Weinberg, R.A. Stromal fibroblasts in cancer: a novel tumor-promoting cell type. *Cell Cycle* **5**, 1597-1601 (2006).
64. Watnick, R.S. The role of the tumor microenvironment in regulating angiogenesis. *Cold Spring Harb Perspect Med* **2**, a006676 (2012).
65. Orimo, A., *et al.* Stromal fibroblasts present in invasive human breast carcinomas promote tumor growth and angiogenesis through elevated SDF-1/CXCL12 secretion. *Cell* **121**, 335-348 (2005).
66. Deryugina, E.I. & Quigley, J.P. Tumor angiogenesis: MMP-mediated induction of intravasation- and metastasis-sustaining neovasculature. *Matrix Biol* **44-46**, 94-112 (2015).
67. Carmeliet, P. & Jain, R.K. Molecular mechanisms and clinical applications of angiogenesis. *Nature* **473**, 298-307 (2011).
68. Gordon, M.S., Mendelson, D.S. & Kato, G. Tumor angiogenesis and novel antiangiogenic strategies. *Int J Cancer* **126**, 1777-1787 (2010).
69. Jabbour, E.J., Estey, E. & Kantarjian, H.M. Adult acute myeloid leukemia. *Mayo Clin Proc* **81**, 247-260 (2006).
70. Behrmann, L., Wellbrock, J. & Fiedler, W. Acute Myeloid Leukemia and the Bone Marrow Niche-Take a Closer Look. *Front Oncol* **8**, 444 (2018).
71. Fiedler, W., *et al.* Vascular endothelial growth factor, a possible paracrine growth factor in human acute myeloid leukemia. *Blood* **89**, 1870-1875 (1997).
72. Yoder, M.C., *et al.* Redefining endothelial progenitor cells via clonal analysis and hematopoietic stem/progenitor cell principals. *Blood* **109**, 1801-1809 (2007).
73. Pizzo, R.J., *et al.* Phenotypic, genotypic, and functional characterization of normal and acute myeloid leukemia-derived marrow endothelial cells. *Exp Hematol* **44**, 378-389 (2016).
74. Hussong, J.W., Rodgers, G.M. & Shami, P.J. Evidence of increased angiogenesis in patients with acute myeloid leukemia. *Blood* **95**, 309-313 (2000).
75. Trujillo, A., McGee, C. & Cogle, C.R. Angiogenesis in acute myeloid leukemia and opportunities for novel therapies. *J Oncol* **2012**, 128608 (2012).
76. Gordon, S. & Pluddemann, A. Tissue macrophages: heterogeneity and functions. *BMC Biol* **15**, 53 (2017).
77. Kratofil, R.M., Kubes, P. & Deniset, J.F. Monocyte Conversion During Inflammation and Injury. *Arterioscler Thromb Vasc Biol* **37**, 35-42 (2017).
78. Twum, D.Y.F., Burkard-Mandel, L. & Abrams, S.I. The Dr. Jekyll and Mr. Hyde complexity of the macrophage response in disease. *J Leukoc Biol* **102**, 307-315 (2017).
79. Atri, C., Guerfali, F.Z. & Laouini, D. Role of Human Macrophage Polarization in Inflammation during Infectious Diseases. *Int J Mol Sci* **19**(2018).
80. Najafi, M., *et al.* Macrophage polarity in cancer: A review. *J Cell Biochem* **120**, 2756-2765 (2019).

## REFERENCES

---

81. Pinto, M.L., *et al.* The Two Faces of Tumor-Associated Macrophages and Their Clinical Significance in Colorectal Cancer. *Front Immunol* **10**, 1875 (2019).
82. Lawrence, T. & Natoli, G. Transcriptional regulation of macrophage polarization: enabling diversity with identity. *Nat Rev Immunol* **11**, 750-761 (2011).
83. Luo, Y., *et al.* Targeting tumor-associated macrophages as a novel strategy against breast cancer. *J Clin Invest* **116**, 2132-2141 (2006).
84. Gazzaniga, S., *et al.* Targeting tumor-associated macrophages and inhibition of MCP-1 reduce angiogenesis and tumor growth in a human melanoma xenograft. *J Invest Dermatol* **127**, 2031-2041 (2007).
85. Zeisberger, S.M., *et al.* Clodronate-liposome-mediated depletion of tumour-associated macrophages: a new and highly effective antiangiogenic therapy approach. *Br J Cancer* **95**, 272-281 (2006).
86. Schmid, M.C. & Varner, J.A. Myeloid cell trafficking and tumor angiogenesis. *Cancer Lett* **250**, 1-8 (2007).
87. Mantovani, A., Sozzani, S., Locati, M., Allavena, P. & Sica, A. Macrophage polarization: tumor-associated macrophages as a paradigm for polarized M2 mononuclear phagocytes. *Trends Immunol* **23**, 549-555 (2002).
88. Oosterling, S.J., *et al.* Macrophages direct tumour histology and clinical outcome in a colon cancer model. *J Pathol* **207**, 147-155 (2005).
89. Pulverini, P.J. & Leibovich, S.J. Effect of macrophage depletion on growth and neovascularization of hamster buccal pouch carcinomas. *J Oral Pathol* **16**, 436-441 (1987).
90. Leek, R.D. & Harris, A.L. Tumor-associated macrophages in breast cancer. *J Mammary Gland Biol Neoplasia* **7**, 177-189 (2002).
91. Condeelis, J. & Pollard, J.W. Macrophages: obligate partners for tumor cell migration, invasion, and metastasis. *Cell* **124**, 263-266 (2006).
92. Nozawa, H., Chiu, C. & Hanahan, D. Infiltrating neutrophils mediate the initial angiogenic switch in a mouse model of multistage carcinogenesis. *Proc Natl Acad Sci U S A* **103**, 12493-12498 (2006).
93. Talmadge, J.E. & Fidler, I.J. AACR centennial series: the biology of cancer metastasis: historical perspective. *Cancer Res* **70**, 5649-5669 (2010).
94. Fidler, I.J. Metastasis: quantitative analysis of distribution and fate of tumor emboli labeled with 125 I-5-iodo-2'-deoxyuridine. *J Natl Cancer Inst* **45**, 773-782 (1970).
95. Bielenberg, D.R. & Zetter, B.R. The Contribution of Angiogenesis to the Process of Metastasis. *Cancer J* **21**, 267-273 (2015).
96. Ghose, S.M., *et al.* Therapeutic Targeting of Vasculature in the Premetastatic and Metastatic Niches Reduces Lung Metastasis. *J Immunol* **204**, 990-1000 (2020).
97. Folkman, J. Role of angiogenesis in tumor growth and metastasis. *Semin Oncol* **29**, 15-18 (2002).
98. Cho, T., *et al.* The role of microvessel density, lymph node metastasis, and tumor size as prognostic factors of distant metastasis in colorectal cancer. *Oncol Lett* **13**, 4327-4333 (2017).
99. Tsuji, T., Ibaragi, S. & Hu, G.F. Epithelial-mesenchymal transition and cell cooperativity in metastasis. *Cancer Res* **69**, 7135-7139 (2009).
100. Guillerey, C. & Smyth, M.J. NK Cells and Cancer Immunoediting. *Curr Top Microbiol Immunol* **395**, 115-145 (2016).
101. Labelle, M. & Hynes, R.O. The initial hours of metastasis: the importance of cooperative host-tumor cell interactions during hematogenous dissemination. *Cancer Discov* **2**, 1091-1099 (2012).
102. Martinelli, R., *et al.* Probing the biomechanical contribution of the endothelium to lymphocyte migration: diapedesis by the path of least resistance. *J Cell Sci* **127**, 3720-3734 (2014).
103. Hedley, B.D. & Chambers, A.F. Tumor dormancy and metastasis. *Adv Cancer Res* **102**, 67-101 (2009).
104. Valastyan, S. & Weinberg, R.A. Tumor metastasis: molecular insights and evolving paradigms. *Cell* **147**, 275-292 (2011).
105. Cristofanilli, M., *et al.* Circulating tumor cells, disease progression, and survival in metastatic breast cancer. *N Engl J Med* **351**, 781-791 (2004).

106. Takahashi, H., *et al.* Biologically Aggressive Phenotype and Anti-cancer Immunity Counterbalance in Breast Cancer with High Mutation Rate. *Sci Rep* **10**, 1852 (2020).
107. Siemann, D.W. The unique characteristics of tumor vasculature and preclinical evidence for its selective disruption by Tumor-Vascular Disrupting Agents. *Cancer Treat Rev* **37**, 63-74 (2011).
108. Dvorak, H.F., Weaver, V.M., Tlsty, T.D. & Bergers, G. Tumor microenvironment and progression. *J Surg Oncol* **103**, 468-474 (2011).
109. Nagy, J.A., Chang, S.H., Shih, S.C., Dvorak, A.M. & Dvorak, H.F. Heterogeneity of the tumor vasculature. *Semin Thromb Hemost* **36**, 321-331 (2010).
110. Abdollahi, A. & Folkman, J. Evading tumor evasion: current concepts and perspectives of anti-angiogenic cancer therapy. *Drug Resist Updat* **13**, 16-28 (2010).
111. Lohmann, A.E. & Chia, S. Patients with metastatic breast cancer using bevacizumab as a treatment: is there still a role for it? *Curr Treat Options Oncol* **13**, 249-262 (2012).
112. Eskander, R.N. & Tewari, K.S. Incorporation of anti-angiogenesis therapy in the management of advanced ovarian carcinoma--mechanistics, review of phase III randomized clinical trials, and regulatory implications. *Gynecol Oncol* **132**, 496-505 (2014).
113. Bilusic, M. & Wong, Y.N. Anti-angiogenesis in prostate cancer: knocked down but not out. *Asian J Androl* **16**, 372-377 (2014).
114. Sun, H., Zhu, M.S., Wu, W.R., Shi, X.D. & Xu, L.B. Role of anti-angiogenesis therapy in the management of hepatocellular carcinoma: The jury is still out. *World J Hepatol* **6**, 830-835 (2014).
115. Ellis, P.M. Anti-angiogenesis in Personalized Therapy of Lung Cancer. *Adv Exp Med Biol* **893**, 91-126 (2016).
116. Marien, K.M., *et al.* Predictive tissue biomarkers for bevacizumab-containing therapy in metastatic colorectal cancer: an update. *Expert Rev Mol Diagn* **15**, 399-414 (2015).
117. Giuliano, S. & Pages, G. Mechanisms of resistance to anti-angiogenesis therapies. *Biochimie* **95**, 1110-1119 (2013).
118. Bellou, S., Pentheroudakis, G., Murphy, C. & Fotsis, T. Anti-angiogenesis in cancer therapy: Hercules and hydra. *Cancer Lett* **338**, 219-228 (2013).
119. Teleanu, R.I., Chircov, C., Grumezescu, A.M. & Teleanu, D.M. Tumor Angiogenesis and Anti-Angiogenic Strategies for Cancer Treatment. *J Clin Med* **9**(2019).
120. Koutras, A.K., Krikelis, D., Alexandrou, N., Starakis, I. & Kalofonos, H.P. Brain metastasis in renal cell cancer responding to sunitinib. *Anticancer Res* **27**, 4255-4257 (2007).
121. Itatani, Y., Kawada, K., Yamamoto, T. & Sakai, Y. Resistance to Anti-Angiogenic Therapy in Cancer-Alterations to Anti-VEGF Pathway. *Int J Mol Sci* **19**(2018).
122. Carmeliet, P. & Jain, R.K. Principles and mechanisms of vessel normalization for cancer and other angiogenic diseases. *Nat Rev Drug Discov* **10**, 417-427 (2011).
123. Thurston, G., *et al.* Leakage-resistant blood vessels in mice transgenically overexpressing angiopoietin-1. *Science* **286**, 2511-2514 (1999).
124. Dong, X., Han, Z.C. & Yang, R. Angiogenesis and antiangiogenic therapy in hematologic malignancies. *Crit Rev Oncol Hematol* **62**, 105-118 (2007).
125. Ribatti, D. Is angiogenesis essential for the progression of hematological malignancies or is it an epiphenomenon? *Leukemia* **23**, 433-434 (2009).
126. Hurwitz, H., *et al.* Bevacizumab plus irinotecan, fluorouracil, and leucovorin for metastatic colorectal cancer. *N Engl J Med* **350**, 2335-2342 (2004).
127. Miller, K., *et al.* Paclitaxel plus bevacizumab versus paclitaxel alone for metastatic breast cancer. *N Engl J Med* **357**, 2666-2676 (2007).
128. Escudier, B., *et al.* Bevacizumab plus interferon alfa-2a for treatment of metastatic renal cell carcinoma: a randomised, double-blind phase III trial. *Lancet* **370**, 2103-2111 (2007).
129. Sandler, A., *et al.* Paclitaxel-carboplatin alone or with bevacizumab for non-small-cell lung cancer. *N Engl J Med* **355**, 2542-2550 (2006).
130. Rose, S. FDA pulls approval for avastin in breast cancer. *Cancer Discov* **1**, OF1-2 (2011).
131. Bergers, G. & Hanahan, D. Modes of resistance to anti-angiogenic therapy. *Nat Rev Cancer* **8**, 592-603 (2008).
132. Chung, A.S., *et al.* An interleukin-17-mediated paracrine network promotes tumor resistance to anti-angiogenic therapy. *Nat Med* **19**, 1114-1123 (2013).

## REFERENCES

---

133. Mackey, J.R., *et al.* Primary results of ROSE/TRIO-12, a randomized placebo-controlled phase III trial evaluating the addition of ramucirumab to first-line docetaxel chemotherapy in metastatic breast cancer. *J Clin Oncol* **33**, 141-148 (2015).
134. Ebos, J.M. & Kerbel, R.S. Antiangiogenic therapy: impact on invasion, disease progression, and metastasis. *Nat Rev Clin Oncol* **8**, 210-221 (2011).
135. Escudier, B., *et al.* Sorafenib for treatment of renal cell carcinoma: Final efficacy and safety results of the phase III treatment approaches in renal cancer global evaluation trial. *J Clin Oncol* **27**, 3312-3318 (2009).
136. Escudier, B., *et al.* Phase II study of sunitinib administered in a continuous once-daily dosing regimen in patients with cytokine-refractory metastatic renal cell carcinoma. *J Clin Oncol* **27**, 4068-4075 (2009).
137. Raymond, E., *et al.* Sunitinib malate for the treatment of pancreatic neuroendocrine tumors. *N Engl J Med* **364**, 501-513 (2011).
138. Llovet, J.M., *et al.* Sorafenib in advanced hepatocellular carcinoma. *N Engl J Med* **359**, 378-390 (2008).
139. Goel, S., *et al.* Normalization of the vasculature for treatment of cancer and other diseases. *Physiol Rev* **91**, 1071-1121 (2011).
140. Casanovas, O., Hicklin, D.J., Bergers, G. & Hanahan, D. Drug resistance by evasion of antiangiogenic targeting of VEGF signaling in late-stage pancreatic islet tumors. *Cancer Cell* **8**, 299-309 (2005).
141. Batchelor, T.T., *et al.* AZD2171, a pan-VEGF receptor tyrosine kinase inhibitor, normalizes tumor vasculature and alleviates edema in glioblastoma patients. *Cancer Cell* **11**, 83-95 (2007).
142. Shojaei, F., *et al.* Bv8 regulates myeloid-cell-dependent tumour angiogenesis. *Nature* **450**, 825-831 (2007).
143. Shojaei, F., *et al.* Tumor refractoriness to anti-VEGF treatment is mediated by CD11b+Gr1+ myeloid cells. *Nat Biotechnol* **25**, 911-920 (2007).
144. Mitsuhashi, A., *et al.* Fibrocyte-like cells mediate acquired resistance to anti-angiogenic therapy with bevacizumab. *Nat Commun* **6**, 8792 (2015).
145. Sun, J., *et al.* Inhibiting angiogenesis and tumorigenesis by a synthetic molecule that blocks binding of both VEGF and PDGF to their receptors. *Oncogene* **24**, 4701-4709 (2005).
146. Bergers, G., Song, S., Meyer-Morse, N., Bergsland, E. & Hanahan, D. Benefits of targeting both pericytes and endothelial cells in the tumor vasculature with kinase inhibitors. *J Clin Invest* **111**, 1287-1295 (2003).
147. Pennacchietti, S., *et al.* Hypoxia promotes invasive growth by transcriptional activation of the met protooncogene. *Cancer Cell* **3**, 347-361 (2003).
148. Ebos, J.M., *et al.* Accelerated metastasis after short-term treatment with a potent inhibitor of tumor angiogenesis. *Cancer Cell* **15**, 232-239 (2009).
149. Paez-Ribes, M., *et al.* Antiangiogenic therapy elicits malignant progression of tumors to increased local invasion and distant metastasis. *Cancer Cell* **15**, 220-231 (2009).
150. Uribealago, I., *et al.* Apelin inhibition prevents resistance and metastasis associated with anti-angiogenic therapy. *EMBO Mol Med* **11**, e9266 (2019).
151. Donnem, T., *et al.* Vessel co-option in primary human tumors and metastases: an obstacle to effective anti-angiogenic treatment? *Cancer Med* **2**, 427-436 (2013).
152. Maniotis, A.J., *et al.* Vascular channel formation by human melanoma cells in vivo and in vitro: vasculogenic mimicry. *Am J Pathol* **155**, 739-752 (1999).
153. van der Schaft, D.W., *et al.* Tumor cell plasticity in Ewing sarcoma, an alternative circulatory system stimulated by hypoxia. *Cancer Res* **65**, 11520-11528 (2005).
154. Shirakawa, K., *et al.* Hemodynamics in vasculogenic mimicry and angiogenesis of inflammatory breast cancer xenograft. *Cancer Res* **62**, 560-566 (2002).
155. Sood, A.K., *et al.* Molecular determinants of ovarian cancer plasticity. *Am J Pathol* **158**, 1279-1288 (2001).
156. Keunen, O., *et al.* Anti-VEGF treatment reduces blood supply and increases tumor cell invasion in glioblastoma. *Proc Natl Acad Sci U S A* **108**, 3749-3754 (2011).
157. Sounni, N.E., *et al.* Blocking lipid synthesis overcomes tumor regrowth and metastasis after antiangiogenic therapy withdrawal. *Cell Metab* **20**, 280-294 (2014).

158. O'Dowd, B.F., *et al.* A human gene that shows identity with the gene encoding the angiotensin receptor is located on chromosome 11. *Gene* **136**, 355-360 (1993).
159. Tatemoto, K., *et al.* Isolation and characterization of a novel endogenous peptide ligand for the human APJ receptor. *Biochem Biophys Res Commun* **251**, 471-476 (1998).
160. Cox, C.M., D'Agostino, S.L., Miller, M.K., Heimark, R.L. & Krieg, P.A. Apelin, the ligand for the endothelial G-protein-coupled receptor, APJ, is a potent angiogenic factor required for normal vascular development of the frog embryo. *Dev Biol* **296**, 177-189 (2006).
161. Devic, E., Paquereau, L., Vernier, P., Knibiehler, B. & Audigier, Y. Expression of a new G protein-coupled receptor X-msr is associated with an endothelial lineage in *Xenopus laevis*. *Mech Dev* **59**, 129-140 (1996).
162. Kalin, R.E., *et al.* Paracrine and autocrine mechanisms of apelin signaling govern embryonic and tumor angiogenesis. *Dev Biol* **305**, 599-614 (2007).
163. Ishimaru, Y., Shibagaki, F., Yamamuro, A., Yoshioka, Y. & Maeda, S. An apelin receptor antagonist prevents pathological retinal angiogenesis with ischemic retinopathy in mice. *Sci Rep* **7**, 15062 (2017).
164. Zhao, H., Yao, P., Li, L. & Chen, L. Apelin receptor signaling: a novel mechanism of endothelial cell polarization. *Acta Biochim Biophys Sin (Shanghai)* **48**, 1138-1139 (2016).
165. Kidoya, H., Naito, H. & Takakura, N. Apelin induces enlarged and nonleaky blood vessels for functional recovery from ischemia. *Blood* **115**, 3166-3174 (2010).
166. Shin, K., Kenward, C. & Rainey, J.K. Apelinergic System Structure and Function. *Compr Physiol* **8**, 407-450 (2017).
167. Szokodi, I., *et al.* Apelin, the novel endogenous ligand of the orphan receptor APJ, regulates cardiac contractility. *Circ Res* **91**, 434-440 (2002).
168. Ashley, E.A., *et al.* The endogenous peptide apelin potently improves cardiac contractility and reduces cardiac loading in vivo. *Cardiovasc Res* **65**, 73-82 (2005).
169. Zhang, Z., Yu, B. & Tao, G.Z. Apelin protects against cardiomyocyte apoptosis induced by glucose deprivation. *Chin Med J (Engl)* **122**, 2360-2365 (2009).
170. Boucher, J., *et al.* Apelin, a newly identified adipokine up-regulated by insulin and obesity. *Endocrinology* **146**, 1764-1771 (2005).
171. Heinonen, M.V., *et al.* Apelin, orexin-A and leptin plasma levels in morbid obesity and effect of gastric banding. *Regul Pept* **130**, 7-13 (2005).
172. Sörhede Winzell, M., Magnusson, C. & Ahrén, B. The apj receptor is expressed in pancreatic islets and its ligand, apelin, inhibits insulin secretion in mice. *Regulatory Peptides* **131**, 12-17 (2005).
173. Chen, H., *et al.* Apelin alleviates diabetes-associated endoplasmic reticulum stress in the pancreas of Akita mice. *Peptides* **32**, 1634-1639 (2011).
174. De Mota, N., *et al.* Apelin, a potent diuretic neuropeptide counteracting vasopressin actions through inhibition of vasopressin neuron activity and vasopressin release. *Proceedings of the National Academy of Sciences of the United States of America* **101**, 10464 (2004).
175. Roberts, E.M., *et al.* Stimulus-Specific Neuroendocrine Responses to Osmotic Challenges in Apelin Receptor Knockout Mice. *Journal of Neuroendocrinology* **22**, 301-308 (2010).
176. Kasai, A., *et al.* Apelin is a novel angiogenic factor in retinal endothelial cells. *Biochem Biophys Res Commun* **325**, 395-400 (2004).
177. Kidoya, H. & Takakura, N. Biology of the apelin-APJ axis in vascular formation. *J Biochem* **152**, 125-131 (2012).
178. Kasai, A., *et al.* Apelin is a crucial factor for hypoxia-induced retinal angiogenesis. *Arterioscler Thromb Vasc Biol* **30**, 2182-2187 (2010).
179. Wang, G., *et al.* Apelin, a new enteric peptide: localization in the gastrointestinal tract, ontogeny, and stimulation of gastric cell proliferation and of cholecystokinin secretion. *Endocrinology* **145**, 1342-1348 (2004).
180. Wang, G., *et al.* Ontogeny of apelin and its receptor in the rodent gastrointestinal tract. *Regul Pept* **158**, 32-39 (2009).
181. Ohno, S., *et al.* Apelin-12 stimulates acid secretion through an increase of histamine release in rat stomachs. *Regul Pept* **174**, 71-78 (2012).
182. Habata, Y., *et al.* Apelin, the natural ligand of the orphan receptor APJ, is abundantly secreted in the colostrum. *Biochim Biophys Acta* **1452**, 25-35 (1999).

## REFERENCES

---

183. Horiuchi, Y., Fujii, T., Kamimura, Y. & Kawashima, K. The endogenous, immunologically active peptide apelin inhibits lymphocytic cholinergic activity during immunological responses. *J Neuroimmunol* **144**, 46-52 (2003).
184. Edinger, A.L., *et al.* An orphan seven-transmembrane domain receptor expressed widely in the brain functions as a coreceptor for human immunodeficiency virus type 1 and simian immunodeficiency virus. *J Virol* **72**, 7934-7940 (1998).
185. Zou, M.X., *et al.* Apelin peptides block the entry of human immunodeficiency virus (HIV). *FEBS Lett* **473**, 15-18 (2000).
186. O'Donnell, L.A., *et al.* Apelin, an endogenous neuronal peptide, protects hippocampal neurons against excitotoxic injury. *J Neurochem* **102**, 1905-1917 (2007).
187. Xie, H., *et al.* Apelin suppresses apoptosis of human osteoblasts. *Apoptosis* **12**, 247-254 (2007).
188. Wattanachanya, L., *et al.* Increased bone mass in mice lacking the adipokine apelin. *Endocrinology* **154**, 2069-2080 (2013).
189. Ostrom, R.S. & Insel, P.A. The evolving role of lipid rafts and caveolae in G protein-coupled receptor signaling: implications for molecular pharmacology. *Br J Pharmacol* **143**, 235-245 (2004).
190. Wheatley, M. & Hawtin, S.R. Glycosylation of G-protein-coupled receptors for hormones central to normal reproductive functioning: its occurrence and role. *Hum Reprod Update* **5**, 356-364 (1999).
191. Zhou, N., *et al.* Cell-cell fusion and internalization of the CNS-based, HIV-1 co-receptor, APJ. *Virology* **307**, 22-36 (2003).
192. Masri, B., Morin, N., Pedebernade, L., Knibiehler, B. & Audigier, Y. The apelin receptor is coupled to Gi1 or Gi2 protein and is differentially desensitized by apelin fragments. *J Biol Chem* **281**, 18317-18326 (2006).
193. Devic, E., Rizzoti, K., Bodin, S., Knibiehler, B. & Audigier, Y. Amino acid sequence and embryonic expression of msr/apj, the mouse homolog of Xenopus X-msr and human APJ. *Mech Dev* **84**, 199-203 (1999).
194. O'Carroll, A.M., Selby, T.L., Palkovits, M. & Lolait, S.J. Distribution of mRNA encoding B78/apj, the rat homologue of the human APJ receptor, and its endogenous ligand apelin in brain and peripheral tissues. *Biochim Biophys Acta* **1492**, 72-80 (2000).
195. Margulies, B.J., Hauer, D.A. & Clements, J.E. Identification and comparison of eleven rhesus macaque chemokine receptors. *AIDS Res Hum Retroviruses* **17**, 981-986 (2001).
196. O'Carroll, A.M., Lolait, S.J. & Howell, G.M. Transcriptional regulation of the rat apelin receptor gene: promoter cloning and identification of an Sp1 site necessary for promoter activity. *J Mol Endocrinol* **36**, 221-235 (2006).
197. Hata, J., *et al.* Functional SNP in an Sp1-binding site of AGTRL1 gene is associated with susceptibility to brain infarction. *Hum Mol Genet* **16**, 630-639 (2007).
198. Sarzani, R., *et al.* The 212A variant of the APJ receptor gene for the endogenous inotrope apelin is associated with slower heart failure progression in idiopathic dilated cardiomyopathy. *J Card Fail* **13**, 521-529 (2007).
199. Zhao, Q., *et al.* Association of genetic variants in the apelin-APJ system and ACE2 with blood pressure responses to potassium supplementation: the GenSalt study. *Am J Hypertens* **23**, 606-613 (2010).
200. O'Carroll, A.M., Don, A.L. & Lolait, S.J. APJ receptor mRNA expression in the rat hypothalamic paraventricular nucleus: regulation by stress and glucocorticoids. *J Neuroendocrinol* **15**, 1095-1101 (2003).
201. O'Carroll, A.M., Lolait, S.J., Harris, L.E. & Pope, G.R. The apelin receptor APJ: journey from an orphan to a multifaceted regulator of homeostasis. *J Endocrinol* **219**, R13-35 (2013).
202. Dray, C., *et al.* Apelin and APJ regulation in adipose tissue and skeletal muscle of type 2 diabetic mice and humans. *Am J Physiol Endocrinol Metab* **298**, E1161-1169 (2010).
203. Pope, G.R., Roberts, E.M., Lolait, S.J. & O'Carroll, A.M. Central and peripheral apelin receptor distribution in the mouse: species differences with rat. *Peptides* **33**, 139-148 (2012).
204. Medhurst, A.D., *et al.* Pharmacological and immunohistochemical characterization of the APJ receptor and its endogenous ligand apelin. *J Neurochem* **84**, 1162-1172 (2003).



205. Matsumoto, M., *et al.* Low stringency hybridization study of the dopamine D4 receptor revealed D4-like mRNA distribution of the orphan seven-transmembrane receptor, APJ, in human brain. *Neurosci Lett* **219**, 119-122 (1996).
206. Hansen, A., *et al.* Sensitive and specific method for detecting G protein-coupled receptor mRNAs. *Nat Methods* **4**, 35-37 (2007).
207. Katugampola, S.D., Maguire, J.J., Matthewson, S.R. & Davenport, A.P. [(125)I]-[Pyr(1)]Apelin-13 is a novel radioligand for localizing the APJ orphan receptor in human and rat tissues with evidence for a vasoconstrictor role in man. *Br J Pharmacol* **132**, 1255-1260 (2001).
208. Kleinz, M.J., Skepper, J.N. & Davenport, A.P. Immunocytochemical localisation of the apelin receptor, APJ, to human cardiomyocytes, vascular smooth muscle and endothelial cells. *Regul Pept* **126**, 233-240 (2005).
209. Kidoya, H., *et al.* Spatial and temporal role of the apelin/APJ system in the caliber size regulation of blood vessels during angiogenesis. *EMBO J* **27**, 522-534 (2008).
210. De Mota, N., Lenkei, Z. & Llorens-Cortes, C. Cloning, pharmacological characterization and brain distribution of the rat apelin receptor. *Neuroendocrinology* **72**, 400-407 (2000).
211. Regard, J.B., Sato, I.T. & Coughlin, S.R. Anatomical profiling of G protein-coupled receptor expression. *Cell* **135**, 561-571 (2008).
212. Hosoya, M., *et al.* Molecular and functional characteristics of APJ. Tissue distribution of mRNA and interaction with the endogenous ligand apelin. *J Biol Chem* **275**, 21061-21067 (2000).
213. Chapman, N.A., Dupre, D.J. & Rainey, J.K. The apelin receptor: physiology, pathology, cell signalling, and ligand modulation of a peptide-activated class A GPCR. *Biochem Cell Biol* **92**, 431-440 (2014).
214. Masri, B., Lahlou, H., Mazarguil, H., Knibiehler, B. & Audigier, Y. Apelin (65-77) activates extracellular signal-regulated kinases via a PTX-sensitive G protein. *Biochem Biophys Res Commun* **290**, 539-545 (2002).
215. Kang, Y., *et al.* Apelin-APJ signaling is a critical regulator of endothelial MEF2 activation in cardiovascular development. *Circ Res* **113**, 22-31 (2013).
216. Ahmed, S.M. & Angers, S. Emerging non-canonical functions for heterotrimeric G proteins in cellular signaling. *J Recept Signal Transduct Res* **33**, 177-183 (2013).
217. Bai, B., Cai, X., Jiang, Y., Karteris, E. & Chen, J. Heterodimerization of apelin receptor and neurotensin receptor 1 induces phosphorylation of ERK(1/2) and cell proliferation via Galphaq-mediated mechanism. *J Cell Mol Med* **18**, 2071-2081 (2014).
218. Sun, X., *et al.* Non-activated APJ suppresses the angiotensin II type 1 receptor, whereas apelin-activated APJ acts conversely. *Hypertens Res* **34**, 701-706 (2011).
219. Siddiquee, K., Hampton, J., McAnally, D., May, L. & Smith, L. The apelin receptor inhibits the angiotensin II type 1 receptor via allosteric trans-inhibition. *Br J Pharmacol* **168**, 1104-1117 (2013).
220. Ishida, J., *et al.* Regulatory roles for APJ, a seven-transmembrane receptor related to angiotensin-type 1 receptor in blood pressure in vivo. *J Biol Chem* **279**, 26274-26279 (2004).
221. Li, Y., *et al.* Heterodimerization of human apelin and kappa opioid receptors: roles in signal transduction. *Cell Signal* **24**, 991-1001 (2012).
222. Rapoport, T.A. Protein translocation across the eukaryotic endoplasmic reticulum and bacterial plasma membranes. *Nature* **450**, 663-669 (2007).
223. Lee, D.K., *et al.* Characterization of apelin, the ligand for the APJ receptor. *J Neurochem* **74**, 34-41 (2000).
224. Yang, P., Maguire, J.J. & Davenport, A.P. Apelin, Elabela/Toddler, and biased agonists as novel therapeutic agents in the cardiovascular system. *Trends Pharmacol Sci* **36**, 560-567 (2015).
225. Kalea, A.Z. & Batlle, D. Apelin and ACE2 in cardiovascular disease. *Curr Opin Investig Drugs* **11**, 273-282 (2010).
226. Sato, T., *et al.* Apelin is a positive regulator of ACE2 in failing hearts. *J Clin Invest* **123**, 5203-5211 (2013).
227. Yang, P., *et al.* [Pyr(1)]Apelin-13(1-12) Is a Biologically Active ACE2 Metabolite of the Endogenous Cardiovascular Peptide [Pyr(1)]Apelin-13. *Front Neurosci* **11**, 92 (2017).

## REFERENCES

---

228. Wang, W., *et al.* Angiotensin-Converting Enzyme 2 Metabolizes and Partially Inactivates Pyr-Apelin-13 and Apelin-17: Physiological Effects in the Cardiovascular System. *Hypertension* **68**, 365-377 (2016).
229. Lee, D.K., Ferguson, S.S., George, S.R. & O'Dowd, B.F. The fate of the internalized apelin receptor is determined by different isoforms of apelin mediating differential interaction with beta-arrestin. *Biochem Biophys Res Commun* **395**, 185-189 (2010).
230. Fan, X., *et al.* Structural and functional study of the apelin-13 peptide, an endogenous ligand of the HIV-1 coreceptor, APJ. *Biochemistry* **42**, 10163-10168 (2003).
231. Shin, K., *et al.* Bioactivity of the putative apelin proprotein expands the repertoire of apelin receptor ligands. *Biochim Biophys Acta Gen Subj* **1861**, 1901-1912 (2017).
232. Shin, K., Pandey, A., Liu, X.Q., Anini, Y. & Rainey, J.K. Preferential apelin-13 production by the proprotein convertase PCSK3 is implicated in obesity. *FEBS Open Bio* **3**, 328-333 (2013).
233. Pisarenko, O., *et al.* Structural apelin analogues: mitochondrial ROS inhibition and cardiometabolic protection in myocardial ischaemia reperfusion injury. *Br J Pharmacol* **172**, 2933-2945 (2015).
234. Maguire, J.J., Kleinz, M.J., Pitkin, S.L. & Davenport, A.P. [Pyr1]apelin-13 identified as the predominant apelin isoform in the human heart: vasoactive mechanisms and inotropic action in disease. *Hypertension* **54**, 598-604 (2009).
235. Daviaud, D., *et al.* TNFalpha up-regulates apelin expression in human and mouse adipose tissue. *FASEB J* **20**, 1528-1530 (2006).
236. Han, S., Wang, G., Qi, X., Englander, E.W. & Greeley, G.H., Jr. Involvement of a Stat3 binding site in inflammation-induced enteric apelin expression. *Am J Physiol Gastrointest Liver Physiol* **295**, G1068-1078 (2008).
237. Han, S., *et al.* A possible role for hypoxia-induced apelin expression in enteric cell proliferation. *Am J Physiol Regul Integr Comp Physiol* **294**, R1832-1839 (2008).
238. Kleinz, M.J. & Davenport, A.P. Immunocytochemical localization of the endogenous vasoactive peptide apelin to human vascular and endocardial endothelial cells. *Regul Pept* **118**, 119-125 (2004).
239. Ronkainen, V.P., *et al.* Hypoxia inducible factor regulates the cardiac expression and secretion of apelin. *FASEB J* **21**, 1821-1830 (2007).
240. Glassford, A.J., *et al.* HIF-1 regulates hypoxia- and insulin-induced expression of apelin in adipocytes. *Am J Physiol Endocrinol Metab* **293**, E1590-1596 (2007).
241. Chng, S.C., Ho, L., Tian, J. & Reversade, B. ELABELA: a hormone essential for heart development signals via the apelin receptor. *Dev Cell* **27**, 672-680 (2013).
242. Reichman-Fried, M. & Raz, E. Small proteins, big roles: the signaling protein Apela extends the complexity of developmental pathways in the early zebrafish embryo. *Bioessays* **36**, 741-745 (2014).
243. Pauli, A., *et al.* Toddler: an embryonic signal that promotes cell movement via Apelin receptors. *Science* **343**, 1248636 (2014).
244. Yang, P., *et al.* Elabela/Toddler Is an Endogenous Agonist of the Apelin APJ Receptor in the Adult Cardiovascular System, and Exogenous Administration of the Peptide Compensates for the Downregulation of Its Expression in Pulmonary Arterial Hypertension. *Circulation* **135**, 1160-1173 (2017).
245. Fang, C., *et al.* SCNH2 is a novel apelinergic family member acting as a potent mitogenic and chemotactic factor for both endothelial and epithelial cells. *Open J Clin Diagn* **3**, 37-51 (2013).
246. Cuttitta, F. A report on Selective Apelin-36 Cutting and Amidation peptide. (ed. Sciences, N.C.I.D.o.B.) (2010).
247. Maloney, P.R., *et al.* Discovery of 4-oxo-6-((pyrimidin-2-ylthio)methyl)-4 H -pyran-3-yl 4-nitrobenzoate (ML221) as a functional antagonist of the apelin (APJ) receptor. *Bioorganic & Medicinal Chemistry Letters* **22**, 6656-6660 (2012).
248. Macaluso, N.J., Pitkin, S.L., Maguire, J.J., Davenport, A.P. & Glen, R.C. Discovery of a competitive apelin receptor (APJ) antagonist. *ChemMedChem* **6**, 1017-1023 (2011).
249. Harford-Wright, E., *et al.* Pharmacological targeting of apelin impairs glioblastoma growth. *Brain* **140**, 2939-2954 (2017).
250. Le Gonidec, S., *et al.* Protamine is an antagonist of apelin receptor, and its activity is reversed by heparin. *FASEB J* **31**, 2507-2519 (2017).

251. Abraham, S., Moss, S.E. & Greenwood, J. Regulation Of Angiogenesis By Apelin And Its Receptor Apj. *Investigative Ophthalmology & Visual Science* **53**, 3001-3001 (2012).
252. Wu, L., Chen, L. & Li, L. Apelin/APJ system: A novel promising therapy target for pathological angiogenesis. *Clin Chim Acta* **466**, 78-84 (2017).
253. Kasai, A., *et al.* Inhibition of apelin expression switches endothelial cells from proliferative to mature state in pathological retinal angiogenesis. *Angiogenesis* **16**, 723-734 (2013).
254. Wysocka, M.B., Pietraszek-Gremplewicz, K. & Nowak, D. The Role of Apelin in Cardiovascular Diseases, Obesity and Cancer. *Front Physiol* **9**, 557 (2018).
255. Wang, Z., *et al.* Using apelin-based synthetic Notch receptors to detect angiogenesis and treat solid tumors. *Nat Commun* **11**, 2163 (2020).
256. Berta, J., *et al.* Apelin expression in human non-small cell lung cancer: role in angiogenesis and prognosis. *J Thorac Oncol* **5**, 1120-1129 (2010).
257. Muto, J., *et al.* The apelin-APJ system induces tumor arteriogenesis in hepatocellular carcinoma. *Anticancer Res* **34**, 5313-5320 (2014).
258. Mastrella, G., *et al.* Targeting APLN/APLNR Improves Antiangiogenic Efficiency and Blunts Proinvasive Side Effects of VEGFA/VEGFR2 Blockade in Glioblastoma. *Cancer Res* **79**, 2298-2313 (2019).
259. Hall, C., *et al.* Inhibition of the apelin/apelin receptor axis decreases cholangiocarcinoma growth. *Cancer Lett* **386**, 179-188 (2017).
260. Feng, M., Yao, G., Yu, H., Qing, Y. & Wang, K. Tumor apelin, not serum apelin, is associated with the clinical features and prognosis of gastric cancer. *BMC Cancer* **16**, 794 (2016).
261. Amoozgar, Z., Jain, R.K. & Duda, D.G. Role of Apelin in Glioblastoma Vascularization and Invasion after Anti-VEGF Therapy: What Is the Impact on the Immune System? *Cancer Res* **79**, 2104-2106 (2019).
262. Wang, Z., Greeley, G.H., Jr. & Qiu, S. Immunohistochemical localization of apelin in human normal breast and breast carcinoma. *J Mol Histol* **39**, 121-124 (2008).
263. Hoffmann, M., Fiedor, E. & Ptak, A. Bisphenol A and its derivatives tetrabromobisphenol A and tetrachlorobisphenol A induce apelin expression and secretion in ovarian cancer cells through a peroxisome proliferator-activated receptor gamma-dependent mechanism. *Toxicol Lett* **269**, 15-22 (2017).
264. Hashimoto, Y., *et al.* G protein-coupled APJ receptor signaling induces focal adhesion formation and cell motility. *Int J Mol Med* **16**, 787-792 (2005).
265. Lv, D., *et al.* PAK1-cofilin phosphorylation mediates human lung adenocarcinoma cells migration induced by apelin-13. *Clin Exp Pharmacol Physiol* **43**, 569-579 (2016).
266. Heo, K., *et al.* Hypoxia-induced up-regulation of apelin is associated with a poor prognosis in oral squamous cell carcinoma patients. *Oral Oncol* **48**, 500-506 (2012).
267. Neelakantan, D., *et al.* Multifunctional APJ Pathway Promotes Ovarian Cancer Progression and Metastasis. *Mol Cancer Res* **17**, 1378-1390 (2019).
268. Yang, L., *et al.* ERK1/2 mediates lung adenocarcinoma cell proliferation and autophagy induced by apelin-13. *Acta Biochim Biophys Sin (Shanghai)* **46**, 100-111 (2014).
269. Maden, M., Pamuk, O.N. & Pamuk, G.E. High apelin levels could be used as a diagnostic marker in multiple myeloma: A comparative study. *Cancer Biomark* **17**, 391-396 (2016).
270. Podgorska, M., Diakowska, D., Pietraszek-Gremplewicz, K., Nienartowicz, M. & Nowak, D. Evaluation of Apelin and Apelin Receptor Level in the Primary Tumor and Serum of Colorectal Cancer Patients. *J Clin Med* **8**(2019).
271. Hao, Y.Z., Li, M.L., Ning, F.L. & Wang, X.W. APJ Is Associated with Treatment Response in Gastric Cancer Patients Receiving Concurrent Chemoradiotherapy and Endostar Therapy. *Cancer Biother Radiopharm* **32**, 133-138 (2017).
272. Salman, T., *et al.* Serum apelin levels and body composition changes in breast cancer patients treated with an aromatase inhibitor. *J BUON* **21**, 1419-1424 (2016).
273. Wang, G., Qi, X., Wei, W., Englander, E.W. & Greeley, G.H., Jr. Characterization of the 5'-regulatory regions of the rat and human apelin genes and regulation of breast apelin by USF. *FASEB J* **20**, 2639-2641 (2006).
274. Tolkach, Y., *et al.* Apelin and apelin receptor expression in renal cell carcinoma. *Br J Cancer* **120**, 633-639 (2019).

## REFERENCES

---

275. Wan, Y., *et al.* Dysregulated microRNA-224/apelin axis associated with aggressive progression and poor prognosis in patients with prostate cancer. *Hum Pathol* **46**, 295-303 (2015).
276. Acik, D.Y., Bankir, M., Baylan, F.A. & Aygun, B. Can ELABELA be a novel target in the treatment of chronic lymphocytic leukaemia? *BMC Cancer* **19**, 1086 (2019).
277. Korbelen, J., *et al.* Pulmonary Targeting of Adeno-associated Viral Vectors by Next-generation Sequencing-guided Screening of Random Capsid Displayed Peptide Libraries. *Mol Ther* **24**, 1050-1061 (2016).
278. Murza, A., Belleville, K., Longpre, J.M., Sarret, P. & Marsault, E. Stability and degradation patterns of chemically modified analogs of apelin-13 in plasma and cerebrospinal fluid. *Biopolymers* **102**, 297-303 (2014).
279. Hamilton, T.C., *et al.* Characterization of a human ovarian carcinoma cell line (NIH:OVCAR-3) with androgen and estrogen receptors. *Cancer Res* **43**, 5379-5389 (1983).
280. Michelfelder, S., *et al.* Vectors selected from adeno-associated viral display peptide libraries for leukemia cell-targeted cytotoxic gene therapy. *Exp Hematol* **35**, 1766-1776 (2007).
281. Xiao, X., Li, J. & Samulski, R.J. Production of high-titer recombinant adeno-associated virus vectors in the absence of helper adenovirus. *J Virol* **72**, 2224-2232 (1998).
282. Cook, J.A. & Mitchell, J.B. Viability measurements in mammalian cell systems. *Anal Biochem* **179**, 1-7 (1989).
283. Andersen, C.U., Markvardsen, L.H., Hilberg, O. & Simonsen, U. Pulmonary apelin levels and effects in rats with hypoxic pulmonary hypertension. *Respir Med* **103**, 1663-1671 (2009).
284. Bradford, M.M. A rapid and sensitive method for the quantitation of microgram quantities of protein utilizing the principle of protein-dye binding. *Anal Biochem* **72**, 248-254 (1976).
285. Untergasser, A., *et al.* Primer3Plus, an enhanced web interface to Primer3. *Nucleic Acids Res* **35**, W71-74 (2007).
286. Pfaffl, M.W. A new mathematical model for relative quantification in real-time RT-PCR. *Nucleic Acids Res* **29**, e45 (2001).
287. Addgene. Bacterial Transformation. Vol. 2017 (2017).
288. Martinez-Salas, E., Francisco-Velilla, R., Fernandez-Chamorro, J. & Embarek, A.M. Insights into Structural and Mechanistic Features of Viral IRES Elements. *Frontiers in Microbiology* **8**(2018).
289. Riecken, K. Homepage of the Lentiviral Gene Ontology Vectors. Vol. 2018 (2012).
290. Körbelin, J. Doctoral thesis, (2013).
291. Hermens, W.T., *et al.* Purification of recombinant adeno-associated virus by iodixanol gradient ultracentrifugation allows rapid and reproducible preparation of vector stocks for gene transfer in the nervous system. *Hum Gene Ther* **10**, 1885-1891 (1999).
292. Weber, K., Thomaschewski, M., Benten, D. & Fehse, B. RGB marking with lentiviral vectors for multicolor clonal cell tracking. *Nat Protoc* **7**, 839-849 (2012).
293. Dunmore, B.J., *et al.* The lysosomal inhibitor, chloroquine, increases cell surface BMPR-II levels and restores BMP9 signalling in endothelial cells harbouring BMPR-II mutations. *Hum Mol Genet* **22**, 3667-3679 (2013).
294. Odaka, C. & Mizuochi, T. Role of macrophage lysosomal enzymes in the degradation of nucleosomes of apoptotic cells. *J Immunol* **163**, 5346-5352 (1999).
295. Kather, J.N., *et al.* Continuous representation of tumor microvessel density and detection of angiogenic hotspots in histological whole-slide images. *Oncotarget* **6**, 19163-19176 (2015).
296. Harbaum, L., *et al.* M2 macrophages derived from patients with idiopathic pulmonary arterial hypertension are susceptible for apelin-mediated suppression of pro-inflammatory cytokines. *European Respiratory Journal* **44**, P311 (2014).
297. Bertani, F.R., *et al.* Classification of M1/M2-polarized human macrophages by label-free hyperspectral reflectance confocal microscopy and multivariate analysis. *Sci Rep* **7**, 8965 (2017).
298. Heinrich, F., *et al.* Morphologic, phenotypic, and transcriptomic characterization of classically and alternatively activated canine blood-derived macrophages in vitro. *PLoS One* **12**, e0183572 (2017).
299. Raggi, F., *et al.* Regulation of Human Macrophage M1-M2 Polarization Balance by Hypoxia and the Triggering Receptor Expressed on Myeloid Cells-1. *Front Immunol* **8**, 1097 (2017).

300. Turrini, R., *et al.* TIE-2 expressing monocytes in human cancers. *Oncoimmunology* **6**, e1303585 (2017).
301. Martinez, F.O., Gordon, S., Locati, M. & Mantovani, A. Transcriptional profiling of the human monocyte-to-macrophage differentiation and polarization: new molecules and patterns of gene expression. *J Immunol* **177**, 7303-7311 (2006).
302. Patel, S.J., *et al.* Identification of essential genes for cancer immunotherapy. *Nature* **548**, 537-542 (2017).
303. Stamm, H., *et al.* Immune checkpoints PVR and PVRL2 are prognostic markers in AML and their blockade represents a new therapeutic option. *Oncogene* **37**, 5269-5280 (2018).
304. Stamm, H., Wellbrock, J. & Fiedler, W. Interaction of PVR/PVRL2 with TIGIT/DNAM-1 as a novel immune checkpoint axis and therapeutic target in cancer. *Mamm Genome* **29**, 694-702 (2018).
305. Gomez-Cuadrado, L., Tracey, N., Ma, R., Qian, B. & Brunton, V.G. Mouse models of metastasis: progress and prospects. *Dis Model Mech* **10**, 1061-1074 (2017).
306. del Toro, R., *et al.* Identification and functional analysis of endothelial tip cell-enriched genes. *Blood* **116**, 4025-4033 (2010).
307. Cassetta, L., *et al.* Isolation of Mouse and Human Tumor-Associated Macrophages. *Adv Exp Med Biol* **899**, 211-229 (2016).
308. Lin, Y., Xu, J. & Lan, H. Tumor-associated macrophages in tumor metastasis: biological roles and clinical therapeutic applications. *J Hematol Oncol* **12**, 76 (2019).
309. Lee, C., *et al.* Targeting of M2-like tumor-associated macrophages with a melittin-based pro-apoptotic peptide. *J Immunother Cancer* **7**, 147 (2019).
310. Martinez, F.O. & Gordon, S. The M1 and M2 paradigm of macrophage activation: time for reassessment. *F1000Prime Rep* **6**, 13 (2014).
311. Glatzel, A.K. University of Hamburg (2018).
312. Venneri, M.A., *et al.* Identification of proangiogenic TIE2-expressing monocytes (TEMs) in human peripheral blood and cancer. *Blood* **109**, 5276-5285 (2007).
313. van der Bij, G.J., *et al.* Tumor infiltrating macrophages reduce development of peritoneal colorectal carcinoma metastases. *Cancer Lett* **262**, 77-86 (2008).
314. Atanasov, G., *et al.* TIE2-expressing monocytes and M2-polarized macrophages impact survival and correlate with angiogenesis in adenocarcinoma of the pancreas. *Oncotarget* **9**, 29715-29726 (2018).
315. Atanasov, G., *et al.* Prognostic significance of TIE2-expressing monocytes in hilar cholangiocarcinoma. *J Surg Oncol* **114**, 91-98 (2016).
316. Latroche, C., *et al.* Coupling between Myogenesis and Angiogenesis during Skeletal Muscle Regeneration Is Stimulated by Restorative Macrophages. *Stem Cell Reports* **9**, 2018-2033 (2017).
317. Hara, C., *et al.* Laser-induced choroidal neovascularization in mice attenuated by deficiency in the apelin-APJ system. *Invest Ophthalmol Vis Sci* **54**, 4321-4329 (2013).
318. Picault, F.X., *et al.* Tumour co-expression of apelin and its receptor is the basis of an autocrine loop involved in the growth of colon adenocarcinomas. *Eur J Cancer* **50**, 663-674 (2014).
319. Kidoya, H., *et al.* The apelin/APJ system induces maturation of the tumor vasculature and improves the efficiency of immune therapy. *Oncogene* **31**, 3254-3264 (2012).
320. Liang, P. & Pardee, A.B. Analysing differential gene expression in cancer. *Nat Rev Cancer* **3**, 869-876 (2003).
321. Wagenblast, E., *et al.* A model of breast cancer heterogeneity reveals vascular mimicry as a driver of metastasis. *Nature* **520**, 358-362 (2015).
322. Zhao, H., *et al.* Apj(+) Vessels Drive Tumor Growth and Represent a Tractable Therapeutic Target. *Cell Rep* **25**, 1241-1254 e1245 (2018).
323. Sorli, S.C., Le Gonidec, S., Knibiehler, B. & Audigier, Y. Apelin is a potent activator of tumour neoangiogenesis. *Oncogene* **26**, 7692-7699 (2007).
324. Venkatesh, V.S. Victoria University of Wellington (2018).
325. Saper, C.B. A guide to the perplexed on the specificity of antibodies. *J Histochem Cytochem* **57**, 1-5 (2009).
326. Hutchings, C.J. A review of antibody-based therapeutics targeting G protein-coupled receptors: an update. *Expert Opin Biol Ther*, 1-11 (2020).

## REFERENCES

---

327. Gulati, S., *et al.* Targeting G protein-coupled receptor signaling at the G protein level with a selective nanobody inhibitor. *Nat Commun* **9**, 1996 (2018).
328. Podgorska, M., Pietraszek-Gremplewicz, K. & Nowak, D. Apelin Effects Migration and Invasion Abilities of Colon Cancer Cells. *Cells* **7**(2018).
329. Crawford, Y. & Ferrara, N. VEGF inhibition: insights from preclinical and clinical studies. *Cell Tissue Res* **335**, 261-269 (2009).
330. Eyries, M., *et al.* Hypoxia-induced apelin expression regulates endothelial cell proliferation and regenerative angiogenesis. *Circ Res* **103**, 432-440 (2008).
331. Obara, S., Akifusa, S. , Ariyoshi, W. , Okinaga, T. , Usui, M. , Nakashima, K. and Nishihara, T. Pyroglutamated Apelin-13 Inhibits Lipopolysaccharide-Induced Production of Pro-Inflammatory Cytokines in Murine Macrophage J774.1 Cells. *Modern Research in Inflammation* **3**, 59-66 (2014).
332. Stamm, H., *et al.* Targeting the TIGIT-PVR immune checkpoint axis as novel therapeutic option in breast cancer. *Oncoimmunology* **8**, e1674605 (2019).
333. Coffelt, S.B., *et al.* IL-17-producing gammadelta T cells and neutrophils conspire to promote breast cancer metastasis. *Nature* **522**, 345-348 (2015).
334. Cruz-Munoz, W., Man, S., Xu, P. & Kerbel, R.S. Development of a preclinical model of spontaneous human melanoma central nervous system metastasis. *Cancer Res* **68**, 4500-4505 (2008).
335. Speak, A.O., *et al.* A high-throughput in vivo screening method in the mouse for identifying regulators of metastatic colonization. *Nat Protoc* **12**, 2465-2477 (2017).
336. Garon, E.B., *et al.* Ramucirumab plus docetaxel versus placebo plus docetaxel for second-line treatment of stage IV non-small-cell lung cancer after disease progression on platinum-based therapy (REVEL): a multicentre, double-blind, randomised phase 3 trial. *Lancet* **384**, 665-673 (2014).
337. Duignan, I.J., *et al.* Pleiotropic stromal effects of vascular endothelial growth factor receptor 2 antibody therapy in renal cell carcinoma models. *Neoplasia* **13**, 49-59 (2011).
338. Jaiprasart, P., Dogra, S., Neelakantan, D., Devapatla, B. & Woo, S. Identification of signature genes associated with therapeutic resistance to anti-VEGF therapy. *Oncotarget* **11**, 99-114 (2020).
339. Yang, S., Zhang, J.J. & Huang, X.-Y. Mouse models for tumor metastasis. *Methods in molecular biology (Clifton, N.J.)* **928**, 221-228 (2012).
340. Puchalapalli, M., *et al.* NSG Mice Provide a Better Spontaneous Model of Breast Cancer Metastasis than Athymic (Nude) Mice. *PLOS ONE* **11**, e0163521 (2016).
341. Eswaraka, J. & Giddabasappa, A. Chapter 6 - Humanized Mice and PDX Models. in *Patient Derived Tumor Xenograft Models* (eds. Uthamanthil, R. & Tinkey, P.) 75-89 (Academic Press, 2017).
342. Kryczek, I., Wei, S., Szeliga, W., Vatan, L. & Zou, W. Endogenous IL-17 contributes to reduced tumor growth and metastasis. *Blood* **114**, 357-359 (2009).
343. Al-Hajj, M., Wicha, M.S., Benito-Hernandez, A., Morrison, S.J. & Clarke, M.F. Prospective identification of tumorigenic breast cancer cells. *Proceedings of the National Academy of Sciences of the United States of America* **100**, 3983-3988 (2003).
344. Muller, W.J., Sinn, E., Pattengale, P.K., Wallace, R. & Leder, P. Single-step induction of mammary adenocarcinoma in transgenic mice bearing the activated c-neu oncogene. *Cell* **54**, 105-115 (1988).
345. Tatin, F., *et al.* Apelin modulates pathological remodeling of lymphatic endothelium after myocardial infarction. *JCI Insight* **2**(2017).
346. Yamazaki, S., *et al.* Apelin/APJ signaling suppresses the pressure ulcer formation in cutaneous ischemia-reperfusion injury mouse model. *Sci Rep* **10**, 1349 (2020).

## 7. Supplementary data

**Supplementary Table 1. Reaction conditions for Real-time qPCR**

<b>Sample volume</b>	2 $\mu$ L of sample cDNA + 18 $\mu$ L of master mix (10 $\mu$ L SYBR® + 4 $\mu$ L primer mix + 4 $\mu$ L water)	
<b>Preincubation</b>	Initial denaturation: 1 cycle, 95°C for 45 s	
<b>3 Step amplification</b>	40 cycles	Denaturation 95°C for 5 s
		Annealing 61°C for 45 s
		Extension 72°C for 26 s
<b>Melting</b>	95°C for 1 s	
<b>Cooling</b>	37°C for 30 s	

**Supplementary Table 2. PCR conditions for High Fidelity Phusion S7 Polymerase.** Annealing temperature depends on the primer and it is listed in the material section. Extension time varies on PCR product length.

Cycles	Step	Temperature	Time
1	Initial denaturation	98°C	30 s
25-35	Denaturation	98°C	10 s
	Annealing	X°C	25 s
	Extension	72°C	25 s/kb
1	Final extension	72°C	10 min
1	Cooling	4°C	hold

**Supplementary Table 3. PCR reaction setup for High Fidelity Phusion S7 Polymerase**

Component	50 $\mu$ L reaction	Final concentration
Water	Add to 50 $\mu$ L	
5X HF Buffer	10 $\mu$ L	1X
10 mM dNTPs	1 $\mu$ L	
Forward primer	2.5 $\mu$ L*	0.5 $\mu$ M
Reverse primer	2.5 $\mu$ L*	0.5 $\mu$ M

SUPPLEMENTARY DATA

Template DNA	Up to 10 ng	
S7 Fusion Polymerase	0.5 $\mu$ L	0.02 U/ $\mu$ L
* 1:10 from the original solution (5 $\mu$ L)		

**Supplementary Table 4. Recommended thermal cycling conditions for qualitative PCR.** Annealing temperature depends on each specific primer pair.

Cycles	Step	Temperature	Time
1	Initial denaturation	95°C	3 min
25-35	Denaturation	95°C	30 s
	Annealing	X°C	30 s
	Extension	72°C	1 min
1	Final extension	72°C	10 min
1	Cooling	4°C	hold

**Supplementary Table 5. List of transgenic cell lines**

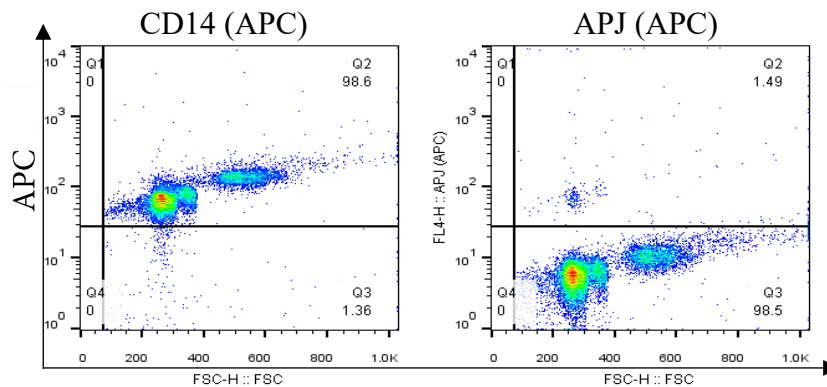
Cell line	Gene of interest	Vector	Reporter	Selection antibiotic
MOLM13	hAPJ	LeGO	eGFP	Puromycin
THP1	hAPJ	LeGO	eGFP	Puromycin
TF1	hAPJ	LeGO	eGFP	Puromycin
HT29	hAPJ	LeGO	mCherry	Puromycin
A549	hAPJ	LeGO	mCherry	Puromycin
MDA MB231	hAPJ	LeGO	mCherry	Puromycin
U118	hAPJ	LeGO	mCherry	Puromycin
OVCAR8	hAPLN	LeGO	mCherry	Puromycin
HT29	hAPLN	LeGO	mCherry	Puromycin
A549	hAPLN	LeGO	mCherry	Puromycin
MDA MB231	hAPLN	LeGO	mCherry	Puromycin
U118	hAPLN	LeGO	mCherry	Puromycin



OVCAR8	hAPLN	LeGO	mCherry	Puromycin
HT29	hAPLN shRNA	LeGO	eGFP	Puromycin
A549	hAPLN shRNA	LeGO	eGFP	Puromycin
MDA MB231	hAPLN shRNA	LeGO	eGFP	Puromycin
U118	hAPLN shRNA	LeGO	eGFP	Puromycin
OVCAR8	hAPLN shRNA	LeGO	eGFP	Puromycin
MC38	-	LeGO	eGFP	Puromycin
LLC1	-	LeGO	eGFP	Puromycin
MC38	mAPJ	LeGO	mCherry	Puromycin
LLC1	mAPJ	LeGO	mCherry	Puromycin

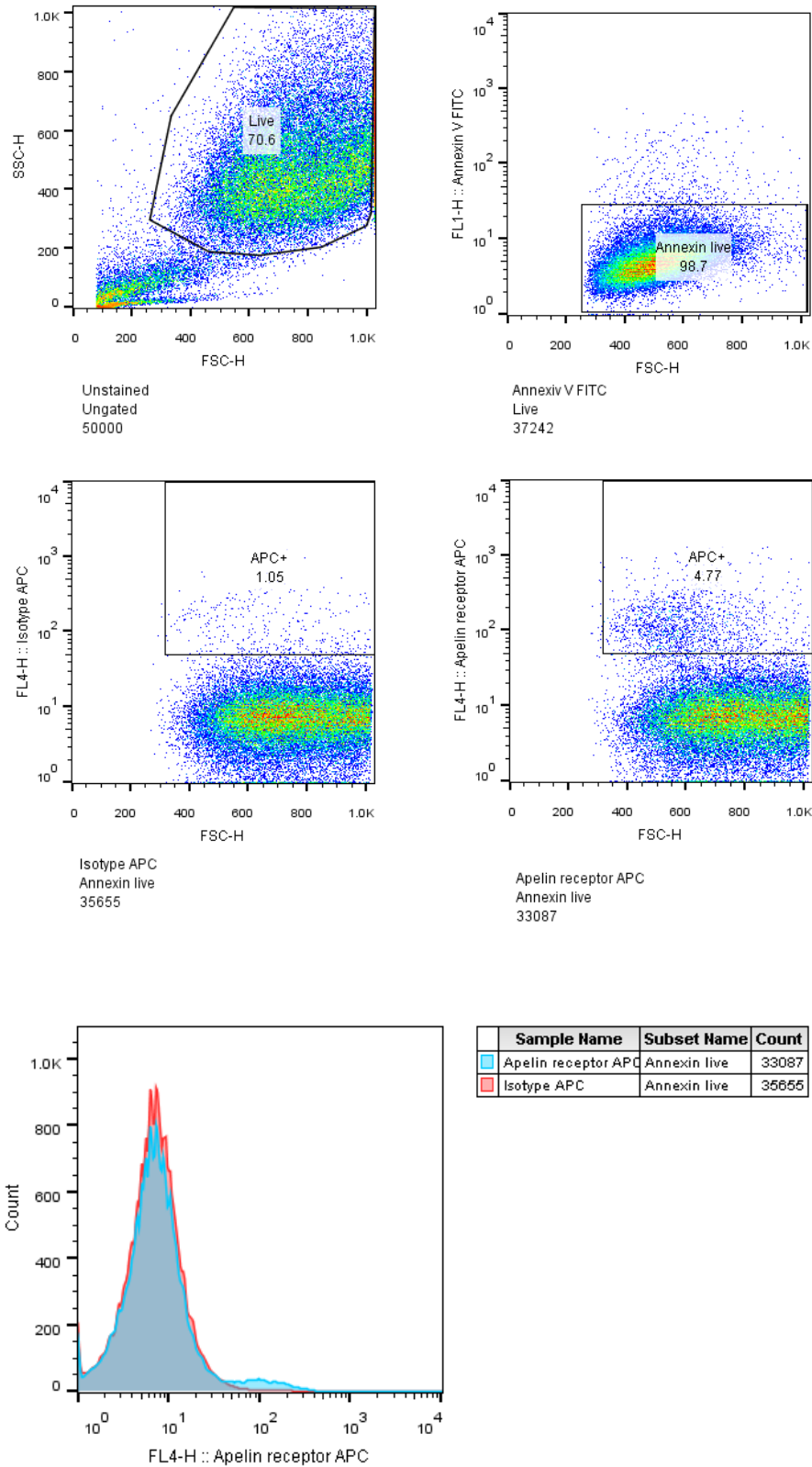
*Functionality of APC-labeled APJ antibody*

To investigate its functionality, binding properties of APC-coupled antibody were tested by using standard beads. The results indicated low binding affinity of the antibody, which is shown on Supplementary Figure 1.

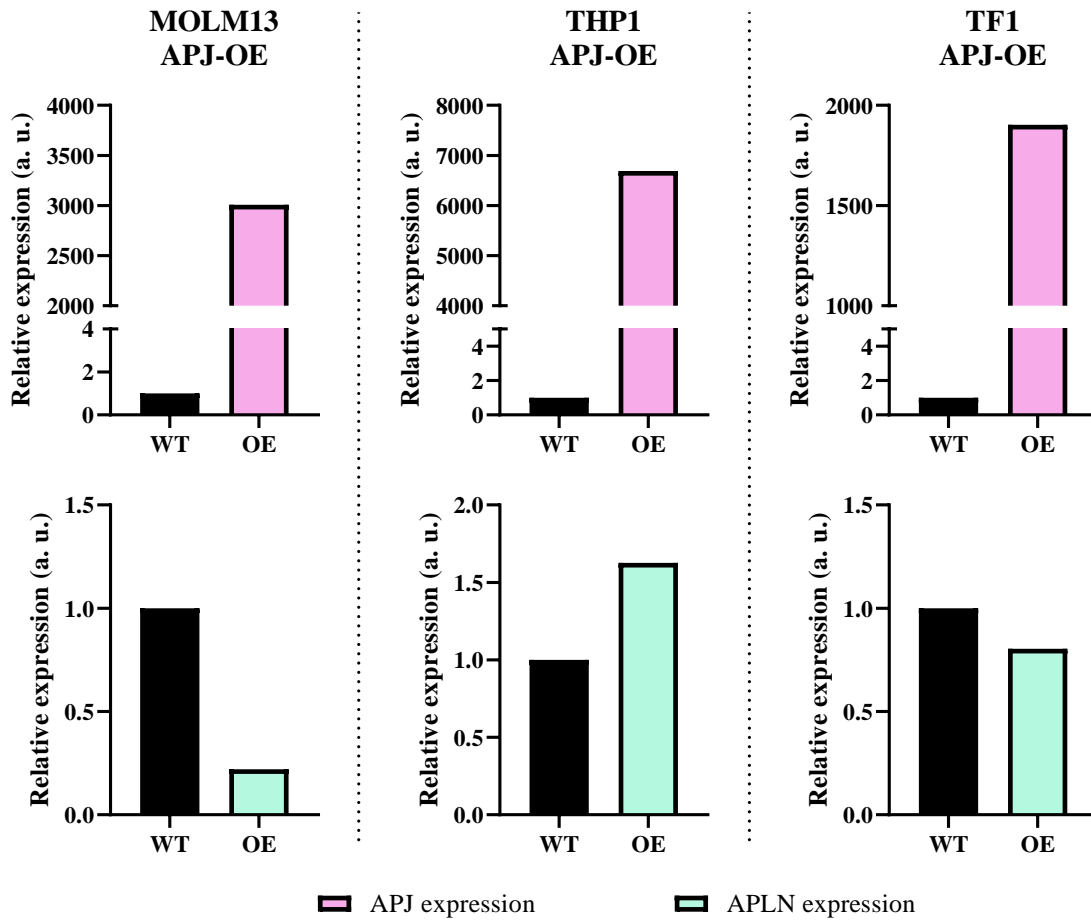


**Supplementary Figure 1. APJ (APC) antibody functionality.** Flow cytometric data, representing low binding affinity of APC-coupled antibody against APJ. Binding affinity of the antibody against APJ was compared to antibody against CD14. Both antibodies are coupled to APC fluorochrome. APJ-antibody showed very low binding affinity (less than 2%).

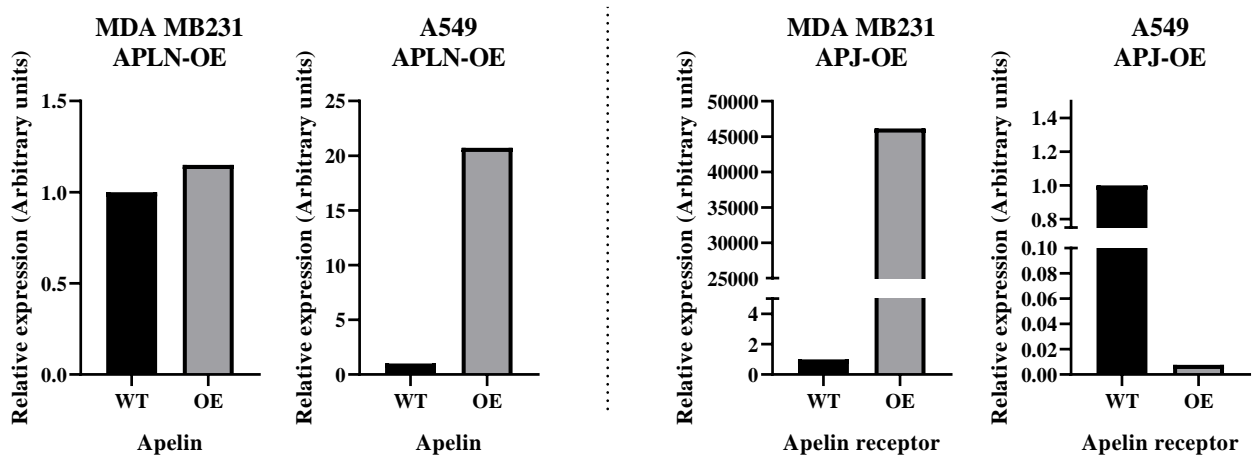
SUPPLEMENTARY DATA



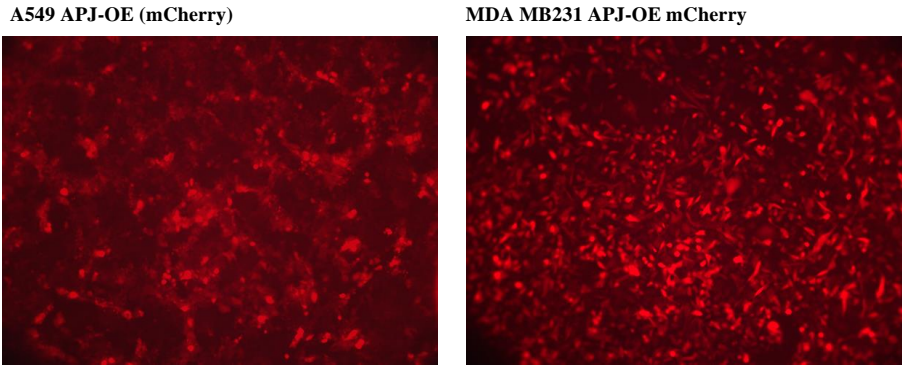
**Supplementary Figure 2. Flow cytometric analysis of U118 APJ surface expression.** APJ surface expression was analyzed using APC-labeled antibody. Annexin V was used to exclude dead cells.



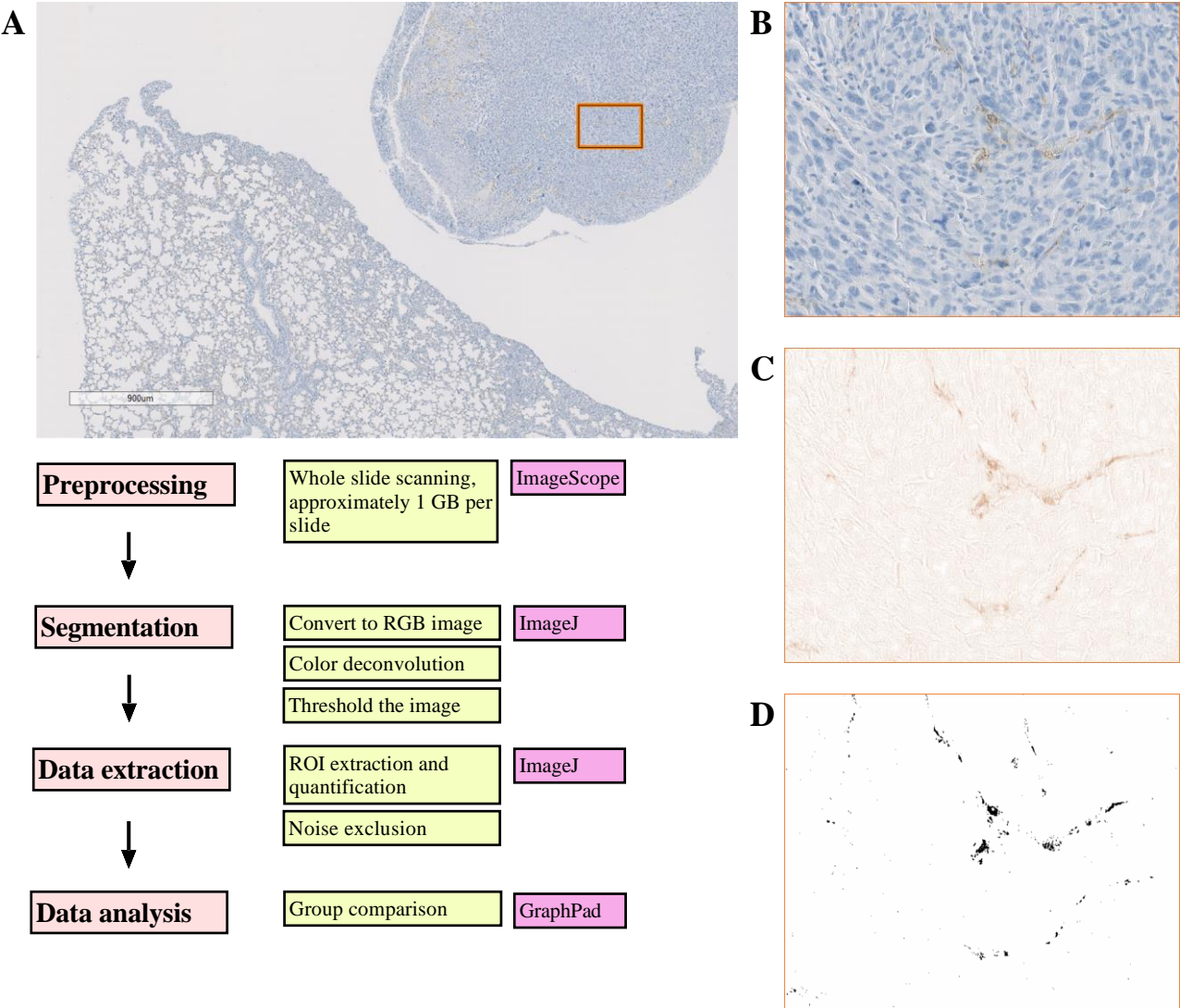
**Supplementary Figure 3. APJ and APLN gene expression analysis of transgenic AML cell lines.** Gene expression was analyzed by Pfaffl method. All samples were analyzed in triplicates and the results were normalized to the expression of glyceraldehyde-3-phosphate dehydrogenase (GAPDH).



**Supplementary Figure 4. APJ and APLN gene expression analysis of solid tumor cell lines.** Gene expression was analyzed by Pfaffl method. All samples were analyzed in triplicates and the results were normalized to the expression of glyceraldehyde-3-phosphate dehydrogenase (GAPDH).



**Supplementary Figure 5. Microscopic image of transduced solid tumor cell lines. APJ-OE A549 and MDA MB231, 7 days after transduction. Magnification 10x.**



**Supplementary Figure 6. Representation and analysis of tumor microvessel density. CD31 stained blood vessels are automatically segmented in whole-slide images. (A) Original image region, (B) Extracted region that will be processed; (C) Extraction of the immunostained area by color deconvolution; (D) Segmentation of blood vessels by thresholding and image post-processing.**

---

## 8. Appendix

### 8.1 Hazard statements

H225	Highly flammable liquid and vapor.
H226	Flammable liquid and vapor.
H228	Flammable solid.
H300	Fatal if swallowed.
H301	Toxic if swallowed.
H302	Harmful if swallowed.
H311	Toxic in contact with skin.
H312	Harmful in contact with skin.
H314	Causes severe skin burns and eye damage.
H315	Causes skin irritation.
H317	May cause an allergic skin reaction.
H318	Causes serious eye damage.
H319	Causes serious eye irritation.
H320	Causes eye irritation.
H331	Toxic if inhaled.
H332	Harmful if inhaled.
H334	May cause allergy or asthma symptoms or breathing difficulties if inhaled.
H335	May cause respiratory irritation.
H336	May cause drowsiness or dizziness.
H340	May cause genetic defects.
H350	May cause cancer.
H360	May damage fertility or the unborn child.
H361f	Suspected of damaging fertility or the unborn child.
H370	Causes damage to organs.
H372	Causes damage to organs through prolonged or repeated exposure.
H373	May cause damage to organs through prolonged or repeated exposure if inhaled.
H400	Very toxic to aquatic life.
H410	Very toxic to aquatic life with long-lasting effects.
H412	Harmful to aquatic life with long lasting effects.

### 8.2 Precautionary statements

P101	If medical advice is needed, have product container or label at hand.
P102	Keep out of reach of children.
P103	Read label before use.
P201	Obtain special instructions before use.
P202	Do not handle until all safety precautions have been read and understood.

## APPENDIX

---

P210	Keep away from heat/sparks/open flames/hot surfaces. No smoking.
P233	Keep container tightly closed.
P240	Ground and bond container and receiving equipment.
P241	Use explosion-proof [electrical/ventilating/lighting/...] equipment.
P242	Use non-sparking tools.
P243	Take action to prevent static discharges.
P260	Do not breathe dusts or mists.
P260D	Do not breathe vapors.
P261	Avoid breathing (dust/fume/gas/mist/vapors/spray).
P261sh	Avoid breathing dust/vapors. P280sh Wear protective gloves/eye protection.
P264	Wash (hands) thoroughly after handling.
P264W	Wash with water thoroughly after handling.
P270	Do not eat, drink or smoke when using this product.
P271	Use only outdoors or in a well-ventilated area.
P272	Contaminated work clothing should not be allowed out of the workplace.
P273	Avoid release to the environment.
P280	Wear (protective gloves/protective clothing/eye protection/face protection).
P280sh	Wear protective gloves/eye protection.
P285	In case of inadequate ventilation wear respiratory protection.
P301+310	IF SWALLOWED: Immediately call a POISON CENTER/doctor.
P301+312	IF SWALLOWED: Call a POISON CENTER or doctor/physician if you feel unwell.
P301+330+331	IF SWALLOWED: Rinse mouth. Do NOT induce vomiting.
P302+352	IF ON SKIN: Wash with plenty of soap and water.
P303+361+353	IF ON SKIN (or hair): Take off immediately all contaminated clothing. Rinse skin with water [or shower].
P304+340	IF INHALED: Remove person to fresh air and keep comfortable for breathing.
P304+340+310	IF INHALED: Remove person to fresh air and keep comfortable for breathing. Immediately call a POISON CENTER/doctor.
P304+341	IF INHALED: If breathing is difficult, remove to fresh air and keep at rest in a position comfortable for breathing.
P305+351+338	IF IN EYES: Rinse cautiously with water for several minutes. Remove contact lenses, if present and easy to do. Continue rinsing.
P305+351+338+310	IF IN EYES: Rinse cautiously with water for several minutes. Remove contact lenses, if present and easy to do. Continue rinsing. Immediately call a POISON CENTER/doctor.
P305+P351+P338	IF IN EYES: Rinse cautiously with water for several minutes. Remove contact lenses, if present and easy to do. Continue rinsing.
P308+313	IF exposed or concerned: Get medical attention/advice.
P310	Immediately call a POISON CENTER/doctor.
P312	Call a POISON CENTER/doctor/... if you feel unwell.
P314	Get medical attention/advice if you feel unwell.
P321	Specific treatment (see ... on this label).
P330	Rinse mouth.
P332+313	If skin irritation occurs: Get medical advice/attention.

---

P333+313	If skin irritation or rash occurs, seek medical advice/attention.
P337+313	If eye irritation persists: Get medical advice/attention.
P342+311	If experiencing respiratory symptoms: Call a POISON CENTER/doctor.
P363	Wash contaminated clothing before reuse.
P391	Collect spillage.
P405	Store locked up.
P501	Dispose of contents/container in accordance with local/regional/national/international regulations.

### 8.3 Physical and health hazards pictograms



GHS02: Flammable



GHS05: Corrosive



GHS06: Toxic



GHS07: Harmful



GHS08: Health hazard

GHS09:  
Environmental hazard

## Acknowledgments

For the past three years and four months, I have had the honor and fortune to work in the team of Prof. Dr. Walter Fiedler and PD Dr. Jasmin Wellbrock. Professor Fiedler, I owe you my gratitude for your sincere and selfless help and kindness during these years. Thank you for finding time for me, for taking care of me, in addition to all your responsibilities at the clinic. Your cheerful spirit has always given me hope for successful completion of my doctorate. I owe a great deal of gratitude to Jasmin, without whom this thesis would not have been possible to finish. Jasmin, thank you for the detailed organization and for your willingness to always answer my questions. Thank you for allowing me to learn techniques and methods that I did not know until now. I am especially grateful for your time given for useful advice and words of consolation when the experiments did not go as planned. Apart from science stuff, I must not forget the parties of our group at your home, including one of the best masquerades I have ever attended.

To Dr. Lena Behrmann and PD Dr. Sabine Hoffmeister-Ullerich I am thankful for every advice given during gene expression analyses. Sabine, thank you for every moment spent to answer my numerous questions during difficult times and for agreeing to participate as a member of the examination committee.

I also owe a great deal of gratitude to professor Wolfgang Maison, who, in addition to all his obligations, agreed to be the evaluator of this doctoral thesis. I am also very grateful to co-supervisor of this doctorate, Prof. Dr. Elke Oetjen for all her understanding, support and constructive comments in moments when things did not go according to the plan and when I wasn't as organized as I should have been. Thank you for your willingness to always help. Also, help from the student service of MIN Faculty, Department of Chemistry, has never been lacking thanks to Ms. Waltraud Wallenius. Ms. Wallenius, thank you for making everything more comfortable and for always finding a way to overcome difficulties.

I am especially grateful to professor Lejla Kapur-Pojškić and professor Hans Joachim Seitz, who, through joint efforts, made it possible for me to come to Hamburg. Yet, none of this would have been possible without my dear friend Dr. Jasmina Hindija. Jasmina, I'm sure I can't thank you enough for your constant support all these years, starting from the time we worked together on my diploma thesis. Thank you for initiating all this, for contacting me at the right time. Thank you for your trust. During our numerous conversations, I could always sense your



positivity, no matter how difficult the situation was at the time. Thank you for your understanding, which I sometimes missed during my doctorate.

Thanks to the technical staff of our lab, Gabi, Antonia, Vanessa, Jana, for every helpful advice. Without you, it would not be possible to perfect the methods necessary for this doctorate. I owe the greatest gratitude to Gabi and Antonia, who were helping me until the very end of the doctorate. Thank you so much for your support when my time for experiments was limited. Antonia and Gabi, despite all obligations, you were also there for me. It was a great pleasure working with you.

This doctorate has spawned some wonderful friendships in my life. Frauke, Alex, it was an honor and joy to work with you. Thank you for sharing your good and bad moments with me. Thank you for sharing not only the space in the lab, but also sharing your Ph.D. life with me. Every piece of advice and comfort after every experiment conducted, successful or unsuccessful, came from you. Thank you for every lunch we had together around 2 pm, especially for Pizza-Thursdays, full of calories. I will remember all of our jokes which made our work atmosphere more than pleasant. You have so often been responsible for the smile on my face. Alex, thank you for understanding every joke that few could understand. Thank you for refreshing and sticking my corner of the office with amusing stickers. Not to forget – thanks to you, I always had the latest information from the world of rap music. To Frauke, my Ph.D. sister and a great friend, I am immensely grateful for all given advice and suggestions during these years. Thank you for your patience and selfless sharing of your knowledge. Thank you for all the good news over the years. Your friendly support and understanding when it was the hardest is something that few could do and cannot be easily forgotten. In the middle of all the science stuff we were dealing with, we always managed to talk about our general life plans, travel plans... Simply, talking to you has always been positively refreshing. Thank you for allowing me to discover you both as a person and as a researcher.

I owe immense gratitude to some of the most brilliant minds in our clinic, Dr. Stefan Horn and Prof. Dr. Jakob Körbelin. Stefan, without your technical support, everything would have been much more difficult. Thank you for all your help in the organization of the mouse experiments, especially for your help when I was not in the lab. It was a pleasure working with you.

Jakob, you have been there all these years and you always had interesting and inspiring comments during our conversation. Thank you for always being full of patience, compassion and goodwill to listen. Thank you for every word of support and understanding in very difficult

moments. Thank you for your great optimism and for spreading scientific enthusiasm; for pointing out that every result, in addition to being bad, also has a good side. I am happy to have had such support.

Jelena Ivanković, Aleksandra Spasojević, Aljoša Šljuka, Ana Šipikovjanović, Daniela Bajdevska, Nina Matić thank you for your friendly support at all times. Aljoša, your programming ability was of great help in this doctorate. Aleksandra, thank you for always finding time to talk about the difficult path to our doctorates. We shared the same view on so many life questions... Our coffee breaks have always been the reason for additional brainstorming. Ana, thank you for all your optimism and for endless goodwill. Daniela, despite all your commitments and the difficult period you had, you always found time for me. Thank you for your cordial help in analyzing IHC samples and for the countless questions you have always been ready to answer. Nina, your words were always full of hope. Our audio messages will surely hold a record in length for a long time. Jelena, Jeca, what would I do without our ice cream gourmet moments, full of positivism?

Vladimir Lakić, Dejana Kulina, Ivana Parađina, Srđan Čegar, thank you for your optimism, jokes, thank you for your interest in everything I have done in the past years. Jovana Gajović, it would be difficult to endure without your enthusiasm in the days when I needed help. Thank you all for maintaining our friendship despite me being away from you. Veca, Goga... Without you, there would be no spiritual in me. Thank you for every message full of good feelings and kindness. Veca, thank you for the surprise cake every time I visit you. Goga, our tea parties have become a tradition.

Dr. Vuk Vuković is someone who left an indelible mark in my life. Someone who made me a better person, a better scientist. Who helped me to keep the faith. Our correspondence, our stories until late at night, is something that will not be forgotten. Thank you for being there when I wasn't on the right track. Thank you for not forgetting me when I needed help so much. Thank you for helping in the most difficult moments when I doubted myself. Your goodness, as a mountain spring, is infinite.

Flávia Oliveira Geraldés, thank you for every thoughtful advice given during this doctorate. Your willingness to help was always there. Thank you for understanding my jokes, for our cooperation in scientific projects in Russia and long lasting friendship.

I hope I haven't forgotten anyone by now.

After all, I want to thank the people to whom I dedicate this doctoral thesis – my family, my loved ones. My family is the reason I'm here where I am. Although we were often so far from each other, I always felt you with me. Thank you for always being light in the dark. Dragan, Anna, don't be surprised that I put your names here. You are my family. You have always been there, from my beginning. Anna, thank you for the words of comfort when it was so hard to start a new life. Dragan, your optimism and support is something that kept me going forward.

To family Nastav I am grateful for every positive thought given. Although we haven't seen each other over the years, I could feel your support in every moment. Dear aunt Ružica, thank you for supporting me in such difficult times of my life.

The Grabovac, Marić and Stojanović families, thank you for never forgetting me. Aunt Ljubinka, Uncle Savo, I am so proud to have had you by my side.

My dear grandmothers, unfortunately, left us near the end of this doctorate. Baka Bosa, Baka Vuka, thank you for your true goodness. Thank you for not hiding your happiness every time we see each other. I hope you would have been proud of me. I am proud of you.

You deserve special credit for this doctorate, Adri. I am here because of you. Your incredible patience over the years is something that is rarely found. Thank you for your words of comfort when it was the hardest. Thank you for every trip, for every dinner you made, for the inexhaustible optimism and above all, for your infinite kindness. Thank you for encouraging me, for making my life better every day. And I am blessed that you are always here and will be, you and Nukli. You have been that necessary firefly.

My mother Gospa and my father Velimir are the reason for my every success. Dear Mom and Dad, thank you for every support. Thank you for reminding me to eat regularly, to have more sleep (even when it wasn't physically possible), and above all for your patience. It wasn't easy being physically separated from you, that's for sure. Thank you for the assurance that I will successfully complete this Ph.D. I want to thank my big brother Goran for his eternal support and for every well-intentioned criticism. Thank you for understanding the moments when I felt hopeless. Thank you for every good thought and good word.

My loved ones, I want you to know that I am immensely grateful to have you. You are the pillars of my life, you are my inspiration and my safety. Without you, I would be left in the dark to wander aimlessly. Every thought of you creates a warm feeling around my heart, the same feeling I experience when I come to my mountain Jahorina. Your support is everything.

Thank you, reader of this thesis, for your interest. I hope you will found the thesis useful.

Eidesstattliche Versicherung /*Declaration on Oath*

Hiermit versichere ich, dass ich die vorliegende Dissertationsschrift mit dem Titel „Apelinergic system and its role in the development of resistance to antiangiogenic therapy in cancer treatment“ selbstständig verfasst, keine anderen als die angegebenen Quellen und Hilfsmittel benutzt und die den benutzen Werken wörtlich oder inhaltlich entnommenen Stellen als solche kenntlich gemacht habe. Ferner versichere ich, dass diese Arbeit noch nie in derselben oder einer ähnlichen Fassung, auch nicht in Teilen, in einem anderen Prüfungsverfahren eingereicht oder veröffentlicht wurde.

*I hereby declare, on oath, that I have written the presented dissertation with the title “Apelinergic system and its role in the development of resistance to antiangiogenic therapy in cancer treatment” on my own, that I have not used other than the acknowledged sources or aids and that all passages adopted literally or with regard to their content are marked as such. I further declare that this work has never been published or submitted in a previous doctoral procedure, in this or any other form, not even partially.*

Hamburg, 17.05.2020

Zoran Knežević

A handwritten signature in blue ink, appearing to read 'Zoran Knežević', with a stylized flourish extending from the top right.